

**IMPACT OF UV TREATMENT ON DISINFECTION BYPRODUCT
PRECURSORS AND SUBSEQUENT BYPRODUCT FORMATION FROM
CHLORINE AND CHLORAMINE**

Bonnie A. Lyon

A dissertation submitted to the faculty of the University of North Carolina at Chapel Hill
in partial fulfillment of the requirements for the degree of Doctor of Philosophy in the
Department of Environmental Sciences and Engineering, Gillings School of Global
Public Health.

Chapel Hill
2012

Approved by:

Howard S. Weinberg

Rose M. Cory

Karl G. Linden

Philip C. Singer

Steven C. Whalen

© 2012
Bonnie A. Lyon
ALL RIGHTS RESERVED

Abstract

BONNIE A. LYON: Impact of UV Treatment on Disinfection Byproduct Precursors and Subsequent Byproduct Formation from Chlorine and Chloramine
(Under the direction of Howard S. Weinberg)

As natural source water quality becomes increasingly impacted by anthropogenic activity, utilities are looking towards alternative disinfection techniques to meet regulations related to the delivery of quality drinking water to consumers. Ultraviolet (UV) irradiation is one process that is being used to address this issue, but there have been few comprehensive studies that have looked at the effect of UV treatment on the formation of disinfection byproducts (DBPs) and in particular, emerging DBP classes that are thought to be more geno- and cytotoxic than the regulated trihalomethanes and haloacetic acids. The objective of this research was to evaluate the impact of UV irradiation on organic and inorganic DBP precursors and the formation of a range of DBPs from subsequent addition of chlorine or chloramine. Disinfection doses of UV (40-186 mJ/cm²) followed by chlorination/chloramination had little effect on the formation of regulated trihalomethanes and haloacetic acids, but the formation of several emerging DBPs were increased by UV and chlorination/chloramination in waters containing 1-10 mg N/L nitrate (halonitromethanes and cyanogen chloride) or regardless of nitrate content (chloral hydrate). Their formation was affected to a greater extent with medium pressure (MP) compared to low pressure (LP) UV. The higher potential toxicity of these byproducts compared to the regulated DBPs warrants consideration of practices

that could reduce their formation. If MP UV is being implemented on source waters containing elevated nitrate, utilities should consider options for nitrate reduction upstream from UV processes. The use of fluorescence spectroscopy allowed for the observation of changes to organic precursor components following combinations of UV, chlorine, and chloramine treatment that were not detectable by UV/visible absorbance spectroscopy or dissolved organic carbon analysis. Results of an *in vitro* cytotoxicity assay employing human colon cells showed that concentrated waters treated with MP UV followed by chloramination had a higher cytotoxicity than those treated with only chloramine, suggesting that further research is needed to evaluate the effect of byproduct mixtures produced during UV-chloramine treatment. The findings of this research have implications for the design and optimization of combined UV-chlorine/chloramine processes for drinking water treatment.

Acknowledgments

I am grateful to Howard Weinberg for his mentoring and guidance throughout my time at UNC. I appreciate the dedication he has for helping his students succeed in graduate school and beyond. I would like to thank Rose Cory, Karl Linden, Phil Singer, and Steve Whalen for serving as additional mentors and contributing to this research. I would like to acknowledge the Gillings School of Global Public Health Dissertation Award and Royster Society of Fellows for providing financial support in my final year of graduate school. I am grateful for the expertise of Glenn Walters and D.J. Fedor in the ESE Design Shop, who built and maintained the UV system used for this work. Thanks to Orange County Water & Sewer Authority Drinking Water Treatment Plant and in particular, Rachel Monschein, for providing laboratory space at OWASA. Thanks to Katie Harrold for her assistance and training on fluorescence analysis and PARAFAC modeling. I would like to acknowledge the support and guidance of Tony DeAngelo and Jane Ellen Simmons of the U.S. EPA on the toxicity component of this project. Thanks also to Rebecca Milsk for performing the cytotoxicity assay for this work and to past and present Weinberg group members for their contributions and motivation. I am truly grateful for the endless support, love, and encouragement of my family, friends, and Pat.

Table of Contents

List of Tables.....	ix
List of Figures.....	xii
List of Abbreviations.....	xvi
Chapter 1: Introduction.....	1
1.1 Drinking Water Treatment and Disinfection Byproducts.....	1
1.2 Natural Organic Matter.....	3
1.3 Inorganic Species: Bromide and Iodide.....	7
1.4 Ultraviolet (UV) Irradiation.....	9
1.5 Potential for UV Treatment to Impact Disinfection Byproduct Formation.....	10
1.6 Toxicology Studies.....	16
1.7 Research Gaps.....	17
1.8 Research Hypotheses.....	21
1.9 Research Objectives.....	21
1.10 Dissertation Organization.....	22
Sources Cited for Chapter 1.....	23
Chapter 2: The Effect of Inorganic Precursors on Disinfection Byproduct Formation during UV-Chlorine/Chloramine Drinking Water Treatment.....	32
2.1 Introduction.....	32
2.2 Materials and Methods.....	36
2.3 Results and Discussion.....	44

2.4 Conclusions.....	62
Sources Cited for Chapter 2.....	66
Chapter 3: Disinfection Byproduct Formation from UV- Chlorine/Chloramine Treatment of Whole and Fractionated Dissolved Organic Matter	71
3.1 Introduction.....	71
3.2 Materials and Methods.....	73
3.3 Results and Discussion	83
3.4 Conclusions.....	107
Sources Cited for Chapter 3.....	110
Chapter 4: Investigating Changes in Dissolved Organic Matter Fluorescence and Disinfection Byproduct Formation from UV and Subsequent Chlorination/Chloramination	115
4.1 Introduction.....	115
4.2 Materials and Methods.....	119
4.3 Results and Discussion	125
4.4 Conclusions.....	141
Sources Cited for Chapter 4.....	142
Chapter 5: Formation and Cytotoxicity of Disinfection Byproduct Mixtures Produced from UV-Chlorine/Chloramine Treatment	148
5.1 Introduction.....	148
5.2 Materials and Methods.....	153
5.3 Results.....	161
5.4 Discussion.....	179
5.5 Conclusions.....	182
Sources Cited for Chapter 5.....	184
Chapter 6: Conclusions and Implications	189

6.1 Summary of Results	189
6.2 Examination of Individual Hypotheses.....	193
6.3 Implications.....	195
Appendix 1: Reverse Osmosis (RO) Concentration Standard Operating Procedure (SOP)	199
Appendix 2: Supplemental Information for Chapter 2	205
Appendix 3: SOP for Medium Pressure (MP) UV System	210
Appendix 4: Preparation of Monochloramine Dosing Solution	214
Appendix 5: DBP Extractions.....	218
5.A Halogenated Volatiles/Haloacetamides Extraction SOP	218
5.B Cyanogen Chloride Extraction SOP	226
5.C Haloacetic Acids Extraction SOP	230
Appendix 6: Supplemental Information for Chapter 4	237
Appendix 7: Supplemental Information for Chapter 5	242
Appendix 8: Growth Inhibition Assay SOP.....	248
Sources Cited for Chapter 6.....	255

List of Tables

Table 1-1. Types of DOM associated with EEM wavelength regions.	6
Table 1-2. Reactions involving reactive nitrogen species formed during photolysis of nitrate/nitrite.	12
Table 1-3. Reactions involving reactive halogen species produced by indirect photolysis.	14
Table 1-4. Reactions rates involving radical species and model NOM components.	14
Table 2-1. Water quality data for filter effluent (Utilities A and B) and reconstituted settled water RO concentrate (Utility C).	37
Table 2-2. 24-hour chlorine demands (mg Cl ₂ /mg C) for ambient (unspiked) and spiked samples treated with LP and MP UV.	45
Table 2-3. 24-hour chloramine demands (mg Cl ₂ /mg C) for ambient and spiked samples treated with LP and MP UV.	46
Table 2-4. 24-hour chlorine and chloramine demands for ambient and spiked Utility C samples treated with MP UV.	46
Table 2-5. Effect of bromide- and nitrate-spiking on chloropicrin and bromopicrin formation from MP UV irradiation followed by chlorination and chloramination in Utility C samples.	55
Table 2-6. Summary of conditions under which a U.S. EPA regulation, WHO guideline value, or maximum level measured in a U.S. occurrence study (for compounds with no current regulation or guideline value) was reached or exceeded.	65
Table 3-1. Sample characterization and disinfectant doses based on chlorine/chloramine demand tests.	86
Table 3-2. Effect of MP UV (1000 mJ/cm ²) on the 72-hour chlorine demand of ambient (unspiked) spiked (10 mg N/L nitrate and 1 mg/L bromide) samples.	88
Table 3-3. Effect of LP (500 mJ/cm ²) and MP UV (1000 mJ/cm ²) on the 72-hour chloramine demand of ambient and spiked (10 mg N/L nitrate and 1 mg/L bromide) samples.	89

Table 3-4. Contribution of hydrophobic acid and hydrophilic DOM to THM4 and HAA9 molar formation in unfractionated RO concentrate.	93
Table 3-5. THM4 bromine incorporation factor (BIF) during chlorination and chloramination of ambient and spiked samples.....	97
Table 3-6. X ₂ AA BIF during chlorination and chloramination of ambient and spiked samples.....	97
Table 3-7. X ₃ AA BIF during chlorination and chloramination in ambient and spiked samples.....	98
Table 3-8. Effect of LP (500 mJ/cm ²) and MP UV (1000 mJ/cm ²) on THM4 bromine incorporation during chlorination and chloramination of ambient and spiked SRNOM.....	99
Table 3-9. Effect of LP (500 mJ/cm ²) and MP UV (1000 mJ/cm ²) on dihaloacetic acid (X ₂ AA) BIF during chlorination and chloramination of ambient and spiked SRNOM.....	99
Table 3-10. Effect of LP (500 mJ/cm ²) and MP UV (1000 mJ/cm ²) on trihaloacetic acid (X ₃ AA) BIF during chlorination and chloramination of ambient and spiked SRNOM.....	100
Table 3-11. Contribution of hydrophobic acids and hydrophilic DOM to chloral hydrate molar formation in unfractionated RO concentrate.	107
Table 4-1. DOC concentration (mg C/L) for ambient (unspiked) and spiked reconstituted RO concentrate samples treated with MP UV.....	126
Table 4-2. Description of four components (C1-C4), excitation and emission peaks (with secondary peaks in parentheses), and comparison to similar peaks identified in previous work (referred to by the peak name and/or letter assigned by the authors of the referenced study).....	129
Table 4-3. Effect of MP UV followed by chlorination (Cl ₂) or chloramination (NH ₂ Cl) on the formation of DBPs in ambient and nitrate-spiked samples	138
Table 5-1. Characteristics of Nordic Reservoir NOM solution prior to UV/chlorine-chloramine treatment and application to cytotoxicity assay.....	155

Table 5-2. Effect of treatment conditions on DBP formation and cell growth inhibition (IC ₂₀ and IC ₅₀ values).....	163
Table 5-3. Results of statistical comparison for IC ₅₀ values (on a DOC basis) between each sample.	166
Table 5-4. Effect of treatment conditions on emerging DBP formation in Nordic Reservoir samples. Detection limits vary due to different dilutions.....	176
Table 5-5. Comparison of 24-hour chlorine/chloramine demand and DBP/total organic halogen yield (molar concentration normalized to DOC) in dilute vs. concentrated (conc.) samples.....	178
Table A2-1. Reverse osmosis (RO) feed and RO concentrate (conc.) characteristics for Orange County Water and Sewer Authority (OWASA) drinking water treatment plant raw and settled waters.	205
Table A2-2. Effect of MP UV (dose is in mJ/cm ²) followed by chlorination and chloramination on THMs in ambient and iodide-spiked Utility C samples.	206
Table A2-3. Chlorine/chloramine residuals at specified time points for kinetics study (mg/L as Cl ₂) in spiked Utility C samples.....	207
Table A2-4. Formation of cyanogen chloride and halogenated volatile species in nitrate- and nitrate- & bromide-spiked Utility C samples following chlorination and 1000 mJ/cm ² MP UV + chlorine treatment, with different chlorine contact times.	208
Table A2-5. Formation of cyanogen chloride and halogenated volatile species in nitrate- and nitrate- & bromide-spiked Utility C samples following chloramination and 1000 mJ/cm ² MP UV + chloramine treatment, with different chloramine contact times.....	209
Table A6-1. Effect of MP UV (dose is in mJ/cm ²) followed by chlorination on the formation of halogenated volatiles in ambient and spiked samples.	239
Table A6-2. Effect of MP UV (dose is in mJ/cm ²) followed by chloramination on the formation of halogenated volatiles in ambient and spiked samples.....	240
Table A6-3. Nitrate concentration and nitrite formation (mg N/L) from MP UV irradiation of ambient and spiked samples	241

List of Figures

Figure 1-1. Generic chemical structure of (a) THMs and (b) HAAs, two classes of DBPs, where X = Cl, Br, or I for THMs and X = Cl, Br, I, or H for HAAs.....	1
Figure 1-2. A typical EEM spectrum.....	6
Figure 1-3. (a) Absorption spectra of NaBr and KI in LGW and (b) LP UV and MP UV spectral output	15
Figure 2-1. (a) Emission spectra of LP (dashed line) and MP (solid line) UV and	49
Figure 2-2. Impact of (a) LP and (b) MP UV followed by chlorination on the molar formation of THM4 in ambient (black shapes) and bromide- and nitrate-spiked (hollow shapes) samples.	50
Figure 2-3. Effect of nitrate concentration on chloropicrin formation from MP UV-chlorine treatment of Utility C samples.....	52
Figure 2-4. Effect of LP and MP UV followed by (a) chlorination and (b) chloramination on the formation of bromopicrin in bromide- and nitrate-spiked samples.....	54
Figure 2-5. Effect of LP and MP UV followed by chlorination on the formation of chloral hydrate in (a) ambient and (b) bromide- and nitrate-spiked Utility A and B samples.	58
Figure 2-6. Effect of MP UV followed by chlorination on the formation of chloral hydrate in ambient and spiked Utility C samples.	59
Figure 2-7. Effect of MP UV followed by chloramination on the formation of cyanogen chloride in Utility C samples.	61
Figure 3-1. RO concentration setup.....	75
Figure 3-2. Procedure for XAD fractionation of DOM by polarity and acid/base properties.	78
Figure 3-3. Composition of OWASA raw water RO concentrate on a carbon mass basis.	85
Figure 3-4. Comparison of (a) OWASA RO concentrate and (b) SRNOM fractions on a carbon mass basis.	85

Figure 3-5. Effect of MP UV followed by chlorination on THM4 formation in ambient and spiked samples.	92
Figure 3-6. Effect of MP UV followed by chlorination on HAA9 formation in ambient and spiked samples.	92
Figure 3-7. Effect of LP and MP UV followed by chloramination on THM4 formation in ambient and spiked samples.	94
Figure 3-8. Effect of LP and MP UV followed by chloramination on HAA9 formation in ambient and spiked samples.	95
Figure 3-9. Effect of MP UV followed by chlorination on chloropicrin formation in ambient samples.	101
Figure 3-10. Effect of LP (500 mJ/cm ²) and MP UV (1000 mJ/cm ²) followed by chlorination and chloramination on chloropicrin formation in nitrate-spiked SRNOM samples.	101
Figure 3-11. Effect of MP UV followed by chlorination on chloral hydrate formation in ambient samples.	105
Figure 4-1. Excitation emission matrices and excitation (solid lines) & emission (dashed) spectra for each component identified in the PARAFAC model.....	128
Figure 4-2. Effect of UV on fluorescence intensity (F_{\max}) in ambient and spiked samples.	130
Figure 4-3. Effect of UV followed by chlorination on component F_{\max} in ambient and spiked samples, with comparison to untreated sample.....	133
Figure 4-4. Effect of UV followed by chloramination on component F_{\max} in ambient and spiked samples, with comparison to untreated sample.....	136
Figure 4-5. Correlation between change in C2 and C4 F_{\max} and formation of chloral hydrate in ambient and nitrate-spiked samples treated with MP UV + chlorine.	139
Figure 4-6. Correlation between change in C2 & C4 F_{\max} and formation of cyanogen chloride in all samples treated with chloramine or MP UV followed by chloramination.....	141
Figure 5-1. Dose-response curves for chlorine and MP UV-chlorine treatment of ambient Nordic Reservoir samples.	167

Figure 5-2. Dose-response curves for chlorine and MP UV-chlorine treatment of nitrate-spiked Nordic Reservoir samples.....	167
Figure 5-3. Dose-response curves for chloramine and MP UV-chloramine treatment of ambient and iodide-spiked Nordic Reservoir samples.....	168
Figure 5-4. Dose-response curves for all treated Nordic Reservoir samples on a DOC basis.....	168
Figure 5-5. Dose-response curves for all treated Nordic Reservoir samples on a total organic halogen formation basis.....	169
Figure A1-1. Schematic of RO concentration procedure.....	202
Figure A1-2. Front of RO concentration unit.	203
Figure A1-3. Back of RO concentration unit.....	204
Figure A1-4. RO membrane enclosure.	204
Figure A3-1. Typical uridine UV/vis absorbance spectra for t=0 and t=5 min.	213
Figure A5-1. Chromatogram of halogenated volatile species for a 100 µg/L calibration point.	225
Figure A5-2. Chromatogram of haloacetamide species for a 200 µg/L calibration point.....	225
Figure A5-3. Cyanogen chloride chromatogram for a 100 µg/L calibration point.....	229
Figure A5-4. Haloacetic acid chromatogram for 500 µg/L (as Br ₃ AA) calibration point.....	236
Figure A6-1. Component 1 excitation (solid line) and emission (dashed line) spectra of four validation splits compared to modeled component.	237
Figure A6-2. Component 2 excitation (solid line) and emission (dashed line) spectra of four validation splits compared to modeled component.	237
Figure A6-3. Component 3 excitation (solid line) and emission (dashed line) spectra of four validation splits compared to modeled component.	238

Figure A6-4. Component 4 excitation (solid line) and emission (dashed line) spectra of four validation splits compared to modeled component.	238
Figure A7-1. Dose-response curves for commercially available Nordic Reservoir NOM compared to Orange County Water & Sewer Authority Drinking Water Treatment Plant raw water (OWASA) reverse osmosis (RO) concentrate.....	242
Figure A7-2. Cytotoxicity results for ascorbic acid, unquenched disinfectants and disinfectants quenched with ascorbic acid.	243
Figure A7-4. Dose-response curve for nitrate in 20 mM phosphate buffer.	244
Figure A7-5. Dose-response curve for iodide in 20 mM phosphate buffer.	244
Figure A7-6. Dose-response curves for tribromonitromethane ($IC_{50} = 2.1 \times 10^{-5} M$), chloral hydrate ($IC_{50} = 5.4 \times 10^{-5} M$), and diiodoacetamide ($IC_{50} = 6.1 \times 10^{-6} M$) standards.	245

List of Abbreviations

ANOVA	Analysis of variance
BIF	Bromine incorporation factor
BV	Bed volume
C1-4	Fluorescing components 1-4 determined from parallel factor analysis (Chapter 4)
CCD	Charge-coupled device
CH	Chloral hydrate
CHO	Chinese hamster ovary
CNCl	Cyanogen chloride
DBP	Disinfection byproduct
DOC	Dissolved organic carbon
DOM	Dissolved organic matter
DON	Dissolved organic nitrogen
DPD	<i>N,N</i> -diethyl- <i>p</i> -phenylenediamine
EEM	Excitation-emission matrix
F _{max}	Maximum fluorescence intensity
GC-ECD	Gas chromatograph with electron capture detector
HAA	Haloacetic acid
HAA5	Five regulated haloacetic acids (chloro-, bromo-, dichloro-, trichloro-, and dibromo-acetic acid)
HAA9	Nine chlorine- and bromine-containing haloacetic acids
IC _x	Inhibitory concentration at which x=10, 20, 50% cell death occurs
IHSS	International Humic Substances Society
IIF	Iodine incorporation factor
IR	Infrared

LGW	Laboratory grade water
LP	Low pressure
MCL	Maximum contaminant level
MEM	Minimum essential medium
MP	Medium pressure
MRL	Minimum reporting limit
MtBE	Methyl tert-butyl ether
NA	Not applicable
NCM460	Normal derived colon mucosa cell line
N-DBP	Nitrogen-containing disinfection byproduct
NM	Not measured
NOM	Natural organic matter
OWASA	Orange County Water and Sewer Authority
PARAFAC	Parallel factor analysis
PTFE	Polytetrafluoroethylene (Teflon)
RO	Reverse osmosis
RPD	Relative percent difference
SOP	Standard operating procedure
SRNOM	Suwannee River natural organic matter
SUVA ₂₅₄	Specific UV absorbance at 254 nm
TBNM	Tribromonitromethane (bromopicrin)
TCNM	Trichloronitromethane (chloropicrin)
TDN	Total dissolved nitrogen
THM	Trihalomethane
THM4	Four regulated chlorine- and bromine-containing trihalomethanes

THM10	Ten chlorine-, bromine-, and iodine-containing trihalomethanes
TN	Total nitrogen
TOC	Total organic carbon
TOX	Total organic halogen
U.S. EPA	United States Environmental Protection Agency
UV	Ultraviolet
WHO	World Health Organization
X ₂ AA	Dihaloacetic acid
X ₃ AA	Trihaloacetic acid

Chapter 1: Introduction

1.1 Drinking Water Treatment and Disinfection Byproducts

Drinking water disinfection was one of the greatest public health advances of the 20th century. The introduction of drinking water chlorination vastly reduced cholera and typhoid incidences and the deaths associated with these outbreaks. In the mid-1970's, by-products of the chlorination process were discovered, including chloroform and other trihalomethanes (Rook 1974; Bellar et al. 1974). Disinfection byproducts (DBPs) are formed when a disinfectant reacts with ubiquitous decaying plant and microbial matter, chemicals in water which can be of natural origin such as bromide and iodide, or anthropogenic pollutants. Figure 1-1 shows the structures of two common classes of DBPs: trihalomethanes (THMs) and haloacetic acids (HAAs).

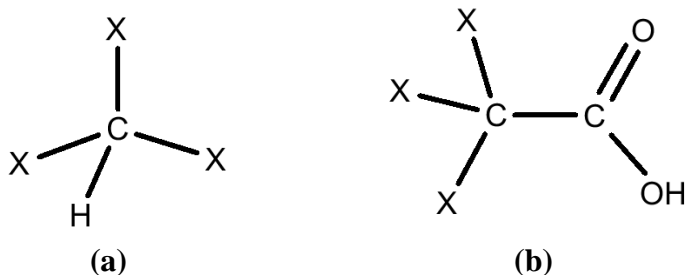


Figure 1-1. Generic chemical structure of (a) THMs and (b) HAAs, two classes of DBPs, where X = Cl, Br, or I for THMs and X = Cl, Br, I, or H for HAAs.

THMs have been found to cause adverse health effects in laboratory animals and concentrated drinking water extracts exhibited toxicological responses in bioassays (National Cancer Institute 1976; Loper et al. 1978). Epidemiological studies have suggested a link between consumption of drinking waters containing elevated levels of DBPs and adverse health outcomes, particularly bladder cancer and reproductive effects (Cantor et al. 1998; Calderon 2000). The Safe Drinking Water Act was introduced in 1974 to ensure high-quality drinking water to consumers by setting in motion the development of standards for naturally-occurring and anthropogenic water contaminants of human health concern. In 1979, the United States Environmental Protection Agency (U.S. EPA) began regulating the sum of four chlorine- and bromine-containing trihalomethanes (THM4) at a maximum contaminant level (MCL) of 100 µg/L (U.S. EPA 1979). The 1998 Stage 1 Disinfectant/Disinfection Byproduct Rule lowered the MCL for THM4 to 80 µg/L and introduced a regulation on the sum of five haloacetic acids (HAA5) at 60 µg/L, as well as bromate (10 µg/L), monitored as a running annual average of all sampling locations within a distribution system (U.S. EPA 1998). In addition, chlorite is regulated “at a level not to exceed” 1000 µg/L, due to potential acute health effects. In 2006, the Stage 2 Disinfectant/Disinfection Byproduct Rule was introduced and will require utilities to comply with MCLs based on *locational* running annual averages (starting in 2012-2013), rather than an average of all sampling points throughout a distribution system (U.S. EPA 2006a). Additionally, under the Unregulated Contaminant Monitoring Rule, the U.S. EPA requires utilities to monitor for a range of unregulated compounds which are on the Drinking Water Contaminant Candidate List for

potential future regulation (U.S. EPA 2007). These increasingly strict regulations have led utilities to look at alternative treatment processes.

As analytical methods have improved, new classes of DBPs of potential health concern have been discovered in drinking water, but at much lower levels than those currently regulated. Krasner and colleagues (2006) conducted an occurrence study at drinking water treatment plants across the U.S. and found that while the use of some alternative disinfectants (chloramines, chlorine dioxide, ozone) decreased the formation of regulated THMs and HAAs, in many cases these processes increased the formation of other DBPs. These include nitrogen-containing DBPs (N-DBPs) such as halonitromethanes and haloacetamides and iodine-containing THMs and HAAs. Although these DBPs are typically formed at lower levels than the regulated THMs and HAAs, toxicological studies of individual species suggest that their geno- and cytotoxicity may be orders of magnitude higher than the regulated DBPs (Plewa et al. 2004; Richardson et al. 2008).

1.2 Natural Organic Matter

Natural organic matter (NOM) is a complex mixture of decaying plant and microbial material found in all natural waters and it is the main precursor for DBP formation (Christman et al. 1983). There are thousands of chemical moieties that contribute to NOM composition, which can vary spatially, seasonally and over time. NOM properties and characteristics are studied to better understand and predict DBP formation. Typically, NOM is quantified by carbon content, reported as total or dissolved organic carbon (TOC or DOC). Dissolved organic matter (DOM) is the

operationally-defined dissolved fraction (usually defined as the portion passing through a 0.45 μm filter) which comprises most of the NOM mass in water (Thurman 1985).

Analyses such as UV/visible, infrared (IR), and fluorescence spectroscopy can be used for NOM characterization (Croué et al. 2000). The specific ultraviolet absorbance at 254 nm (SUVA_{254}), defined as $\text{UV}_{254}/[\text{DOC}]$, has been shown to correlate with DBP formation and is often used to predict the reactivity of NOM towards disinfectants (Edzwald et al. 1985; Reckhow et al. 1990; Kitis et al. 2001a). A measure referred to as fluorescence index (the ratio of emission intensity at 470 nm to the emission intensity at 520 nm, at an excitation of 370 nm) has been used to characterize organic matter source (e.g. microbial vs. terrestrial-derived) and aromatic content (McKnight et al. 2001; Cory & McKnight 2005). These wavelength pairs were chosen based on the emission intensities for DOM samples acquired from a range of aquatic environments and the excitation minimizing the inner-filter effect (partial absorption of emission by a component of the sample itself) and the instrument background interference.

Some characterization techniques require concentration or isolation of NOM, which can be carried out by evaporation, freeze-drying, membranes, or resin adsorption. Leenheer (1981) proposed a fractionation scheme using resins, pH-adjustment and various eluents to separate DOM by polarity and acid/base properties. Hydrophobic moieties include aromatic and phenolic-type structures while hydrophilic NOM is associated with protein-, carbohydrate-, and amino-type groups (Krasner et al. 1996). Past research has shown that in general, the hydrophobic fraction has greater THM and HAA formation potential compared to hydrophilic precursors. However, the hydrophilic fraction can play an important role in DBP formation, especially in low humic-containing

waters (Kitis et al. 2002; Liang & Singer 2003; Hua & Reckhow 2007a). There are differing views regarding the effectiveness of concentration and isolation methods for characterizing NOM. Some argue that these processes can create artifacts when assessing NOM reactivity as a result of extreme pH adjustments, concentration of salts, and membrane fouling (Malcolm 1991; Town & Powell 1993). Reverse osmosis (RO) isolation has been demonstrated as a method through which high organic carbon recoveries (80-99%) and preservation of original source water reactivity can be obtained (Kitis et al. 2001b; Song et al. 2009). Concentration and fractionation methods are not appropriate for every study but they have provided much insight into DBP formation mechanisms and meaningful results can be obtained, as long as limitations are recognized.

One type of characterization method which does not require intensive sample preparation is fluorescence spectroscopy. Fluorescence occurs when an electron in a molecule absorbs energy and re-emits light as it returns to its ground state. Molecules which exhibit this property are called fluorophores. DOM fluorescence is associated with the delocalized electron structure of aromatic components. Past work has identified different types and sources of organic matter that correspond with specific fluorescence excitation-emission matrix (EEM) regions (Coble 1996). An example EEM spectrum is shown in Figure 1-2 and Table 1-1 lists the types of DOM associated with EEM regions.

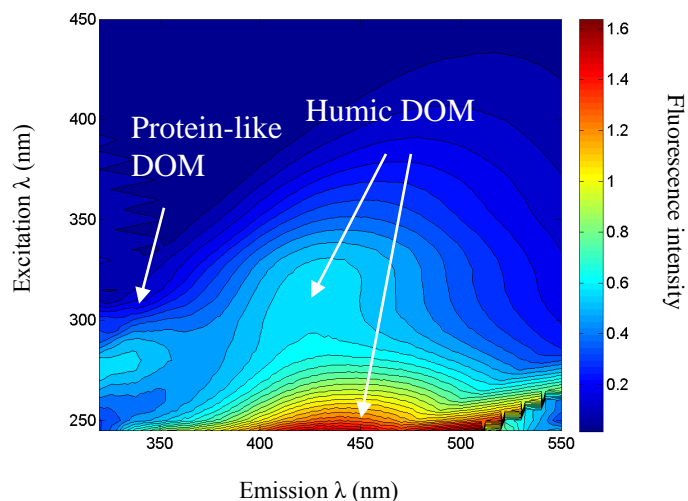


Figure 1-2. A typical EEM spectrum.

Table 1-1. Types of DOM associated with EEM wavelength regions.

$\lambda_{\text{ex}}/\lambda_{\text{em}}$ (nm)	DOM type	Associated with
275/310-340	Protein-like	agriculturally or wastewater-impacted source water
260-400/380-500	Humic-like	DOM color
230-260/380-500	Fulvic acid-like	DOM

Limited conclusions can be drawn by looking at EEM spectra alone. The application of parallel factor analysis (PARAFAC), a statistical modeling technique, to EEM data allows for quantitative identification of specific chemical components within the fluorescing material of DOM (Stedmon et al. 2003). These components can be associated with aliphatic or aromatic character, microbial- vs. terrestrial-derived DOM, and some have been identified as quinone- or protein-like compounds (Cory & McKnight 2005). Understanding the presence and changes in these DOM constituents that result from various treatment processes can provide information on DBP precursors and

formation pathways. A recent study that used fluorescence spectroscopy and PARAFAC to investigate DOM fluorescence during chlorination found a strong correlation between quinone-like components and THM4 and HAA5 formation (Beggs et al. 2009).

The formation of halogen-containing DBPs during chlorination is thought to occur by halogen substitution and oxidation reactions (Rook 1977; Norwood et al. 1980). Model compounds have typically been used to study these pathways due to the complexity of NOM. Boyce and Hornig (1983) proposed a mechanism for the formation of chloroform from chlorination of a 1,3-dihydroxyaromatic compound (e.g. resorcinol) involving chlorine substitution and oxidative decarboxylation. Dissolved organic nitrogen (DON) species are important precursors for the formation of N-DBPs (Reckhow et al. 1990; Lee et al. 2007). Labeled $^{15}\text{NH}_2\text{Cl}$ experiments have demonstrated that both DON and chloramine can contribute as nitrogen sources in the formation of N-DBPs such as dichloroacetonitrile and cyanogen chloride during chloramination (Yang et al. 2010).

1.3 Inorganic Species: Bromide and Iodide

Inorganic species (in particular, bromide and iodide) can also contribute to DBP formation and speciation. Sources of bromide in surface and groundwaters include: saltwater intrusion, rock weathering, and anthropogenic emissions (Wegman et al. 1981; Flury & Papritz 1993). Bromide levels in U.S. source waters were measured for the Information Collection Rule and ranged from below detection (<0.02 mg/L) to 1 mg/L, with a mean of 0.03 mg/L (U.S. EPA 2000). Rainfall, rock weathering, and saltwater intrusion are sources of iodide in surface and groundwaters, where concentrations typically occur in the low $\mu\text{g/L}$ range (Fuge & Johnson 1986).

If bromide is present during chlorination it can be oxidized by free chlorine (HOCl, $pK_a=7.5$) to form hypobromous acid (HOBr, $pK_a=8.8$), an important halogenating agent, which results in the formation of bromine-substituted DBPs upon reaction with NOM. Aqueous bromine reacts faster with NOM than aqueous chlorine and when both are present, bromine tends to act more as a substituting agent while chlorine reacts preferentially as an oxidant (Rook et al. 1978; Westerhoff et al. 2004). When bromide is present during chloramination, a similar reaction occurs to form active bromine species, including HOBr, NHBrCl, and NHBr₂ (Trofe et al. 1980; Bousher et al. 1989), which can react with NOM to form bromine-containing DBPs.

More recently, iodine-substituted DBPs have been measured after disinfection of waters containing iodide. Their formation is favored during chloramination rather than chlorination because hypoiodous acid (HOI, $pK_a=10.6$), the reactive iodine species, is quickly oxidized to inert iodate when free chlorine is present. However, in the presence of monochloramine the reaction to iodate is much slower, giving HOI a chance to react with NOM (Bichsel & von Gunten 2000). Halogen speciation is of importance because iodine-containing DBPs have been shown to be more geno- and cytotoxic relative to their bromine-substituted counterparts, which are more toxic than the corresponding chlorine-containing byproducts (Richardson et al. 2008). A bromine incorporation factor (BIF) can be calculated among a class of halogenated DBPs, allowing for a simplified comparison of halogen substitution across samples (Gould et al. 1983; Obolensky & Singer 2005).

$$BIF = \frac{\sum(\text{molar conc.} \times \# Br)}{\sum(\text{molar conc.}) \times (\# \text{ halogens})}$$

An example calculation for the BIF for THM4:

Species	Conc. (µM)
CHCl ₃	2.12
BrCl ₂ CH	2.43
Br ₂ ClCH	1.57
CHBr ₃	0.31
THM4	6.43

$$BIF = \frac{(2.12 \times 0) + (2.43 \times 1) + (1.57 \times 2) + (0.31 \times 3)}{(2.12 + 2.43 + 1.57 + 0.31) \times 3} = 0.34$$

1.4 Ultraviolet (UV) Irradiation

Utilities have been examining alternative treatment schemes in order to comply with increasingly stringent DBP regulations and to continue delivering quality drinking water to consumers. UV irradiation is one such process that is being used in drinking water treatment plants as a primary disinfectant prior to secondary disinfection by chlorination or chloramination. Advantages associated with UV treatment are: it is highly effective at inactivating waterborne pathogens which are resistant to chlorine/chloramines, such as *Cryptosporidium* (Clancy et al. 2000), and there are no taste and odor problems associated with UV. UV irradiation is a physical process and disinfection only occurs while water is in the pathway of UV light, so in North America it must be used in combination with a chemical disinfectant to provide a residual for distribution of drinking water.

For water treatment applications, the two commonly used lamp types are low and medium pressure UV (LP and MP UV). LP UV emits nearly monochromatic light at 254 nm while MP UV emits light over a wide range and throughout the germicidal wavelengths of 200 to 300 nm (Bolton & Linden 2003). In practice, UV dose is commonly determined using a mathematical model and validated using biological assay results (Linden & Darby 1997). A typical UV disinfection dose for drinking water

treatment is 40 mJ/cm^2 and the dose required by the U.S. EPA Long Term 2 Enhanced Surface Water Treatment Rule to achieve 4-log inactivation of adenovirus is 186 mJ/cm^2 (U.S. EPA 2006b). Accurately modeling and determining a polychromatic (MP UV) dose is more difficult than monochromatic (LP UV) dose because the germicidal effectiveness varies across the MP output wavelengths. In bench-scale experiments, biosimetry, chemical actinometry, or mathematical modeling can be used to determine the effective germicidal fluence (dose) (Jin et al. 2006). Chemical actinometers considered suitable for UV fluence measurement are uridine and potassium iodide/potassium iodate (KI/KIO_3). The KI/KIO_3 actinometer is best for estimating total incident fluence, while the uridine actinometer is better for estimating germicidal fluence, because its absorbance spectrum is similar to that of microbial DNA (Jin et al. 2006). Fluence is calculated by multiplying the fluence rate (or irradiance) by exposure time. A common approach is to measure the lamp irradiance with a radiometer, which can be validated through chemical actinometry, applying calculations derived by Morowitz (1950), and correcting for factors which include reflection, divergence, and light absorbance by water (Bolton & Linden 2003).

1.5 Potential for UV Treatment to Impact Disinfection Byproduct Formation

UV alone is not expected to generate halogen-containing DBPs, because a halogenating agent such as HOCl or NH_2Cl is required for their formation. There have been few comprehensive studies to evaluate the impact of UV treatment on DBP formation when combined with a secondary disinfectant to provide a residual, and the majority of research that has taken place focused on the regulated THMs and HAAs

(Malley et al. 1995; Liu et al. 2002) rather than emerging DBP classes which are thought to be more toxicologically potent (Plewa et al. 2004; Richardson et al. 2008). In one study that did look at emerging, unregulated DBPs, Reckhow et al. (2010) observed an increase in trichloronitromethane (chloropicrin) formation following MP UV irradiation (40-140 mJ/cm²) and post-chlorination compared to chlorination alone in source waters containing 1-10 mg/L nitrate as N. The authors hypothesized that MP UV irradiation of waters containing nitrate resulted in photonitration of NOM and chloropicrin formation upon post-chlorination, suggesting that UV could impact the formation of DBPs with subsequent chlorination/chloramination through reactions with inorganic species present in the water during treatment.

The photochemistry of nitrate has been studied extensively over many decades. Nitrate absorbs primarily below 240 nm with a strong $\pi \rightarrow \pi^*$ absorption band at 200 nm (molar absorptivity, $\epsilon = 9900 \text{ M}^{-1} \text{ cm}^{-1}$) but also possesses a weak $n \rightarrow \pi^*$ band at 310 nm ($\epsilon = 7.4 \text{ M}^{-1} \text{ cm}^{-1}$). This weaker absorption band is relevant for solar radiation but for engineered treatment processes, the MP UV output overlaps with the strong nitrate absorption band. A series of photochemically induced reactions, shown in Table 1-2, have been identified and make up a complicated web of reaction pathways resulting from nitrate photolysis. N_2O_4 and $\cdot\text{NO}_2$ can act as nitrating agents (add an $-\text{NO}_2$ group to a compound) and N_2O_3 is a nitrosating agent, in which an $-\text{NO}$ group is added to a chemical (Challis and Kyrtpoulos 1979; Goldstein and Czapski 1996; Vione et al. 2001). These nitrated/nitrosated products may serve as precursors to N-DBP formation with subsequent chlorination/chloramination, as is thought to be the case for the observed

increase in chloropicrin formation from MP UV treatment followed by chlorination (Reckhow et al. 2010; Shah et al. 2011).

Table 1-2. Reactions involving reactive nitrogen species formed during photolysis of nitrate/nitrite.

Reaction	Quantum Yield (Φ)* or Rate	Source
$\text{NO}_3^- + h\nu + \text{H}^+ \rightarrow \cdot\text{NO}_2 + \cdot\text{OH}$	$\Phi_{228\text{ nm}} = 0.1$	Sharpless & Linden 2001
$\text{NO}_3^- + h\nu \rightarrow \text{NO}_2^- + \frac{1}{2}\text{O}_2$	$\Phi_{305\text{ nm}} = 0.01$	Warneck & Wurzinger 1988
$\text{NO}_2^- + h\nu + \text{H}^+ \rightarrow \cdot\text{NO} + \cdot\text{OH}$	$\Phi_{360\text{ nm}} = 0.025$	Fischer & Warneck 1996
$\cdot\text{NO}_2 + \cdot\text{OH} \rightarrow \text{ONO}_2\text{H}$	$k=4.5 \times 10^9 \text{ M}^{-1}\text{s}^{-1}$	Loegager & Sehested 1993
$\text{NO}_2^- + \cdot\text{OH} \rightarrow \cdot\text{NO}_2 + \text{OH}^-$	$k=6.0 \times 10^9 \text{ M}^{-1}\text{s}^{-1}$	Loegager & Sehested 1993
$2 \cdot\text{NO}_2 \rightarrow \text{N}_2\text{O}_4$	$k=4.5 \times 10^8 \text{ M}^{-1}\text{s}^{-1}$	Graetzel et al. 1969
$\cdot\text{NO} + \cdot\text{NO}_2 \rightarrow \text{N}_2\text{O}_3$	$k=1.1 \times 10^9 \text{ M}^{-1}\text{s}^{-1}$	Graetzel et al. 1970

*Quantum yield is defined as: $\Phi_\lambda = \frac{\text{number of molecules transformed}}{\text{number of photons (of wavelength } \lambda) \text{ absorbed}}$

Another pathway by which UV treatment could impact DBP formation is through alteration of NOM structure and reactivity towards chlorine/chloramine. Using electrospray ionization mass spectrometry to investigate the effects of typical UV drinking water disinfection doses on organic matter extracted from Ohio River water, Magnuson et al. (2002) found that with increasing LP and MP UV dose (20-140 mJ/cm²), there was a shift towards smaller NOM molecules. Malley et al. (1995) observed an increase in the ratio of hydrophilic to hydrophobic organic matter in filtered surface water after MP UV irradiation (130 mJ/cm²). Bromide and iodide (after being oxidized by chlorine to HOBr and HOI, respectively) have been shown to be more reactive with hydrophilic and low molecular weight organic precursors than their hydrophobic and high molecular weight precursor counterparts, as measured by the formation and speciation of bromine- and iodine-containing THMs and bromine-containing HAAs (Liang & Singer 2003; Hua & Reckhow 2007a). Therefore, if bromide or iodide are present, bromine- and iodine-incorporation into DBPs could be increased by subsequent

chlorination or chloramination if UV irradiation increases the amount of hydrophilic NOM moieties in water, which is of importance because of the greater toxicity of iodine- and bromine-substituted DBPs compared to their chlorine-containing counterparts. Indeed, this has been demonstrated for solar irradiation of surface water NOM (Chow et al. 2008). The authors observed a significant decrease in UV absorbance and increase in hydrophilic fraction, accompanied by increased bromine incorporation in THMs and HAAs for samples that were subjected to several days of sunlight photolysis and then chlorinated.

Similar to the photo-induced reactions involving reactive nitrogen species, halogen ions (chloride, bromide, and iodide) can be activated indirectly by hydroxyl radicals ($\cdot\text{OH}$) produced during UV irradiation, forming reactive halogen species shown in Table 1-3 (Nowell & Hoigne 1992; Grebel et al. 2009). $\cdot\text{OH}$ can be formed by UV photolysis of NOM, nitrate, and dissolved or colloidal Fe(III) (Mopper & Zhou 1990; Vione et al. 2003). The extent to which reactive halogen species may be involved in DBP formation is not well understood; however, general predictions can be made based on measured rate constants. For example, the reaction between $\cdot\text{OH}$ and Br^- or I^- is about twice as fast as that of $\cdot\text{OH}$ with NO_2^- (Table 1-2) and similar to that of $\cdot\text{OH}$ with an organic precursor (Table 1-4), suggesting that the activation of halogen ions to reactive halogen species are important pathways in $\cdot\text{OH}$ reactions, especially in waters that are lacking other $\cdot\text{OH}$ scavengers (e.g. a low DOC, low alkalinity water). Table 1-4 shows reactions and rate constants between radical species and organic compounds which contain some of the reactive NOM components. $\cdot\text{OH}$ itself may participate in DBP formation. Ozonation and UV/ H_2O_2 are processes which employ $\cdot\text{OH}$ radicals as the

primary oxidant during treatment, and byproducts associated with these oxidation processes include those with oxygenated functional groups: halonitromethanes, haloketones, aldehydes, carboxylic acids, and bromate (Goldstone et al. 2002; Krasner et al. 2006).

Table 1-3. Reactions involving reactive halogen species produced by indirect photolysis.

Reaction	Rate constant	Reference
$\text{Cl}^- + \cdot\text{OH} \rightarrow \text{ClOH}\cdot^-$	$4.3 \times 10^9 \text{ M}^{-1} \text{ s}^{-1}$	Jayson et al. 1973
$\text{Br}^- + \cdot\text{OH} \rightarrow \text{BrOH}\cdot^-$	$1.1 \times 10^{10} \text{ M}^{-1} \text{ s}^{-1}$	Matthew & Anastasio 2006
$\text{I}^- + \cdot\text{OH} \rightarrow \text{IOH}\cdot^-$	$1.2 \times 10^{10} \text{ M}^{-1} \text{ s}^{-1}$	Elliot & Simsons 1984
$\text{ClOH}\cdot^- \rightarrow \text{Cl}^- + \cdot\text{OH}$	$6.1 \times 10^9 \text{ s}^{-1}$	Jayson et al. 1973
$\text{BrOH}\cdot^- \rightarrow \text{Br}^- + \cdot\text{OH}$	$3.3 \times 10^7 \text{ s}^{-1}$	Zehavi & Rabani 1972
$\text{BrOH}\cdot^- \rightarrow \text{Br}\cdot + \text{OH}^-$	$4.2 \times 10^6 \text{ s}^{-1}$	Zehavi & Rabani 1972
$\text{ClOH}\cdot^- + \text{Cl}^- \rightarrow \text{Cl}_2\cdot^- + \text{OH}^-$	$1.0 \times 10^4 \text{ M}^{-1} \text{ s}^{-1}$	Grigor'ev et al. 1987
$\text{BrOH}\cdot^- + \text{Br}^- \rightarrow \text{Br}_2\cdot^- + \text{OH}^-$	$1.9 \times 10^8 \text{ M}^{-1} \text{ s}^{-1}$	Zehavi & Rabani 1972
$\text{Cl}^- + \text{Cl}\cdot \rightarrow \text{Cl}_2\cdot^-$	$8 \times 10^9 \text{ M}^{-1} \text{ s}^{-1}$	Nagarajan & Fessenden 1985
$\text{Br}^- + \text{Br}\cdot \rightarrow \text{Br}_2\cdot^-$	$9 \times 10^9 \text{ M}^{-1} \text{ s}^{-1}$	Nagarajan & Fessenden 1985
$\text{I}^- + \text{I}\cdot \rightarrow \text{I}_2\cdot^-$	$1.1 \times 10^{10} \text{ M}^{-1} \text{ s}^{-1}$	Nagarajan & Fessenden 1985

Table 1-4. Reactions involving radical species and model NOM components.

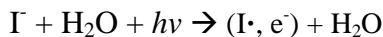
Reaction	Rate constant	Reference
$\cdot\text{OH} + 1,3\text{-C}_6\text{H}_4(\text{OH})_2$	$1.2 \times 10^{10} \text{ M}^{-1} \text{ s}^{-1}$	Savel'eva et al. 1972
$\text{Br}_2\cdot^- + 1,3\text{-C}_6\text{H}_4(\text{OH})_2$	$1.7 \times 10^8 \text{ M}^{-1} \text{ s}^{-1}$	Land 1993
$\text{I}_2\cdot^- + 1,3\text{-C}_6\text{H}_4(\text{OH})_2$	$1.3 \times 10^8 \text{ M}^{-1} \text{ s}^{-1}$	Alfassi et al. 1995
$\text{Br}_2\cdot^- + \text{C}_6\text{H}_5\text{OH}$	$6.1 \times 10^6 \text{ M}^{-1} \text{ s}^{-1}$	Alfassi et al. 1990
$\text{I}_2\cdot^- + \text{C}_6\text{H}_5\text{O}^-$	$2.2 \times 10^7 \text{ M}^{-1} \text{ s}^{-1}$	Alfassi et al. 1990
$\text{Br}_2\cdot^- + \text{C}_6\text{H}_5\text{O}^-$	$5.1 \times 10^7 \text{ M}^{-1} \text{ s}^{-1}$	Alfassi et al. 1990
$\text{NO}_2\cdot + \text{C}_6\text{H}_5\text{O}^-$	$1.5 \times 10^7 \text{ M}^{-1} \text{ s}^{-1}$	Alfassi et al. 1990

Direct photo-excitation of halogen ions can also form reactive halogen species.

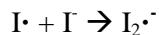
Figure 1-3 shows the absorption spectra of bromide and iodide in laboratory grade water (LGW) from 200-300 nm (germicidal wavelengths) compared with the LP and MP UV lamp spectral output. Bromide absorbs largely below 220 nm, but iodide has significant

absorbance up to 260 nm, overlapping with the LP and MP UV emission spectra.

Photolysis of iodide in aqueous solution forms an iodine atom and a solvated electron through a charge transfer reaction (Jortner et al. 1961):



From here, the iodine and hydrated electron can re-form iodide, which is the predominant reaction in the absence of electron scavengers. However, if electron scavengers are present (e.g. nitrate, iodate) to react with the hydrated electron, iodine is available to react with iodide, forming additional reactive halogen species (Fox 1970; Rahn 1997), shown by the following reactions:



Little is known about the extent to which iodine radicals may become involved in DBP formation, but the production of these reactive species presents a potential pathway for iodine incorporation into DBPs.

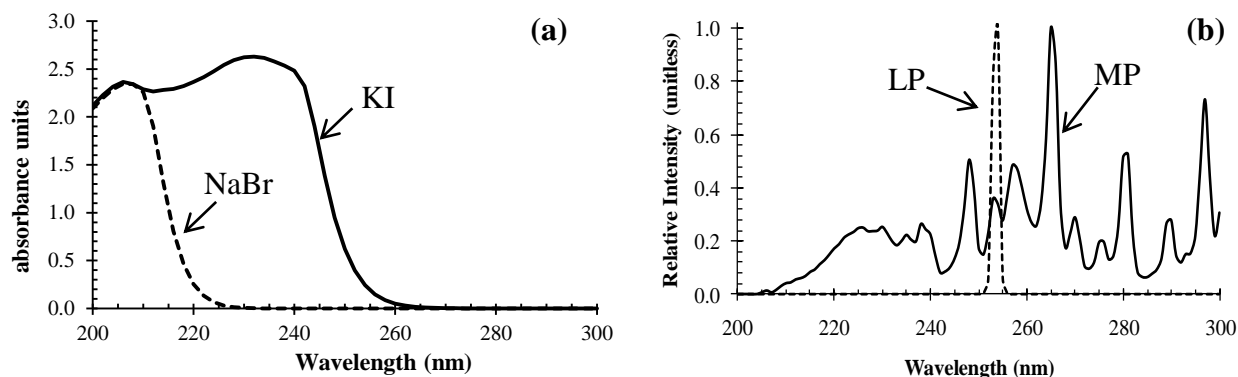


Figure 1-3. (a) Absorption spectra of NaBr and KI in LGW and (b) LP UV and MP UV spectral output¹.

¹Absorption spectra of NaBr (1 mM) and KI (0.6 mM) were measured at the University of North Carolina at Chapel Hill (unpublished data). LP and MP UV lamp spectra were measured at the University of Colorado at Boulder (Linden et al. 2012).

Lastly, while past research has shown little impact on the formation of regulated THMs and HAAs resulting from UV at disinfection doses, a recent survey of utilities showed that many were operating at a higher UV dose than originally designed for (Linden et al. 2012). Two of the utilities that were designed to deliver 40 mJ/cm² were actually dosing closer to 200 mJ/cm² as a result of improved upstream treatment processes. UV dose is a function of contact time as well as water absorbance, so if the water quality changes (for example, water absorbance decreases) but the contact time and lamp intensity remain the same, the dose being delivered could be much higher than expected.

1.6 Toxicology Studies

Since the discovery of DBPs in drinking water, much research has been focused on understanding their potential human health effects. Single compound *in vitro* assays have helped to identify the relative toxicity within and across DBP classes. For example, toxicological assays have shown that N-DBPs are more geno- and cytotoxic than the regulated THMs and HAAs and that bromine- and iodine-substituted DBPs are more toxic than their corresponding chlorine-containing analogues (Plewa et al. 2004; Richardson et al. 2008). Combining single compound geno- and cytotoxicity data with DBP occurrence information can provide insight into which DBPs or DBP classes are of most concern (Richardson et al. 2007a). However, much less research has been directed at identifying the potential health effects of DBP mixtures and “real” water samples which are more representative of what consumers are actually exposed to on a regular

basis. Toxicological studies comparing waters treated with alternative disinfection techniques are lacking, especially those involving UV disinfection.

A study that looked at mutagenicity in *Salmonella* for organic extracts of treated waters showed that those treated with ozone and post-chlorination were less mutagenic than those treated with chlorine at a dose adjusted to leave a similar target residual (Claxton et al. 2008; Miltner et al. 2008). Backlund (1995) observed an increase in *Salmonella* mutagenicity for a concentrated extract of a surface water treated with 10-60 mJ/cm² LP UV prior to chlorination, compared to the same water treated with only chlorine at the same dose. Most biological assays require sample concentration to induce a measurable response. A common technique is the use of XAD resin concentration followed by elution with an organic solvent such as ethyl acetate (Loper et al. 1978; Simmons et al. 2002). While this process allows for the application of a toxicological assay to complex mixtures, the concentration method itself may result in the loss of volatile DBPs and resin retention of unidentified byproducts, and thereby, part of the toxicological fraction. For this reason, an approach in which the sample is pre-concentrated using RO before disinfection has been developed (Pressman et al. 2010).

1.7 Research Gaps

It is important to understand the implications of a process that is being used as an integral part of drinking water treatment. The literature is lacking in comprehensive studies that evaluate the impact of combined UV-chlorine/chloramine treatment on DBP formation, especially for the unregulated, emerging DBPs. One of the few studies that looked at the formation of N-DBPs focused on MP and LP UV followed by chlorination,

but not chloramination (Reckhow et al. 2010). The use of chloramination for drinking water treatment is expected to grow as increasingly strict regulations come into effect (Richardson 2007b). Chloramination favors the formation of some DBPs (e.g., iodine-containing THMs and HAAs, cyanogen halides, nitrosamines) which are thought to be more toxicologically potent than the regulated THMs and HAAs (Bichsel & von Gunten 2000; Krasner et al. 1989; Choi & Valentine 2002; Richardson et al. 2008).

To date, there have not been any published studies looking at the formation of iodine-containing DBPs during combined UV-chlorine/chloramine treatment. Little is known about the role of reactive halogen species in DBP formation but the overlap of iodide absorption with MP UV output provides a pathway by which iodine could become incorporated into DBPs. This is especially relevant as population growth continues along coastal regions where salt-water intrusion could raise bromide and iodide levels in surface and groundwaters that are drinking water sources. Although the extent of salt-water intrusion at a particular location depends on various hydrogeological factors, anthropogenic activity such as increased demand on aquifers can further increase salt-water intrusion (NOAA 2011). It is estimated that by 2015, coastal populations in the United States will increase by more than 12 million (Crossett et al. 2005).

Though previous studies have investigated changes in organic precursor size distribution and polarity resulting from UV irradiation, most of this work used methods involving pH adjustment, concentration, and harsh solvents or were not able to discern differences at disinfection doses relevant to full-scale drinking water treatment. Approaches that have recently been applied to organic matter characterization allow for analysis of samples using very little preparation and can provide valuable information on

NOM source, structure and reactivity (Helms et al. 2008; Stedmon et al. 2003).

Fluorescence spectroscopy and associated modeling techniques are just starting to be used for characterizing organic precursor changes during drinking water chlorination and other engineered treatment processes (Beggs et al. 2009; Baghoth et al. 2011; Murphy et al. 2011). A recent review focused on a limitation of this approach, the lack of component behavior comparison between studies (Ishii and Boyer 2012). Inconsistent data processing by researchers is another factor that could limit the application of fluorescence and PARAFAC to predicting DOM behavior and reactivity across different source waters (Cory et al. 2010, Murphy et al. 2011). However, if these limitations can be recognized and addressed, fluorescence spectroscopy and PARAFAC modeling offer a promising tool to help in understanding linkages between DOM source and DBP formation.

While over 500 individual DBPs have been identified in laboratory and field studies using a variety of treatments and disinfectants, there remains a large percentage of unidentified byproducts as indicated by analysis of total organic halogen (TOX) (Hua & Reckhow 2007b). A measure of TOX can be compared to the chlorine equivalents of individually measured halogen-containing DBPs, to determine a percentage of “unknown” halogenated organics. Little is known about what is contained within this “unknown” fraction and how it contributes to the total toxicity of a treated water, especially for alternative treatment processes. Drinking water toxicity studies using individual compound data to predict human health impacts do not capture synergistic or antagonistic effects of mixtures, and are potentially missing an important fraction of unknown byproducts. Studies evaluating real disinfected waters have used concentration

techniques that result in the loss of volatile DBPs. One technique is to spike back these DBPs, but by this approach, unknown volatile losses remain unaccounted for. Another question that remains is the ability of many toxicological assays employing *Salmonella* or rodents to be extrapolated to estimated human responses. Clearly, *in vivo* tests administered to human subjects with concentrated DBP mixtures cannot be performed, but *in vitro* studies using human cells, which should be more applicable to human health endpoints, have not yet been widely used. This proposed research will attempt to answer some of the questions related to these research gaps.

1.8 Research Hypotheses

1. The formation of reactive chemical species from UV photolysis of waters containing nitrate, bromide, and/or iodide will influence nitrogen- and halogen-containing DBP formation with subsequent chlorination or chloramination and, thereby, the toxicity of the treated water.

2. UV irradiation changes the molecular weight distribution of NOM, which will impact its reactivity towards disinfectants (chlorine, chloramine) and the speciation of DBPs.

1.9 Research Objectives

Objective 1: Determine the effect of UV photolysis on the involvement of inorganic water constituents (specifically nitrate, bromide, and iodide) in the formation of, or incorporation into, DBPs when followed by chlorination or chloramination.

Objective 2: Investigate the impact of UV irradiation on DOM structure using EEM fluorescence spectroscopy, relating observed changes to subsequent DBP formation and speciation.

Objective 3: Use a toxicological assay as a complimentary tool to DBP analysis and precursor characterization studies to compare relative toxicity of various drinking water treatments involving UV irradiation.

1.10 Dissertation Organization

This dissertation is comprised of six chapters, four of which are written as stand-alone papers for publication. Objective 1 is primarily addressed in Chapter 2, although inorganic spiking results are also presented in Chapters 3, 4, and 5. Chapter 2 has already been published in the journal *Water Research* (Volume 46, Issue 15, 1 October 2012, 4653-4664), as a paper titled “The Effect of Inorganic Precursors on Disinfection Byproduct Formation During UV-Chlorine/Chloramine Drinking Water Treatment,” with co-authors Aaron D. Dotson, Karl G. Linden, and Howard S. Weinberg.

Objective 2 is presented in Chapter 4 and is currently being prepared for publication under the title “Changes in Dissolved Organic Matter Fluorescence and Disinfection Byproduct Formation from UV and Subsequent Chlorination/Chloramination,” with co-authors Rose M. Cory and Howard S. Weinberg.

Objective 3 is addressed in Chapter 5, and a publication is currently being prepared with the tentative title of “Cytotoxicity of Disinfection Byproduct Mixtures Produced from UV-Chlorine/Chloramine Treatment,” with co-authors Rebecca Y. Milsik, Anthony B. DeAngelo, Jane Ellen Simmons, and Howard S. Weinberg.

While not derived from a specific chapter, a methods paper detailing the halogenated volatiles/haloacetamides DBP suite extraction is also in preparation.

Sources Cited for Chapter 1

- Alfassi, Z.B. et al., 1990. Temperature dependence of the rate constants for reaction of inorganic radicals with organic reductants. *Journal of Physical Chemistry*, 94(25), pp.8800-8805.
- Alfassi, Z.B. et al., 1995. Rate constants for reactions of iodine atoms in solution. *International Journal Chemical Kinetics*, 27, pp.181-188.
- Backlund, P., 1995. Introduction and removal of disinfection byproducts and mutagenic activity by chemical and photolytic treatments. *Revue des sciences de l'eau*, 8(3), pp.387-401.
- Baghoth, S.A. et al., 2011. Tracking natural organic matter (NOM) in a drinking water treatment plant using fluorescence excitation-emission matrices and PARAFAC. *Water Research*, 45(2), pp.797-809.
- Beggs, K.M.H. et al., 2009. Characterizing chlorine oxidation of dissolved organic matter and disinfection by-product formation with fluorescence spectroscopy and parallel factor analysis. *Journal of Geophysical Research*, 114, GO4001.
- Bellar, T.A. et al., 1974. The occurrence of organohalides in chlorinated drinking waters. *Journal American Water Works Association*, 66(12), pp.703-706.
- Bichsel, Y. & von Gunten, U., 2000. Formation of iodo-trihalomethanes during disinfection and oxidation of iodide-containing waters. *Environmental Science & Technology*, 34(13), pp.2784-2791.
- Bolton, J.R. & Linden, K.G., 2003. Standardization of methods for fluence (UV dose) determination in bench-scale UV experiments. *Journal of Environmental Engineering*, 129(3), pp.209-216.
- Bousher, A. et al., 1989. Kinetics of reactions in solutions containing monochloramine and bromide. *Water Research*, 23(8), pp.1049-1058.
- Boyce, S.D. & Hornig, J.F., 1983. Reaction pathways of trihalomethane formation from the halogenation of dihydroxyaromatic model compounds for humic acid. *Environmental Science & Technology*, 17(4), pp.202-211.
- Calderon, R.L., 2000. The epidemiology of chemical contaminants of drinking water. *Food and Chemical Toxicology*, 38(S1), pp.S13-20.
- Cantor, K.P. et al., 1998. Drinking water source and chlorination byproducts I. Risk of bladder cancer. *Epidemiology*, 9(1), pp.21-28.

- Challis, B.C. and Kyrtopoulos, S.A., 1979. Chemistry of nitroso-compounds. 11. nitrosation of amines by the 2-phase interaction of amines in solution with gaseous oxides of nitrogen. *Journal of the Chemical Society – Perkin Transactions 1, 2*, pp.299-304.
- Choi, J. & Valentine, R.L., 2002. Formation of N-nitrosodimethylamine (NDMA) from reaction of monochloramine: a new disinfection by-product. *Water Research*, 36(4), pp.817-824.
- Chow, A.T. et al., 2008. Impact of simulated solar irradiation on disinfection byproduct precursors. *Environmental Science & Technology*, 42(15), pp.5586-5593.
- Christman, R.F. et al., 1983. Identity and yields of major halogenated products of aquatic fulvic acid chlorination. *Environmental Science & Technology*, 17(10), pp.625-628.
- Clancy, J.L. et al., 2000. Using UV to inactivate Cryptosporidium. *Journal American Water Works Association*, 92(9), pp.97-104.
- Claxton, L.D. et al., 2008. Integrated disinfection by-products research: salmonella mutagenicity of water concentrates disinfected by chlorination and ozonation/postchlorination. *Journal of Toxicology and Environmental Health, Part A*, 71(17), pp.1187-1194.
- Coble, P.G., 1996. Characterization of marine and terrestrial DOM in seawater using excitation-emission matrix spectroscopy. *Water Research*, 51(4), pp.325-346.
- Cory, R.M. & McKnight, D.M., 2005. Fluorescence spectroscopy reveals ubiquitous presence of oxidized and reduced quinones in dissolved organic matter. *Environmental Science & Technology*, 39(21), pp.8142-8149.
- Cory, R.M. et al., 2010. Effect of instrument-specific response on the analysis of fulvic acid fluorescence spectra. *Environmental Science & Technology*, 8, pp.67-78.
- Crossett, K.M. et al., 2005. *Population Trends Along the Coastal United States: 1980-2008*. U.S. Department of Commerce, National Oceanic and Atmospheric Administration: Silver Spring, Maryland.
- Croué, J.-P. et al., 2000. *Characterization of Natural Organic Matter in Drinking Water*. American Water Works Association and Water Research Foundation: Denver, Colorado.
- Edzwald, J.K. et al., 1985. Surrogate parameters for monitoring organic matter and THM precursors. *Journal American Water Works Association*, 77(4), pp.122-132.
- Elliot, A.J. & Simons, A.S., 1984. Rate constants for reactions of hydroxyl radicals as a function of temperature. *Radiation Physics and Chemistry*, 24, pp.229-231.

- Fischer, M. & Warneck, Peter, 1996. Photodecomposition of nitrite and undissociated nitrous acid in aqueous solution. *Journal of Physical Chemistry*, 100(48), pp.18749-18756.
- Flury, M. & Papritz, A., 1993. Bromide in the natural environment: occurrence and toxicity. *Journal of Environmental Quality*, 22, pp.747-758.
- Fox, M.F., 1970. The photolysis of simple inorganic anions in solution. *Quarterly Reviews of the Chemical Society*, 24, pp.565-584.
- Fuge, R. & Johnson, C.C., 1986. The geochemistry of iodine - a review. *Environmental Geochemistry and Health*, 8(2), pp.31-54.
- Goldstein, S. and Czapski, G., 1996. Mechanism of the nitrosation of thiols and amines by oxygenated $\cdot\text{NO}$ solutions: the nature of the nitrosating intermediates. *Journal of the American Chemical Society*, 118(14), pp.3419-3425.
- Goldstone, J.V. et al., 2002. Reactions of hydroxyl radical with humic substances: bleaching, mineralization, and production of bioavailable carbon substrates. *Environmental Science & Technology*, 36(3), pp.364-372.
- Gould, J.P. et al., 1983. Formation of Brominated Trihalomethanes: Extent and Kinetics. In: R. L. Jolley et al., eds. *Water Chlorination: Environmental Impact and Health Effects*. Ann Arbor, Michigan: Ann Arbor Science Publishers, pp. 297-310.
- Graetzel, M. et al., 1969. Pulsradiolytische untersuchung einiger elementarprozesse der oxydation und reduktion des nitritions. *Berichte der Bunsen-Gesellschaft fur Physikalische Chemie*, 73, pp.646-653.
- Graetzel, M. et al., 1970. Pulsradiolytische untersuchung der NO-oxydation und des gleichgewichts $\text{N}_2\text{O}_3 \leftrightarrow \text{NO} + \text{NO}_2$ in waessriger loesung. *Berichte der Bunsen-Gesellschaft fur Physikalische Chemie*, 74, pp.488-492.
- Grebel, J.E. et al., 2009. Impact of halides on the photobleaching of dissolved organic matter. *Marine Chemistry*, 115(1-2), pp.134-144.
- Grigor'ev, A.E. et al., 1987. Formation of Cl_2^- in the bulk solution during the radiolysis of concentrated aqueous solutions of chlorides. *High Energy Chemistry*, 21, pp.99-102.
- Helms, J.R. et al., 2008. Absorption spectral slopes and slope ratios as indicators of molecular weight, source, and photobleaching of chromophoric dissolved organic matter. *Limnology and Oceanography*, 53(3), pp.955-969.

- Hua, G. & Reckhow, D.A., 2007a. Characterization of disinfection byproduct precursors based on hydrophobicity and molecular size. *Environmental Science & Technology*, 41(9), pp.3309-3315.
- Hua, G. & Reckhow, D.A., 2007b. Comparison of disinfection byproduct formation from chlorine and alternative disinfectants. *Water Research*, 41(8), pp.1667-1678.
- Ishii, S.K.L. & Boyer, T.H., 2012. Behavior of reoccurring PARAFAC components in fluorescent dissolved organic matter in natural and engineered systems: a critical review. *Environmental Science & Technology*, 46(4), pp.2006-2017.
- Jayson, G.G. et al., 1973. Some simple, highly reactive, inorganic chlorine derivatives in aqueous solution. *Journal of the Chemical Society, Faraday Transactions 1*, 69, pp.1597-1607.
- Jin, S. et al., 2006. Polychromatic UV fluence measurement using actinometry, biodosimetry, and mathematical techniques. *Journal of Environmental Engineering*, 132(8), pp.831-842.
- Jortner, J. et al., 1961. The photochemistry of the iodide ion in aqueous solution. *Journal of Physical Chemistry*, 65(7), pp.1232-1238.
- Kitis, M. et al., 2001a. The reactivity of natural organic matter to disinfection by-products formation and its relation to specific ultraviolet absorbance. *Water Science and Technology*, 43(2), pp.9-16.
- Kitis, M. et al., 2001b. Isolation of dissolved organic matter (DOM) from surface waters using reverse osmosis and its impact on the reactivity of DOM to formation and speciation of disinfection by-products. *Water Research*, 35(9), pp.2225-2234.
- Kitis, M. et al., 2002. Probing reactivity of dissolved organic matter for disinfection by-product formation using XAD-8 resin adsorption and ultrafiltration fractionation. *Water Research*, 36(15), pp.3834-3848.
- Krasner, S.W. et al., 1989. The occurrence of disinfection by-products in US drinking water. *Journal American Water Works Association*, 81(8), pp.41-53.
- Krasner, S.W. et al., 1996. Three approaches for characterizing NOM. *Journal American Water Works Association*, 88(6), pp.66-79.
- Krasner, S.W. et al., 2006. Occurrence of a new generation of disinfection byproducts. *Environmental Science & Technology*, 40(23), pp.7175-7185.
- Land, E.J., 1993. Preparation of unstable quinones in aqueous solution via pulse radiolytic one-electron oxidation of dihydroxybenzenes. *Journal of the Chemical Society, Faraday Transactions 1*, 89(5), pp.803-810.

- Lee, W. et al., 2007. Dissolved organic nitrogen as a precursor for chloroform, dichloroacetonitrile, N-nitrosamine, and trichloronitromethane. *Environmental Science & Technology*, 41(15), pp.5485-5490.
- Leenheer, J.A., 1981. Comprehensive approach to preparative isolation and fractionation of dissolved organic carbon from natural waters and wastewaters. *Environmental Science & Technology*, 15(5), pp.578-587.
- Liang, L. & Singer, P.C., 2003. Factors influencing the formation and relative distribution of haloacetic acids and trihalomethanes in drinking water. *Environmental Science & Technology*, 37(13), pp.2920-2928.
- Linden, K.G. & Darby, J.L., 1997. Estimating effective germicidal dose from medium pressure UV lamps. *Journal of Environmental Engineering*, 123(11), pp.1142-1149.
- Linden, K.G. et al., 2012. *Impact of UV Location and Sequence on Byproduct Formation*. American Water Works Association and Water Research Foundation: Denver, Colorado.
- Liu, W. et al., 2002. Comparison of disinfection byproduct (DBP) formation from different UV technologies at bench scale. *Water Science & Technology: Water Supply*, 2(5-6), pp.515-521.
- Loeager, T. & Sehested, K., 1993. Formation and decay of peroxyxynitrous acid: a pulse radiolysis study. *The Journal of Physical Chemistry*, 97(25), pp.6664-6669.
- Loper, J.C. et al., 1978. Residue organic mixtures from drinking water show in vitro mutagenic and transforming activity. *Journal of Toxicology and Environmental Health, Part A*, 4(5-6), pp.919-38.
- Magnuson, M.L. et al., 2002. Effect of UV irradiation on organic matter extracted from treated Ohio River water studied through the use of electrospray mass spectrometry. *Environmental Science & Technology*, 36(23), pp.5252-5260.
- Malcolm, R.L., 1991. Factors to be Considered in the Isolation and Characterization of Aquatic Humic Substances. In: B. Allard, H. Boren, & A. Grimvall, eds. *Humic Substances in the Aquatic and Terrestrial Environment*. USA: Springer.
- Malley, J.P. et al., 1995. *Evaluation of the Byproducts Produced from the Treatment of Groundwaters with Ultraviolet Irradiation*. American Water Works Association and Water Research Foundation: Denver, Colorado.
- Matthew, B.M. & Anastasio, C., 2006. A chemical probe technique for the determination of reactive halogen species in aqueous solution: part 1 – bromide solutions. *Atmospheric Chemistry and Physics*, 6, pp.2423-2437.

- McKnight, D.M. et al., 2001. Spectrofluorometric characterization of dissolved organic matter for indication of precursor organic material and aromaticity. *Limnology and Oceanography*, 46(1), pp.38-48.
- Miltner, R.J. et al., 2008. Integrated disinfection by-products mixtures research: disinfection of drinking waters by chlorination and ozonation/postchlorination treatment scenarios. *Journal of Toxicology and Environmental Health, Part A*, 71(17), pp.1133-1148.
- Mopper, K. & Zhou, X., 1990. Hydroxyl radical photoproduction in the sea and its potential impact on marine processes. *Science*, 250(4981), pp.661-664.
- Morowitz, H.J., 1950. Absorption effects of volume irradiation of microorganisms. *Science*, 111(2879), pp.229-230.
- Murphy, K.R. et al., 2011. Organic matter fluorescence in municipal water recycling schemes: toward a unified PARAFAC model. *Environmental Science & Technology*, 45(7), pp.2909-2916.
- Nagarajan, V. & Fessenden, R.W., 1985. Flash photolysis of transient radicals. 1. X_2^- with X = Cl, Br, I, and SCN. *Journal of Physical Chemistry*, 89, pp.2330-2335.
- National Cancer Institute, 1976. *Report on the Carcinogenesis Bioassay of Chloroform (CAS No. 67-66-3)*. National Cancer Institute: Bethesda, Maryland.
- NOAA (National Oceanic and Atmospheric Association), 2011. *State of the Coast Report*. U.S. Department of Commerce, National Oceanic and Atmospheric Association: Silver Spring, Maryland. <<http://stateofthecoast.noaa.gov>>
- Norwood, D.L. et al., 1980. Reactions of chlorine with selected aromatic models of aquatic humic material. *Environmental Science & Technology*, 14(2), pp.187-190.
- Nowell, L.H. & Hoigne, J., 1992. Photolysis of aqueous chlorine at sunlight and ultraviolet wavelengths 2. Hydroxyl radical production. *Water Research*, 26(5), pp.559-605.
- Obolensky, A. & Singer, P.C., 2005. Halogen substitution patterns among disinfection byproducts in the information collection rule database. *Environmental Science & Technology*, 39(8), pp.2719-2730.
- Plewa, M.J. et al., 2004. Halonitromethane drinking water disinfection byproducts: chemical characterization and mammalian cell cytotoxicity and genotoxicity. *Environmental Science & Technology*, 38(1), pp.62-68.

- Pressman, J.G. et al., 2010. Concentration, chlorination, and chemical analysis of drinking water for disinfection byproduct mixtures health effects research: U.S. EPA's Four Lab Study. *Environmental Science & Technology*, 44(19), pp.7184-7192.
- Rahn, R.O., 1997. Potassium iodide as a chemical actinometer for 254 nm radiation: use of iodate as an electron scavenger. *Photochemistry and Photobiology*, 66(4), pp.450-455.
- Reckhow, D.A. et al., 1990. Chlorination of humic materials: byproduct formation and chemical interpretations. *Environmental Science & Technology*, 24(11), pp.1655-1664.
- Reckhow, D.A. et al., 2010. Effect of UV treatment on DBP formation. *Journal American Water Works Association*, 102(6), pp.100-113.
- Richardson, S.D. et al., 2007a. Occurrence, genotoxicity, and carcinogenicity of regulated and emerging disinfection by-products in drinking water: a review and roadmap for research. *Mutation Research*, 636, pp.178-242.
- Richardson, S.D., 2007b. Water analysis: emerging contaminants and current issues. *Analytical Chemistry*, 79(12), pp.4295-4324.
- Richardson, S.D. et al., 2008. Occurrence and mammalian cell toxicity of iodinated disinfection byproducts in drinking water. *Environmental Science & Technology*, 42(22), pp.8330-8338.
- Rook, J.J., 1974. Formation of haloforms during chlorination of natural waters. *Water Treatment and Examination*, 23(2), pp.234-243.
- Rook, J.J., 1977. Chlorination reactions of fulvic acids in natural waters. *Environmental Science & Technology*, 11(5), pp.478-482.
- Rook, J.J. et al., 1978. Bromide oxidation and organic substitution in water treatment. *Journal of Environmental Science and Health, Part A*, A13(2), pp.91-116.
- Savel'eva, O.S. et al., 1972. Reactions of substituted phenols with hydroxyl radicals and their dissociated form O⁻. *Journal of Organic Chemistry of the USSR*, 8, pp.283-286.
- Shah, A.D. et al., 2011. Impact of UV disinfection combined with chlorination/chloramination on the formation of halonitromethanes and haloacetonitriles in drinking water. *Environmental Science & Technology*, 45(8), pp.3657-3664.

- Sharpless, C.M. & Linden, K.G., 2001. UV photolysis of nitrate: effects of natural organic matter and dissolved inorganic carbon and implications for UV water disinfection. *Environmental Science & Technology*, 35(14), pp.2949-2955.
- Simmons, J.E. et al., 2002. Development of research strategy for integrated technology-based toxicological and chemical evaluation of complex mixtures of drinking water disinfection byproducts. *Environmental Health Perspectives*, 110(S6), pp.1013-1024.
- Song, H. et al., 2009. Isolation and fractionation of natural organic matter: evaluation of reverse osmosis performance and impact of fractionation parameters. *Environmental Monitoring and Assessment*, 153(1-4), pp.307-321.
- Stedmon, C.A. et al., 2003. Tracing dissolved organic matter in aquatic environments using a new approach to fluorescence spectroscopy. *Marine Chemistry*, 82(3-4), pp.239-254.
- Thurman, E.M., 1985. *Organic Geochemistry of Natural Waters*. Dordrecht, the Netherlands: M. Nijhoff Publishers.
- Town, R. & Powell, H., 1993. Limitations of XAD resins for the isolation of the non-colloidal humic fraction in soil extracts and aquatic samples. *Analytica Chimica Acta*, 271(2), pp.195-202.
- Trofe, T.W. et al., 1980. Kinetics of monochloramine decomposition in the presence of bromide. *Environmental Science & Technology*, 14(5), pp.544-549.
- U.S. EPA (Environmental Protection Agency), 1979. *National Interim Primary Drinking Water Regulations: Control of Trihalomethanes in Drinking Water: Final Rules*. Federal Register 44, pp.68624-68705.
- U.S. EPA (Environmental Protection Agency), 1998. *National Primary Drinking Water Regulations: Disinfectants and Disinfection Byproducts: Final Rule*. Federal Register 63(241), pp.69390-69476.
- U.S. EPA (Environmental Protection Agency), 2000. ICR Auxiliary 1 Database Version 5.0, Query Tool Version 2.0 [EPA 815-C-00-002, CD-ROM].
- U.S. EPA (Environmental Protection Agency), 2006a. *National Primary Drinking Water Regulations: Stage 2 Disinfectants and Disinfection Byproducts Rule*. Federal Register 71(2), pp.387-493.
- U.S. EPA (Environmental Protection Agency), 2006b. *National Primary Drinking Water Regulations: Long Term 2 Enhanced Surface Water Treatment Rule, Final Rule*. Federal Register 71(3), pp.653-702.

- U.S. EPA (Environmental Protection Agency), 2007. *Unregulated Contaminant Monitoring Regulation (UCMR) for Public Water Systems Revisions: Final Rule*. Federal Register 72(2), pp.367-398.
- Vione, D. et al., 2001. Formation of nitrophenols upon UV irradiation of phenol and nitrate in aqueous solutions and in TiO₂ aqueous suspensions. *Chemosphere*, 44(2), pp.237-248.
- Vione, D. et al., 2003. New processes in the environmental chemistry of nitrite. 2. The role of hydrogen peroxide. *Environmental Science & Technology*, 37(20), pp.4635-4641.
- Warneck, P & Wurzinger, C., 1988. Product quantum yields for the 305-nm photodecomposition of NO₃⁻ in aqueous solution. *Journal of Physical Chemistry*, 92(22), pp.6278-6283.
- Wegman, R.C.C. et al., 1981. Methyl bromide and bromide-ion in drainage water after leaching of glasshouse soils. *Water, Air, and Soil Pollution*, 16(1), pp.3-11.
- Westerhoff, P. et al., 2004. Reactivity of natural organic matter with aqueous chlorine and bromine. *Water Research*, 38(6), pp.1502-1513.
- Yang, X. et al., 2010. Nitrogenous disinfection byproducts formation and nitrogen origin exploration during chloramination of nitrogenous organic compounds. *Water Research*, 44(9), pp.2691-2702.
- Zehavi, D. & Rabani, J., 1972. The oxidation of aqueous bromide ions by hydroxyl radicals: a pulse radiolytic investigation. *Journal of Physical Chemistry*, 76(3), pp.312-319.

Chapter 2: The Effect of Inorganic Precursors on Disinfection Byproduct Formation during UV-Chlorine/Chloramine Drinking Water Treatment

2.1 Introduction

Utilities have been examining alternative treatment schemes in order to comply with increasingly stringent regulations related to the delivery of quality drinking water to consumers. Ultraviolet (UV) irradiation is one such process that is highly effective at inactivating waterborne pathogens which are resistant to chlorine/chloramines, such as *Cryptosporidium* (Clancy et al. 2000), and has no taste and odor problems. In North America, when UV is applied to surface waters, it must be used in combination with a secondary chemical disinfectant to provide a residual for distribution of drinking water. Two UV lamp types are commonly used for irradiation: low pressure (LP), which emits nearly monochromatic light at 254 nm, and medium pressure (MP), which emits polychromatic light over a range of wavelengths, including those associated with germicidal effects between 200 and 300 nm. A recent survey of United States utilities which employ UV showed that the majority of those responding use MP UV (62%) compared to LP UV (38%). In addition, chlorine is more commonly applied to maintain a residual disinfectant for distribution (68%) compared to chloramines (32%) (Dotson et al. 2012).

One goal of drinking water treatment processes is to minimize the formation of disinfection byproducts (DBPs) produced when a disinfectant reacts with ubiquitous

dissolved organic matter (DOM), salts in water that may be of natural origin such as bromide and iodide, and anthropogenic pollutants. Epidemiological studies have suggested a link between consumption of drinking waters containing elevated levels of DBPs and adverse human health outcomes, particularly bladder cancer and reproductive effects (Cantor et al. 1998). Trihalomethanes (THMs), a major class of DBPs, have been found to cause adverse health effects in laboratory animals, and concentrated disinfected drinking water extracts exhibited toxicological responses in bioassays (National Cancer Institute 1976; Loper et al. 1978). Krasner and colleagues (2006) conducted an occurrence study at drinking water treatment plants across the United States and found that the use of some alternative disinfectants (chloramines, chlorine dioxide, ozone) decreased the formation of THMs and haloacetic acids (HAAs), another class of DBPs for which a subset are currently regulated, but in many cases, these processes increased the formation of other DBPs, which are thought to be more geno- and cytotoxic than the regulated THMs and HAAs (Plewa et al. 2008).

UV alone, at disinfection doses, does not form halogen-containing DBPs, because a halogenating agent such as chlorine or chloramine is required for their formation. However, there have been few comprehensive studies to evaluate the impact of UV treatment on DBP formation when combined with a secondary disinfectant. The majority of research that has taken place focused on the regulated THMs and HAAs (Malley et al. 1995; Liu et al. 2002; Dotson et al. 2010) rather than emerging DBP classes which are thought to be more toxicologically potent but are not currently regulated in the United States. In one study that did look at emerging, unregulated DBPs, Reckhow et al. (2010) observed an increase in chloropicrin (trichloronitromethane) formation following MP UV

irradiation (40-140 mJ/cm²) and post-chlorination compared to chlorination alone in source waters containing nitrate (1-10 mg N/L). Nitrate in drinking water is regulated by the United States Environmental Protection Agency (U.S. EPA) at a maximum contaminant level of 10 mg N/L (U.S. EPA, 1992). The authors hypothesized that MP UV irradiation of waters containing nitrate resulted in photonitration of DOM and chloropicrin formation upon post-chlorination, suggesting that UV could impact the formation of DBPs with subsequent chlorination through reactions with inorganic species present in the water during treatment.

Another pathway by which UV treatment could impact DBP formation is through alteration of DOM structure and reactivity towards chlorine/chloramines. At extremely high doses (greater than 20,000 mJ/cm²), LP UV photolysis has been shown to break down DOM into smaller, more hydrophilic molecules with lower molar absorptivity than the parent material (Buchanan et al. 2005). The UV doses used were several orders of magnitude higher than those typically employed in drinking water disinfection, but other studies have reported DOM changes for more relevant doses. Using electrospray ionization mass spectrometry to investigate the effects of typical UV drinking water disinfection doses on organic matter extracted from the Ohio River, Magnuson et al. (2002) found that with increasing LP and MP UV dose (20-140 mJ/cm²), there was a shift towards smaller DOM molecules. Malley and colleagues (1995) observed an increase in the ratio of hydrophilic to hydrophobic organic matter in filtered surface water after MP UV irradiation (130 mJ/cm²). Bromide and iodide (after being oxidized by chlorine to HOBr and HOI, respectively) have been shown to be more reactive with hydrophilic and low molecular weight organic precursors than their hydrophobic and high molecular

weight precursor counterparts, as measured by the formation and speciation of bromine- and iodine-containing THMs and bromine-containing HAAs (Liang & Singer 2003; Hua & Reckhow 2007). Therefore, if bromide or iodide are present, their incorporation into DBPs could be increased by subsequent chlorination or chloramination if UV irradiation increased the amount of hydrophilic DOM moieties in water. This has significant implications because of the greater toxicity of iodine- and bromine-substituted DBPs compared to their chlorine-containing counterparts (Plewa et al. 2008). Indeed, this has been demonstrated for solar irradiation of surface water DOM, where a significant decrease in UV absorbance and increase in hydrophilic fraction were observed, accompanied by increased bromine incorporation in THMs and HAAs for samples that were subjected to several days of sunlight photolysis and then chlorinated (Chow et al. 2008).

While past research has shown little impact on the formation of regulated THMs and HAAs resulting from UV at disinfection doses, a recent survey of utilities showed that many were operating at a higher UV dose than originally designed for (Dotson et al. 2012). For example, two utilities that were designed to deliver 40 mJ/cm^2 were actually dosing closer to 200 mJ/cm^2 as a result of improved upstream treatment processes. UV dose is a function of contact time as well as water absorbance, so if the water quality changes (for example, water absorbance decreases) but the contact time and lamp intensity remain the same, the dose being delivered could be much higher than expected.

In order to balance microbial inactivation and chemical byproduct risk during the production of drinking water, it is important to understand the potential impacts of UV disinfection process sequences. This study investigated the formation of a range of

halogen- and nitrogen-containing DBPs from UV-chlorine/chloramine treatment of three pre-treated (coagulation/flocculation, sedimentation, and filtration) drinking waters. The specific waters were chosen because of their different organic and inorganic DBP precursor content. A subset of samples were spiked with additional bromide, nitrate, and iodide to investigate the role of inorganic precursors. LP and MP UV doses ranging from typical disinfection doses (40 and 186 mJ/cm²) to higher doses (1000 mJ/cm²) were used to study trends in DBP formation. The results of DBP analysis were compared to the same samples without UV treatment and with a disinfectant dose adjusted for a similar target chlorine/chloramine residual.

2.2 Materials and Methods

Water Collection—Utilities A and B

Samples were collected from Utilities A and B, located in the United States (U.S.), after coagulation/flocculation, sedimentation, and filtration but prior to disinfectant addition. Utility A is supplied by a surface water from a watershed with no known agricultural, industrial, or wastewater inputs at the time of sampling. This water had a higher specific UV absorbance at 254 nm (SUVA₂₅₄) than those from other sources but a lower ambient bromide content. Utility B treats water from a major river, which is known to be impacted by agricultural, industrial, and wastewater discharge. Ambient (unspiked) water quality parameters are shown in Table 2-1. A subset of samples were spiked with 0.5 mg/L bromide and 8 mg N/L nitrate, administered in the sodium salt form.

Table 2-1. Water quality data for ambient (unspiked) filter effluent (Utilities A and B) and ambient reconstituted settled water RO concentrate (Utility C).

parameter (units)	Utility A	Utility B	Utility C
dissolved organic carbon (mg C/L)	1.6	1.4	2.8
total dissolved nitrogen (mg N/L)	0.2	1.1	0.2
nitrate (mg N/L)	<0.02	0.8	<0.02
bromide ($\mu\text{g/L}$)	8	60	28
SUVA ₂₅₄ (L/mg C·m)	2.4	2.0	1.5

Water Collection–Utility C

Water from Utility C, also in the U.S. and supplied by a surface water, was collected after coagulation/flocculation and sedimentation. Settled water was concentrated using a custom-built portable reverse osmosis (RO) system so that a large amount of DOM could be collected and stored to provide the same matrix for a series of experiments. RO concentration has previously been demonstrated as a method through which high organic carbon recoveries (80-99%) and preservation of original source water reactivity can be obtained (Kitis et al. 2001; Song et al. 2009). The RO system included a spiral wound membrane (cellulosic acetate), four filter cartridge filters (10, 5, 1, and 0.45 μm) (Graver Technologies, Glasgow, DE, USA) and a cation exchange resin cartridge (H^+). The system was operated in two stages. First, source water was pumped through the filters and ion exchange resin and collected in a high density polypropylene 80-gallon reservoir (RO feed reservoir). Second, a high pressure pump fed the collected water through the RO membrane. The retentate (RO concentrate) was recycled in the RO feed reservoir and the filtrate (permeate) discarded. The RO membrane was operated until a desired concentration factor of approximately 15 (by volume) was achieved (180 L

settled water concentrated to 12 L). On a dissolved organic carbon (DOC) basis, the concentration factor was 14.2, which represents 95% DOC recovery through the RO concentration process. The standard operating procedure for RO concentration is provided in Appendix 1 and characteristics of the RO feed and concentrate are shown in Appendix 2. The RO concentrate was filtered (0.45 μm) in the laboratory and stored in amber glass bottles at 4°C until use. Prior to an experiment, the RO concentrate was diluted in laboratory grade water (LGW) to obtain a DOC concentration of approximately 3 mg C/L, chosen to represent the higher end of the average settled water DOC for this source. Characteristics of this ambient reconstituted RO concentrate are shown in Table 2-1. LGW was prepared in-house from a Dracor system (Durham, NC, USA), which pre-filters inlet 7 M Ω deionized water to 1 μm , removes residual disinfectants, reduces total organic carbon (TOC) to less than 0.2 mg C/L with an activated carbon cartridge, and removes ions to 18 M Ω with mixed bed ion-exchange resins. Sample pH was approximately 6.5 after dilution. A subset of samples were spiked with 0.1 mg/L iodide, 1 mg/L bromide, 10 mg N/L nitrate, or both bromide and nitrate, administered in the sodium salt (bromide and nitrate) or potassium salt (iodide) form. An additional experiment was carried out to evaluate the impact of lower nitrate spiking levels (1 and 5 mg N/L) on chloropicrin formation following MP UV and chlorine treatment.

UV Treatment

UV treatment was performed using quasi-collimated LP and MP lamps. The LP UV system consisted of four 15 W LP lamps (General Electric, Fairfield, CT, USA) mounted above a 4-inch circular aperture. Two different MP UV systems were used for

this work, the first for Utility A and B samples and the second for Utility C experiments. The first was a commercially-built system with a 1 kW MP lamp (Calgon Carbon, Pittsburgh, PA, USA) mounted above a 3-inch circular aperture, and the second was a custom-built unit containing a 550 W MP lamp (Ace-Hanovia, Vineland, NJ, USA) with a 4-inch aperture. Samples were placed in a 250- or 500-mL capacity Pyrex crystallization dish and stirred during irradiation. Constant sample temperature was maintained at 20-25°C by placing the dish inside a copper coil which was connected to a programmable refrigerated recirculating water unit. A manual (LP UV and second MP UV system) or pneumatic shutter (first MP UV system) was used to rapidly begin or end the irradiation. UV doses ranged from 40 to 1000 mJ/cm² and were determined using calculation techniques described by Bolton and Linden (2003) and Jin et al. (2006). Briefly, UV irradiance was measured at the water surface using an SED240 detector with a W diffuser connected to an IL1400A radiometer (International Light, Peabody, MA, USA). The irradiance between 200 and 300 nm was multiplied by a Petri factor (0.80 for the LP UV system, 0.83 for the first MP UV system, and 0.92 for the second MP UV system), water factor, radiometer sensor factor, reflection factor, and germicidal factor (MP UV only) to obtain an average irradiance (LP UV) or germicidal irradiance (MP UV) in mW/cm². The irradiation time (s) was then determined by dividing the desired UV dose (mJ/cm² or mW·s/cm²) by the average or germicidal irradiance.

Uridine actinometry was used to calculate MP UV irradiance in the second MP UV system following the procedure described by Jin et al. (2006). Chemical actinometry uses a compound (uridine, in this case) that has a known response (quantum yield) to UV exposure and an easily measured absorbance spectra to calculate lamp incident irradiance

(mW/cm²). From this value, the germicidal irradiance and time required to deliver a desired dose can be calculated. For this work, a molar extinction coefficient ($\epsilon_{262\text{nm}}$) of 10185 M⁻¹ cm⁻¹ and quantum yield (Φ) of 0.020 mol/einstein (assumed to be constant over germicidal range) were used (Jin et al. 2006). The operating procedure for the second MP UV system (University of North Carolina at Chapel Hill lamp setup) is provided in Appendix 3.

Chlorine and Chloramine Addition

After irradiation, samples were buffered to pH 7.5 with 5 mM phosphate buffer (to be consistent with typical pH for treatment at Utilities A and B) and immediately dosed with chlorine from a dilution of a concentrated sodium hypochlorite stock solution (Fisher laboratory grade, 5.6-6%) or pre-formed monochloramine. This dose was based on a target residual of 1.0±0.4 mg Cl₂/L (for all chlorinated samples and Utility C chloraminated samples) or 2.4±0.4 mg Cl₂/L (for Utility A and B chloraminated samples) after 24 hours, calculated from demand tests performed prior to treatment. Duplicate samples were treated with UV-chlorine/chloramine and held in headspace-free amber glass bottles with caps and PTFE-lined septa for 24 hours at 20°C. Demand tests were carried out by applying a range of chlorine or monochloramine doses to 25 mL aliquots of each sample. After these demand test samples were held headspace-free for 24 hours at 20°C, the chlorine or monochloramine residuals were measured and plotted against disinfectant dose, and the appropriate dose to achieve the target residual was selected. Free chlorine residuals were measured in duplicate using the *N,N*-diethyl-*p*-phenylenediamine (DPD) colorimetric method following Standard Method 4500-Cl G

(APHA 1999). A pre-formed monochloramine solution was prepared by adding free chlorine drop-wise to an ammonium chloride solution (adjusted to pH 8.5 with NaOH) at a 1:1.2 Cl:N molar ratio (standard operating procedure is provided in Appendix 4). Monochloramine is referred to as chloramine throughout this paper for the purpose of discussion, but the pre-formed chloramine solution was prepared such that monochloramine was the primary species formed (dichloramine negligible) and ammonium chloride was present in excess so that no free chlorine remained. Chloramine speciation and concentration in the pre-formed solution were verified by UV spectrometry and solving simultaneous Beer's Law equations as described by Schreiber and Mitch (2005). Chloramine residuals in samples were analyzed in duplicate using an adaptation of the indophenol method (Hach Method 10171) with MonochlorF reagent (Hach Company, Loveland, CO, USA).

DBP Analysis

After the 24-hour holding time, chlorine/chloramine residuals were measured and samples were transferred to glass vials containing quenching agent (ammonium sulfate in 40 mL vials for HAAs and ascorbic acid in 60 mL vials for all other DBPs) and sealed with caps and PTFE-lined septa. Quenching agent amounts were calculated from the stoichiometric ratios of ammonium sulfate or ascorbic acid to chlorine, assuming a residual of 1 mg/L Cl_2 , with a safety factor of two. Confirmation of this approach was established by selecting several samples, adding an equivalent ratio of quenching agent to an extra aliquot of that sample, and measuring residual chlorine/chloramine. In all selected samples, no residual was detected. Quenched samples were then stored

headspace-free at 4°C until DBP analysis, which was carried out as three separate extractions: (1) THMs (including all 10 chlorine-, bromine-, and iodine-containing species), 4 haloacetonitriles (trichloro-, dichloro-, bromochloro-, and dibromo-acetonitrile), two haloketones (1,1-dichloro- and 1,1,1-trichloro-propanone), two halonitromethanes (trichloro- and tribromo-nitromethane), chloral hydrate, and 8 haloacetamides (bromo-, dichloro-, bromochloro-, trichloro-, dibromo-, bromodichloro-, dibromochloro-, and tribromo-acetamide) were co-extracted within 24 hours of quenching; (2) cyanogen chloride was extracted within 48 hours of quenching, and (3) 9 HAAs (chlorine- and bromine-containing species) were analyzed within 72 hours of quenching. DBPs were liquid-liquid extracted with methyl tert-butyl ether (MtBE) and analyzed on a Hewlett-Packard 5890 gas chromatograph with ⁶³Ni electron capture detector (GC-ECD) following the procedures described by Scilimenti et al. (1994) (cyanogen chloride), Brophy et al. (2000) (HAAs), and Weinberg et al. (2002) (remaining DBPs). Standard operating procedures for these extractions are provided in Appendices 5A-5C. The 4 regulated THMs, HAAs, chloral hydrate, chloropicrin, haloacetonitriles, haloketones, and bromo-, dichloro- and trichloro-acetamide standards were obtained from Supelco and Sigma-Aldrich (Sigma Chemical Co., St. Louis, MO, USA). Bromopicrin (tribromonitromethane), iodine-containing THMs, and remaining haloacetamide standards were obtained from Orchid Cellmark (New Westminster, BC, Canada). Cyanogen chloride was obtained from SPEX Certiprep (Metuchen, NJ, USA). A Zebron (Phenomenex, Torrance, CA, USA) ZB-1 capillary column (30 m length, 0.25 mm inner diameter, 1.0-µm film thickness) was used for chromatographic separation of compounds, except for cyanogen chloride which was analyzed on a ZB-1701 capillary column (30 m

length, 0.25 mm inner diameter, 1.0- μm film thickness). The following temperature program was used for THMs, halonitromethanes, haloacetonitriles, chloral hydrate, and haloketones: oven held at 35°C for 22 min, increased at 10°C/min to 145°C and held for 2 min, increased at 20°C/min to 225°C and held for 10 min, then increased at 20°C/min to 260°C and held for 5 min. Injection volume was 2 μL (splitless) and after 0.5 minutes the sample was split at a 1:1 ratio. The injection temperature was set at 117°C to minimize the breakdown of bromopicrin (Chen et al. 2002), and the detector temperature was 290°C. Haloacetamides were run using the following oven temperature program: held at 37°C for 1 min, increased at 5°C/min to 110°C and held for 10 min, then increased at 5°C/min to 280°C. Injection volume was 2 μL (splitless) and after 0.5 minutes the sample was split at a 1:1 ratio, injector temperature was 200°C and detector temperature was 300°C. Cyanogen chloride was extracted separately and run with the following oven temperature program: held at 35°C for 9 min and then increased at 10°C/min to 250°C and held for 10 min. Injection volume was 2 μL (splitless), injector temperature was 150°C and detector temperature was 300°C. HAA extracts were analyzed using the following oven temperature program: initial temperature was 37°C, held for 21 min, increased at 5°C/min to 136°C, held for 3 min, increased at 20°C/min to 250°C and held for 3 min. Injection volume was 1 μL (splitless) and after 0.5 minutes the sample was split at a 1:1 ratio, injector temperature was 180°C and detector temperature was 300°C. All samples were analyzed in duplicate and 1,2-dibromopropane was used as an internal standard. The minimum reporting limit (MRL) for all compounds except HAAs was 0.1 $\mu\text{g/L}$. The MRL for HAAs ranged from 0.4 to 4 $\mu\text{g/L}$ for individual species.

Water Characterization

DOC and total dissolved nitrogen were measured with a Shimadzu TOC-V_{CPH} Total Organic Carbon Analyzer with a TNM-1 Total Nitrogen Measuring Unit (Shimadzu Corp., Atlanta, GA, USA) following Standard Method 5310 (APHA 1999). DBP results were normalized to DOC content for comparison across different waters. UV absorbance was measured using a Varian-Cary 100 spectrophotometer (Agilent, Santa Clara, CA, USA) for Utility A and B samples and a Hewlett Packard 8452A Diode Array spectrophotometer (Agilent, Santa Clara, CA, USA) for Utility C samples. Inorganic anions (bromide and nitrate) were measured using a Dionex ion chromatograph (Sunnyvale, CA, USA) following Standard Method 4110 (APHA 1999).

2.3 Results and Discussion

Chlorine/Chloramine Demand

Chlorine and chloramine demands increased with increasing UV dose but at disinfection doses (40 and 186 mJ/cm²) these changes were minor (0.1-0.6 mg Cl₂/L for chlorine and 0.1-0.3 mg Cl₂/L for chloramine). Lamp type (LP vs. MP UV) did not make a difference in chlorine demand for ambient samples at disinfection doses, but for higher UV doses and samples spiked with bromide and nitrate, MP UV induced greater changes in demand than LP UV. When normalized by carbon content, Utility B had the highest chlorine and chloramine demand (Tables 2-2 and 2-3). Utility B water had the highest background bromide content (0.06 mg/L), but its SUVA₂₅₄ value was between that of the other samples (2.0 L/mg C·m for Utility B compared to 2.4 and 1.5 L/mg C·m for Utilities A and C, respectively). Additional spiking conditions were included for Utility

C samples to investigate the relative contribution of each inorganic precursor during MP UV treatment. Table 2-4 shows the 24-hour chlorine and chloramine demands for ambient samples and those spiked with bromide, nitrate, or bromide and nitrate.

Table 2-2. 24-hour chlorine demands (mg Cl₂/mg C) for ambient and spiked samples treated with LP and MP UV. Values shown represent the average for duplicate samples and are normalized by DOC for comparison across the three utilities. Relative percent difference (RPD) between duplicate measurements was ≤15%.

Lamp type	UV dose (mJ/cm ²)	Utility A		Utility B		Utility C	
		ambient	Br ⁻ + NO ₃ ⁻ spiked ^a	ambient	Br ⁻ + NO ₃ ⁻ spiked	ambient	Br ⁻ + NO ₃ ⁻ spiked
LP UV	0	0.8	1.0	1.0	1.4	- ^b	-
	40	0.8	1.1	1.3	1.4	-	-
	186	0.8	1.1	1.3	1.4	-	-
	1000	0.9	1.2	1.2	1.5	-	-
MP UV	0	0.8	1.0	1.0	1.4	0.6	0.8
	40	0.7	1.1	1.1	1.6	0.6	0.8
	186	0.9	1.2	1.3	1.8	0.6	1.0
	1000	1.0	1.6	1.5	1.8	0.8	1.5

^aSpiking amounts were 0.5 mg/L bromide and 8 mg N/L nitrate for Utilities A & B and 1 mg/L bromide and 10 mg N/L nitrate for Utility C.

^bUtility C samples were not treated with LP UV.

Table 2-3. 24-hour chloramine demands (mg Cl₂/mg C) for ambient and spiked samples treated with LP and MP UV. Values shown represent the average for duplicate samples (RPD between duplicates ≤8%) and are normalized by DOC for comparison across the three utilities.

Lamp type	UV dose (mJ/cm ²)	Utility A		Utility B		Utility C	
		ambient	Br ⁻ + NO ₃ ⁻ spiked ^a	ambient	Br ⁻ + NO ₃ ⁻ spiked	ambient	Br ⁻ + NO ₃ ⁻ spiked
LP UV	0	0.3	0.4	0.4	0.5	- ^b	-
	40	0.2	0.3	0.4	0.5	-	-
	186	0.4	0.4	0.4	0.5	-	-
	1000	0.4	0.6	0.5	0.5	-	-
MP UV	0	0.3	0.4	0.4	0.5	0.1	0.2
	40	0.3	0.4	0.4	0.5	0.1	0.2
	186	0.3	0.5	0.5	0.5	0.1	0.2
	1000	0.3	0.8	0.6	0.9	0.2	0.4

^aSpiking amounts were 0.5 mg/L bromide and 8 mg N/L nitrate for Utilities A & B and 1 mg/L bromide and 10 mg N/L nitrate for Utility C.

^bUtility C samples were not treated with LP UV.

Table 2-4. 24-hour chlorine and chloramine demands for ambient and spiked Utility C samples treated with MP UV. Values shown represent the average for duplicate samples (RPD between duplicates <10%).

post-disinfectant	UV dose (mJ/cm ²)	Chlorine/chloramine demand (mg/L as Cl ₂)			
		ambient	Br ⁻ spiked ^a	NO ₃ ⁻ spiked ^b	Br ⁻ + NO ₃ ⁻ spiked
chlorine	0	1.6	2.1	1.6	2.2
	40	1.6	2.2	1.8	2.3
	186	1.8	2.3	2.2	2.8
	1000	2.1	2.6	3.8	4.2
chloramine	0	0.4	0.5	0.3	0.4
	40	0.3	0.4	0.4	0.4
	186	0.3	0.3	0.6	0.6
	1000	0.4	0.5	1.0	1.1

^aBromide was spiked at 1 mg/L.

^bNitrate was spiked at 10 mg N/L.

Regardless of UV dose, the presence of bromide increased the chlorine demand but did not affect the chloramine demand. Bromide can be oxidized by free chlorine to form hypobromous acid, which reacts faster with DOM than free chlorine, contributing to the overall chlorine demand (Rook et al. 1978; Westerhoff et al. 2004). When bromide is present during chloramination, a similar reaction occurs to form active bromine species, including NH_2Br , NHBr_2 , and NHBrCl (Trofe et al. 1980). Although the rate of bromide oxidation by chloramine is comparable or faster than that of free chlorine in deionized water, the formation of reactive bromine species from chloramine can vary in real waters because these reactions are sensitive to pH, chloramine speciation, and bromide concentration. The formation of active bromine species in a surface water containing bromide and treated with preformed monochloramine at pH 7.5 (i.e. the samples used for this work) is slow and not likely to be significant enough to change the chloramine demand (Diehl et al. 2000; Benotti et al. 2011). Reactions 1-4 below show the oxidation of bromide by free chlorine (HOCl/OCl^- , $\text{pK}_a = 7.5$) and chloramine (Kumar and Margerum 1987; Bousher et al. 1989). Reactions 5-10 show the activation of nitrate by UV and subsequent reactions with post-disinfectants (Graetzel et al. 1969; Warneck and Wurzinger 1988; Margerum et al. 1994; Goldstein and Rabani 2007).

Reaction	Quantum yield (Φ_λ) or second order rate constant
(1) $\text{HOCl} + \text{Br}^- \rightarrow \text{HOBr} + \text{Cl}^-$	$1.55 \times 10^3 \text{ M}^{-1} \text{ s}^{-1}$
(2) $\text{OCl}^- + \text{Br}^- \rightarrow \text{OBr}^- + \text{Cl}^-$	$9.0 \times 10^{-4} \text{ M}^{-1} \text{ s}^{-1}$
(3) $\text{NH}_2\text{Cl} + \text{H}^+ \rightleftharpoons \text{NH}_3\text{Cl}^+$	
(4) $\text{NH}_3\text{Cl}^+ + \text{Br}^- \rightarrow \text{NH}_2\text{Br} + \text{Cl}^-$	$6 \times 10^4 \text{ M}^{-1} \text{ s}^{-1}$
(5) $\text{NO}_3^- + h\nu + \text{H}^+ \rightarrow \cdot\text{NO}_2 + \cdot\text{OH}$	$\Phi_{205 \text{ nm}} = 0.13, \Phi_{254 \text{ nm}} = 0.037$
(6) $\text{NO}_3^- + h\nu + \text{H}^+ \rightarrow \text{ONOOH}$	$\Phi_{205 \text{ nm}} = 0.28, \Phi_{254 \text{ nm}} = 0.10$
(7) $\text{NO}_3^- + h\nu \rightarrow \text{NO}_2^- + \frac{1}{2} \text{O}_2$	$\Phi_{305 \text{ nm}} = 0.001$
(8) $2 \cdot\text{NO}_2 \rightarrow \text{N}_2\text{O}_4$	$4.5 \times 10^8 \text{ M}^{-1} \text{ s}^{-1}$
(9) $\text{HOCl} + \text{NO}_2^- + \text{H}_2\text{O} \rightarrow \text{H}_3\text{O}^+ + \text{Cl}^- + \text{NO}_3^-$	$4.4 \times 10^4 \text{ M}^{-1} \text{ s}^{-1}$
(10) $\text{NH}_2\text{Cl} + \text{NO}_2^- + \text{H}_2\text{O} \rightarrow \text{NH}_4^+ + \text{Cl}^- + \text{NO}_3^-$	$0.24 \text{ M}^{-1} \text{ s}^{-1}$

Nitrate, rather than bromide, contributed to the more significant increase in chlorine/chloramine demand observed after MP UV treatment of spiked samples. This may be partly attributed to the reaction of nitrite, which is produced from photolysis of nitrate, with free chlorine or chloramine (Reactions 9 and 10). For comparison, the reaction rate constant of HOCl/OCl⁻ with Suwannee River DOM is 2.4 M⁻¹ s⁻¹ after a rapid initial stage reaction with an estimated rate constant of 500-5000 M⁻¹ s⁻¹ (Westerhoff et al. 2004), and the reaction rate constant of monochloramine with a range of DOM isolates was reported by Duirk and colleagues (2005) to be 2.9 to 9.6 M⁻¹ s⁻¹. As would be expected from the nitrate absorbance spectra, shown with the MP and LP UV emission spectra in Figure 2-1, the quantum yield of reactive nitrogen species in Reactions 5 and 6 is greater at 205 nm compared to 254 nm (corresponding to the increasing absorbance with decreasing wavelength from 254 to 205 nm) and, thus, LP UV should result in lower formation of reactive nitrogen species from nitrate photolysis compared to MP UV.

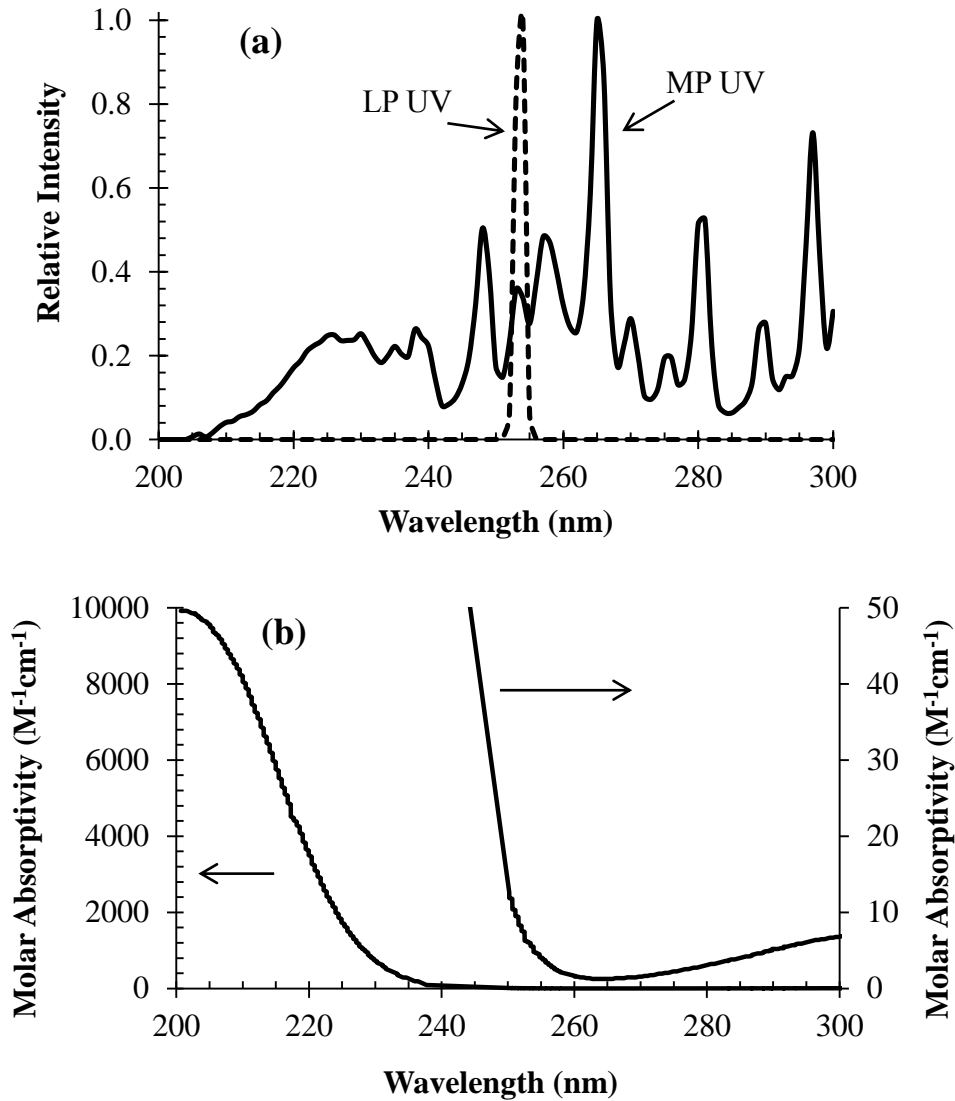


Figure 2-1. (a) Emission spectra of LP (dashed line) and MP (solid line) UV and (b) absorbance spectrum of nitrate.

Formation of THMs and HAAs

The formation of THM4 (sum of four regulated THMs) was not affected by pre-treatment with LP or MP UV at disinfection doses during subsequent chlorination or chloramination. THM4 formation increased 15-20% with MP UV doses of 1000 mJ/cm^2 followed by chlorination compared to chlorination alone in Utility A and B samples and

30-40% in Utility C samples, shown in Figure 2-2. RPD between experimental duplicates was <9%. Spiking with bromide caused a shift to the bromine-substituted species and increased the molar yield of THM4 following chlorination for Utilities A and B (38% and 16%, respectively), but not Utility C. Spiking with nitrate did not impact THM formation or speciation regardless of UV dose.

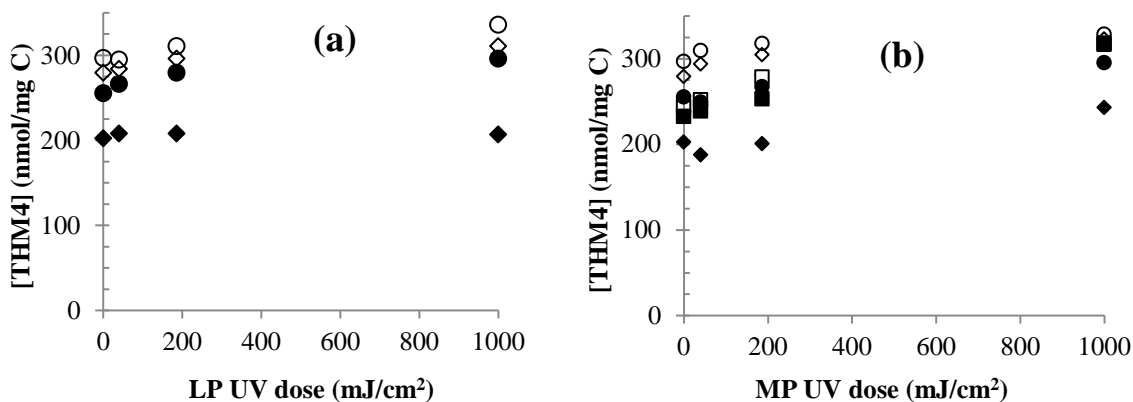


Figure 2-2. Impact of (a) LP and (b) MP UV followed by chlorination on the molar formation of THM4 in ambient (black shapes) and bromide- and nitrate-spiked (hollow shapes) samples. Utility A= diamonds, Utility B= circles and Utility C= squares. THM4 concentration is normalized to DOC. Spiking amounts were 0.5 mg/L bromide (6.3 μ M) and 8 mg N/L nitrate (0.57 mM) for Utilities A & B and 1 mg/L bromide (12.5 μ M) and 10 mg N/L nitrate (0.71 mM) for Utility C. Utility C samples were not treated with LP UV. Value shown represents the average between experimental duplicate samples (RPD <9%).

THM4 formation was significantly lower in chloraminated compared to chlorinated samples, as expected. With 1000 mJ/cm² MP UV followed by chloramination in bromide- and nitrate-spiked Utility B and C samples, THM4 formation doubled compared to chloramination alone, but even with this increase, the THM4 levels were below 23 nmol/mg C (7 μ g/L). The increased chlorine demand accompanied by elevated THM4 formation with 1000 mJ/cm² suggests that at high doses, UV irradiation affects THM precursors, making them more susceptible to reaction with chlorine.

HAAs were only measured for Utility A samples and UV had little effect on their formation, aside from two cases. Trichloroacetic acid formation decreased with increasing MP UV dose in ambient samples that were subsequently treated with chlorine (55 nmol/mg C (14.1 µg/L) from chlorine alone compared to 51, 48, and 43 nmol/mg C (13.0, 12.2, and 10.8 µg/L) for 40, 186, and 1000 mJ/cm² MP UV followed by chlorine, with the same 1 mg/L residual). Bromochloroacetic acid formation increased with increasing MP UV dose in bromide-spiked samples (15 nmol/mg C (3.9 µg/L) for chlorine alone compared to 18, 21, and 29 nmol/mg C (4.8, 5.6, and 7.9 µg/L) for 40, 186, and 1000 mJ/cm² MP UV followed by chlorine). The RPD between duplicate samples ranged from 5-15%. In all cases, the sum of 5 regulated HAAs (as well as the sum of all 9 measured HAAs) remained below the maximum contaminant level of 60 µg/L.

UV effects on haloacetamides, haloacetonitriles, and halo ketones were minimal. In ambient samples, 1,1,1-trichloropropanone formation was increased 40-170% with 1000 mJ/cm² MP UV followed by chlorination, but no significant changes were observed at lower UV doses. Spiking with iodide resulted in the formation of iodine-substituted THMs during chloramination (dichloroiodo-, bromochloroiodo-, chlorodiiodo- and triiodo-methane) but pre-treatment with MP UV did not further affect their formation (results are not shown here, but are presented in Appendix 2). Trihalonitromethanes, chloral hydrate, and cyanogen chloride formation were impacted by UV irradiation, the extent of which varied with lamp type, dose, and spiking conditions. These results are discussed in detail in the following sections.

Halonitromethanes

Chloropicrin and bromopicrin formation increased in UV treated samples containing nitrate (1-10 mg N/L) when followed by chlorination or chloramination, compared to the same samples without UV treatment. Utility C samples spiked with 1, 5, and 10 mg N/L nitrate generated the same amount of chloropicrin with 1000 mJ/cm² MP UV followed by chlorination (9.9-10.3 µg/L (20.8-21.6 nmol/mg C)), compared to 0.7 µg/L (1.5 nmol/mg C) for chlorine alone at a dose adjusted to provide the same target residual. For doses of 40 or 186 mJ/cm² MP UV followed by chlorination, chloropicrin formation was 24-32% lower in samples spiked with 1 mg N/L nitrate compared to 5 or 10 mg N/L nitrate where the chloropicrin concentrations were similar, but still showed a three- to twelve-fold increase in chloropicrin formation compared to chlorination alone. These collective results, shown in Figure 2-3, demonstrate that even with lower nitrate levels, MP UV enhances chloropicrin formed by subsequent chlorination.

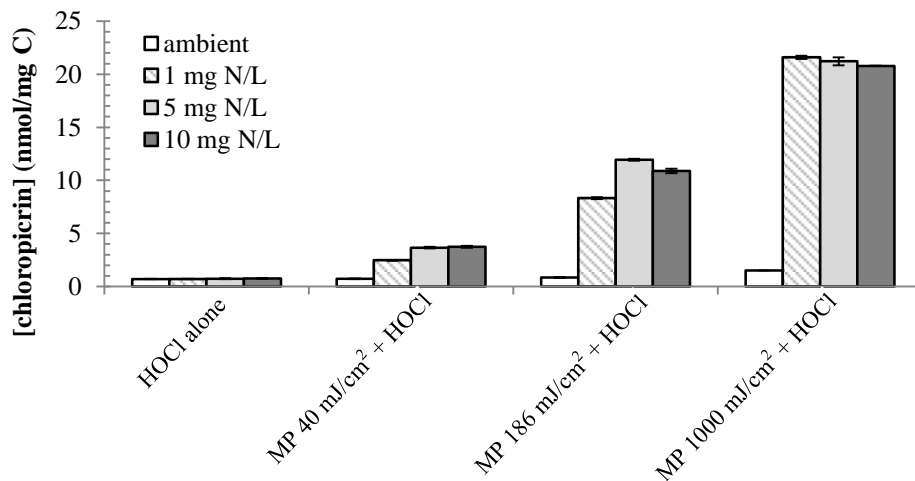


Figure 2-3. Effect of nitrate concentration on chloropicrin formation from MP UV-chlorine treatment of Utility C samples. Chloropicrin molar concentration is normalized to DOC. Bar height represents average value and the range between experimental duplicate values is shown by the inset lines. Ambient nitrate was <0.02 mg N/L (<0.001 mM).

Bromopicrin formation was favored over chloropicrin in samples spiked with bromide, and the molar yield of bromopicrin resulting from chlorination alone in bromide- and nitrate-spiked samples was greater than that of chloropicrin in nitrate-spiked samples (1.9 compared to 0.5 nmol/mg C), shown in Table 2-5. Similar trends were observed during chloramination, but the overall levels were 5- to 16-fold lower compared to chlorination. Both LP and MP UV increased bromopicrin formation when followed by chlorination in samples containing elevated bromide and nitrate (8-10 mg N/L), but to a greater extent with MP UV, shown in Figure 2-4. There are currently no regulations or guidelines for halonitromethanes in drinking water in the United States, but the median and maximum chloropicrin levels measured in surface waters during the Information Collection Rule (ICR) were 0.2 and 2.4 $\mu\text{g/L}$ (U.S. EPA 2005). The median and maximum concentrations measured in a nationwide occurrence study of 12 treatment plants across the United States were 0.2 and 2.0 $\mu\text{g/L}$ for chloropicrin and <0.5 and 5.0 $\mu\text{g/L}$ for bromopicrin (Krasner et al. 2006).

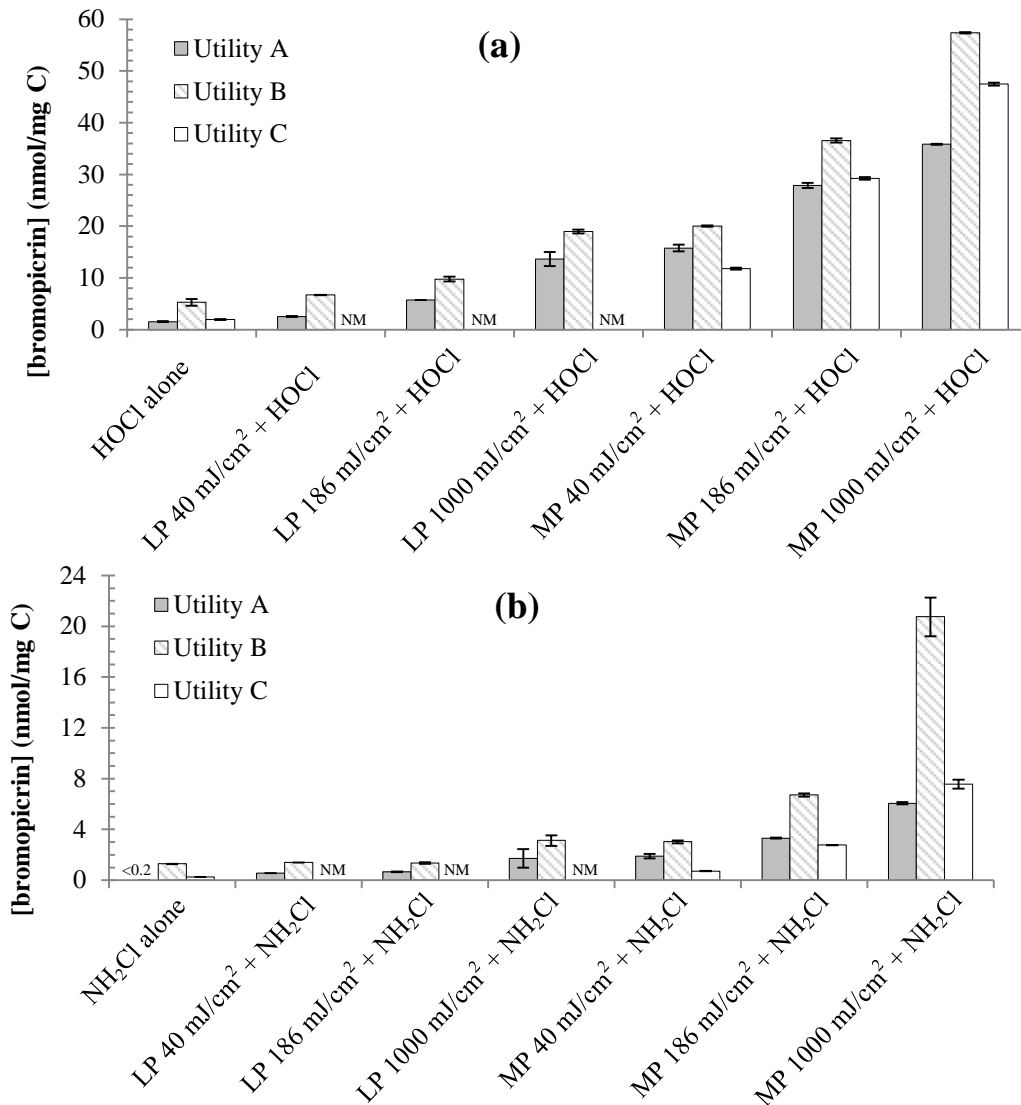


Figure 2-4. Effect of LP and MP UV followed by (a) chlorination and (b) chloramination on the formation of bromopicrin in bromide- and nitrate-spiked samples. Bromopicrin molar concentration is normalized to DOC. Bar height represents average value and the range between experimental duplicate values is shown by the inset lines. Spiking amounts were 0.5 mg/L bromide (6.3 μ M) and 8 mg N/L nitrate (0.57 mM) for Utilities A & B and 1 mg/L bromide (12.5 μ M) and 10 mg N/L nitrate (0.71 mM) for Utility C. NM = not measured since Utility C samples were not treated with LP UV.

Table 2-5. Effect of bromide- and nitrate-spiking on chloropicrin and bromopicrin formation from MP UV irradiation followed by chlorination and chloramination in Utility C samples. Chloropicrin and bromopicrin molar concentration are normalized to DOC. Value shown represents average between experimental duplicates (RPD \leq 10%).

post-disinfectant	UV dose (mJ/cm ²)	chloropicrin formation (nmol/mg C)			
		ambient	Br ⁻ spiked ^a	NO ₃ ⁻ spiked ^b	Br ⁻ + NO ₃ ⁻ spiked
chlorine	0	0.5	<0.2	0.5	<0.2
	40	0.5	<0.2	2.8	<0.2
	186	0.6	<0.2	8.8	<0.2
	1000	1.2	<0.2	17	<0.2
chloramine	0	<0.2	<0.2	<0.2	<0.2
	40	<0.2	<0.2	0.5	0.3
	186	<0.2	<0.2	1.1	0.6
	1000	<0.2	<0.2	1.8	0.3

post-disinfectant	UV dose (mJ/cm ²)	bromopicrin formation (nmol/mg C)			
		ambient	Br ⁻ spiked	NO ₃ ⁻ spiked	Br ⁻ + NO ₃ ⁻ spiked
chlorine	0	<0.1	1.9	<0.1	1.9
	40	<0.1	2.6	0.2	12
	186	<0.1	5.0	0.4	29
	1000	<0.1	12	0.7	48
chloramine	0	0.2	0.3	0.2	0.3
	40	0.2	0.2	0.2	0.7
	186	0.2	0.2	0.2	2.8
	1000	0.2	0.3	0.2	7.6

^aBromide was spiked at 1 mg/L (12.5 μ M).

^bNitrate was spiked at 10 mg N/L (0.71 mM).

Increased formation of chloropicrin with MP UV (40-140 mJ/cm²), but not LP UV, and subsequent chlorination in nitrate-containing waters (1-10 mg N/L) has been previously observed (Reckhow et al. 2010). The authors attributed this to the formation of reactive nitrogen species from MP UV photolysis of nitrate (e.g. Reactions 5-8) that can act as nitrating agents towards DOM. The resulting nitro organics can further react

with chlorine to form chloropicrin. Recent work has further probed these reactions, indicating that $\cdot\text{NO}_2$ is the primary species responsible for increased chloropicrin formation during UV treatment (Shah et al. 2011). However, this mechanism does not completely explain the observed increase in bromopicrin formation from LP UV, since the majority of nitrate absorption occurs below 240 nm and LP UV emits essentially monochromatic light at 254 nm, shown in Figure 2-1. Assuming that ortho-nitrophenol, a representative precursor that has been shown to produce chloropicrin upon chlorination (Merlet et al. 1985), produces comparable bromopicrin and chloropicrin yields (5.7%), only about 0.05% of the 0.6 mM (as N) nitrate would be required to account for the additional 19.5 nM bromopicrin that was formed with an LP UV dose of 1000 mJ/cm^2 followed by chlorination in Utility B water. If it is assumed that bromopicrin has a greater molar yield per mg DOC than chloropicrin (as was observed in this work), even less of the nitrate would be required to account for the increased bromopicrin formation. Thus, even though nitrate only absorbs a small amount of irradiation at 254 nm (molar absorptivity (ϵ) = $4.7 \text{ M}^{-1}\text{cm}^{-1}$ at 254 nm, compared to $9900 \text{ M}^{-1}\text{cm}^{-1}$ at 200 nm), it could be enough to form nM amounts of bromopicrin during sequenced UV processes (i.e. UV followed by chlorine or chloramine). This calculation also assumes that activated nitrate is converted to a nitrating agent (such as $\cdot\text{NO}_2$ or N_2O_4) which reacts quantitatively with DOM. Aqueous bromine reacts faster with DOM than aqueous chlorine, and bromine tends to act more as a substituting/halogenating agent while chlorine reacts preferentially as an oxidant (Rook et al. 1978; Westerhoff et al. 2004). This could explain why a similar increase in chloropicrin formation from LP UV and subsequent chlorination has not been observed and also why there was a greater molar yield of bromopicrin compared

to chloropicrin. Westerhoff et al. (2004) calculated rate constants for the reactions of HOCl/OCl⁻ and HOBr/OBr⁻ with a DOM isolate (Suwannee River) at pH 8 to be 2.4 and 167 M⁻¹ s⁻¹, respectively (after a rapid initial stage reaction with an estimated rate constant of 500-5000 M⁻¹ s⁻¹). In comparison, the rate constant for the reaction of •NO₂ with an organic precursor (C₆H₅O⁻) is on the order of 1.5x10⁷ M⁻¹ s⁻¹ (Alfassi et al. 1990). Increased chloropicrin formation has also been previously observed for waters treated with pre-ozonation followed by chlorine, compared to the same waters treated with chlorine only (Hoigne and Bader 1988).

Chloral Hydrate

Chloral hydrate (the hydrated form of trichloroacetaldehyde) formation increased with increasing UV dose and to a greater extent with MP UV compared to LP UV, as shown in Figure 2-5. Its formation during chlorination was higher in ambient samples compared to bromide-spiked samples, suggesting a possible shift to the bromine-substituted counterpart (not analyzed), as observed with THMs and chloropicrin/bromopicrin. Nitrate spiking had no effect on the production of chloral hydrate, shown in Figure 2-6, which suggests that precursors for chloral hydrate are not affected by the production of reactive species from UV irradiation of nitrate. Utility A water, which had the highest SUVA₂₅₄, formed the most chloral hydrate per mg DOC in samples that were chlorinated only (not UV treated), but the lower SUVA₂₅₄ water (Utility C) had greater changes in chloral hydrate formation resulting from UV irradiation. Overall chloral hydrate formation was greater with chlorination (12.6 and 16.9 nmol/mg C (2.9 and 7.8 µg/L)) compared to chloramination (0.76 and 0.39 nmol/mg

C (0.2 $\mu\text{g/L}$ in both cases)) in Utilities B and C, respectively. Chloral hydrate was below detection limit ($<0.6 \text{ nM}$ ($<0.1 \mu\text{g/L}$)) in all chloraminated Utility A samples.

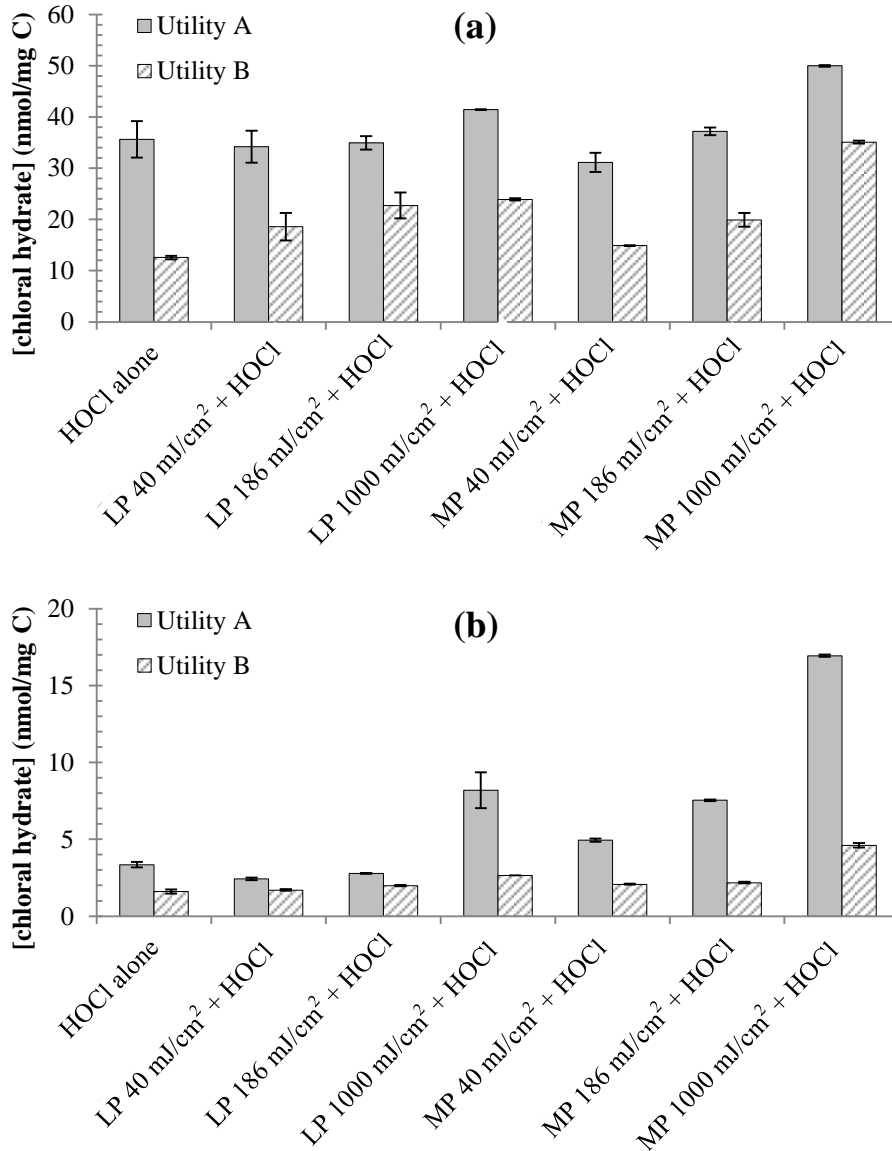


Figure 2-5. Effect of LP and MP UV followed by chlorination on the formation of chloral hydrate in (a) ambient and (b) bromide- and nitrate-spiked Utility A and B samples. Chloral hydrate molar concentration is normalized by DOC. Bar height represents average value and the range between experimental duplicate values is shown by the inset lines. Spiking amounts were 0.5 mg/L bromide (6.3 μM) and 8 mg N/L nitrate (0.57 mM).

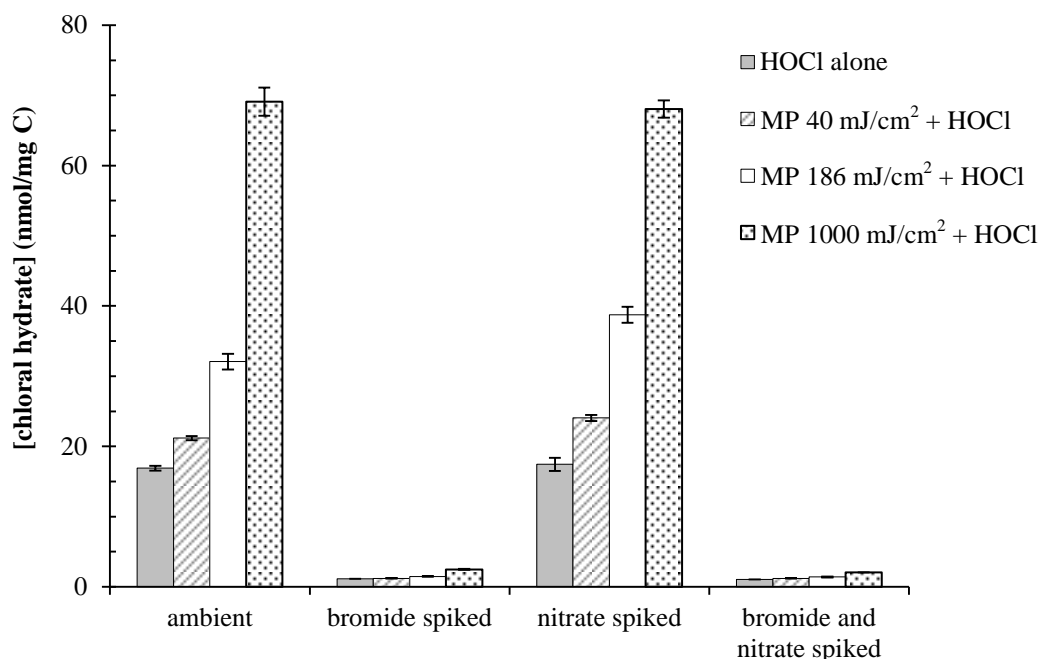


Figure 2-6. Effect of MP UV followed by chlorination on the formation of chloral hydrate in ambient and spiked Utility C samples. Chloral hydrate molar concentration is normalized by DOC. Bar height represents average value and the range between experimental duplicate values is shown by the inset lines. Spiking amounts were 1 mg/L bromide (12.5 μ M) and 10 mg N/L nitrate (0.71 mM).

Increased chloral hydrate formation has been previously observed in waters pre-treated with ozone prior to chlorination, compared to those not ozonated and with a chlorine dose adjusted to provide a similar residual (Singer et al. 1999). This was likely due to the formation of acetaldehyde, known to be produced during ozonation of DOM (Yamada and Somiya 1989), which can then further react with chlorine to produce chlorine-substituted acetaldehydes (McKnight and Reckhow 1992). Aldehydes are also known to be produced during UV irradiation (Liu et al. 2002), so a similar pathway could explain the increased chloral hydrate formation resulting from UV followed by chlorination compared to chlorination alone that was observed here. The World Health Organization has set a provisional guideline of 10 μ g/L (60.5 nM) for chloral hydrate in

drinking water (WHO 1993). This level was exceeded in ambient Utility A samples treated with 1000 mJ/cm² LP or MP UV followed by chlorination, ambient Utility C samples treated with 186 or 1000 mJ/cm² MP UV followed by chlorination, and nitrate-spiked Utility C samples treated with 40-1000 mJ/cm² MP UV followed by chlorine (although the formation from chlorine alone in ambient and nitrate-spiked Utility C samples was already 7.8 and 8.1 µg/L, respectively).

Cyanogen Chloride

Cyanogen chloride was only analyzed in Utility B and C chloraminated samples. Its formation doubled with 186 mJ/cm² and increased three-fold with 1000 mJ/cm² MP UV followed by chloramination in nitrate-spiked Utility C samples, compared to chloramination alone, shown in Figure 2-7. In samples that were not spiked with nitrate, only the highest dose of MP UV (1000 mJ/cm²) affected cyanogen chloride (formation doubled compared to chloramination alone). For Utility B, cyanogen chloride was only detected in ambient samples pretreated with 186 mJ/cm² MP UV (9.8 nM) or ambient and bromide- and nitrate-spiked samples pretreated with 1000 mJ/cm² MP UV (22 and 19 nM, respectively). Spiking with bromide had little effect on the overall cyanogen chloride formation. This supports the earlier observation that the reaction of chloramine with bromide to form reactive bromine species is not likely to be significant under the experimental conditions used for this work and, thus, does not compete with the availability of chloramine to form cyanogen chloride.

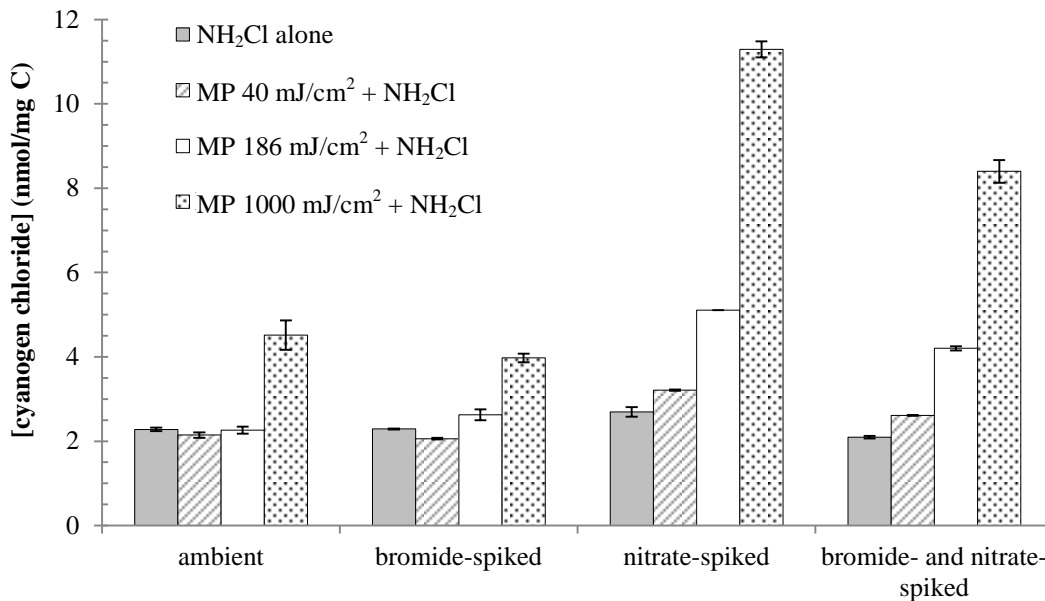


Figure 2-7. Effect of MP UV followed by chloramination on the formation of cyanogen chloride in Utility C samples. Cyanogen chloride molar concentration is normalized by organic carbon content. Bar height represents average value and the range between experimental duplicate values is shown by the inset lines. Spiking amounts were 1 mg/L bromide (12.5 μ M) and 10 mg N/L nitrate (0.71 mM).

Liu and colleagues (2006) previously observed an increase in cyanogen chloride formation following 60 mJ/cm² MP UV and chloramination, compared to chloramination alone. Cyanogen chloride is typically observed as a chloramination byproduct and past work has identified amino acids and other organic nitrogen compounds as precursors (Hirose et al. 1988; Krasner et al. 1989). A potential mechanism for the formation of cyanogen chloride resulting from UV treatment is through chloramination of formaldehyde, which is known to be a cyanogen chloride precursor and can be formed during UV irradiation of surface and groundwaters (Malley et al. 1995; Pedersen et al. 1999). Unlike chloral hydrate, which is also hypothesized to form via an aldehyde intermediate, spiking with nitrate resulted in greater cyanogen chloride formation for samples treated with MP UV compared to the same treatment in unspiked samples. This

suggests that there may be multiple pathways by which UV can increase cyanogen chloride precursors (e.g. production of formaldehyde and also formation of reactive nitrogen species from nitrate which can react with DOM). Indeed, recent labeled $^{15}\text{NH}_2\text{Cl}$ experiments have demonstrated that both dissolved organic nitrogen and chloramines can contribute as nitrogen sources in the formation of cyanogen chloride during chloramination (Yang et al. 2010). The World Health Organization has set a guideline value of 70 $\mu\text{g/L}$ (1.1 μM cyanogen chloride) for all cyanide species, which includes cyanogen chloride (WHO 1993). Even with the highest MP UV dose and 10 mg/L nitrate spike, cyanogen chloride was below this guideline value.

2.4 Conclusions

This study investigated the effect of nitrate and bromide on the formation of a range of halogen- and nitrogen-containing DBPs during UV-chlorine/chloramine drinking water treatment. Typical UV disinfection doses (40-186 mJ/cm^2) did not impact the formation of regulated THMs and HAAs with subsequent chlorination or chloramination. Three classes of emerging, unregulated DBPs thought to be more geno- and cytotoxic than the regulated THMs and HAAs were affected by UV-chlorine/chloramine treatment (trihalonitromethanes, chloral hydrate, cyanogen chloride), although the most significant changes were only observed with high UV doses or in waters spiked with high levels of nitrate and/or bromide. The potential toxicity of these compounds warrants consideration of conditions which could minimize their formation (precursors, UV dose, lamp type) during design and implementation of UV drinking water treatment, particularly as water sources become increasingly impaired.

The main findings of this work include:

- 24-hour free chlorine and monochloramine demands were increased by LP and MP UV. At UV disinfection doses ($\leq 186 \text{ mJ/cm}^2$), these changes were minor (0.1-0.6 mg Cl_2/L for chlorine and 0.1-0.3 mg Cl_2/L for chloramine). The most significant increases in chlorine demand (0.6-2.2 mg Cl_2/L) occurred with MP UV treatment of waters spiked with 8-10 mg N/L nitrate.
- UV had minimal impact on the formation of THM4, iodine-containing THMs, HAA9, haloacetonitriles, haloketones, and haloacetamides at disinfection doses. At higher MP UV doses (1000 mJ/cm^2) THM4 formation was increased by up to 40%.
- Chloropicrin formation doubled and increased six-fold with 40 mJ/cm^2 MP UV followed by chloramination and chlorination, respectively, in nitrate-spiked samples (8-10 mg N/L). Even at lower nitrate spiking levels (1 and 5 mg N/L), MP UV and subsequent chlorination increased chloropicrin formation. Compared to the same samples treated with chlorine alone, chloropicrin was increased three- and twelve-fold with doses of 40 and 186 mJ/cm^2 followed by chlorination, respectively, in samples spiked with 1 mg N/L nitrate.
- Bromopicrin formation was influenced to a greater extent by UV (both LP and MP) than chloropicrin. In samples containing bromide and nitrate, bromopicrin formation increased 30-60% with 40 mJ/cm^2 LP UV and four- to ten-fold with 40 mJ/cm^2 MP UV, after subsequent chlorination.
- Chloral hydrate formation was increased with LP (1000 mJ/cm^2) and MP UV during chlorination, compared to chlorination alone. With 40 mJ/cm^2 MP UV followed by chlorine, up to a 40% increase in chloral hydrate formation was observed.

- Cyanogen chloride formation doubled with 1000 mJ/cm² MP UV followed by chloramination in ambient samples, compared to chloramination alone. Samples spiked with nitrate showed greater increases in cyanogen chloride with increasing MP UV dose. For samples spiked with nitrate or nitrate and bromide, cyanogen chloride formation doubled with 186 mJ/cm² MP UV and increased three-fold with 1000 mJ/cm² MP UV followed by chloramination, compared to chloramination alone.

A summary of UV treatment conditions in which regulations or guideline values for selected DBPs were reached or exceeded is shown in Table 2-6. It should be noted that this study only looked at three source waters and that DBP precursors can vary considerably across different locations. If UV, and in particular MP UV, is being implemented on source waters containing nitrate (greater than 1 mg N/L), utilities should consider options for nitrate reduction upstream from UV processes. If this is not feasible, the use of LP over MP UV can reduce the effect on halonitromethane formation.

Table 2-6. Summary of conditions under which a U.S. EPA regulation, WHO guideline value, or maximum level measured in the Information Collection Rule (ICR) or U.S. occurrence study (for chloropicrin and bromopicrin, respectively, which currently have no regulation or guideline value) was reached or exceeded. Spiking amounts, unless otherwise noted, were 0.5 mg/L bromide and 8 mg N/L nitrate for Utilities A & B and 1 mg/L bromide and 10 mg N/L nitrate for Utility C.

DBP or DBP class	Regulation, guideline value, or ICR/U.S. occurrence study maximum concentration (µg/L)	Conditions under which this value was reached or exceeded
THM4	80 (U.S. EPA 2006)	None ¹
HAA5	60 (U.S. EPA 2006)	None ²
Chloral hydrate	10 (WHO 1993)	<i>Utility A</i> : ambient, 1000 mJ/cm ² LP or MP UV + HOCl; <i>Utility C</i> ³ : ambient, 186-1000 mJ/cm ² MP UV + HOCl; nitrate-spiked, 40-1000 mJ/cm ² MP UV + HOCl
Cyanogen chloride	70 (WHO 1993)	None
Chloropicrin	2.4 (U.S. EPA 2005)	<i>Utility C</i> : nitrate-spiked (1-10 mg N/L), 186-1000 mJ/cm ² MP UV + HOCl
Bromopicrin	5.0 (Krasner et al. 2006)	<i>Utilities A and B</i> : bromide- & nitrate-spiked, 1000 mJ/cm ² LP UV or 40-1000 mJ/cm ² MP UV + HOCl; <i>Utility B</i> : bromide- & nitrate-spiked, 1000 mJ/cm ² MP UV + NH ₂ Cl; <i>Utility C</i> : bromide-spiked, 1000 mJ/cm ² MP UV + HOCl; bromide- & nitrate-spiked, 40-1000 mJ/cm ² MP UV + HOCl; bromide- & nitrate-spiked, 1000 mJ/cm ² MP UV + NH ₂ Cl

¹THM4 formation was greater than 80 µg/L in all samples spiked with 0.5-1 mg/L bromide and chlorinated, regardless of UV treatment.

²HAAs were only measured for Utility A.

³Chloral hydrate formation from chlorine alone in Utility C ambient and nitrate-spiked samples was 7.8 and 8.1 µg/L, respectively.

Sources Cited for Chapter 2

- Alfassi, Z.B. et al., 1990. Temperature dependence of the rate constants for reaction of inorganic radicals with organic reductants. *Journal of Physical Chemistry*, 94(25), pp.8800-8805.
- APHA (American Public Health Association), American Water Works Association, and Water Environment Federation, 1999. Standard Methods for the Examination of Water and Wastewater. 20th Edition, American Public Health Association: Washington DC.
- Bolton, J.R. & Linden, K.G., 2003. Standardization of methods for fluence (UV dose) determination in bench-scale UV experiments. *Journal of Environmental Engineering*, 129(3), pp.209-215.
- Benotti, M.J. et al., 2011. *Role of Bromamines on DBP Formation and Impact on Chloramination and Ozonation*. American Water Works Association and Water Research Foundation: Denver, Colorado.
- Bousher, A. et al., 1989. Kinetics of reactions in solutions containing monochloramine and bromide. *Water Research*, 23(8), pp.1049-1058.
- Brophy, K.S. et al., 2000. Quantification of nine haloacetic acids using gas chromatography with electron capture detection. In: *Natural Organic Matter and Disinfection By-Products*. ACS Symposium Series 761. American Chemical Society, pp.343-355.
- Buchanan, W. et al., 2005. Fractionation of UV and VUV pretreated natural organic matter from drinking water. *Environmental Science & Technology*, 39(12), pp.4647-4654.
- Cantor, K.P. et al., 1998. Drinking water source and chlorination byproducts I. Risk of bladder cancer. *Epidemiology*, 9(1), pp.21-28.
- Chen, P.H. et al., 2002. Hydrogen abstraction and decomposition of bromopicrin and other trihalogenated disinfection byproducts by GC/MS. *Environmental Science & Technology*, 36(15), pp.3362-3371.
- Chow, A.T. et al., 2008. Impact of simulated solar irradiation on disinfection byproduct precursors. *Environmental Science & Technology*, 42(15), pp.5586-5593.
- Clancy, J.L. et al., 2000. Using UV to inactivate cryptosporidium. *Journal of the American Water Works Association*, 92(9), pp.97-104.
- Diehl, A.C. et al., 2000. DBP formation during chloramination. *Journal of the American Water Works Association*, 92(6), pp.76-90.

- Duirk, S.E. et al., 2005. Modeling monochloramine loss in the presence of natural organic matter. *Water Research*, 39(14), pp.3418-3431.
- Dotson, A.D. et al., 2010. UV/H₂O₂ treatment of drinking water increases post-chlorination DBP formation. *Water Research*, 44(12), pp.3703-3713.
- Dotson, A.D. et al., 2012. UV disinfection implementation status in United States water treatment plants. *Journal American Water Works Association*, 104(5), pp.E318-E324.
- Goldstein, S. & Rabani, J., 2007. Mechanism of nitrite formation by nitrate photolysis in aqueous solutions: the role of peroxyxynitrite, nitrogen dioxide, and hydroxide radical. *Journal of the American Chemical Society*, 129(34), pp.10597-10601.
- Graetzel, M. et al., 1969. Pulsradiolytische untersuchung einiger elemntarprozesse der oxidation und reduction des nitritions. *Berichte der Bunsen-Gesellschaft fur Physikalische Chemie*, 73, pp.646-653.
- Hirose, J. et al., 1988. Formation of cyanogen chloride by the reaction of amino acids with hypochlorous acid in the presence of ammonium ion. *Chemosphere*, 17(5), pp.865-873.
- Hoigne, J. & Bader, H., 1988. The formation of trichloronitromethane (chloropicrin) and chloroform in a combined ozonation/chlorination treatment of drinking water. *Water Research* 22(3), pp.313-319.
- Hua, G. & Reckhow, D.A., 2007. Characterization of disinfection byproduct precursors based on hydrophobicity and molecular size. *Environmental Science & Technology*, 41(9), pp.3309-3315.
- Jin, S. et al., 2006. Polychromatic UV fluence measurement using chemical actinometry, biodosimetry, and mathematical techniques. *Journal of Environmental Engineering*, 132(8), pp.831-841.
- Kitis, M. et al., 2001. Isolation of dissolved organic matter (DOM) from surface waters using reverse osmosis and its impact on the reactivity of DOM to formation and speciation of disinfection by-products. *Water Research*, 35(9), pp.2225-2234.
- Krasner, S.W. et al., 1989. The occurrence of disinfection by-products in US drinking water. *Journal of the American Water Works Association*, 81(8), pp.41-53.
- Krasner, S.W. et al., 2006. Occurrence of a new generation of disinfection byproducts. *Environmental Science & Technology*, 40(23), pp.7175-7185.

- Kumar, K. & Margerum, D.W., 1987. Kinetics and mechanism of general-acid-assisted oxidation of bromide by hypochlorite and hypochlorous acid. *Inorganic Chemistry*, 26(16), pp.2706-2711.
- Liang, L. & Singer, P.C., 2003. Factors influencing the formation and relative distribution of haloacetic acids and trihalomethanes in drinking water. *Environmental Science & Technology*, 37(13), pp.2920-2928.
- Liu, W. et al., 2002. Comparison of disinfection byproduct (DBP) formation from different UV technologies at bench scale. *Water Science and Technology: Water Supply*, 2(5-6), pp.515-521.
- Liu, W. et al., 2006. THM, HAA and CNCl formation from UV irradiation and chlor(am)ination of selected organic waters. *Water Research*, 40(10), pp.2033-2043.
- Loper, J.C. et al., 1978. Residue organic mixtures from drinking water show *in vitro* mutagenic and transforming activity. *Journal of Toxicology and Environmental Health*, 4(5-6), pp.919-938.
- Magnuson, M.L. et al., 2002. Effect of UV irradiation on organic matter extracted from treated Ohio River water studied through the use of electrospray mass spectrometry. *Environmental Science & Technology*, 36(23), pp.5252-5260.
- Malley, J.P. et al., 1995. *Evaluation of the Byproducts Produced by the Treatment of Groundwaters with Ultraviolet Irradiation*. American Water Works Association and Water Research Foundation: Denver, Colorado.
- Margerum, D.W. et al., 1994. Water chlorination chemistry: nonmetal redox kinetics of chloramine and nitrite ion. *Environmental Science & Technology*, 28(2), pp.331-337.
- McKnight, A. & Reckhow, D.A., 1992. Reactions of ozonation by-products with chlorine and chloramines. In: *Proceedings of the AWWA Annual Conference*, Vancouver, British Columbia.
- Merlet, N. et al., 1985. Chloropicrin formation during oxidative treatments in the preparation of drinking water. *Science of the Total Environment*, 47, pp.223-228.
- National Cancer Institute, 1976. Report on the Carcinogenesis Bioassay of Chloroform (CAS No. 67-66-3). National Cancer Institute: Bethesda, Maryland.
- Pedersen, E.J. et al., 1999. Formation of cyanogen chloride from the reaction of monochloramine with formaldehyde. *Environmental Science & Technology*, 33(23), pp.4239-4249.

- Plewa, M.J. et al., 2008. Comparative mammalian cell toxicity of N-DBPs and C-DBPs. In: *Disinfection By-Products in Drinking Water: Occurrence, Formation, Health Effects, and Control*. ACS Symposium Series 995. American Chemical Society, pp.36-50.
- Reckhow, D.A. et al., 2010. Effect of UV treatment on DBP formation. *Journal of the American Water Works Association*, 102(6), pp.100-113.
- Rook, J.J. et al., 1978. Bromide oxidation and organic substitution in water treatment. *Journal of Environmental Science and Health, Part A*, 13(2), pp.91-116.
- Schreiber, I.M. & Mitch, W.A., 2005. Influence of the order of reagent addition on NDMA formation during chloramination. *Environmental Science & Technology*, 39(10), pp.3811-3818.
- Sclimenti, M.J. et al., 1994. The simultaneous determination of cyanogen chloride and cyanogen bromide in chloraminated waters by a simplified microextraction GC/ECD technique. In: *Proceedings of the AWWA Water Quality Technology Conference*, Charlotte, North Carolina.
- Shah, A.D. et al., 2011. Impact of UV disinfection combined with chlorination/chloramination on the formation of halonitromethanes and haloacetonitriles in drinking water. *Environmental Science & Technology*, 45(8), pp.3657-3664.
- Singer, P.C. et al., 1999. *Impacts of Ozonation on the Formation of Chlorination and Chloramination By-products*. American Water Works Association and Water Research Foundation: Denver, Colorado.
- Song, H., et al., 2009. Isolation and fractionation of natural organic matter: evaluation of reverse osmosis performance and impact of fractionation parameters. *Environmental Monitoring and Assessment*, 153(1-4), pp.307-321.
- Trofe, T.W. et al., 1980. Kinetics of monochloramine decomposition in the presence of bromide. *Environmental Science & Technology*, 14(5), pp.544-549.
- U.S. EPA (Environmental Protection Agency), 1992. *National Primary Drinking Water Regulations: Synthetic Organic Chemicals and Inorganic Chemicals, Final Rule*. Federal Register 57(138), pp.31776-31849.
- U.S. EPA (Environmental Protection Agency), 2005. *Occurrence Assessment for the Final Stage 2 Disinfectants and Disinfection Byproducts Rule*. EPA/815/R-05/011, U.S. EPA: Athens, Georgia.

- U.S. EPA (Environmental Protection Agency), 2006. *National Primary Drinking Water Regulations: Stage 2 Disinfectants and Disinfection Byproducts Rule*. Federal Register 71(2), pp.387-493.
- Warneck, P. & Wurzinger, C., 1988. Product quantum yields for the 305-nm photodecomposition of NO_3^- in aqueous solution. *Journal of Physical Chemistry*, 92(22), pp.6278-6283.
- Weinberg, H.S. et al., 2002. *The Occurrence of Disinfection By-Products (DBPs) of Health Concern in Drinking Water: Results of a Nationwide DBP Occurrence Study*. EPA/600/R-02/068, U.S. EPA: Athens, Georgia.
- Westerhoff, P. et al., 2004. Reactivity of natural organic matter with aqueous chlorine and bromine. *Water Research*, 38(6), pp.1502-1513.
- WHO (World Health Organization), 1993. *Guidelines for Drinking-Water Quality*. 2nd Edition, World Health Organization: Geneva.
- Yamada, H. & Somiya, I., 1989. The determination of carbonyl compounds in ozonated water by the PFBOA Method. *Ozone: Science & Engineering*, 11(2), pp.127-141.
- Yang, X. et al., 2010. Nitrogenous disinfection byproducts formation and nitrogen origin exploration during chloramination of nitrogenous organic compounds. *Water Research*, 44(9), pp.2691-2702.

Chapter 3: Disinfection Byproduct Formation from UV-Chlorine/Chloramine Treatment of Whole and Fractionated Dissolved Organic Matter

3.1 Introduction

Natural organic matter (NOM) is a complex mixture of decaying plant and microbial material found in all natural waters, and it is the main precursor for disinfection byproduct (DBP) formation (Christman et al. 1983). NOM properties and characteristics are studied to better understand and predict formation of DBPs of potential human health concern (Loper et al. 1978; Cantor et al. 1998; Calderon 2000). Trihalomethanes (THMs) and haloacetic acids (HAAs) are two major DBP classes formed during chlorination, and a subset of these are regulated in the United States (U.S. EPA 2006). Dissolved organic matter (DOM) is the operationally-defined dissolved fraction (usually defined as the portion passing through a 0.45 μm filter) which comprises most of the NOM mass in water (Thurman 1985). The specific ultraviolet absorbance of a water sample at 254 nm (SUVA_{254}), defined as the UV absorbance at 254 nm divided by dissolved organic carbon (DOC) concentration, has been shown to correlate with DBP formation during chlorination and is often used to predict the reactivity of NOM towards disinfectants (Edzwald et al. 1985; Reckhow et al. 1990; Kitis et al. 2001a). Some characterization techniques require concentration or isolation of NOM. Leenheer (1981) proposed a fractionation scheme using resins, pH-adjustment, and various eluents to separate NOM by polarity and acid/base properties. Hydrophobic moieties include

aromatic and phenolic-type structures while hydrophilic NOM is associated with protein-, carbohydrate-, and amino-type groups (Krasner et al. 1996). Past research has shown that in general, the hydrophobic fraction has greater THM and HAA formation potential compared to hydrophilic precursors, which typically comprise a smaller amount of the total NOM. However, the hydrophilic fraction can play an important role in DBP formation, especially in low humic-containing waters (Kitis et al. 2002; Liang & Singer 2003; Hua & Reckhow 2007a).

As anthropogenic activity continues to stress source water quality and increasingly stringent DBP regulations come into effect (U.S. EPA 2006), utilities are looking to alternative treatment processes to balance microbial inactivation and chemical byproduct risk. One such process is ultraviolet (UV) irradiation, which is being increasingly used as a primary disinfectant in treatment plants that employ chlorination or chloramination for secondary disinfection. UV alone is not expected to generate halogen-containing DBPs, because a halogenating agent such as chlorine (HOCl) or chloramine (NH₂Cl) is required for their formation. However, there have been few comprehensive studies to evaluate the impact of UV treatment on DBP formation when combined with a secondary disinfectant, and the majority of research that has taken place focused on the regulated THMs and HAAs (Malley et al. 1995; Liu et al. 2002) rather than emerging DBP classes which are thought to be more toxicologically potent (Plewa et al. 2004; Richardson et al. 2008). It is important to understand the implications of a process that is being used as an integral part of drinking water treatment. The use of NOM fractions can help to elucidate a better understanding of DBP formation mechanisms and organic precursor reactivity as affected by UV treatment.

The objective of this study was to investigate DBP formation and speciation from UV-chlorine/chloramine treatment of hydrophilic and hydrophobic DOM fractions. Concentrated organic precursors (DOC concentration of 9.5-10.7 mg C/L) were treated with correspondingly scaled-up doses of UV and chlorine/chloramines to allow for the observation of emerging DBPs (haloketones, haloacetamides, halonitromethanes) that are often below detection in disinfected natural waters, along with other commonly measured DBPs (THMs, HAAs, chloral hydrate, haloacetonitriles). DBP results were compared to those obtained with the same treatments on the whole (unfractionated) water and a commercially available NOM isolate, Suwannee River natural organic matter (SRNOM).

3.2 Materials and Methods

Reverse Osmosis Concentration

A custom-built portable reverse osmosis (RO) unit was used to concentrate NOM from Orange County Water and Sewer Authority (OWASA, Carrboro, NC, USA) raw water (drinking water source). The raw water that was concentrated for these experiments differs from that used in Chapters 2 and 4, which was settled water (collected after coagulation/flocculation and sedimentation). Raw water was chosen for these experiments because a higher organic carbon content was desired to ensure sufficient organic precursors following fractionation. The characteristics of OWASA raw and settled waters, before and after RO concentration are shown in Appendix 2. RO concentration has previously been demonstrated as a method through which high organic carbon recoveries (80-99%) and preservation of original source water reactivity can be obtained (Kitis et al. 2001b; Song et al. 2009). The RO system included a spiral wound

cellulose triacetate membrane (4x21 inch membrane in a 600 psi-rated fiberglass vessel, part number MC4025AHF, Dracor Water Systems, Durham, NC, USA), four cartridge filters (10, 5, 1, and 0.45 μm , QMA Polypropylene Filter Series, 10 inch height, double open end, Graver Technologies, Glasgow, DE, USA) and a cation exchange (H^+) resin cartridge (10 inch height, Graver Technologies). The tubing between filters and pumps was polyvinyl chloride (PVC). A process flow diagram of the RO unit is shown in Figure 3-1 and the operating procedure can be found in Appendix 1. The system was operated in two stages. First, source water was pumped through the filters and ion exchange resin and collected in a high density polypropylene 80-gallon reservoir (RO feed reservoir). Second, a high pressure pump fed the collected water through the RO membrane. The retentate (RO concentrate) was recycled in the RO feed reservoir and the filtrate (permeate) discarded. The RO membrane was operated until a desired concentration factor of approximately 50 by volume was achieved (180 L raw water concentrated to about 3.5 L RO concentrate). The RO concentrate was filtered in the laboratory (0.45 μm nylon membrane, 47 mm diameter, Whatman International Ltd., Maidstone, England) and stored in amber glass bottles at 4°C until use.

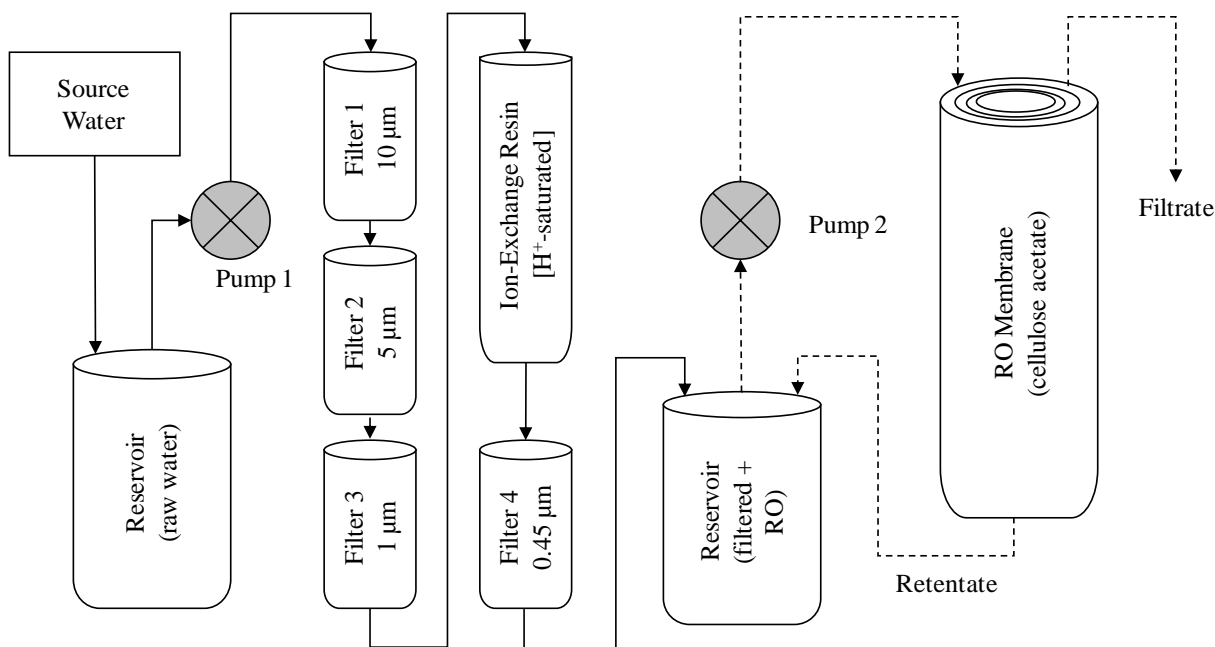


Figure 3-1. RO concentration setup.

XAD Fractionation

A portion of the RO concentrate was fractionated by polarity and acid/base properties on Amberlite XAD-8 and XAD-4 resins (Rohm & Haas, Philadelphia, PA, USA), following the approach of Leenheer (1981). Banked XAD-8 resin was used for this study, because it has not been commercially available for many years. Alternative resins of similar properties are available (e.g. XAD-7HP). Before use, the resins were rinsed in a large glass beaker of 0.1 N NaOH for five days. Each day, the fine particles were decanted off and the NaOH solution replaced. NaOH solutions were prepared from ACS grade pellets (Mallinckrodt, St. Louis, MO, USA). After five days, the resins were washed with laboratory grade water (LGW) several times. LGW was prepared in-house from a Dracor system, which pre-filters inlet 7 MΩ deionized water to 1 µm, removes residual disinfectants, reduces total organic carbon (TOC) to less than 0.2 mg C/L with an

activated carbon cartridge, and removes ions to 18 MΩ with mixed bed ion-exchange resins. The XAD resins were then Soxhlet-extracted sequentially with methanol, acetonitrile, and methanol for 24 hours each. Methanol and acetonitrile were Fisher HPLC grade (ThermoFisher Scientific, Waltham, MA, USA). After extraction, approximately 475 mL of each XAD resin (as a resin/methanol slurry) was packed into a separate glass column containing polytetrafluoroethylene (PTFE) fittings and mesh frits at their base and rinsed with LGW to remove residual methanol, until the TOC in the column effluent was less than 0.5 mg C/L.

Dowex Marathon H⁺ cation-exchange resin (Dow Chemical Co., Midland, MI, USA) was packed into two glass columns (approximately 150 mL resin per column) and each rinsed with 4 bed volumes (BV) of 5% HCl, 7 BV LGW, 4 BV 4% NaOH, and 7 BV LGW. The columns were then filled with 10% Fisher ACS Plus grade HCl and left overnight. The next day, the columns were rinsed with several liters of LGW to remove residual acid. The amount of RO concentrate to pass through the column in one run was calculated according to the following equation (Leenheer 1981):

$$V_{0.5r} = 2 \times V_0 \times (1 + k'_{0.5r})$$

where $V_{0.5r}$ is the volume of RO concentrate applied to the resin, V_0 is the void volume (approximately 65% of the total resin volume), and $k'_{0.5r}$ is the capacity factor of the resin (mass solute sorbed to resin)/(mass of solute in column void volume). A $k'_{0.5r}$ of 50 is commonly used for XAD-4 and XAD-8 resins. The fraction that passes through both resins is operationally defined as hydrophilic DOM. The hydrophobic acid fraction was obtained by reverse eluting the XAD-8 column with 0.1 N NaOH and then passing the eluent through the cation exchange resin. Hydrophobic neutrals were desorbed from the

XAD-8 column with 2 BV of a 75% acetonitrile:25% LGW solution after rinsing the column with 1 BV LGW. The transphilic acid fraction was desorbed from the XAD-4 column by reverse eluting with 0.1 N NaOH and then passing the eluent through a separate cation exchange resin. Transphilic neutrals were desorbed from the XAD-4 column with 2 BV of a 75% acetonitrile:25% LGW solution after rinsing the column with 1 BV LGW. Between runs, XAD resins were regenerated by rinsing with 6 BV 0.1 N NaOH, 2 BV LGW, 6 BV 0.1 N HCl, and 2 BV LGW. Cation exchange resins were regenerated by rinsing with 15 BV 10% HCl and standing overnight in 10% HCl, followed by LGW rinsing. The aqueous samples and solvents were passed through resin columns using a peristaltic pump (Masterflex Model number 7568-00, Cole-Parmer, Vernon Hills, IL, USA). The columns were connected with PTFE fittings and tubing, except for a 10-inch section contained in the pump heads, which required flexible tubing (Masterflex Tygon®, part number 06409-14, Cole-Parmer).

The acetonitrile used to desorb the hydrophilic and transphilic neutral fractions was evaporated using a rotary evaporator prior to lyophilization. The remaining fractions were freeze-dried with a Virtis Genesis-12 SQXL lyophilizer (SP Scientific, Gardiner, NY, USA). DBP formation experiments were carried out using the hydrophobic acid and hydrophilic DOM fractions obtained from this procedure, in addition to the whole water (unfractionated RO concentrate) and SRNOM. The remaining fractions (hydrophobic neutrals, transphilic acids, and transphilic neutrals) were not used in these experiments due to time constraints but were stored in amber glass vials at room temperature (lyophilized neutrals) or 4°C (aqueous transphilic acids) for future experiments. The fractionation procedure is illustrated in Figure 3-2. One limitation of this study is that the

hydrophilic DOM fraction did not undergo any additional desalting steps. Salts (e.g., NaCl) are not retained on the XAD resins and therefore accumulate in the hydrophilic DOM (Leenheer 1981). Desalting often results in lower overall DOM recovery (Leenheer et al. 2000), but since this step was not included, the hydrophilic DOM fraction likely contained more salts than other fractions, which may have impacted the hydrophilic DOM characteristics and subsequent reactivity. For example, Suwannee River Humic Acid has been shown to undergo aggregation with increasing NaCl concentration (Baalousha et al. 2006).

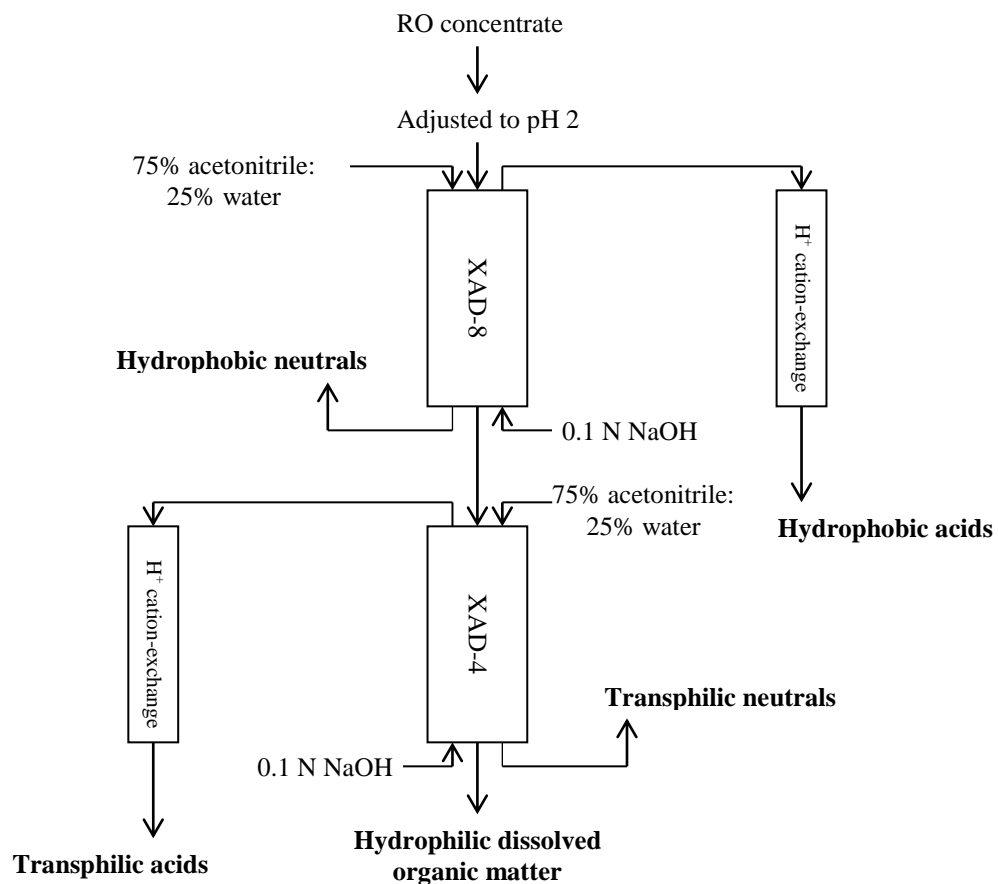


Figure 3-2. Procedure for XAD fractionation of DOM by polarity and acid/base properties.

SRNOM was obtained from the International Humic Substance Society (IHSS, St. Paul, MN, USA). Prior to UV-chlorine/chloramine treatments, the sample to be treated (hydrophobic acids, hydrophilic DOM, unfractionated RO concentrate, or SRNOM) was diluted in LGW to achieve a DOC concentration of approximately 10 mg C/L and adjusted to pH 7 with NaOH or H₂SO₄ (Fisher ACS Plus grade). TOC and DOC were measured using a Shimadzu TOC-V_{CPH} Total Organic Carbon Analyzer (Shimadzu Corp., Atlanta, GA, USA) following Standard Method 5310 (APHA 1999). A subset of samples were spiked with 1 mg/L bromide and 10 mg N/L nitrate, administered in the sodium salt form (Fisher ACS grade).

UV Treatment

UV treatment was performed using quasi-collimated LP and MP lamps, which were located at Duke University (Durham, NC, USA) at the time of these experiments. The LP UV system consisted of four 15 W LP lamps (General Electric, Fairfield, CT, USA) mounted above a 4-inch circular aperture. The MP UV system was commercially built with a 1 kW MP lamp (Calgon Carbon, Pittsburgh, PA, USA) mounted above a 3-inch circular aperture. Samples were retained in a 250-mL capacity Pyrex crystallization dish and stirred during irradiation. Constant sample temperature was maintained at 20-25°C by placing the dish in a copper coil which was connected to a programmable refrigerated recirculating water unit. A manual (LP UV system) or pneumatic shutter (MP UV system) was used to rapidly begin or end the irradiation. Higher doses than those typically used for UV disinfection were applied for this study to investigate trends (500 mJ/cm² for LP UV and 1000 mJ/cm² for MP UV). Doses were determined using

calculation techniques described by Bolton and Linden (2003). Briefly, UV irradiance was measured at the water surface using an SED240 detector with a W diffuser connected to an IL1400A radiometer (International Light, Peabody, MA, USA). The irradiance between 200 to 300 nm was multiplied by a Petri factor (0.97 for LP system, 0.96 for MP system), water factor, radiometer sensor factor, reflection factor, and germicidal factor (MP UV only) to obtain an average irradiance (LP UV) or germicidal irradiance (MP UV) in mW/cm^2 . The irradiation time (s) was then determined by dividing the desired UV dose (mJ/cm^2 or $\text{mW}\cdot\text{s}/\text{cm}^2$) by the average or germicidal irradiance.

Chlorine and Chloramine Addition

After irradiation, samples were immediately dosed with chlorine from a dilution of a concentrated sodium hypochlorite stock solution (Fisher laboratory grade, 5.65-6%) or pre-formed monochloramine. The dose required to leave 1.0 mg Cl_2/L after 72 hours of contact time in the sample with the highest demand was chosen and applied to all samples of the same water type (i.e. RO concentrate, hydrophilic DOM, hydrophobic acids, and SRNOM) so each sample received an equivalent dose. This is a different approach to the experiments described in Chapter 2, in which samples were compared on an equivalent residual basis and also held for only 24 hours, rather than 72 hours. Results of a kinetics study that was carried out to determine the effect of chlorine/chloramine contact time on DBP formation for a subset of the spiking and UV conditions is presented in Appendix 2, and shows the differences in DBP formation between 24 and 72 hour chlorine/chloramine contact times. Demand tests were performed by applying a range of chlorine or monochloramine doses to 25 mL aliquots of each sample. After these samples were held headspace-free for 72 hours at 20°C, the chlorine or monochloramine

residuals were measured and plotted against disinfectant dose, to determine the dose required to achieve the target residual for the sample with the highest demand. Free chlorine residuals were measured in duplicate using the *N,N*-diethyl-*p*-phenylenediamine (DPD) colorimetric method following Standard Method 4500-Cl G (APHA 1999). A pre-formed monochloramine solution was prepared by adding free chlorine drop-wise to an ammonium chloride (ACS grade, Mallinckrodt) solution (adjusted to pH 8.5 with NaOH) at a 1:1.2 Cl:N molar ratio (standard operating procedure is provided in Appendix 4). Monochloramine is referred to as chloramine throughout this paper for the purpose of discussion, but the pre-formed chloramine solution was prepared such that monochloramine was the primary species formed (dichloramine negligible) and ammonium chloride was present in excess so that no free chlorine remained. Chloramine speciation and concentration in the pre-formed solution were verified by UV spectrometry and solving simultaneous Beer's Law equations as described by Schreiber and Mitch (2005). Chloramine residuals in samples were analyzed in duplicate using an adaption of the indophenol method (Hach Method 10171) with MonochlorF reagent (Hach Company, Loveland, CO). Samples were held in headspace-free amber glass bottles with caps and PTFE-lined septa for 72 hours at 20°C.

DBP Analysis

THM4 (four regulated chlorine- and bromine-containing THM species), HAA9 (five regulated (HAA5) and four unregulated chlorine- and bromine-containing HAA species), chloral hydrate, chloropicrin (trichloronitromethane), 4 haloacetonitriles (trichloro-, dichloro-, bromochloro-, and dibromo-acetonitrile), two haloketones (1,1-

dichloro- and 1,1,1-trichloro-propanone), and monobromo-, dichloro- and trichloro-acetamide standards were obtained from Supelco and Sigma-Aldrich (Sigma Chemical Co., St. Louis, MO, USA). Bromochloro-, dibromo-, bromodichloro-, dibromochloro-, and tribromo-acetamide standards were obtained from Orchid Cellmark (New Westminster, BC, Canada). After the 72-hour reaction time, chlorine/chloramine residuals were measured and samples were transferred to 40-mL vials containing ammonium sulfate (ACS grade, Mallinckrodt) for HAA9 extractions or 60-mL vials with L-ascorbic acid (ACS grade, Sigma) for all other compounds. Samples were then stored headspace-free at 4°C until DBP analysis, which was carried out as two separate extractions: (1) THM4, 4 haloacetonitriles, two haloketones, chloropicrin, chloral hydrate, and 8 haloacetamides were co-extracted within 24 hours of quenching; and (2) HAA9 were analyzed within 72 hours of quenching. DBPs were liquid-liquid extracted with methyl tert butyl ether (OmniSolv, EMD Chemicals Inc., Gibbstown, NJ) and analyzed on a Hewlett-Packard 5890 gas chromatograph with ⁶³Ni electron capture detector (GC-ECD) following the procedures described by Brophy et al. (2000) (HAA9) and Weinberg et al. (2002) (remaining DBPs). The standard operating procedures for these extractions are provided in Appendices 5A and 5C. A Zebron (Phenomenex, Torrance, CA) ZB-1 capillary column (30 m length, 0.25 mm inner diameter, 1.0-µm film thickness) was used for chromatographic separation of compounds. The following temperature program was used for THMs, chloral hydrate, haloacetonitriles, chloral hydrate, and haloketones: oven held at 35°C for 22 min, increased at 10°C/min to 145°C and held for 2 min, increased at 20°C/min to 225°C and held for 10 min, then increased at 20°C/min to 260°C and held for 5 min. Injection volume was 2 µL (splitless) and after

0.5 minutes the sample was split at a 1:1 ratio. The injection temperature was 200°C and the detector temperature was 290°C. Haloacetamides were run using the following oven temperature program: held at 37°C for 1 min, increased at 5°C/min to 110°C and held for 10 min, then increased at 5°C/min to 280°C. Injection volume was 2 µL (splitless) and after 0.5 minutes the sample was split at a 1:1 ratio, injector temperature was 200°C and detector temperature was 300°C. HAA9 extracts were analyzed using the following oven temperature program: initial temperature was 37°C, held for 21 min, increased at 5°C/min to 136°C, held for 3 min, increased at 20°C/min to 250°C and held for 3 min. Injection volume was 1 µL (splitless) and after 0.5 minutes the sample was split at a 1:1 ratio, injector temperature was 180°C and detector temperature was 300°C. All samples were analyzed in duplicate and 1,2-dibromopropane was used as an internal standard. The minimum reporting limit (MRL) for all compounds except HAAs was 0.1 µg/L. The MRL for HAAs ranged from 0.4 to 4 µg/L for individual species.

3.3 Results and Discussion

Fractionation

Figure 3-3 shows the contribution of isolated DOM fractions accounting for 97% of the organic carbon measured in the unfractionated RO concentrate and Figure 3-4 is a comparison of OWASA RO concentrate and a SRNOM sample isolated by Croué et al. (2000). The RO concentrate had a higher hydrophilic/transphilic content and lower hydrophobic organic carbon content compared to SRNOM. The OWASA hydrophobic acid fraction and SRNOM used for these experiments had the same SUVA₂₅₄ (3.7), which was higher than that of the OWASA hydrophilic DOM (1.5) or unfractionated RO

concentrate (3.1). The relative percent difference (RPD) between duplicate SUVA₂₅₄ measurements was ≤9%, so the difference between the OWASA hydrophobic acid/SRNOM and unfractionated RO SUVA₂₅₄ values (17%) is meaningful. The higher SUVA₂₅₄ for the hydrophobic acid fraction, which contains more aromatic, higher molecular weight precursors, compared to the hydrophilic DOM, is consistent with previous work (Croué et al. 2000). UV absorbance data was not collected for the other fractions of the RO concentrate in this study. The contribution of properties such as SUVA₂₅₄ and DBP formation from the isolated fractions studied here (hydrophobic acids and hydrophilic DOM) was compared to those of the whole, unfractionated RO concentrate for a partial mass balance using Equation 3-1:

$$\% \text{ contribution} = \frac{x_i C_i}{C_{RO}} \quad (3-1)$$

where x_i is the fraction of carbon mass to the whole water (0.59 for hydrophobic acids, 0.15 for hydrophilic DOM), C_i is the SUVA₂₅₄ or DBP yield (molar concentration normalized by mg DOC) of that fraction, and C_{RO} is the SUVA₂₅₄ or DBP molar yield of the unfractionated RO concentrate. Using Equation 3-1, the SUVA₂₅₄ values in the hydrophobic acids and hydrophilic DOM were found to account for 70% and 7%, respectively, of the unfractionated RO concentrate SUVA₂₅₄. Similar values were obtained for SRNOM fractions isolated by Croué et al. (2000), with hydrophobic acids and hydrophilic fractions contributing 72% and 7%, respectively, to the unfractionated SRNOM SUVA₂₅₄.

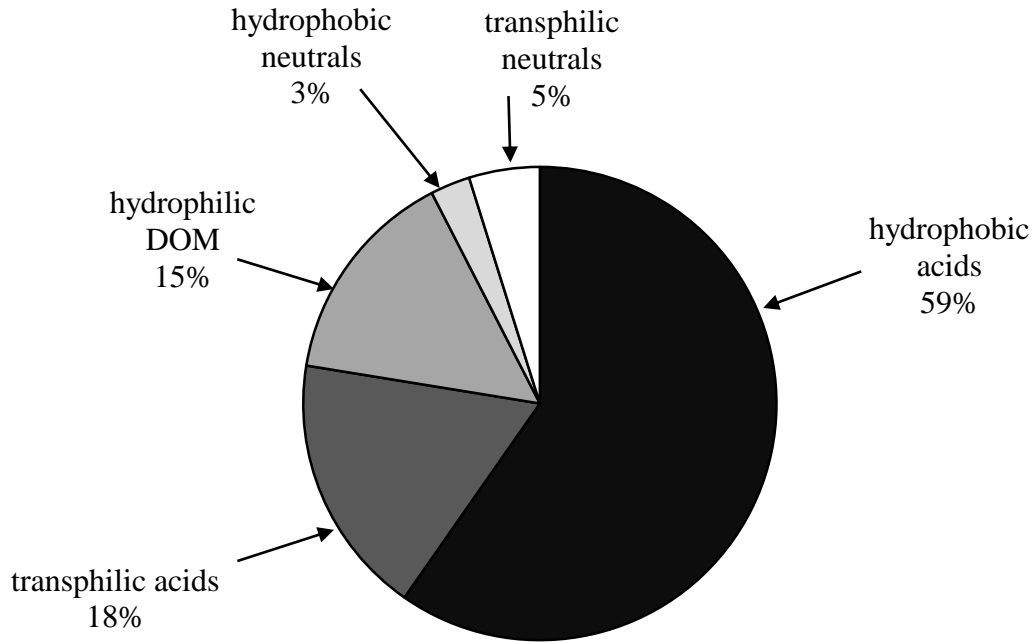


Figure 3-3. Composition of OWASA raw water RO concentrate on a carbon mass basis.

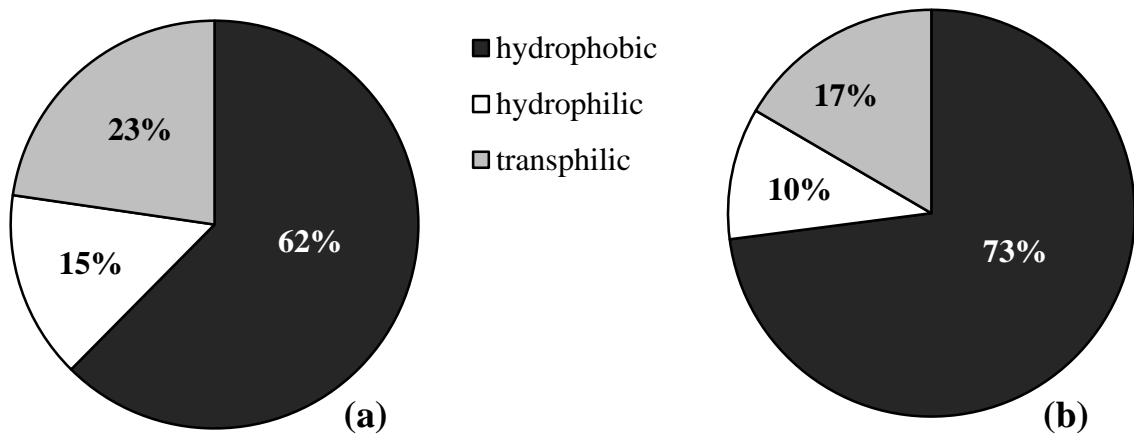


Figure 3-4. Comparison of (a) OWASA RO concentrate and (b) SRNOM fractions on a carbon mass basis.

Chlorine and Chloramine Demand

Characteristics and treatment conditions of each water type (unfractionated OWASA RO concentrate, hydrophobic acids, hydrophilic DOM, and SRNOM) are shown in Table 3-1. The specified chlorine or chloramine dose was applied to all samples within that water type, including those spiked with bromide and nitrate and treated with UV, so the results presented in this chapter are compared on an equivalent chlorine or chloramine dose basis.

Table 3-1. Sample characterization and disinfectant doses based on chlorine/chloramine demand tests.

Parameter	OWASA			
	RO concentrate	hydrophobic acids	hydrophilic DOM	SRNOM
DOC (mg C/L)	9.5	9.9	10.7	10.4
SUVA ₂₅₄ (L/mg C·m)	3.1	3.7	1.5	3.7
chlorine dose (mg Cl ₂ /L)	16	16	20	23
chloramine dose (mg Cl ₂ /L)	4.2	5.3	6.0	6.6

The 72-hour chlorine demand of the OWASA RO concentrate was increased 33% by MP UV irradiation (1000 mJ/cm²) in ambient (unspiked) samples, but was not affected in bromide- and nitrate-spiked RO concentrate samples, shown in Table 3-2. The change in SRNOM chlorine demand with MP UV pre-treatment, compared to the sample without UV treatment, was within the analytical error associated with replicate residual measurements (RPD ≤10%), and, thus, not significant. Results presented in Chapter 2 showed that the use of 1000 mJ/cm² MP UV increased the chlorine demand of ambient samples (DOC concentrations of 1.4-2.8 mg C/L) by between 25 to 50%, but this increase was not observed for ambient samples other than the OWASA RO concentrate

in these experiments. It is not clear why this would be the case for only ambient OWASA RO concentrate and not for bromide- and nitrate-spiked OWASA RO concentrate or the other OWASA fractions and SRNOM treated here. The THM4 formation results following MP UV irradiation and chlorination of the ambient RO concentrate shown in the next section also suggest that this sample may be anomalous.

Spiking with bromide (1 mg/L) and nitrate (10 mg N/L) also had little effect on chlorine demand. Results presented in Chapter 2 showed that samples spiked with bromide had an increased chlorine demand relative to ambient samples, presumably due to the formation of hypobromous acid (HOBr) from the oxidation of bromide by free chlorine (HOCl), which is known to react faster with organic precursors than aqueous chlorine (Rook et al. 1978; Westerhoff et al. 2004). However, the ratios of bromide to chlorine in those samples were much higher (0.18-0.38) compared to the samples treated for experiments reported here (0.04-0.06), which could explain why a similar increase was not observed. In addition, the longer chlorine contact time (72 hr here compared to 24 hr in Chapter 2 samples) allows the chlorine reaction to go further to completion and potentially “catch up” to the HOBr reaction. Spiking with nitrate was also shown to increase the chlorine demand 20-140% with the use of MP UV (186-1000 mJ/cm²) in Chapter 2, thought to be in part due to the reaction of chlorine with nitrite formed from nitrate photolysis (Margerum et al. 1994). The chlorine demand of the bromide- and nitrate-spiked hydrophobic acid fraction was increased 19% when MP UV was added, but other samples were not affected. The lack of change in chlorine demand for samples spiked with nitrate and treated with MP UV could also be a result of the lower nitrate to chlorine ratio in samples treated here compared to those described in Chapter 2.

Table 3-2. Effect of MP UV (1000 mJ/cm²) on the 72-hour chlorine demand of ambient (unspiked) spiked (10 mg N/L nitrate and 1 mg/L bromide) samples. Value is normalized by DOC content for comparison across the four water types.

Spiking	Treatment	Chlorine demand (mg Cl ₂ /mg C)			
		OWASA			SRNOM
		RO concentrate	hydrophobic acids	hydrophilic DOM	
ambient	HOCl alone	1.2	1.1	1.1	1.8
	MP UV + HOCl	1.6	1.1	1.1	2.0
bromide + nitrate	HOCl alone	1.3	1.1	1.2	1.9
	MP UV + HOCl	1.4	1.3	1.2	2.0

LP UV (500 mJ/cm²) and MP UV (1000 mJ/cm²) increased the chloramine demand in ambient and bromide- and nitrate-spiked SRNOM, but had no effect on the demand in the hydrophobic acid fraction, shown in Table 3-3. The chloramine demand in the ambient hydrophilic DOM fraction was decreased 12.5% with the use of either LP or MP UV, which was not observed for any other samples, including the bromide- and nitrate-spiked hydrophilic DOM. The error associated with replicate monochloramine residual measurements was ≤10%, so this change was not much greater than the analytical error. Regardless of UV dose, spiking with bromide and nitrate did not change the chloramine demand in the hydrophobic acid fraction, but increased the chloramine demand in the hydrophilic DOM fraction by between 22 and 40%, compared to the corresponding ambient sample. As previously noted, spiking with bromide did not significantly affect the chlorine demand in any of the samples, which may have been due to the lower bromide to chlorine ratio during chlorination (0.04-0.06) compared to that of chloramination (0.15-0.24).

Table 3-3. Effect of LP (500 mJ/cm²) and MP UV (1000 mJ/cm²) on the 72-hour chloramine demand of ambient and spiked (10 mg N/L nitrate and 1 mg/L bromide) samples. Value is normalized by DOC content for comparison across the three water types. Unfractionated RO concentrate samples were not treated with chloramine.

Spiking	Treatment	Chloramine demand (mg Cl ₂ /mg C)		
		OWASA		SRNOM
		hydrophobic acids	hydrophilic DOM	
ambient	NH ₂ Cl alone	0.38	0.45	0.33
	LP UV + NH ₂ Cl	0.38	0.40	0.38
	MP UV + NH ₂ Cl	0.39	0.40	0.38
bromide + nitrate	NH ₂ Cl alone	0.38	0.55	0.36
	LP UV + NH ₂ Cl	0.38	0.56	0.41
	MP UV + NH ₂ Cl	0.39	0.56	0.55

THM/HAA Formation

THM4 yields during chlorination ranged from 0.15 to 1.1 µmol/mg C. Values reported in the literature for chlorination of whole waters and isolated DOM fractions typically range from 0.2 to 0.7 µmol/mg C (Reckhow et al. 1990; Croué et al. 2000; Liang & Singer 2003; Hua & Reckhow 2007a) although higher values have been found. Miller and Uden (1983) showed a chloroform yield of 1.2 µmol/mg C following chlorination of fulvic acid extracts at pH 8. The addition of MP UV prior to chlorination increased THM4 formation in the OWASA RO concentrate, hydrophobic acid fraction, and SRNOM, compared to samples treated with only chlorine, suggesting that at these doses, UV irradiation increases the reactivity of THM precursors towards chlorine (Figure 3-5). The 120% increase in THM4 formation after MP UV pre-treatment in the ambient RO concentrate sample is significantly higher than what was observed in the

other water types here or in samples described in Chapter 2, where THM4 formation was increased up to 40% with 1000 mJ/cm² MP UV followed by chlorination, compared to chlorination alone with a dose adjusted to achieve the same target residual. Another recent study showed a 30-50% increase in THM4 formation when 1000 mJ/cm² MP UV was used prior to chlorination in coagulated and filtered drinking source waters, compared to samples treated with only chlorine, at a dose adjusted to achieve the same target residual (Dotson et al. 2010).

Spiking with bromide in the SRNOM and hydrophilic and hydrophobic acid fractions resulted in a shift to bromine-substituted THM4 species but did not change the THM4 molar yield. A shift to bromine-containing species was also observed for the OWASA RO concentrate, but THM4 molar yield increased 43% between ambient and bromide-spiked chlorinated samples. With MP UV treatment followed by chlorination in the RO concentrate, the molar THM4 yield was decreased by 52% between ambient and bromide-spiked samples, again suggesting that the ambient RO concentrate sample may have been anomalous. Bromine incorporation into THM4 and HAA9 is discussed in more detail in the following section.

The use of MP UV prior to chlorination increased HAA9 formation by 18% in the ambient RO concentrate, but had little effect on HAA9 production in other samples, shown in Figure 3-6. Precursors in the hydrophobic acid fraction of the OWASA RO concentrate contributed more to THM4 and HAA9 formation during chlorination than the hydrophilic DOM. This is consistent with previous studies that have shown hydrophobic DOM, which is rich in aromatic and phenolic-type structures, to be the main source of THM and HAA precursors during chlorination (Liang & Singer 2003, Hua & Reckhow

2007a). The contributions of THM4 formation from the hydrophobic acid and hydrophilic DOM fractions to that of the unfractionated RO concentrate were calculated using Equation 3-1 and are shown in Table 3-4. The combined THM4 formation in these fractions accounted for 95% of THM4 produced in the chlorinated ambient RO concentrate, which is higher than the corresponding bromide- and nitrate-spiked sample (63%). This is consistent with the anomalous THM4 formation and chlorine demand results noted earlier for ambient RO concentrate samples. Although Kitis and colleagues (2002) demonstrated nearly 100% recovery of THM4 and HAA9 formation potential during chlorination of hydrophilic and hydrophobic fractions obtained through XAD fractionation of an RO concentrate compared to the unfractionated water, this was significantly higher than the THM4 or HAA9 mass balance by these fractions for other samples in the present study (41-66%). Another study reported a 57% THM4 formation potential recovery from the sum of individual XAD fractions compared to the whole water, which is closer to the values that were obtained here (Chang et al. 2000).

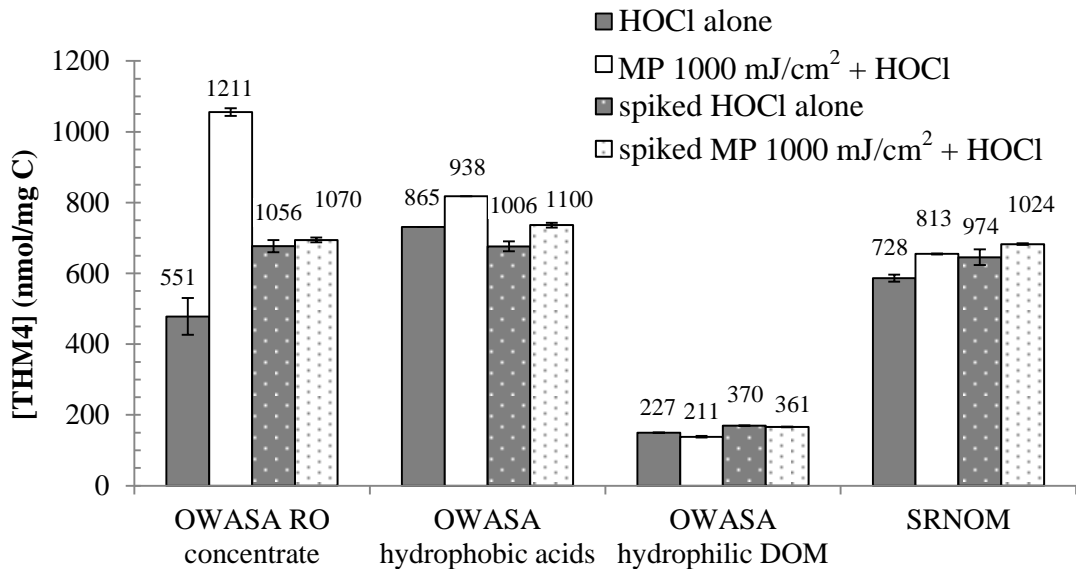


Figure 3-5. Effect of MP UV followed by chlorination on THM4 formation in ambient and spiked samples. THM4 molar concentration is normalized by DOC content for comparison across the four water types and value shown above bar is concentration in $\mu\text{g/L}$. Bar height represents average value and the range between duplicate samples is shown by the inset lines. Spiking amounts were 10 mg N/L nitrate and 1 mg/L bromide.

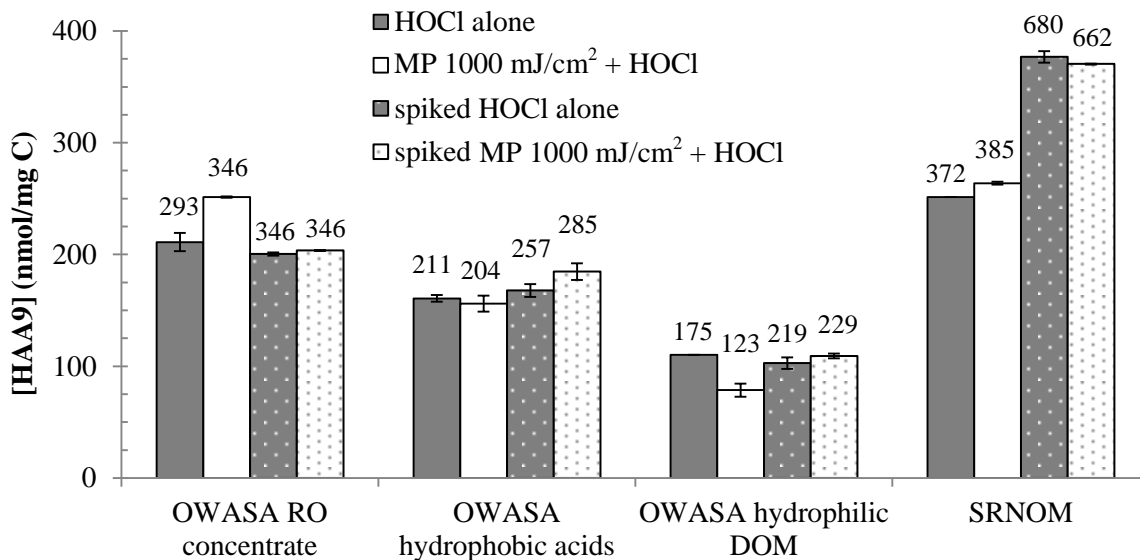


Figure 3-6. Effect of MP UV followed by chlorination on HAA9 formation in ambient and spiked samples. HAA9 molar concentration is normalized by DOC content for comparison across the four water types and value shown above bar is concentration in $\mu\text{g/L}$. Bar height represents average value and the range between duplicate samples is shown by the inset lines. Spiking amounts were 10 mg N/L nitrate and 1 mg/L bromide.

Table 3-4. Contribution of hydrophobic acid and hydrophilic DOM to THM4 and HAA9 molar formation in unfractionated RO concentrate.

Spiking	Treatment	% THM4 contribution		% HAA9 contribution	
		hydrophobic acids	hydrophilic DOM	hydrophobic acids	hydrophilic DOM
ambient	HOCl alone	90%	4.7%	45%	7.8%
	MP 1000 mJ/cm ² + HOCl	46%	2.0%	37%	4.7%
bromide + nitrate	HOCl alone	59%	3.8%	49%	7.7%
	MP 1000 mJ/cm ² + HOCl	63%	3.6%	53%	8.0%

LP and MP UV irradiation had little impact on THM4 formation from subsequent chloramination, shown in Figure 3-7. Spiking with bromide increased the molar yield of THM4 in the hydrophilic DOM fraction, which is consistent with the observed increase in chloramine demand compared to the corresponding ambient samples. UV had varying effects on HAA9 formation during chloramination (Figure 3-8). The use of MP UV prior to chloramination increased HAA9 formation by 24% in the bromide- and nitrate-spiked hydrophobic acid fraction, compared to the sample treated with only chloramine, but did not affect the corresponding ambient sample. HAA9 formation was increased 30% with the use of MP UV prior to chloramination in ambient SRNOM but not in the bromide- and nitrate-spiked SRNOM.

Overall, THM4 and HAA9 formation was higher during chlorination compared to chloramination, particularly for THM4 in the hydrophobic acid fraction. As observed with chlorination, the hydrophobic acid fraction had higher HAA9 formation compared to the hydrophilic fraction during chloramination. However, the hydrophilic fraction contributed more to THM4 formation during chloramination. Less research has looked at the formation of DBPs from chloramination of isolated organic precursor fractions in

comparison to chlorination, but Hua & Reckhow (2007a) showed that THM precursors were more hydrophilic compared to trihaloacetic acid precursors.

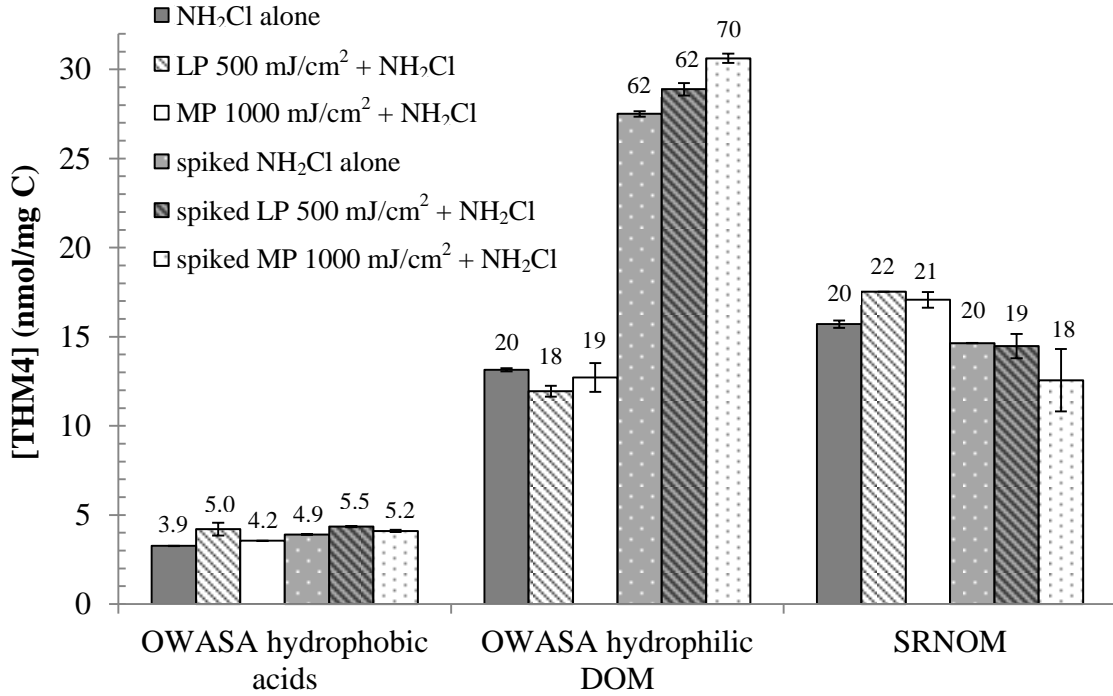


Figure 3-7. Effect of LP and MP UV followed by chloramination on THM4 formation in ambient and spiked samples. THM4 molar concentration is normalized by DOC content for comparison across the three water types and value shown above bar is concentration in $\mu\text{g/L}$. Bar height represents average value and the range between duplicate samples is shown by the inset lines.

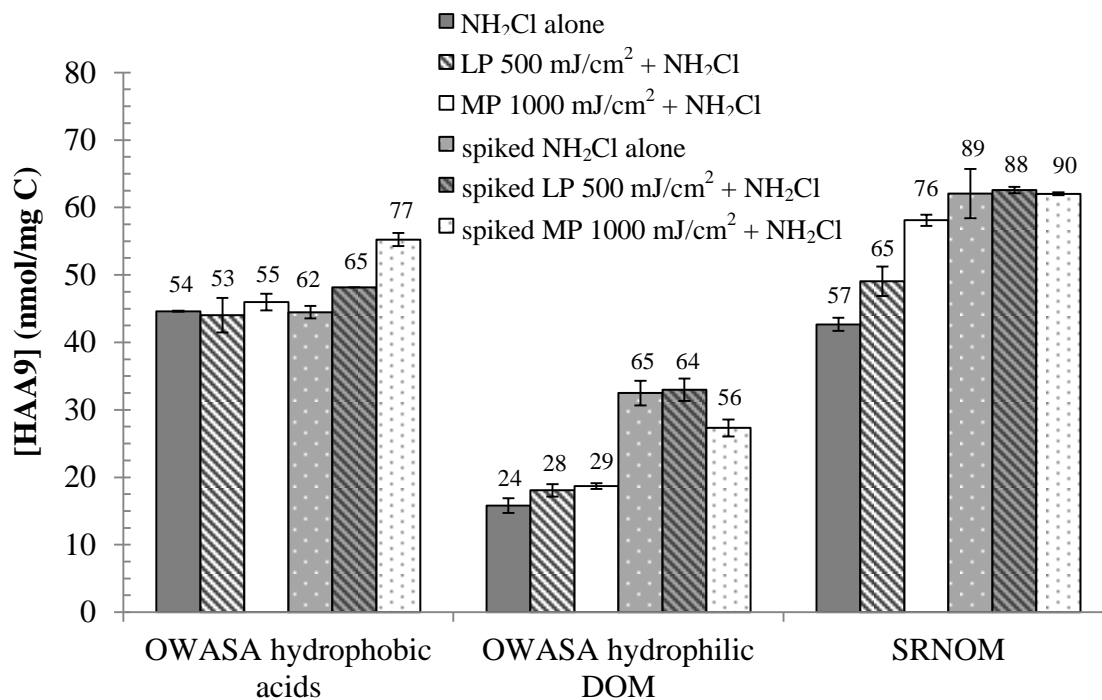


Figure 3-8. Effect of LP and MP UV followed by chloramination on HAA9 formation in ambient and spiked samples. HAA9 molar concentration is normalized by DOC content for comparison across the three water types and value shown above bar is concentration in $\mu\text{g/L}$. Bar height represents average value and the range between duplicate samples is shown by the inset lines.

Bromine Incorporation

Toxicological studies have shown that bromine-containing DBPs are more genotoxic and cytotoxic than their chlorine-containing counterparts (Richardson et al. 2008). For this reason, halogen speciation is of interest when evaluating DBP formation. If bromide is present during chlorination, it can be oxidized by free chlorine (HOCl) to form hypobromous acid (HOBr), an important halogenating agent, which results in the formation of bromine-substituted DBPs upon reaction with DOM. Aqueous bromine reacts faster with DOM than aqueous chlorine and when both are present, bromine tends to act more as a substituting agent while chlorine reacts preferentially as an oxidant

(Rook et al. 1978; Westerhoff et al. 2004). When bromide is present during chloramination, a similar reaction occurs to form active bromine species, including HOBr, NHBrCl, and NHBr₂ (Trofe et al. 1980; Bousher et al. 1989), which can react with DOM to form bromine-containing DBPs. A bromine incorporation factor (BIF) can be calculated among a class of halogenated DBPs using Equation 3-2 (Gould et al. 1981; Obolensky & Singer 2005):

$$BIF = \frac{\sum(\text{molar conc.} \times \# \text{ Br atoms})}{\sum(\text{molar conc.}) \times (\# \text{ halogen atoms})} \quad (3-2)$$

An example calculation for the BIF in THM4:

Species	Conc. (μM)
CHCl ₃	2.12
BrCl ₂ CH	2.43
Br ₂ ClCH	1.57
CHBr ₃	0.31
THM4	6.43

$$BIF = \frac{(2.12 \times 0) + (2.43 \times 1) + (1.57 \times 2) + (0.31 \times 3)}{(2.12 + 2.43 + 1.57 + 0.31) \times 3} = 0.34$$

The BIF was calculated for THM4 and di- and tri- haloacetic acids (X₂AA, X₃AA) for each of the waters used in this study. Tables 3-5, 3-6, and 3-7 show the THM4, X₂AA, and X₃AA BIF, respectively, for ambient compared to bromide- and nitrate-spiked samples during chlorination and chloramination. Bromine incorporation during chlorination was similar for each water across THM4, X₂AA, and X₃AA (e.g. OWASA RO concentrate = 0.34, 0.39, and 0.40 and SRNOM = 0.19, 0.20, and 0.26, respectively). Bromine incorporation was higher in the hydrophilic fraction compared to the hydrophobic acid fraction, which was expected based on previous research showing bromine to be more reactive with lower molecular weight, hydrophilic precursors (Liang & Singer 2003, Hua & Reckhow 2007a). This was further confirmed by a higher BIF in

the more hydrophilic OWASA RO concentrate compared to the SRNOM. During chloramination, dihaloacetic acids dominated the HAA9 pool, which was expected, as past work has shown only trace X₃AA formation after chloramination and suggests that X₂AA and X₃AA have different precursors and formation occurs by distinct pathways (Hua & Reckhow 2007b).

Table 3-5. THM4 bromine incorporation factor (BIF) during chlorination and chloramination of ambient and spiked samples.

Secondary disinfectant		THM4 BIF			
		OWASA			
		RO concentrate	hydrophobic acids	hydrophilic DOM	SRNOM
HOCl	ambient	0.02	0.001	0.17	<0.00003 ²
	bromide + nitrate	0.34	0.23	0.63	0.19
NH ₂ Cl	ambient	NA	<0.006	0.17	<0.001
	bromide + nitrate	NA	0.06	0.67	0.07

NA = not applicable, unfractionated RO concentrate was not treated with chloramine.

Table 3-6. X₂AA BIF during chlorination and chloramination of ambient and spiked samples.

Secondary disinfectant		X ₂ AA BIF			
		OWASA			
		RO concentrate	hydrophobic acids	hydrophilic DOM	SRNOM
HOCl	ambient	0.03	<0.002	0.15	<0.001
	bromide + nitrate	0.39	0.29	0.54	0.20
NH ₂ Cl	ambient	NA	<0.005	0.12	<0.004
	bromide + nitrate	NA	0.25	0.69	0.13

NA = not applicable, unfractionated RO concentrate was not treated with chloramine.

²The THM4 BIF detection limit was calculated for each sample using the detection limit for BrCl₂CH (0.1 µg/L, 0.61 nM) and the measured Cl₃CH concentration for that specific sample. For example, chlorinated ambient SRNOM formed 728 µg/L (6.1 µM) of Cl₃CH and <0.1 µg/L of BrCl₂CH, Br₂CICH, and Br₃CH (<0.61, <0.48, and <0.40 nM, respectively). The calculation for BIF detection limit would then be: (1*0.00061)/(3*6.1) = 0.00003. The same approach was used for X₂AA and X₃AA BIF detection limit calculations, using the detection limit of Br₂AA (0.4 µg/L, 1.8 nM) for X₂AA and BrCl₂AA (0.8 µg/L, 3.8 nM) for X₃AA. In some cases, all X₃AA species were below their detection limit, so a BIF detection limit could not be calculated.

Table 3-7. X₃AA BIF during chlorination and chloramination in ambient and spiked samples.

Secondary disinfectant		X ₃ AA BIF			
		OWASA			SRNOM
		RO concentrate	hydrophobic acids	hydrophilic DOM	
HOCl	ambient	0.05	<0.01	0.09	<0.001
	bromide + nitrate	0.40	0.19	0.62	0.26
NH ₂ Cl	ambient	NA	-*	0.10	-
	bromide + nitrate	NA	0.33	0.24	<0.0006

NA = not applicable, unfractionated RO concentrate was not treated with chloramine.

*BIF detection limit could not be calculated because all X₃AA species were below detection limit.

The effect of UV on THM₄, X₂AA, and X₃AA BIF in SRNOM samples is shown in Tables 3-8, 3-9, and 3-10, respectively. Spiking with bromide resulted in a shift to the bromine-containing species in all samples, but in general, UV did not further change the BIF. In one case (SRNOM spiked with bromide and nitrate) the THM₄ bromine incorporation doubled between chloramination alone and MP UV followed by chloramination (0.07 to 0.15), which was not observed in the corresponding ambient or bromide-only spiked samples. This suggests that the presence of nitrate during MP UV irradiation caused the increase in bromine incorporation, which could result from a change in DOM composition to smaller, more hydrophilic precursors. MP UV photolysis of nitrate produces hydroxyl radicals, which can break down DOM to form lower molecular weight, more hydrophilic structures (**Mopper and Zhou 1990; Goldstone et al. 2002, Sarathy and Mohseni 2007**). Although a change in precursor composition would also be expected to affect bromine incorporation during chlorination, the BIF in that case was already 0.19 without MP UV, so a small change might not be detectable or further influence bromine incorporation. The levels of THM₄ during chloramination

were much lower than those produced from chlorination (35- to 55-fold lower in SRNOM samples), and this shift in bromine incorporation corresponds to a 5 µg/L (3 nmol/mg C) increase in bromodichloromethane and 5 µg/L (1 nmol/mg C) decrease in trichloromethane (chloroform).

Table 3-8. Effect of LP (500 mJ/cm²) and MP UV (1000 mJ/cm²) on THM4 bromine incorporation during chlorination and chloramination of ambient and spiked SRNOM.

Treatment	THM4 BIF		
	ambient	bromide	bromide + nitrate
HOCl	<0.00003	0.20	0.19
LP UV + HOCl	<0.00003	0.19	0.19
MP UV + HOCl	<0.00003	0.18	0.19
NH ₂ Cl	<0.001	0.07	0.07
LP UV + NH ₂ Cl	<0.001	0.06	0.05
MP UV + NH ₂ Cl	<0.001	0.04	0.15

Table 3-9. Effect of LP (500 mJ/cm²) and MP UV (1000 mJ/cm²) on dihaloacetic acid (X₂AA) BIF during chlorination and chloramination of ambient and spiked SRNOM.

Treatment	X ₂ AA BIF		
	ambient	bromide	bromide + nitrate
HOCl	<0.001	0.20	0.20
LP UV + HOCl	<0.001	0.19	0.19
MP UV + HOCl	<0.001	0.19	0.19
NH ₂ Cl	<0.004	0.13	0.13
LP UV + NH ₂ Cl	<0.004	0.12	0.11
MP UV + NH ₂ Cl	<0.003	0.10	0.16

Table 3-10. Effect of LP (500 mJ/cm²) and MP UV (1000 mJ/cm²) on trihaloacetic acid (X₃AA) BIF during chlorination and chloramination of ambient and spiked SRNOM.

Treatment	X ₃ AA BIF		
	ambient	bromide	bromide + nitrate
HOCl	<0.001	0.25	0.26
LP UV + HOCl	<0.001	0.25	0.22
MP UV + HOCl	<0.001	0.24	0.26
NH ₂ Cl	.*	<0.0006	<0.0006
LP UV + NH ₂ Cl	-	<0.0006	<0.0007
MP UV + NH ₂ Cl	-	<0.0006	<0.0006

*BIF detection limit could not be calculated because all X₃AA species were below detection limit.

Chloropicrin and Chloral Hydrate Formation

Results presented in Chapter 2 showed that the use of UV prior to chlorination or chloramination increased halonitromethane (chloropicrin and bromopicrin) formation in the presence of nitrate and increased production of chloral hydrate, regardless of nitrate content. The contribution of different organic precursors to these formation processes was further explored in this fractionation study.

Chloropicrin formation increased more than three-fold in ambient RO concentrate and hydrophilic DOM samples when MP UV was used prior to chlorination (Figure 3-9), but was below detection limit (<0.1 µg/L, <0.06 nmol/mg C) in all ambient SRNOM and hydrophobic acid fraction samples. MP UV followed by chlorination or chloramination formed 23 µg/L (13 nmol/mg C) and 17 µg/L (9.9 nmol/mg C) of chloropicrin, respectively, in SRNOM samples spiked with bromide and nitrate (Figure 3-10). The corresponding LP UV + chlorine/chloramine or chlorine/chloramine alone samples formed less than 0.1 µg/L (0.06 nmol/mg C) chloropicrin. Bromide- and nitrate-spiked

RO concentrate samples that were treated with chlorine and MP UV + chlorine formed 1.5 $\mu\text{g/L}$ (1.0 nmol/mg C) and 2.8 $\mu\text{g/L}$ (1.8 nmol/mg C) chloropicrin, respectively.

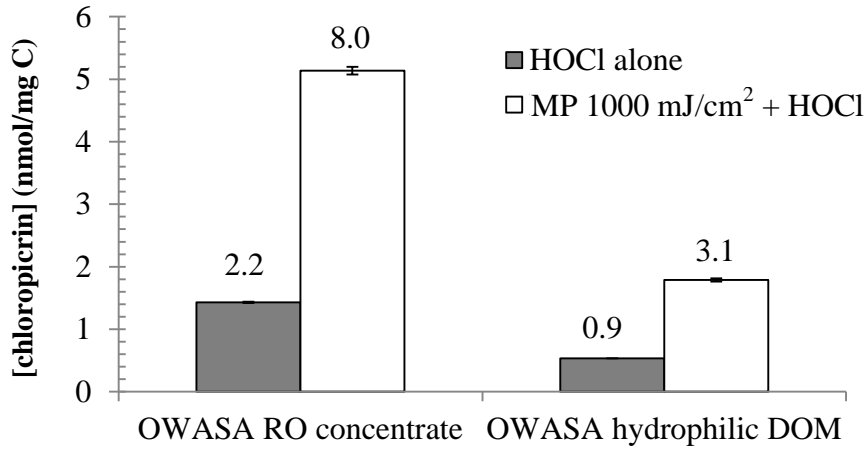


Figure 3-9. Effect of MP UV followed by chlorination on chloropicrin formation in ambient samples. Chloropicrin molar concentration is normalized by DOC content for comparison between the two water types and value shown above bar is concentration in $\mu\text{g/L}$. Bar height represents average value and the range between duplicate samples is shown by the inset lines.

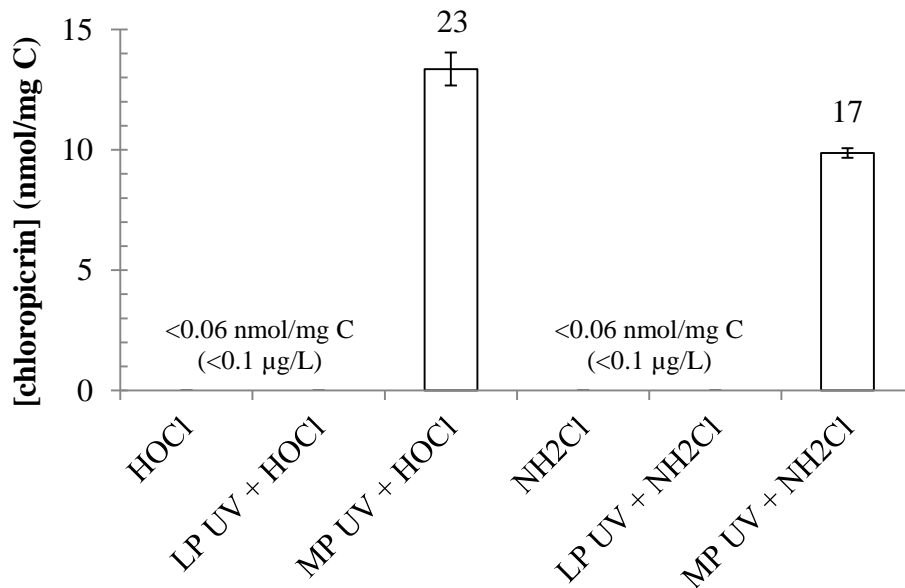


Figure 3-10. Effect of LP (500 mJ/cm²) and MP UV (1000 mJ/cm²) followed by chlorination and chloramination on chloropicrin formation in nitrate-spiked SRNOM samples. Chloropicrin molar concentration is normalized by DOC content and value shown above bar is concentration in $\mu\text{g/L}$. Bar height represents average value and the range between duplicate samples is shown by the inset lines.

An increase in chloropicrin formation with MP UV, but not LP UV, has been previously observed by Reckhow et al. (2010), and is thought to be due to the formation of reactive nitrogen species (e.g. $\cdot\text{NO}_2$) from MP UV photolysis of nitrate that can act as nitrating agents towards aromatic DOM components. The resulting nitro organics can further react with chlorine or chloramine to form chloropicrin. These reactions are discussed in more detail in Chapter 2. Nitrate absorbs primarily below 240 nm so LP UV, which has a nearly monochromatic output at 254 nm, results in less formation of reactive nitrogen species than MP UV, which has a polychromatic output from 200 to 400 nm. The quantum yields of $\cdot\text{NO}_2$ from UV photolysis of nitrate at 205 and 254 nm are 0.13 and 0.037, respectively (Goldstein & Rabani 2007). Pre-ozonation followed by chlorination has been shown to increase chloropicrin formation (Merlet et al. 1985; Hoigne & Bader 1988; Krasner et al. 2006) although the actual mechanism has not been experimentally proven.

In this study, samples were spiked with bromide and nitrate or just bromide, but not nitrate alone. Spiking with bromide likely resulted in a shift to the bromine-substituted counterpart, bromopicrin (tribromonitromethane). At the time of these analyses, however, a GC injector temperature of 200°C was being used, which can result in degradation of bromopicrin (Chen et al. 2002). The injector temperature was changed to 117°C for subsequent experiments to minimize this breakdown, but quantitative bromopicrin results were not obtained for the fractionation study. One explanation for the higher chloropicrin yield in bromide- and nitrate-spiked SRNOM samples compared to the spiked RO concentrate is that since bromine incorporation was higher in the RO concentrate, bromopicrin formation was favored and less chloropicrin was produced.

Similarly, this makes interpretation of chloropicrin formation between chlorination and chloramination of bromide- and nitrate-spiked SRNOM difficult. Chlorination typically results in higher levels of chloropicrin compared to chloramination, and to a greater extent with pre-ozonation (Hu et al. 2010), but the results presented here showed only slightly higher formation when MP UV was used prior to chlorination vs. chloramination (23 µg/L vs. 17 µg/L). Bromine incorporation was shown to be higher with chlorination compared to chloramination in SRNOM samples (Tables 3-5 and 3-6) so it is likely that more bromopicrin was formed in MP UV + chlorine treated SRNOM compared to the corresponding chloramine-treated samples, resulting in a higher total halonitromethane formation than apparent from the chloropicrin results alone. Results presented in Chapter 2 (e.g. Table 2-5) showed that chloropicrin formation was ten-fold higher with chlorination compared to chloramination in a sample spiked with nitrate only and pre-treated with 1000 mJ/cm² MP UV.

Chloropicrin was below detection limit (<0.1 µg/L, <0.06 nmol/mg C) in the chlorinated OWASA hydrophobic acid fraction samples, which is consistent with past work that has shown higher chloropicrin yields after chlorination of hydrophilic DOM isolates compared to the hydrophobic acid and transphilic acid fractions (Hu et al. 2010). However, the formation of chloropicrin from chlorine and MP UV + chlorine treatment of the hydrophilic DOM fraction only accounted for 5.6% and 5.2%, respectively, of the chloropicrin produced in corresponding RO concentrate samples, using Equation 3-1. This suggests that chloropicrin precursors are also contained in other DOM fractions. The fractionation carried out by the Hu et al. (2010) only isolated hydrophobic acid and transphilic acid fractions. In another study that isolated an additional 7 fractions, Dotson

et al. (2009) also demonstrated higher formation of chloropicrin following chlorination of hydrophilic DOM compared to hydrophobic acid and transphilic acid fractions, but found that additional fractions (hydrophobic bases/neutrals, transphilic & hydrophobic amphoteric) contributed to chloropicrin formation.

Formation of chloral hydrate (the hydrated version of trichloroacetaldehyde) was increased 60% and 20% in ambient RO concentrate and SRNOM, respectively, when MP UV was used prior to chlorination, compared to chlorination alone (Figure 3-11), which is consistent with the higher chlorine demand and THM4 formation observed for the ambient RO concentrate compared to SRNOM with the addition of MP UV. The corresponding bromide- and nitrate-spiked RO concentrate and SRNOM samples showed chloral hydrate increases of 16% and 20% with MP UV and chlorination, compared to chlorination alone. Its formation in chlorine and MP UV + chlorine treated hydrophobic acid samples was considerably lower (0.3-0.4 µg/L) than in hydrophilic DOM (40 µg/L). With LP UV (500 mJ/cm²) followed by chlorination, chloral hydrate formation was increased 11% in ambient SRNOM samples.

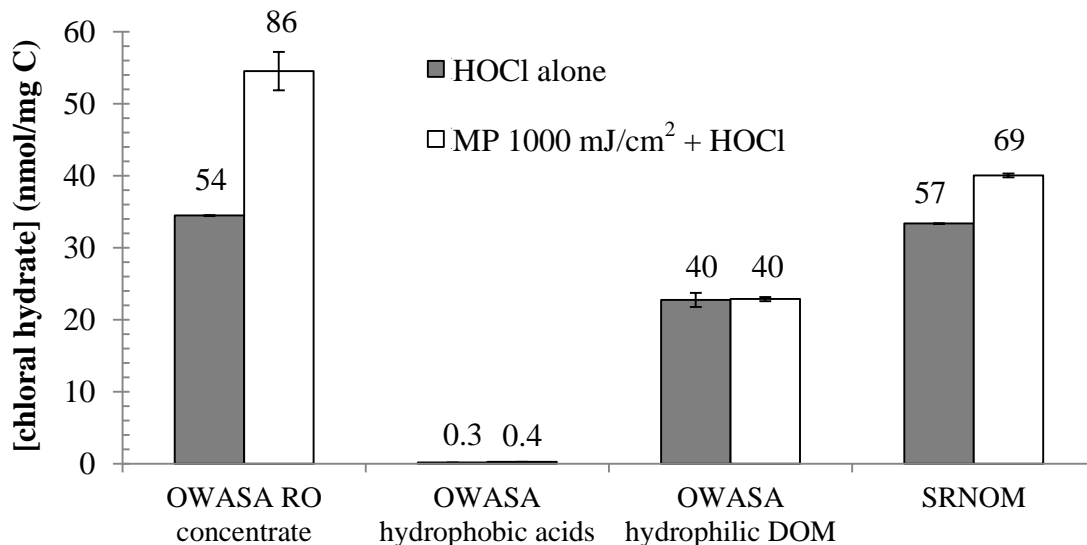


Figure 3-11. Effect of MP UV followed by chlorination on chloral hydrate formation in ambient samples. Chloral hydrate concentration is normalized by DOC content for comparison between the four water types and value shown above bar is concentration in $\mu\text{g/L}$. Bar height represents average value and the range between duplicate samples is shown by the inset lines.

Past work has identified amino acids and acetaldehyde as two main precursors for chloral hydrate formation during chlorination and chloramination (Trehy et al. 1986; McKnight & Reckhow 1992). Amine-type precursors are associated with more hydrophilic NOM (Krasner et al. 1996), which explains the higher chloral hydrate formation observed in the hydrophilic DOM compared to the hydrophobic acid fraction in this study. Aldehydes can be produced from ozonation or UV irradiation of NOM (Yamada & Somiya 1989; Liu et al. 2002). Thus, the increased chloral hydrate formation observed in this work when UV was used prior to chlorination of the unfractionated RO concentrate and SRNOM was likely due to the formation of acetaldehyde which can further react with chlorine to form chloral hydrate. The limited formation of chloral hydrate in the hydrophobic acid fraction and lack of change in the hydrophilic DOM with the addition of MP UV prior to chlorination suggests that UV-induced precursors were

not generated from these fractions and may be present in another fraction, such as the transphilic DOM or base/neutral fractions that were not analyzed in this study.

During chloramination, chloral hydrate was not detected ($<0.1 \mu\text{g/L}$, $<0.06 \text{ nmol/mg C}$) in the hydrophobic acid fraction or SRNOM (RO concentrate was not treated with chloramine) but was formed in the hydrophilic DOM samples, although at much lower levels compared to chlorination ($2.6 \mu\text{g/L}$ for chloramine alone compared to $40 \mu\text{g/L}$ for chlorine alone). This is consistent with previous research that has shown higher chloral hydrate yields during chlorination compared to chloramination (Jacangelo et al. 1989; Koch & Krasner 1989; Dixon & Lee 1991). The use of 1000 mJ/cm^2 MP UV prior to chloramination increased chloral hydrate formation by 16% in the hydrophilic DOM fraction, which corresponded to a change of only $0.4 \mu\text{g/L}$ (0.2 nmol/mg C). If the same amount of UV-induced precursor were to react with chlorine to form chloral hydrate, this change would not be detectable above the background level formed from chlorine alone ($40 \mu\text{g/L}$, 23 nmol/mg C).

The combined contributions of hydrophilic DOM and hydrophobic acid fractions (calculated from Equation 3-1) accounted for 11% and 6% of the chloral hydrate produced in chlorinated and MP UV + chlorine treated RO concentrate samples, respectively (Table 3-11), suggesting that other fractions not analyzed here contained chloral hydrate precursors. Alternatively, the low mass balance recoveries observed for both chloral hydrate and chloropicrin in this study may indicate that the fractionation procedure altered the reactivity of precursors for these DBPs. Previous work has demonstrated that THM4 and HAA9 precursor reactivity can be conserved through XAD fractionation (Kitis et al. 2002), but chloral hydrate and chloropicrin have different

precursors and these may not behave the same as the more hydrophobic THM4 and HAA9 precursors through XAD fractionation procedures.

Table 3-11. Contribution of hydrophobic acids and hydrophilic DOM to chloral hydrate molar formation in unfractionated RO concentrate.

Spiking	Treatment	% chloral hydrate contribution	
		hydrophobic acids	hydrophilic DOM
ambient	HOCl alone	0.3%	10%
	MP 1000 mJ/cm ² + HOCl	0.2%	6.1%

3.4 Conclusions

Although the conditions applied in this study are not typical of full-scale drinking water treatment, the use of waters containing concentrated organic precursors and scaled-up doses of UV-chlorine/chloramine allowed for an investigation of trends and UV effects on different organic precursors. The main findings and implications of this study include:

- SRNOM and OWASA RO concentrate had similar hydrophobic acid/hydrophilic precursor composition based on XAD resin fractionation; however, their reactivities (e.g. chlorine demand, HAA9 and chloropicrin formation, halogen speciation) were quite different. The implication of this finding is that hydrophobic acid/hydrophilic DOM character alone is not sufficient for predicting DBP formation across water types under different treatment conditions. Results presented in Chapter 4 explore the use of another characterization technique, fluorescence, which may be a better tool for predicting DOM reactivity.

- MP UV (1000 mJ/cm^2) increased the chlorine demand in OWASA RO concentrate by 33% and increased THM4 formation in the RO concentrate and hydrophobic acid fraction and SRNOM, suggesting that, at these doses, MP UV irradiation enhances the reactivity of THM4 precursors towards chlorine.
- Bromine incorporation into THM4 and HAA9 was higher in hydrophilic DOM than for hydrophobic acids and was higher in the OWASA RO concentrate compared to the more hydrophobic SRNOM. UV had little effect on bromine incorporation into THMs and HAAs, even with MP UV at 1000 mJ/cm^2 .
- Regardless of UV dose, the hydrophilic DOM contributed more to chloropicrin and chloral hydrate production during chlorination and chloramination compared to the hydrophobic acids fraction.
- Chloropicrin formation increased three-fold in ambient OWASA RO concentrate and the hydrophilic DOM fraction with 1000 mJ/cm^2 MP UV followed by chlorination, compared to samples treated with the same dose of chlorine but without UV. This similar increase suggests that the UV-induced reactions responsible for chloropicrin formation occur to the same extent within hydrophilic DOM as the whole water and that high MP UV doses may result in a shift to more hydrophilic precursors.
- MP UV followed by chlorination increased chloral hydrate formation in ambient OWASA RO concentrate (60%) and SRNOM (20%), compared to samples treated with only chlorine at the same dose. In the corresponding bromide- and nitrate-spiked samples, chloral hydrate was increased 16% (RO concentrate) and 20% (SRNOM) by MP UV. These results suggest that MP UV is increasing hydrophilic

precursors, which were shown to contribute more than hydrophobic acids to chloral hydrate formation.

- If MP UV irradiation increases hydrophilic precursors, as several findings presented here have indicated, the formation potential of these DBPs (and other halonitromethane and haloaldehyde species) would be expected to increase with MP UV pre-treatment and subsequent chlorination and chloramination. This has public health implications, as these DBPs are thought to be more geno- and cytotoxic than the regulated THMs and HAAs.
- There was no change in chloral hydrate formation from the UV-treated hydrophilic DOM fraction when followed by chlorination, compared to the corresponding sample treated with the same dose of chlorine but no UV pre-treatment, suggesting that the main source of UV-induced precursors are not contained in this fraction and may be present in the transphilic DOM, neutral/base or another fraction not analyzed here.
- The relatively low mass balance recoveries of chloral hydrate and chloropicrin formation in XAD fractions of the RO concentrate compared to their formation in the unfractionated water (<10%), in contrast to THM4 and HAA9 recoveries (42-95%), suggests that either the fractions not analyzed for this work may have significant chloral hydrate and chloropicrin precursors or that the XAD fractionation procedure may alter the reactivity of precursors to these DBPs.

Sources Cited for Chapter 3

- APHA (American Public Health Association), American Water Works Association, and Water Environment Federation, 1999. Standard Methods for the Examination of Water and Wastewater. 20th Edition, American Public Health Association: Washington DC.
- Baalousha, M. et al., 2006. Conformation and size of humic substances: effects of major cation concentration and type, pH, salinity, and residence time. *Colloids and Surfaces A: Physicochemical and Engineering Aspects*, 272(1-2), pp.48-55.
- Bolton, J.R. & Linden, K.G., 2003. Standardization of methods for fluence (UV dose) determination in bench-scale UV experiments. *Journal of Environmental Engineering*, 129(3), pp.209-216.
- Bousher, A. et al., 1989. Kinetics of reactions in solutions containing monochloramine and bromide. *Water Research*, 23(8), pp.1049-1058.
- Brophy, K.S. et al., 2000. Quantification of nine haloacetic acids using gas chromatography with electron capture detection. In *Natural Organic Matter and Disinfection By-Products, ACS Symposium Series 761*. American Chemical Society, pp.343-355.
- Calderon, R.L., 2000. The epidemiology of chemical contaminants of drinking water. *Food and Chemical Toxicology*, 38(S1), pp.S13-20.
- Cantor, K.P. et al., 1998. Drinking water source and chlorination byproducts I. Risk of bladder cancer. *Epidemiology*, 9(1), pp.21-28.
- Chang, C.-N. et al., 2000. Characterization and isolation of natural organic matter from a eutrophic reservoir. *Journal of Water Supply: Research and Technology – AQUA*, 49(5), pp.269-280.
- Chen, P.H. et al., 2002. Hydrogen abstraction and decomposition of bromopicrin and other trihalogenated disinfection byproducts by GC / MS. *Environmental Science & Technology*, 36(15), pp.3362-3371.
- Christman, R.F. et al., 1983. Identity and yields of major halogenated products of aquatic fulvic acid chlorination. *Environmental Science & Technology*, 17(10), pp.625-628.
- Croué, J.-P. et al., 2000. *Characterization of Natural Organic Matter in Drinking Water*, American Water Works Association and Water Research Foundation: Denver, Colorado.

- Dixon, K.L. & Lee, R.G., 1991. Disinfection by-products control: A survey of American system treatment plants. In: *Proceedings of the AWWA Annual Conference*, Philadelphia, Pennsylvania.
- Dotson, A.D. et al., 2009. Nitrogen enriched dissolved organic matter (DOM) isolates and their affinity to form emerging disinfection by-products. *Water Science and Technology*, 60(1), pp.135-143.
- Dotson, A.D. et al., 2010. UV/H₂O₂ treatment of drinking water increases post-chlorination DBP formation. *Water Research*, 44(12), pp.3703-3713.
- Edzwald, J.K. et al., 1985. Surrogate parameters for monitoring organic matter and THM precursors. *Journal American Water Works Association*, 77(4), pp.122-132.
- Goldstein, S. & Rabani, J., 2007. Mechanism of nitrite formation by nitrate photolysis in aqueous solutions: the role of peroxyxynitrite, nitrogen dioxide, and hydroxide radical. *Journal of the American Chemical Society*, 129(34), pp.10597-10601.
- Goldstone, J.V. et al., 2002. Reactions of hydroxyl radical with humic substances: bleaching, mineralization, and production of bioavailable carbon substrates. *Environmental Science & Technology*, 36(3), pp.364-372.
- Gould, J.P. et al., 1981. Formation of brominated trihalomethanes-extent and kinetics. In *4th Conference on Water Chlorination*. Ann Arbor, Michigan.
- Hoigne, J. & Bader, H., 1988. The formation of trichloronitromethane (chloropicrin) and chloroform in a combined ozonation/chlorination treatment of drinking water. *Water Research*, 22(3), pp.313-319.
- Hu, J. et al., 2010. Halonitromethane formation potentials in drinking waters. *Water Research*, 44(1), pp.105-114.
- Hua, G. & Reckhow, D.A., 2007a. Characterization of disinfection byproduct precursors based on hydrophobicity and molecular size. *Environmental Science & Technology*, 41(9), pp.3309-3315.
- Hua, G. & Reckhow, D.A., 2007b. Comparison of disinfection byproduct formation from chlorine and alternative disinfectants. *Water Research*, 41(8), pp.1667-1678.
- Kitis, M. et al., 2001a. The reactivity of natural organic matter to disinfection by-products formation and its relation to specific ultraviolet absorbance. *Water Science and Technology*, 43(2), pp.9-16.
- Kitis, M. et al., 2001b. Isolation of dissolved organic matter (DOM) from surface waters using reverse osmosis and its impact on the reactivity of DOM to formation and speciation of disinfection by-products. *Water Research*, 35(9), pp.2225-2234.

- Kitis, M. et al., 2002. Probing reactivity of dissolved organic matter for disinfection by-product formation using XAD-8 resin adsorption and ultrafiltration fractionation. *Water Research*, 36(15), pp.3834-3848.
- Koch, B. & Krasner, S.W., 1989. Occurrence of disinfection byproducts in a distribution system. In: *Proceedings of the AWWA Annual Conference*, Los Angeles, California.
- Krasner, S.W. et al., 1996. Three approaches for characterizing NOM. *Journal American Water Works Association*, 88(6), pp.66-79.
- Krasner, S.W. et al., 2006. Occurrence of a new generation of disinfection byproducts. *Environmental Science & Technology*, 40(23), pp.7175-7185.
- Leenheer, J.A., 1981. Comprehensive approach to preparative isolation and fractionation of dissolved organic carbon from natural waters and wastewaters. *Environmental Science & Technology*, 15(5), pp.578-587.
- Leenheer, J.A. et al., 2000. Comprehensive isolation of natural organic matter from water for spectral characterizations and reactivity testing. In: *Natural Organic Matter and Disinfection By-Products*. ACS Symposium Series 761. American Chemical Society, pp.68-83.
- Liang, L. & Singer, P.C., 2003. Factors influencing the formation and relative distribution of haloacetic acids and trihalomethanes in drinking water. *Environmental Science & Technology*, 37(13), pp.2920-2928.
- Liu, W. et al., 2002. Comparison of disinfection byproduct (DBP) formation from different UV technologies at bench scale. *Water Science & Technology: Water Supply*, 2(5-6), pp.515-521.
- Loper, J.C. et al., 1978. Residue organic mixtures from drinking water show in vitro mutagenic and transforming activity. *Journal of Toxicology and Environmental Health, Part A*, 4(5-6), pp.919-38.
- Malley, J.P. et al., 1995. *Evaluation of the Byproducts Produced from the Treatment of Groundwaters with Ultraviolet Irradiation*, American Water Works Association and Water Research Foundation: Denver, Colorado.
- Margerum, D.W. et al., 1994. Water chlorination chemistry: nonmetal redox kinetics of chloramine and nitrite ion. *Environmental Science & Technology*, 28(2), pp.331-337.
- McKnight, A. & Reckhow, D.A., 1992. Reactions of ozonation by-products with chlorine and chloramines. In: *Proceedings of the AWWA Annual Conference*, Vancouver, British Columbia.

- Merlet, N. et al., 1985. Chloropicrin formation during oxidative treatments in the preparation of drinking water. *Science of the Total Environment*, 47, pp.223-228.
- Miller, J.W. & Uden, C., 1983. Characterization of nonvolatile aqueous chlorination products of humic substances. *Environmental Science & Technology*, 17(3), pp.150-157.
- Mopper, K. & Zhou, X., 1990. Hydroxyl radical photoproduction in the sea and its potential impact on marine processes. *Science*, 250(4981), pp.661-664.
- Obolensky, A. & Singer, P.C., 2005. Halogen substitution patterns among disinfection byproducts in the information collection rule database. *Environmental Science & Technology*, 39(8), pp.2719-2730.
- Plewa, M.J. et al., 2004. Halonitromethane drinking water disinfection byproducts: chemical characterization and mammalian cell cytotoxicity and genotoxicity. *Environmental Science & Technology*, 38(1), pp.62-68.
- Reckhow, D.A. et al., 1990. Chlorination of humic materials: byproduct formation and chemical interpretations. *Environmental Science & Technology*, 24(11), pp.1655-1664.
- Reckhow, D.A. et al., 2010. Effect of UV treatment on DBP formation. *Journal American Water Works Association*, 102(6), pp.100-113.
- Richardson, S.D. et al., 2008. Occurrence and mammalian cell toxicity of iodinated disinfection byproducts in drinking water. *Environmental Science & Technology*, 42(22), pp.8330-8338.
- Rook, J.J. et al., 1978. Bromide oxidation and organic substitution in water treatment. *Journal of Environmental Science and Health, Part A*, A13(2), pp.91-116.
- Sarathy, S.R. & Mohseni, M., 2007. The impact of UV/H₂O₂ advanced oxidation on molecular size distribution of chromophoric natural organic matter. *Environmental Science & Technology*, 41(24), pp.8315-8320.
- Schreiber, I.M. & Mitch, W.A., 2005. Influence of the order of reagent addition on NDMA formation during chloramination. *Environmental Science & Technology*, 39(10), pp.3811-3818.
- Song, H. et al., 2009. Isolation and fractionation of natural organic matter: evaluation of reverse osmosis performance and impact of fractionation parameters. *Environmental Monitoring and Assessment*, 153(1-4), pp.307-321.
- Thurman, E.M., 1985. *Organic Geochemistry of Natural Waters*, Dordrecht, the Netherlands: M. Nijhoff Publishers.

- Trehy, M.L. et al., 1986. Chlorination byproducts of amino acids in natural waters. *Environmental Science & Technology*, 20(11), pp.1117-1122.
- Trofe, T.W. et al., 1980. Kinetics of monochloramine decomposition in the presence of bromide. *Environmental Science & Technology*, 14(5), pp.544-549.
- U.S. EPA (Environmental Protection Agency), 2006. *National Primary Drinking Water Regulations: Long Term 2 Enhanced Surface Water Treatment Rule, Final Rule*. Federal Register, 71(2), pp.653-702.
- Weinberg, H.S. et al., 2002. *The Occurrence of Disinfection By-Products (DBPs) of Health Concern in Drinking Water: Results of a Nationwide DBP Occurrence Study*. EPA/600/R/-02/068, U.S. EPA: Athens, Georgia.
- Westerhoff, P. et al., 2004. Reactivity of natural organic matter with aqueous chlorine and bromine. *Water Research*, 38(6), pp.1502-1513.
- Yamada, H. & Somiya, I., 1989. The determination of carbonyl compounds in ozonated water by the PFBOA method. *Ozone: Science & Engineering*, 11(2), pp.127-141.

Chapter 4: Investigating Changes in Dissolved Organic Matter Fluorescence and Disinfection Byproduct Formation from UV and Subsequent Chlorination/Chloramination

4.1 Introduction

Dissolved organic matter (DOM), formed from plant and microbial decay products, is present in all natural waters and plays an important role in many natural and engineered processes (Christman et al. 1983; Lovley et al. 1996; Markager & Vincent 2000; Maranger & Pullin 2003; Kwon et al. 2005). It is the main precursor in the formation of disinfection byproducts (DBPs) of potential human health concern (Loper et al. 1978; Cantor et al. 1998) during drinking water treatment. DBPs are produced when DOM reacts with a disinfectant, such as chlorine, as well as chemicals in water which can be of natural origin (e.g. bromide, iodide) or anthropogenic pollutants. Trihalomethanes (THMs) and haloacetic acids (HAAs) are two of the major DBP classes formed during chlorination, and a subset of these are regulated in the United States (U.S. EPA 2006).

As anthropogenic activity continues to stress source water quality and more stringent DBP regulations come into effect, utilities are looking towards alternative treatment processes to traditionally practiced chlorination. A nationwide occurrence study of drinking water treatment plants across the United States found that the use of some other disinfectants (chloramine, chlorine dioxide, ozone) decreased the formation of

regulated THMs and HAAs, but in many cases, these processes increased the formation of other DBPs that are thought to be more geno- and cytotoxic than those that are currently regulated (Krasner et al. 2006). An alternative process stream uses ultraviolet (UV) irradiation as a primary disinfectant in treatment plants employing chlorination or chloramination for secondary disinfection. The majority of past work that has evaluated combined UV-chlorine/chloramine treatment found little effect on regulated DBPs when UV was applied at disinfection doses (40-186 mJ/cm²) (Malley et al. 1995; Liu et al. 2002; Dotson et al. 2010), but less research has focused on the formation of emerging, unregulated DBPs which are thought to be more toxicologically potent (Plewa et al. 2008). In one study that did look at additional DBP classes, Reckhow et al. (2010) observed an increase in chloropicrin (trichloronitromethane) formation following medium pressure (MP, polychromatic output 200 to 400 nm) UV irradiation (40-140 mJ/cm²) and post-chlorination compared to chlorination alone in source waters containing nitrate (1-10 mg N/L). The relative importance of source water characteristics (e.g. nitrate or DOM concentration and quality) leading to increased chloropicrin after UV treatment are not well understood and require further study to evaluate the implications of integrating UV into the overall drinking water production process.

Average characteristics of DOM are often studied to better understand and predict DBP formation, because DOM is a dynamic and heterogeneous mixture comprised of thousands of chemical moieties that vary spatially and temporally in source waters (McKnight & Aiken 1998). Fluorescence spectroscopy is a relatively quick, simple, and sensitive technique that is being increasingly applied for DOM characterization and monitoring (Hudson et al. 2007). Past work has identified different types and sources of

organic matter that correspond with fluorescence excitation-emission matrix (EEM) regions such as humic- and protein-like DOM (Coble 1996). The application of parallel factor analysis (PARAFAC), a statistical modeling technique, to EEM data allows for quantitative identification of mathematically and chemically independent components within the fluorescing material of DOM (Stedmon et al. 2003). These components can be associated with aliphatic or aromatic character, microbial- vs. terrestrial-derived DOM, and some have been identified as quinone- or protein-like compounds (Cory & McKnight 2005).

Two recent studies used fluorescence and PARAFAC to track DOM fate through drinking water and recycled water treatment plants (Baghoth et al. 2011; Murphy et al. 2011). Baghoth and colleagues (2011) observed changes in component fluorescence across different drinking water treatment processes that were consistent with previous work that used more laborious techniques (e.g. high performance liquid chromatography, nuclear magnetic resonance spectroscopy) to follow DOM chemistry and removal during treatment. For example, coagulation showed preferential removal of higher molecular weight, humic-like components, and ozone reacted with humic-like components more than with protein-like components.

There is potential to use fluorescence/PARAFAC to understand linkages between DOM source and DBP formation, particularly for evaluating the effects of different treatment processes on these parameters. Promising past work has investigated correlations between fluorescence and DBP formation potential (Yang et al. 2008; Roccaro et al. 2009), and a few studies have related individual fluorescing DOM components with regulated THMs and HAAs (Johnstone et al. 2009; Hua et al. 2010;

Beggs & Summers 2011; Pifer & Fairey 2012). Beggs and Summers (2011) found that an aromatic humic-like component correlated with regulated THM and HAA formation following chlorination ($R^2 = 0.89$ and 0.69 , respectively), while polyphenolic and protein-like components showed little correlation ($R^2 \leq 0.40$). However, while this approach has promise, very little work has investigated the linkages between DOM fluorescence and unregulated byproducts that are potentially more geno- and cytotoxic than the regulated THMs and HAAs.

Because past studies have shown that understanding the changes in DOM constituents that result from various treatment processes can provide valuable information on DBP precursors and DBP formation pathways, the objective of this study was to evaluate and relate changes in DOM fluorescence to DBP formation during sequenced MP UV processes (i.e. UV followed by chlorine or chloramine). Samples were analyzed by fluorescence spectroscopy and a range of DBPs were measured following MP UV-chlorine/chloramine treatment and compared to samples without UV but with a chlorine or chloramine dose adjusted to obtain a similar target residual after 24 hours. In addition, fluorescence was measured for samples treated with UV alone (prior to chlorination/chloramination). Fluorescence data was analyzed using PARAFAC. MP UV doses ranging from disinfection ($40\text{-}186 \text{ mJ/cm}^2$) to higher doses (1000 mJ/cm^2) were used to investigate trends. A subset of samples were spiked with additional bromide and nitrate to investigate the role of inorganic precursors in the formation of DBPs during MP UV-chlorine/chloramine treatment.

4.2 Materials and Methods

Sample Collection

Water from Orange County Water & Sewer Authority Drinking Water Treatment Plant (Carrboro, NC, USA) was concentrated using a custom-built portable reverse osmosis (RO) system so that a large amount of DOM could be collected and stored to provide the same matrix for a series of experiments. RO concentration has previously been demonstrated as a method through which high organic carbon recoveries (80-99%) and preservation of original source water reactivity can be obtained (Kitis et al. 2001; Song et al. 2009). Water for RO concentration was collected after coagulation/flocculation and sedimentation to simulate a location where UV would be applied for primary disinfection of surface waters. The RO system included a spiral wound membrane (cellulosic acetate), four filter cartridge filters (10, 5, 1, and 0.45 μm), and a cation exchange resin cartridge (Graver Technologies, Glasgow, DE, USA). The system was operated in two stages. First, source water was pumped through the filters and ion exchange resin and collected in a high density polypropylene 80 gallon reservoir (RO feed reservoir). Second, a high pressure pump fed the collected water through the RO membrane. The retentate (RO concentrate) was recycled in the RO feed reservoir and the filtrate (permeate) discarded. The RO membrane was operated until a desired concentration factor of approximately 15 (by volume) was achieved (180 L settled water concentrated to 12 L). The RO concentrate was filtered (0.45 μm nylon membrane, 47 mm diameter, Whatman International Ltd., Maidstone, England) in the laboratory and stored in amber glass bottles at 4°C until use. The RO concentrate character was monitored by dissolved organic carbon (DOC) and UV/visible absorbance measurements,

which remained relatively constant between experiments. The characteristics of the water before and after RO concentration are shown in Appendix 2.

Within one week prior to an experiment, the RO concentrate was diluted in laboratory grade water (LGW) to obtain a DOC concentration of approximately 3 mg C/L and stored at 4°C until use. LGW was prepared in-house from a Dracor system (Durham, NC, USA), which pre-filters inlet 7 MΩ deionized water to 1 μm, removes residual disinfectants, reduces total organic carbon to less than 0.2 mg C/L with an activated carbon cartridge, and removes ions to 18 MΩ with mixed bed ion-exchange resins. DOC of samples was measured with a Shimadzu TOC-V_{CPH} Total Organic Carbon Analyzer (Shimadzu Corporation, Atlanta, GA, USA) following Standard Method 5310 (APHA 1999). UV/visible absorbance was measured using a Hewlett Packard 8452A Diode Array spectrophotometer (Agilent, Santa Clara, CA, USA). All glassware was soaked in a detergent solution, rinsed with tap water, soaked in 10% nitric acid, rinsed with LGW, and dried in an oven at 180°C (only non-volumetric glassware was dried in oven). A subset of samples were spiked with additional bromide (1 mg/L) or nitrate (10 mg N/L), administered in the sodium salt form (Fisher ACS grade, ThermoFisher Scientific, Waltham, MA, USA). These levels were chosen to investigate trends and mechanisms, although it is recognized that these are higher concentrations than those typically observed in surface waters. For comparison, the United States Environmental Protection Agency regulates nitrate in drinking water at a maximum contaminant level of 10 mg N/L (U.S. EPA 1992). Ambient samples contained <0.02 mg N/L nitrate and 28 μg/L bromide.

UV Treatment

UV treatment was performed using quasi-collimated irradiation from a custom-built unit containing a 550 W MP lamp (Ace-Hanovia, Vineland, NJ, USA) with a 4-inch aperture. Samples were retained in a 250-mL capacity Pyrex crystallization dish and stirred during irradiation. Constant sample temperature was maintained at 20-25°C by placing the dish in a copper coil which was connected to a programmable refrigerated recirculating water unit. A manual shutter was used to rapidly begin or end the irradiation. UV doses were determined using previously described calculation techniques (Bolton & Linden 2003). Briefly, UV irradiance was measured at the water surface using an SED240 detector with a W diffuser connected to an IL1400A radiometer (International Light, Peabody, MA, USA). The irradiance between 200 and 300 nm was multiplied by a Petri factor (0.92), water factor, radiometer sensor factor, reflection factor, and germicidal factor to obtain a germicidal irradiance in mW/cm^2 . The irradiation time (s) was then determined by dividing the desired UV dose (mJ/cm^2 or $\text{mW}\cdot\text{s}/\text{cm}^2$) by the germicidal irradiance. Uridine actinometry was used to confirm UV irradiance following the procedure described by Jin et al. (2006).

Chlorination/Chloramination

Immediately following irradiation, samples were buffered to pH 7.5 with 5 mM phosphate buffer (prepared from Fisher ACS grade sodium phosphate monobasic monohydrate and sodium phosphate dibasic heptahydrate) and dosed with chlorine from a dilution of a concentrated sodium hypochlorite stock solution (Fisher laboratory grade, 5.6-6%) or pre-formed monochloramine, based on a target residual of 1.0 ± 0.4 mg Cl_2/L

after 24 hours calculated from demand tests performed prior to treatment. Duplicate samples were treated with UV-chlorine/chloramine and held in chlorine demand-free headspace-free 250-mL amber glass bottles with caps and polytetrafluoroethylene (PTFE) lined septa for 24 hours at 20°C. Glassware was made chlorine demand-free no more than a week before use by soaking in a 20 mg/L as Cl₂ solution of sodium hypochlorite for 24 hours and then rinsing with LGW and drying in an oven at 180°C for 24 hours. Free chlorine residuals in samples were measured in duplicate using the *N,N*-diethyl-*p*-phenylenediamine (DPD) colorimetric method following Standard Method 4500-Cl G (APHA 1999). Chloramine residuals in samples were analyzed in duplicate using an adaption of the indophenol method (Hach Method 10171) with MonochlorF reagent (Hach Company, Loveland, CO, USA). Details on how demand tests were carried out are described in Chapter 2. A pre-formed monochloramine solution was prepared by adding free chlorine drop-wise to an ammonium chloride (ACS grade, Mallinckrodt, St. Louis, MO, USA) solution (adjusted to pH 8.5 with NaOH) at a 1:1.2 Cl:N molar ratio. Monochloramine is referred to as chloramine throughout this chapter for the purpose of discussion, but the pre-formed chloramine solution was prepared such that monochloramine was the primary species formed (dichloramine negligible) and ammonium chloride was present in excess so that no free chlorine remained. Chloramine speciation and concentration in the pre-formed solution were verified by UV spectrometry and solving simultaneous Beer's Law equations as described by Schreiber and Mitch (2005).

Disinfection Byproduct Analysis

After the 24-hour holding time, chlorine/chloramine residuals were measured and samples for DBP analysis were transferred to 60-mL glass vials containing quenching agent (ACS grade L-ascorbic acid, Sigma Chemical Co., St. Louis, MO, USA) with caps and PTFE-lined septa. Quenched samples were then stored headspace-free at 4°C until DBP analysis, which was carried out as two separate extractions: (1) THMs (four regulated chlorine- and bromine-containing species), 4 haloacetonitriles (trichloro-, dichloro-, bromochloro-, and dibromo-acetonitrile), two haloketones (1,1-dichloro- and 1,1,1-trichloro-propanone), two halonitromethanes (trichloro- and tribromo-nitromethane), chloral hydrate, and 11 haloacetamides (bromo-, dichloro-, bromochloro-, trichloro-, dibromo-, chloroiodo-, bromodichloro-, bromoiodo-, dibromochloro-, tribromo-, and diiodo-acetamide) were co-extracted within 24 hours of quenching; and (2) cyanogen chloride was extracted within 48 hours of quenching. DBPs were liquid-liquid extracted with methyl tert-butyl ether (MtBE) and analyzed on a Hewlett-Packard 5890 gas chromatograph with ⁶³Ni electron capture detector (GC-ECD) following the procedures described by Scilimenti et al. (1994) (cyanogen chloride) and Weinberg et al. (2002) (all other DBPs). THMs, chloral hydrate, chloropicrin, haloacetonitrile, haloketone, and bromo-, dichloro-, and trichloro-acetamide standards were obtained from Supelco and Sigma-Aldrich (Sigma Chemical Co., St. Louis, MO, USA). Bromopicrin (tribromonitromethane) and remaining haloacetamide standards were obtained from Orchid Cellmark (New Westminster, BC, Canada). Cyanogen chloride was obtained from SPEX Certiprep (Metuchen, NJ, USA). All samples were analyzed in duplicate and 1,2-dibromopropane was used as an internal standard. The minimum reporting limit

(MRL) for all compounds was 0.1 µg/L. Chromatographic conditions for DBP analysis are described in Chapter 2.

Fluorescence

A Fluorolog-321 fluorescence spectrophotometer (Horiba Jobin Yvon, Edison, NJ, USA) with a charge-coupled device (CCD) detector was used to measure fluorescence and generate EEM data following an adaption of the method and correction factors described by Cory et al. (2010). EEMs were collected for samples at excitation wavelengths from 240 to 450 nm at 5 nm intervals and emission wavelengths from 320 to 550 nm at 1 nm intervals. Excitation wavelengths below 250 nm were not included for data processing due to the low signal to noise ratio on the Fluorolog at 240 and 245 nm. Chlorine/chloramine residuals were not quenched prior to fluorescence analysis. At the time of quenching for DBP measurement (24 hours after chlorine/chloramine dosing), samples for fluorescence measurement were transferred to chlorine demand-free headspace-free 25-mL amber glass vials and stored at 4°C until analysis (3 days for chlorinated samples, 5 days for chloraminated samples, and 2-7 days for UV-only samples). Prior to analysis, each sample was allowed to come to room temperature. Samples and LGW blanks (collected daily) were corrected for instrument response by multiplying by the manufacturer-supplied excitation and emission correction factors and then blank EEMs were subtracted from sample EEMs. Intensities were normalized to the area under the water Raman peak (350 nm) of the blank to obtain data in Raman units. Sample absorbance was measured with an Ocean Optics USB4000 spectrometer (Ocean Optics, Dunedin, FL, USA). A total of 269 EEMs were collected and a four component

PARAFAC model was developed using Matlab (Version 7.12.0, Mathworks, Natick, MA, USA) and the DOMFluor toolbox following the tutorial presented by Stedmon and Bro (2008). Components were verified using four-way split-half analysis, which compares the excitation and emission loadings (spectra) between the model and four separate splits of the dataset using Tucker Congruence Coefficients to ensure that component identification was not biased by a local maximum (Lorenzo-Seva and Berge 2006; Stedmon and Bro 2008). The individual loadings of data splits and the model for each component are shown in Appendix 6. Residual EEMs (difference between model and measured excitation/emission loadings) contained mostly background noise, which verified that the four-component model was able to account for the majority of observed fluorescence and fit the data well. Fluorescence intensities of each component in every sample are reported as a maximum fluorescence (F_{\max}) value in Raman units, which correlates with the relative amount of that fluorescing component (Lakowicz 2006; Stedmon & Bro 2008). In addition to fluorescence, samples were analyzed by UV/visible spectroscopy and DOC (for samples treated with UV only) to compare these characterization techniques to results obtained with fluorescence.

4.3 Results and Discussion

DOC characterization

Any observed changes in DOC concentration with treatment were within experimental error (relative percent difference, RPD, between experimental duplicates $\leq 13\%$), shown in Table 4-1. The slope ratio ($S_R = S_{275-295} : S_{350-400}$) of log-transformed UV/visible absorption spectra has been shown to correlate well with DOM molecular weight and has been used to evaluate photochemical changes to DOM (De Haan & De

Boer 1987; Summers et al. 1987, Helms et al. 2008). However, while there were shifts in the absorption spectrum of the water as a function of treatment, there was a high degree of uncertainty (S_R RPD >20% between experimental duplicates), likely due to the low absorbance (specific UV absorbance at 254 nm, $SUVA_{254} = 1.4-1.5$) of the water that was collected after coagulation/flocculation and sedimentation, which preferentially removes higher absorbing material (Collins et al. 1986). Inclusion of MP UV treatment, chlorine addition, and inorganic constituents further complicated interpretations of changes in absorbance and it was difficult to draw any conclusions about changes in DOM composition following treatment. The low sensitivity of DOC combined with non-specificity of absorbance further emphasized the value of fluorescence spectroscopy, which was able to detect and track DOM changes from UV, chlorine, and chloramine treatment in this matrix without the errors associated with UV/visible spectroscopy.

Table 4-1. DOC concentration (mg C/L) for ambient (unspiked) and spiked reconstituted RO concentrate samples treated with MP UV. Value shown represents average between experimental duplicate samples (RPD \leq 13%).

UV dose (mJ/cm ²)	Spiking condition*			
	ambient	bromide	nitrate	bromide + nitrate
0	2.7	2.7	2.8	2.9
40	2.8	2.7	2.9	2.9
186	2.8	2.7	3.0	3.1
1000	2.8	2.7	3.1	3.0

*Spiking amounts, where applicable, were 1 mg/L bromide and 10 mg N/L nitrate.

PARAFAC Analysis

A four-component PARAFAC model was developed and validated for a range of treatment and spiking conditions. Three components (C1, C2, and C3) were humic-like

with terrestrial origin and the fourth (C4) was a protein/tryptophan-like component. The excitation and emission loadings (spectra) of the four modeled components are shown in Figure 4-1, and Table 4-2 describes their characteristics with comparisons to similar components that have been identified in natural and engineered systems. A subset of samples were analyzed in triplicate to determine the reproducibility of component quantification in each sample. The relative standard deviation of component F_{\max} values between triplicates varied by component, ranging from 0.1% to 5.8% with an average of 1.6%. All treatments were carried out in duplicate, and the results presented in Figures 4-2 to 4-4 show the RPD between these experimental duplicate analyses.

Since the water used for this work was collected after coagulation/flocculation and sedimentation, the four components identified here persisted through primary treatment. Similar components observed in past work have exhibited a range of removal/transformation efficiencies under various drinking water and wastewater treatment processes, but ultimately persist through to finished water (Baghoth et al. 2011; Murphy et al. 2011).

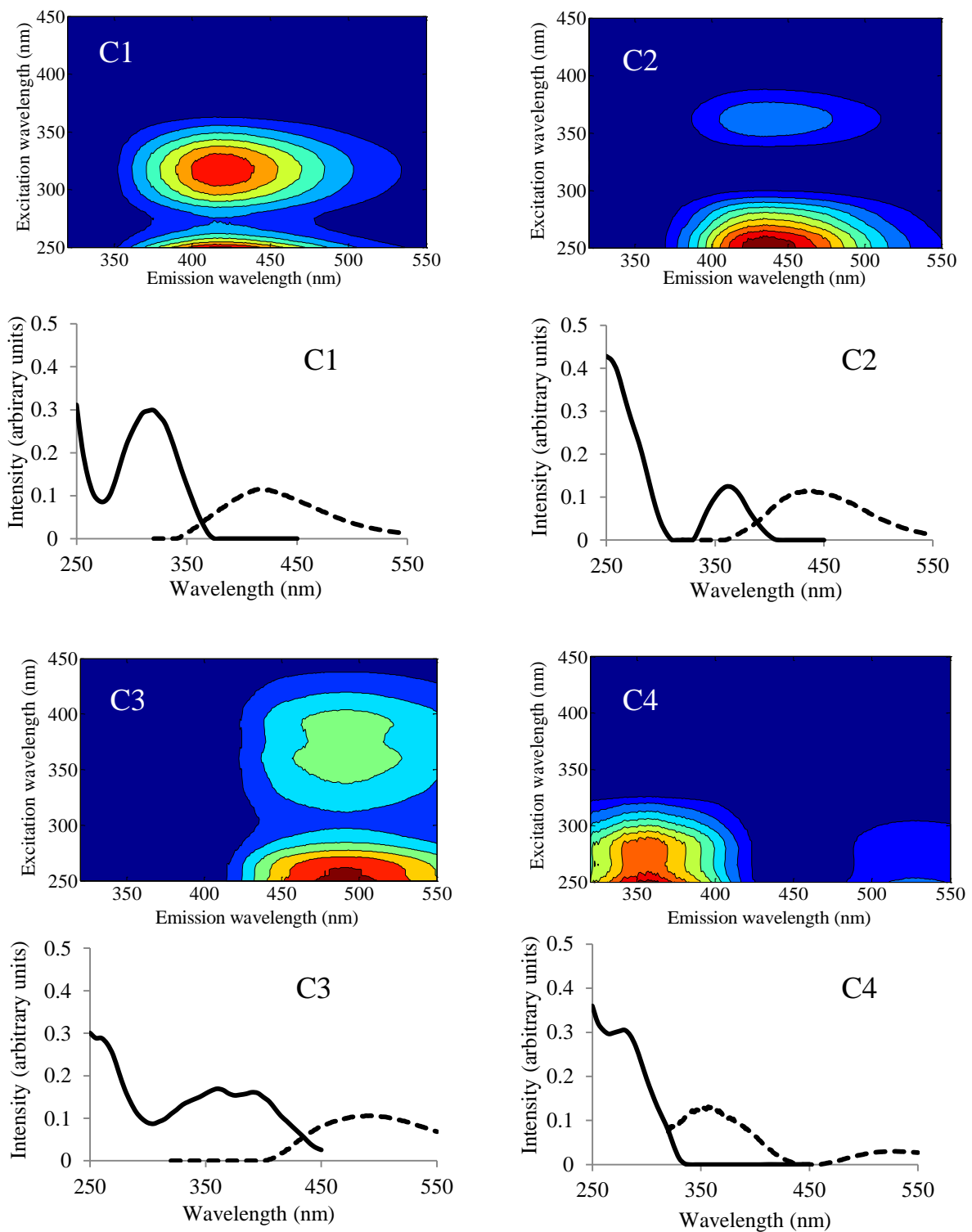


Figure 4-1. Excitation emission matrices and excitation (solid lines) & emission (dashed) spectra for each component identified in the PARAFAC model.

Table 4-2. Description of four components (C1-C4), excitation and emission peaks (with secondary peaks in parentheses), and comparison to similar peaks identified in previous work (referred to by the peak name and/or letter assigned by the authors of the referenced study).

Component	$\lambda_{ex}/\lambda_{em}$	Description	Comparison to past work
C1	<250(320)/414	Terrestrial humic-like	C6: <250(320)/400 ^a C2: 250(320)/410 ^b
C2	<250(360)/434	Terrestrial humic-like	Peaks C or A ^c C4: <250(360)/440 ^a P8: <260(355)/434 ^d C5: 250(340)/440 ^b
C3	<250(360)/489	Terrestrial humic-like	C3: 270(360)/478 ^e C1: 260(360)/480 ^b
C4	<250(280)/357	Protein, tryptophan-like	Peak T ^c C7: 280/344 ^a C4: <250(290)/360 ^b

^aStedmon & Markager 2005

^bBagtho et al. 2011

^cCoble 1996 (“C,” “A,” and “T” are somewhat arbitrary letters assigned by the author to these peaks)

^dMurphy et al. 2008

^eStedmon et al. 2003

Effect of MP UV Treatment on PARAFAC Components

Two components (C2 and C4) decreased in intensity following MP UV treatment of ambient (unspiked) samples, while C1 and C3 did not (see Figure 4-2). C2 and C4 F_{max} values were reduced 27% and 66%, respectively, with the highest UV dose (1000 mJ/cm²). Tryptophan absorbs strongly between 200 and 300 nm (Fasman 1976) and since MP UV lamps have a polychromatic output from 200 to 400 nm, the reactivity of tryptophan-like C4 to UV would be expected. Components similar to the humic-like component “A” absorb light in the UVC region of 100 to 280 nm (Coble 1996; Stedmon et al. 2003) which overlaps with the MP UV lamp output and is consistent with the observed decrease in C2 F_{max} with MP UV irradiation.

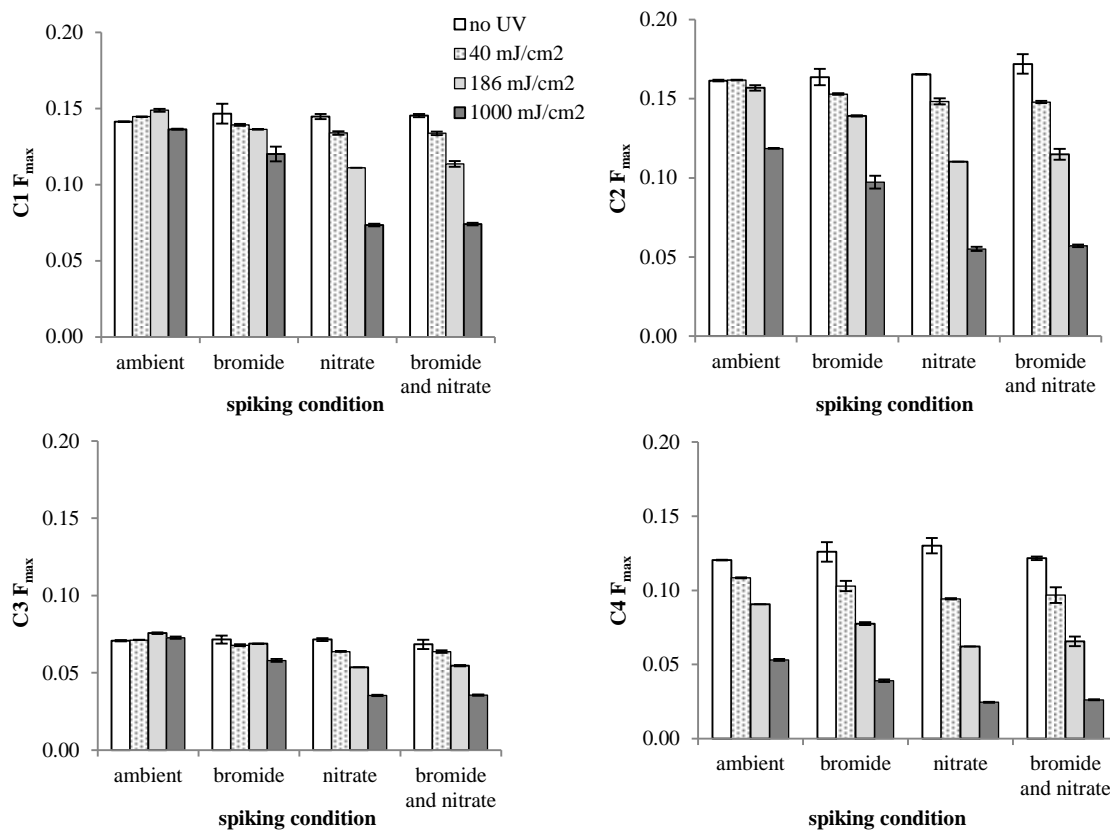


Figure 4-2. Effect of UV on fluorescence intensity (F_{\max}) in ambient and spiked samples. Spiking amounts, where applicable, were 1 mg/L bromide and 10 mg N/L nitrate. Bar height represents average between experimental duplicate samples, with the duplicate values shown by inset bars.

In contrast to ambient samples (where only C2 and C4 were decreased by MP UV), irradiation of nitrate-containing samples decreased the F_{\max} of all components (Figure 4-2). This suggests that all components were amenable to indirect photolysis (i.e. reaction with hydroxyl radicals produced from photolysis of nitrate). Nitrate absorbs strongly below 240 nm, which overlaps with the MP UV emission. UV photolysis of nitrate generates nitrogen dioxide ($\cdot\text{NO}_2$) and hydroxyl radicals ($\cdot\text{OH}$), with decreasing quantum yield (Φ_λ) as wavelength increases between 200 and 300 nm ($\Phi_{205\text{ nm}} = 0.129$ and $\Phi_{253.7\text{ nm}} = 0.037$) (Goldstein & Rabani 2007). Hydroxyl radicals have been shown to react relatively unselectively with DOM, with rate constants on the order of $10^8\text{ M}^{-1}\text{ s}^{-1}$

(Westerhoff et al. 1999) and indeed, similar F_{\max} reductions were observed in this current work among all components for samples treated with UV in the presence of nitrate, relative to the same treatment in ambient samples.

Few studies have used fluorescence spectroscopy to evaluate engineered UV treatment processes. Hofbauer & Andrews (2004) observed a 28% decrease in total fluorescence intensity when 3000 mJ/cm² MP UV was applied to a Suwannee River DOM solution (DOC = 4 mg C/L) but that study did not investigate individual fluorescing components. In another study that did use PARAFAC to evaluate the effects of UV and other advanced wastewater treatment processes on DOM fluorescence, Murphy and colleagues (2011) showed varying results for the F_{\max} of individual components following UV irradiation across six different treatment plants. In general, the authors observed decreases in component fluorescence intensity following UV treatment and to a lesser extent when chlorine was applied prior to UV. In a few cases, however, the F_{\max} of several components appeared to increase following UV, although it was not clear whether these changes were within the associated analytical/experimental error. In addition, the UV dose or lamp type (i.e. MP vs. low pressure, LP, monochromatic output at 254 nm) used in each treatment plant was not reported, which may have contributed to the varying results.

The order of component reactivity to MP UV treatment of ambient samples was: C4>C2>C1~C3, which is opposite to the trend that is typically observed for sunlight photolysis in natural systems (Stedmon & Markager 2005), suggesting that findings on DOM reactivity to sunlight photolysis may be not applicable to predicting behavior in engineered MP UV systems.

The presence of bromide (1 mg/L) resulted in a greater F_{\max} decrease in samples treated with the higher UV doses of 186 mJ/cm² (C2 and C4) or 1000 mJ/cm² (all components) compared to ambient samples. One explanation for this observation could be the formation of reactive halogen species from photolysis of bromide (e.g. $\text{Br}_2^{\cdot-}$, $\text{BrOH}^{\cdot-}$, see Chapter 1 for more discussion), which have been shown to contribute to DOM degradation and react more selectively with electron-rich chromophores than hydroxyl radicals (Grebel et al. 2009). However, this increase in F_{\max} reduction was not observed between nitrate and bromide- & nitrate-spiked samples, suggesting that there may have been a maximum possible F_{\max} reduction already reached from the reactive species formed from nitrate photolysis. Nitrate was also spiked at 10 mg N/L (0.71 mM) compared to bromide at 1 mg/L (0.013 mM), and based on the overlap of their respective absorption spectra with the MP UV output (shown in Chapter 1), nitrate would be expected to produce more reactive species than bromide following irradiation.

Effect of MP UV-Chlorine/Chloramine Treatment on PARAFAC Components

Chlorination decreased the F_{\max} of all components, shown in Figure 4-3. This is in agreement with past work that has shown chlorination to reduce overall fluorescence intensity (Roccaro et al. 2009; Beggs & Summers 2011; Murphy et al. 2011). Regardless of MP UV dose, the addition of bromide during chlorination reduced F_{\max} for all components (47%, 30%, 30%, and 10% F_{\max} reduction for C1, C2, C3, and C4, respectively, compared to ambient samples). Bromide can be oxidized by free chlorine (HOCl) to form hypobromous acid (HOBr), which reacts with DOM faster than aqueous chlorine, and when both are present, bromine tends to act more as a substituting agent while chlorine reacts preferentially as an oxidant (Rook et al. 1978; Westerhoff et al.

2004). These results suggest that the presence of HOBr results in more breakdown of fluorescing DOM constituents and/or that fluorescence is being quenched by bromine substitution reactions.

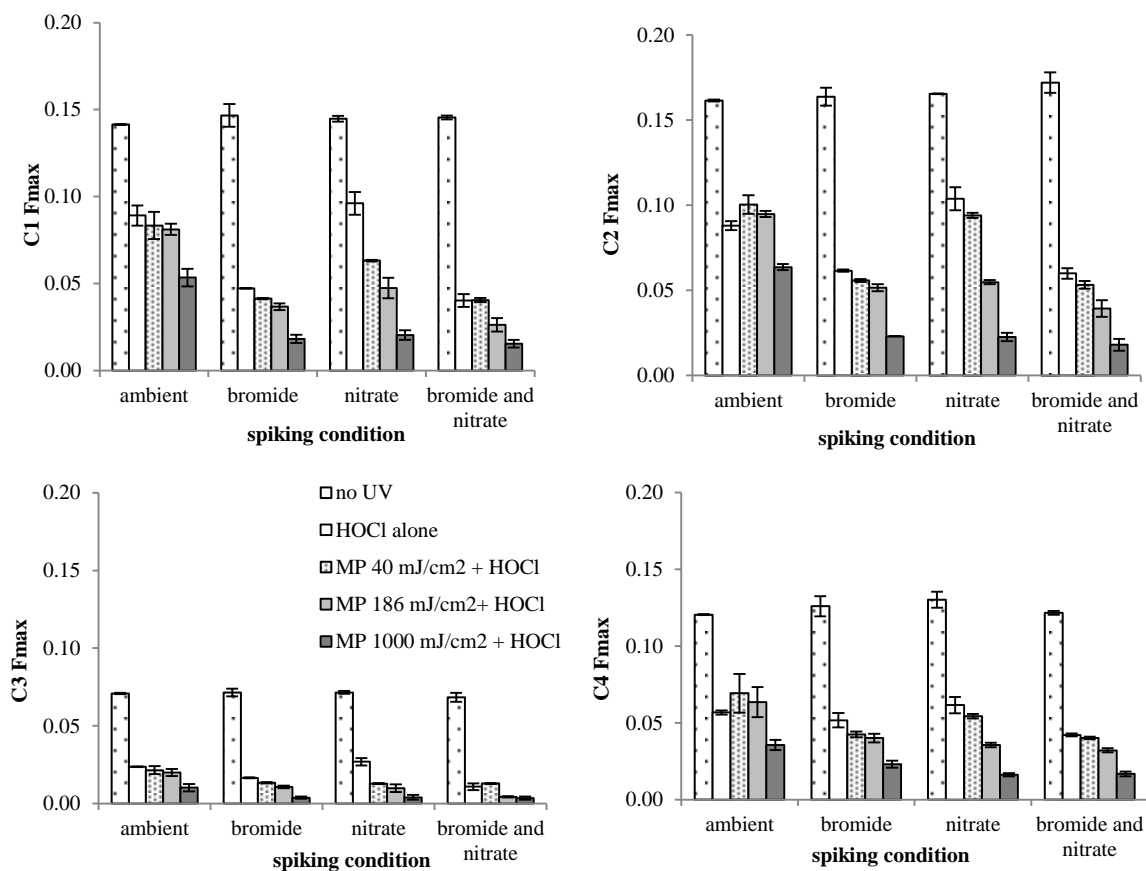


Figure 4-3. Effect of UV followed by chlorination on component F_{max} in ambient and spiked samples, with comparison to untreated sample (no UV in Figure 4-2). Spiking amounts, where applicable, were 1 mg/L bromide and 10 mg N/L nitrate. Bar height represents average between experimental duplicate samples, with the duplicate values shown by inset bars.

The reduction in fluorescence intensity following chlorination is thought to be due to oxidation of fluorescing DOM components, such as the breakdown of carbon double bonds in aromatic molecules, and halogen substitution reactions, which can result in fluorescence quenching (Korshin et al. 1999; Lakowicz 2006). The order of component

reactivity to chlorine was: C3>C4>C2>C1, with F_{\max} reductions of 67%, 53%, 46%, and 37%, respectively, following the addition of chlorine to ambient samples. While the humic-like C3 component was found to be most affected by chlorine in this study, Beggs & Summers (2011) found that the fluorescence intensity of protein-like components was decreased more than that of humic-like upon chlorination (average of 67% compared to 30% reduction, respectively). One explanation for this difference is that the DOM source material in that study was pine needle leachate, which had a higher protein-like fluorescence contribution compared to that of humic-like components. Two of the four identified components in that work were polyphenolic/protein-like, and they accounted for 78-84% of the fluorescence in coagulated fresh leachate samples. In comparison, the tryptophan/protein-like component in the present study accounted for 24% of the fluorescence in an ambient sample (the source of which was coagulated/settled drinking source water).

Treatment of ambient samples with MP UV followed by chlorine resulted in F_{\max} decreases for C1 and C3 that were not observed for those components when treated with either chlorine or MP UV alone. This suggests that MP UV produced precursors that were more amenable to reaction with chlorine compared to the original organic matter. Indeed, the chlorine demand of ambient samples was increased with 1000 mJ/cm^2 MP UV pre-treatment (results presented in Chapter 2). Samples were compared on an equivalent targeted residual basis, so higher chlorine doses were applied to these samples. While some of the increased F_{\max} reduction in C1 and C3 with the use of 1000 mJ/cm^2 MP UV could be due to this higher dose of chlorine, differences were observed even with

40 and 186 mJ/cm² MP UV in ambient samples, which were given the same chlorine dose as ambient samples not treated with MP UV.

Changes in F_{\max} were much smaller with chloramine treatment compared to chlorination, which is consistent with the lower chloramine vs. chlorine demand of samples that was observed (results presented in Chapter 2). C3 and C4, which were also the most affected by chlorine, were slightly affected by chloramine (F_{\max} decreased 15-16% for ambient samples treated with chloramine, compared to no treatment), while C1 and C2 were not, shown in Figure 4-4. The addition of bromide prior to chloramination did not result in greater F_{\max} decreases compared to the same treatment in ambient samples, as observed during chlorination. Bromide can be oxidized by chloramine to produce active bromine species, including NH_2Br , NHBr_2 , and NHBrCl (Trofe et al. 1980), but their formation in a surface water containing bromide and treated with preformed monochloramine at pH 7.5 (i.e. the source waters used for this work) is slow and not likely to be significant (Diehl et al. 2000; Benotti et al. 2011). This was also reflected in the lack of change in chloramine demand with the addition of bromide (results not presented here, but shown in Chapter 2). In general there was more variability in fluorescence intensity between experimental duplicates during chlorination, compared to UV alone or chloramination.

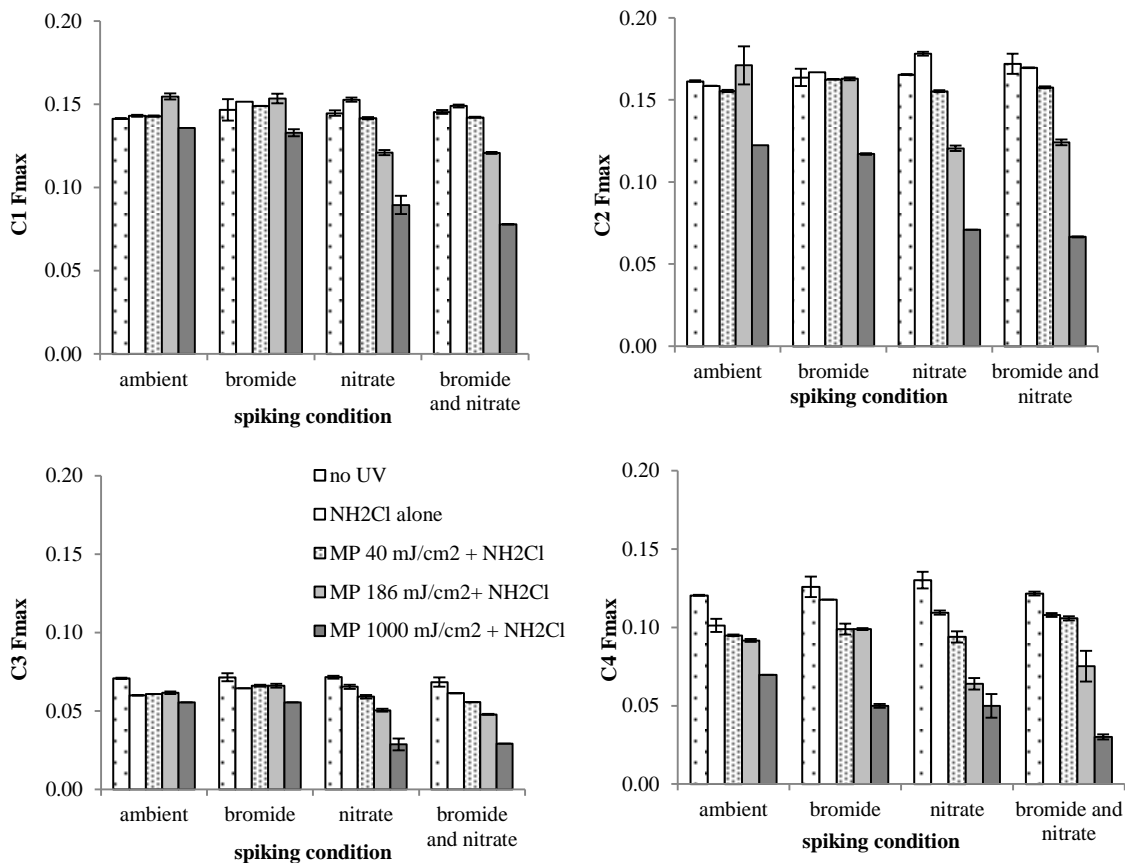


Figure 4-4. Effect of UV followed by chloramination on component F_{\max} in ambient and spiked samples, with comparison to untreated sample (no UV in Figure 4-2). Spiking amounts, where applicable, were 1 mg/L bromide and 10 mg N/L nitrate. Bar height represents average between experimental duplicate samples, with the duplicate values shown by inset bars.

Comparison of Disinfection Byproduct and Fluorescence Results

Only a subset of DBP results will be discussed in this section, focusing on compounds that were affected by MP UV. Additional DBP results can be found in Appendix 6. The use of MP UV at disinfection doses (40-186 mJ/cm²) prior to chlorination or chloramination had little effect on the formation of the four regulated chlorine- and bromine-containing THMs (THM4), which is in agreement with previous research (Malley et al. 1995; Liu et al. 2002). However, when samples were treated with

1000 mJ/cm² MP UV prior to chlorination, THM4 formation increased 30-35% compared to chlorination alone, suggesting that with higher doses, MP UV generates THM4 precursors that are more amenable to reaction with chlorine. This is consistent with the F_{\max} decrease observed for C1 and C3 with the addition of UV prior to chlorination and the increased chlorine demand observed for samples treated with 1000 mJ/cm² MP UV (described in Chapter 2). Past research has shown that in general, hydrophobic DOM has greater THM formation potential compared to hydrophilic precursors, which typically comprise a smaller amount of the total NOM. However, the hydrophilic fraction can play an important role in DBP formation, especially in low humic-containing waters (Kitis et al. 2002; Liang & Singer 2003; Hua & Reckhow 2007). At high doses, UV irradiation can produce smaller, more hydrophilic precursors (Malley et al. 1995; Magnuson et al. 2002), which was also supported by findings presented in Chapter 3.

Trihalonitromethanes (chloropicrin and bromopicrin), chloral hydrate, and cyanogen chloride formation were affected by MP UV with subsequent chlorination or chloramination, compared to samples treated with only chlorine or chloramine, the extent to which depended on nitrate/bromide spiking conditions and MP UV dose³. Results for a subset of treatment conditions and DBPs are shown in Table 4-3.

The increased formation of chloropicrin and bromopicrin following MP UV irradiation and chlorination or chloramination is hypothesized to result from the production of reactive nitrogen species from photolysis of nitrate, which can act as nitrating agents towards DOM. These nitrated organics then generate halonitromethanes after chlorination or chloramination (Reckhow et al. 2010; Shah et al. 2011). Since the

³See Chapter 2 for additional discussion and results on the formation of halonitromethanes, chloral hydrate, and cyanogen chloride during UV-chlorine/chloramine treatment.

F_{\max} of all four components was affected similarly with MP UV irradiation in the presence of nitrate, it is difficult to draw any conclusions from the fluorescence results about which components were most responsible for halonitromethane formation.

Table 4-3. Effect of MP UV followed by chlorination (Cl_2) or chloramination (NH_2Cl) on the formation of DBPs in ambient and nitrate-spiked samples (10 mg N/L). Concentrations are shown in $\mu\text{g/L}$ and represent the average between experimental duplicate samples (RPD $\leq 10\%$).

spiking condition	UV dose (mJ/cm^2)	THM4		chloropicrin		chloral hydrate		cyanogen chloride	
		Cl_2	NH_2Cl	Cl_2	NH_2Cl	Cl_2	NH_2Cl	Cl_2	NH_2Cl
ambient	0	82	1.0	0.2	<0.1	7.8	0.2	<0.1	0.4
	40	84	1.1	0.2	<0.1	9.8	0.2	<0.1	0.4
	186	89	1.0	0.3	<0.1	15	0.2	<0.1	0.4
	1000	111	0.8	0.5	<0.1	32	0.2	<0.1	0.8
nitrate	0	81	1.1	0.2	<0.1	8.1	0.2	<0.1	0.5
	40	85	1.0	1.3	0.2	11	0.2	<0.1	0.6
	186	95	0.9	4.0	0.5	18	0.2	<0.1	0.9
	1000	109	0.6	8.0	0.8	32	0.3	<0.1	1.9

Chloral hydrate formation increased with increasing MP UV dose when followed by chlorination, compared to its formation in samples treated with chlorine alone. Nitrate spiking had no effect on chloral hydrate formation, but samples spiked with bromide had lower chloral hydrate formation, likely due to a shift to the bromine-substituted species (not measured for this work). The mechanism for increased chloral hydrate formation with MP UV and subsequent chlorination is thought to be through the formation of acetaldehyde, which can form chloral hydrate upon chlorination and is known to be produced from MP UV (McKnight & Reckhow 1992; Liu et al. 2002). The reactivity of C2 and C4 to UV suggest that one or both of these components were responsible for the formation of chloral hydrate precursors during MP UV irradiation. This is supported by the strong correlation that was found between the decrease in C2 and C4 F_{\max} and

increase in chloral hydrate formation in ambient and nitrate-spiked samples treated with MP UV followed by chlorination (R^2 values of 0.99 for both C2 and C4 in ambient samples and 0.97 and 0.96 for C2 and C4, respectively, in nitrate-spiked samples), shown in Figure 4-5.

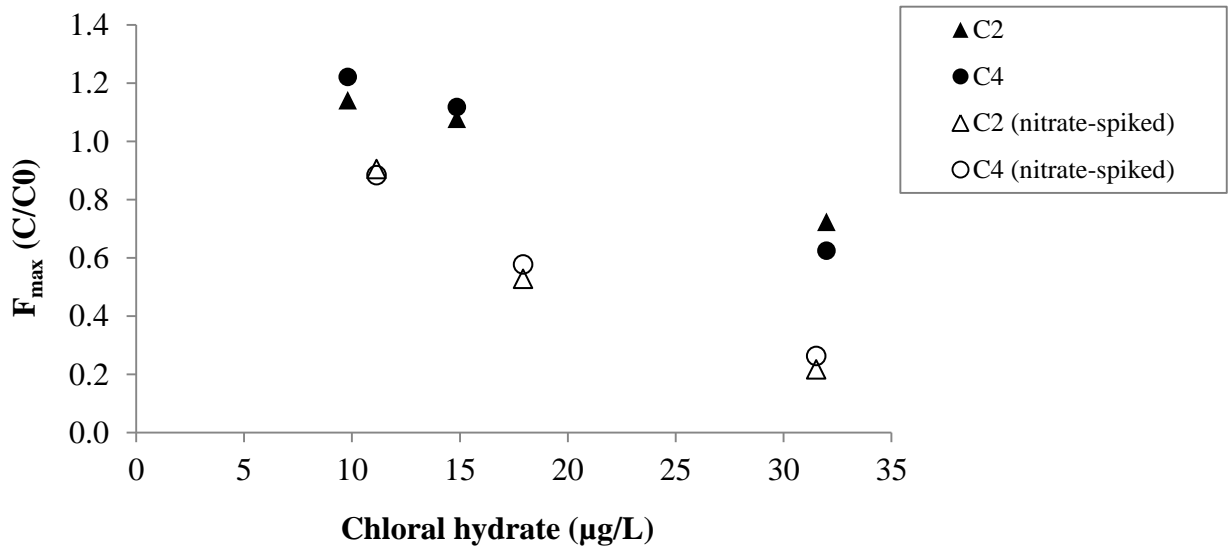


Figure 4-5. Correlation between change in C2 and C4 F_{max} and formation of chloral hydrate in ambient and nitrate-spiked samples treated with MP UV + chlorine. R^2 values were 0.99 for both C2 and C4 in ambient samples and 0.94 and 0.97 for C2 and C4, respectively, in nitrate-spiked samples.

Cyanogen chloride is typically observed as a chloramination byproduct and previous work has identified amino acids, including tryptophan, and other organic nitrogen compounds as precursors (Krasner et al. 1989; Yang et al. 2010). Therefore, C4 or similar non-fluorescing compounds would likely be important precursors for cyanogen chloride during chloramination, and indeed, the C4 F_{max} was decreased with chloramine treatment and formation of cyanogen chloride was observed. The use of MP UV prior to chloramination increased cyanogen chloride formation compared to chloramination

alone, and to a greater extent in nitrate-spiked samples. One proposed pathway for this observed increase is through the formation of formaldehyde, which can produce cyanogen chloride upon chloramination and is known to be generated during engineered UV irradiation and sunlight photolysis of humic materials (Malley et al. 1995; Pedersen et al. 1999). Again, the observed effect of MP UV on the F_{\max} of C2 and C4 suggest UV-induced precursors responsible for increased cyanogen chloride formation originated from one or both of these components or similar non-fluorescing compounds. Decreases in C2 and C4 F_{\max} were correlated to cyanogen chloride formation in samples treated with chloramine or MP UV followed by chloramine (R^2 values of 0.88 and 0.66 for C2 and C4, respectively), shown in Figure 4-6.

Although the proposed pathways for cyanogen chloride and chloral hydrate are similar in that both have an aldehyde intermediate, nitrate-spiking during UV irradiation and subsequent chlorination/chloramination further increased the formation of cyanogen chloride but not chloral hydrate. This suggests either an additional pathway for cyanogen chloride formation involving reactive species produced from nitrate photolysis or different mechanisms in formaldehyde vs. acetaldehyde formation from MP UV. A recent study showed evidence that indirect photolysis was an important pathway in formaldehyde production from DOM in natural waters, while acetaldehyde was primarily formed through direct photolysis (de Bruyn et al. 2011). This would support the observed effect of nitrate spiking on cyanogen chloride formation during UV treatment, if the hypothesized pathways involving acetaldehyde and formaldehyde are correct.

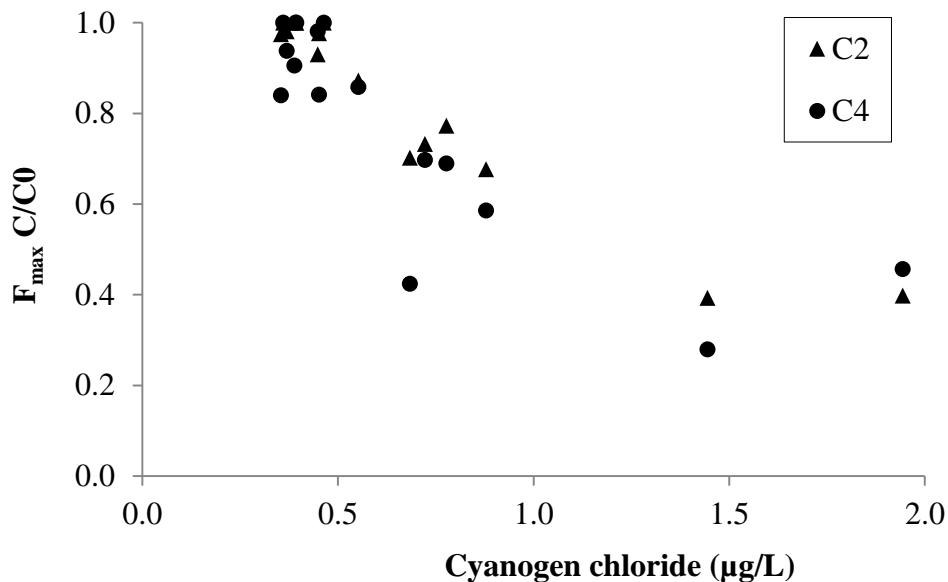


Figure 4-6. Correlation between change in C2 & C4 F_{max} and formation of cyanogen chloride in all samples treated with chloramine or MP UV followed by chloramination. R^2 values were 0.88 and 0.66 for C2 and C4, respectively.

4.4 Conclusions

The use of fluorescence spectroscopy combined with DBP analysis allowed for an investigation into the impact of MP UV treatment on DOM composition and subsequent reactivity with chlorine or chloramine. Fluorescence is well-suited for this application because it is very sensitive and was able to provide more information about changes to specific organic precursors than other characterization techniques such as DOC measurements and UV/visible absorbance spectral slope. This study will add to the limited body of literature that has investigated the effects of engineered treatment processes on fluorescing DOM components, and the results have implications for predicting and controlling DBP formation during UV-chlorine/chloramine drinking water treatment.

Sources Cited for Chapter 4

- APHA (American Public Health Association), American Water Works Association, and Water Environment Federation, 1999. Standard Methods for the Examination of Water and Wastewater. 20th Edition, American Public Health Association: Washington DC.
- Baghoth, S.A. et al., 2011. Tracking natural organic matter (NOM) in a drinking water treatment plant using fluorescence excitation-emission matrices and PARAFAC. *Water Research*, 45(2), pp.797-809.
- Beggs, K.M.H. & Summers, R.S., 2011. Character and chlorine reactivity of dissolved organic matter from a mountain pine beetle impacted watershed. *Environmental Science & Technology*, 45(13), pp.5717-5724.
- Benotti, M.J. et al., 2011. *Role of Bromamines on DBP Formation and Impact on Chloramination and Ozonation*. American Water Works Association and Water Research Foundation: Denver, Colorado.
- Bolton, J.R. & Linden, K.G., 2003. Standardization of methods for fluence (UV dose) determination in bench-scale UV experiments. *Journal of Environmental Engineering*, 129(3), pp.209-216.
- Cantor, K.P. et al., 1998. Drinking water source and chlorination byproducts I. Risk of bladder cancer. *Epidemiology*, 9(1), pp.21-28.
- Christman, R.F. et al., 1983. Identity and yields of major halogenated products of aquatic fulvic acid chlorination. *Environmental Science & Technology*, 17(10), pp.625-628.
- Coble, P.G., 1996. Characterization of marine and terrestrial DOM in seawater using excitation-emission matrix spectroscopy. *Water Research*, 30(4), pp.325-346.
- Collins, M.R. et al., 1986. Molecular weight distribution, carboxylic acidity, and humic substances content of aquatic organic matter: implications for removal during water treatment. *Environmental Science & Technology*, 20(10), pp.1028-1032.
- Cory, R.M. & McKnight, D.M., 2005. Fluorescence spectroscopy reveals ubiquitous presence of oxidized and reduced quinones in dissolved organic matter. *Environmental Science & Technology*, 39(21), pp.8142-8149.
- Cory, R.M. et al., 2010. Effect of instrument-specific response on the analysis of fulvic acid fluorescence spectra. *Environmental Science & Technology*, 44(1), pp.67-78.
- de Bruyn, W.J. et al., 2011. Photochemical production of formaldehyde, acetaldehyde and acetone from chromophoric dissolved organic matter in coastal waters. *Journal of Photochemistry and Photobiology A: Chemistry*, 226(1), pp.16-22.

- De Haan, H. & De Boer, T. 1987. Applicability of light absorbance and fluorescence as measures of concentration and molecular size of dissolved organic carbon in humic Lake Tjeukemeer. *Water Research*, 21(6), pp.731-734.
- Diehl, A.C. et al., 2000. DBP formation during chloramination. *Journal American Water Works Association*, 92(6), pp.76-90.
- Dotson, A.D. et al., 2010. UV/H₂O₂ treatment of drinking water increases post-chlorination DBP formation. *Water Research*, 44(12), pp.3703-3713.
- Fasman, G.D. ed., 1976. *Handbook of Biochemistry and Molecular Biology, Proteins Volume I*. 3rd Edition, CRC Press: Cleveland, Ohio.
- Goldstein, S. & Rabani, J., 2007. Mechanism of nitrite formation by nitrate photolysis in aqueous solutions: the role of peroxyxynitrite, nitrogen dioxide, and hydroxyl radical. *Journal of the American Chemical Society*, 129(34), pp.10597-10601.
- Grebel, J.E. et al., 2009. Impact of halides on the photobleaching of dissolved organic matter. *Marine Chemistry*, 115(1-2), pp.134-144. Helms, J.R. et al., 2008. Absorption spectral slopes and slope ratios as indicators of molecular weight, source, and photobleaching of chromophoric dissolved organic matter. *Limnology and Oceanography*, 53(3), pp.955-969.
- Hofbauer, D.E.W. & Andrews, S.A., 2004. Influence of UV irradiation and UV/hydrogen peroxide oxidation process on natural organic matter fluorescence characteristics. *Water Science & Technology: Water Supply*, 4(4), pp.41-46.
- Hua, B. et al., 2010. Parallel factor analysis of fluorescence EEM spectra to identify THM precursors in lake waters. *Environmental Monitoring and Assessment*, 161(1-4), pp.71-81.
- Hua, G. & Reckhow, D.A., 2007. Characterization of disinfection byproduct precursors based on hydrophobicity and molecular size. *Environmental Science & Technology*, 41(9), pp.3309-3315.
- Hudson, N. et al., 2007. Fluorescence analysis of dissolved organic matter in natural, waste and polluted waters-a review. *River Research and Applications*, 23(6), pp.631-649.
- Jin, S. et al., 2006. Polychromatic UV fluence measurement using actinometry, biodosimetry, and mathematical techniques. *Journal of Environmental Engineering*, 132(8), pp.831-842.
- Johnstone, D.W. et al., 2009. Parallel factor analysis of excitation-emission matrices to assess drinking water disinfection byproduct formation during a peak formation period. *Environmental Engineering Science*, 26(10), pp.1551-1559.

- Kitis, M. et al., 2001. Isolation of dissolved organic matter (DOM) from surface waters using reverse osmosis and its impact on the reactivity of DOM to formation and speciation of disinfection by-products. *Water Research*, 35(9), pp.2225-2234.
- Kitis, M. et al., 2002. Probing reactivity of dissolved organic matter for disinfection by-product formation using XAD-8 resin adsorption and ultrafiltration fractionation. *Water Research*, 36(15), pp.3834-3848.
- Korshin, G.V. et al., 1999. Influence of chlorination on chromophores and fluorophores in humic substances. *Environmental Science & Technology*, 33(8), pp.1207-1212.
- Krasner, S.W. et al., 1989. The occurrence of disinfection by-products in US drinking water. *Journal American Water Works Association*, 81(8), pp.41-53.
- Krasner, S.W. et al., 2006. Occurrence of a new generation of disinfection byproducts. *Environmental Science & Technology*, 40(23), pp.7175-7185.
- Kwon, B. et al., 2005. Biodegradability, DBP formation, and membrane fouling potential of natural organic matter: characterization and controllability. *Environmental Science & Technology*, 39(3), pp.732-739.
- Lakowicz, J.R., 2006. *Principles of Fluorescence Spectroscopy*. 3rd Edition, Springer: New York.
- Liang, L. & Singer, P.C., 2003. Factors influencing the formation and relative distribution of haloacetic acids and trihalomethanes in drinking water. *Environmental Science & Technology*, 37(13), pp.2920-2928.
- Liu, W. et al., 2002. Comparison of disinfection byproduct (DBP) formation from different UV technologies at bench scale. *Water Science & Technology: Water Supply*, 2(5-6), pp.515-521.
- Loper, J.C. et al., 1978. Residue organic mixtures from drinking water show in vitro mutagenic and transforming activity. *Journal of Toxicology and Environmental Health, Part A*, 4(5-6), pp.919-38.
- Lorenzo-Seva, U. and Berge, J.M.F.T., 2006. Tucker's congruence coefficient as a meaningful index of factor similarity. *Methodology: European Journal of Research Methods for Behavioral and Social Sciences*, 2(2), pp.57-64.
- Lovley, D.R. et al., 1996. Humic substances as electron acceptors for microbial respiration. *Nature*, 382(6590), pp.445-448.
- Magnuson, M.L. et al., 2002. Effect of UV irradiation on organic matter extracted from treated Ohio River water studied through the use of electrospray mass spectrometry. *Environmental Science & Technology*, 36(23), pp.5252-5260.

- Malley, J.P. et al., 1995. *Evaluation of the Byproducts Produced from the Treatment of Groundwaters with Ultraviolet Irradiation*. American Water Works Association and Water Research Foundation: Denver, Colorado.
- Maranger, R. & Pullin, M.J., 2003. Elemental complexation by dissolved organic matter in lakes: implications for Fe speciation and the speciation and the bioavailability of Fe and P. In: Findlay, S.E.G. & Sinsabaugh, R.L., eds., *Aquatic Ecosystems - Interactivity of Dissolved Organic Matter*. Academic Press: San Diego, California, pp.185-214.
- Markager, S. & Vincent, W.F., 2000. Spectral light attenuation and absorption of UV and blue light in natural waters. *Limnology and Oceanography*, 45(3), pp.642-650.
- McKnight, A. & Reckhow, D.A., 1992. Reactions of ozonation by-products with chlorine and chloramines. In: *Proceedings of the AWWA Annual Conference*, Vancouver, British Columbia.
- McKnight, D.M. & Aiken, G.R., 1998. Sources and age of aquatic humus. In: Hesson, D.O. & Tranvik, L.J., eds., *Aquatic Humic Substances: Ecology and Biogeochemistry*. Springer-Verlag: New York, pp.9-39.
- Murphy, K.R. et al., 2008. Distinguishing between terrestrial and autochthonous organic matter sources in marine environments using fluorescence spectroscopy. *Marine Chemistry*, 108(1-2), pp.40-58.
- Murphy, K.R. et al., 2011. Organic matter fluorescence in municipal water recycling schemes: toward a unified PARAFAC model. *Environmental Science & Technology*, 45(7), pp.2909-2916.
- Pedersen, E.J. et al., 1999. Formation of cyanogen chloride from the reaction of monochloramine with formaldehyde. *Environmental Science & Technology*, 33(23), pp.4239-4249.
- Pifer, A.D. & Fairey, J.L., 2012. Improving on SUVA₂₅₄ using fluorescence-PARAFAC analysis and asymmetric flow-field flow fractionation for assessing disinfection byproduct formation and control. *Water Research*, 46(9), pp.2927-2936.
- Plewa, M.J. et al., 2008. Comparative mammalian cell toxicity of N-DBPs and C-DBPs. In: *Disinfection By-Products in Drinking Water: Occurrence, Formation, Health Effects, and Control*. ACS Symposium Series 995. American Chemical Society, pp.36-50.
- Reckhow, D.A. et al., 2010. Effect of UV treatment on DBP formation. *Journal American Water Works Association*, 102(6), pp.100-113.

- Roccaro, P. et al., 2009. Changes in NOM fluorescence caused by chlorination and their associations with disinfection by-products formation. *Environmental Science & Technology*, 43(3), pp.724-729.
- Rook, J.J. et al., 1978. Bromide oxidation and organic substitution in water treatment. *Journal of Environmental Science and Health, Part A*, A13(2), pp.91-116.
- Schreiber, I.M. & Mitch, W.A., 2005. Influence of the order of reagent addition on NDMA formation during chloramination. *Environmental Science & Technology*, 39(10), pp.3811-3818.
- Sclimenti, M.J. et al., 1994. The simultaneous determination of cyanogen chloride and cyanogen bromide in chloraminated waters by a simplified microextraction GC/ECD technique. In: *Proceedings of the AWWA Water Quality Technology Conference*, Charlotte, North Carolina, pp.489-506.
- Shah, A.D. et al., 2011. Impact of UV disinfection combined with chlorination/chloramination on the formation of halonitromethanes and haloacetonitriles in drinking water. *Environmental Science & Technology*, 45(8), pp.3657-3664.
- Song, H. et al., 2009. Isolation and fractionation of natural organic matter: evaluation of reverse osmosis performance and impact of fractionation parameters. *Environmental Monitoring and Assessment*, 153(1-4), pp.307-321.
- Stedmon, C.A. et al., 2003. Tracing dissolved organic matter in aquatic environments using a new approach to fluorescence spectroscopy. *Marine Chemistry*, 82(3-4), pp.239-254.
- Stedmon, C.A. & Markager, S., 2005. Resolving the variability in dissolved organic matter fluorescence in a temperate estuary and its catchment using PARAFAC analysis. *Limnology and Oceanography*, 50(2), pp.686-697.
- Stedmon, C.A. & Bro, R., 2008. Characterizing dissolved organic matter fluorescence with parallel factor analysis: a tutorial. *Limnology and Oceanography*, 6, pp.572-579.
- Summers, R.S. et al., 1987. Molecular size distribution and spectroscopic characterization of humic substances. *Science of the Total Environment*, 62, pp.27-37.
- Trofe, T.W. et al., 1980. Kinetics of monochloramine decomposition in the presence of bromide. *Environmental Science & Technology*, 14(5), pp.544-549.
- U.S. EPA (Environmental Protection Agency), 1992. *National Primary Drinking Water Regulations: Synthetic Organic Chemicals and Inorganic Chemicals, Final Rule*. Federal Register 57(138), pp.31776-31849.

- U.S. EPA (Environmental Protection Agency), 2006. *National Primary Drinking Water Regulations: Stage 2 Disinfectants and Disinfection Byproducts Rule*. Federal Register 71(2), pp.387-493.
- Weinberg, H.S. et al., 2002. *The Occurrence of Disinfection By-Products (DBPs) of Health Concern in Drinking Water: Results of a Nationwide DBP Occurrence Study*. EPA/600/R-02/068, U.S. EPA: Athens, Georgia.
- Westerhoff, P. et al., 1999. Relationships between the structure of natural organic matter and its reactivity towards molecular ozone and hydroxyl radicals. *Water Research*, 33(10), pp.2265-2276.
- Westerhoff, P. et al., 2004. Reactivity of natural organic matter with aqueous chlorine and bromine. *Water Research*, 38(6), pp.1502-1513.
- Yang, X., et al., 2008. Correlations between organic matter properties and DBP formation during chloramination. *Water Research*, 42(8-9), pp.2329-2339.
- Yang, X. et al., 2010. Nitrogenous disinfection byproducts formation and nitrogen origin exploration during chloramination of nitrogenous organic compounds. *Water Research*, 44(9), pp.2691-2702.

Chapter 5: Formation and Cytotoxicity of Disinfection Byproduct Mixtures Produced from UV-Chlorine/Chloramine Treatment

5.1 Introduction

Drinking water disinfection was one of the greatest public health advances of the 20th century. The introduction of drinking water chlorination vastly reduced cholera and typhoid incidences and the deaths associated with these outbreaks. In the mid-1970's, byproducts of the chlorination process were discovered, including chloroform and other trihalomethanes (THMs) (Rook 1974; Bellar et al. 1974). Disinfection byproducts (DBPs) are formed when a disinfectant reacts with ubiquitous decaying plant and microbial matter (natural organic matter, NOM), salts in water which can be of natural origin such as bromide and iodide, or anthropogenic pollutants. Shortly after the discovery of DBPs in drinking water, the National Cancer Institute released a report showing that chloroform was carcinogenic to laboratory animals (National Cancer Institute 1976) and another study demonstrated a mutagenic bioassay response from concentrated organic extracts of chlorinated waters (Loper et al. 1978). Epidemiological studies have suggested an association between exposure to waters containing elevated levels of DBPs and adverse human health outcomes, including bladder cancer and reproductive effects (Bove et al. 1995; Cantor et al. 1998), further emphasizing the importance of balancing microbial inactivation and chemical byproduct risk. The United

States Environmental Protection Agency (U.S. EPA) currently regulates a subset of two major DBP classes formed during chlorination, chosen as indicators for overall DBP formation: four chlorine- and bromine-containing THMs (THM4) and five chlorine- and bromine-containing haloacetic acids (HAA5), along with bromate and chlorite (U.S. EPA 2006).

Single compound *in vitro* assays have helped to identify the relative toxicity within and across DBP classes. For example, toxicological assays have shown that nitrogen-containing DBPs are more geno- and cytotoxic than the regulated THM4 and HAA5 and that bromine- and iodine-substituted DBPs are more toxic than their corresponding chlorine-containing byproducts (Plewa et al. 2004; Richardson et al. 2008). Combining single compound toxicity data with DBP occurrence information can provide insight into which DBPs or DBP classes are of most concern (Richardson et al. 2007). However, while more than 500 individual DBPs have been identified in laboratory and field studies using a variety of treatments and disinfectants, there remains a large percentage of unidentified byproducts as indicated by analysis of total organic halogen (Hua & Reckhow 2007). A measure of total organic halogen can be compared to the chlorine equivalents of individually measured halogen-containing DBPs to determine a percentage of unknown halogenated organics. Little is known about what is contained within this unknown fraction and how it contributes to the total toxicity of treated water. Bull and colleagues (2001) reported that epidemiological findings associated with disinfected drinking water could not be accounted for by the regulated DBPs alone. Thus, there is a need for research focused on identifying the potential health effects of DBP mixtures present in treated water samples, which include known and unknown

byproducts and are more representative of what consumers are actually exposed to on a regular basis.

As a result of anthropogenic impacts on source water quality and increasingly stringent DBP regulations, utilities have been looking at alternative treatment processes to chlorination (e.g. chloramines, ozone, chlorine dioxide). An occurrence study of treated drinking waters across the United States found that while the use of these alternative disinfectants reduced regulated THM4 and HAA5 formation, in some cases, these processes also increased the formation of DBPs of toxicological importance (Krasner et al. 2006). Ultraviolet (UV) irradiation is an alternative treatment process that has gained popularity because of its effectiveness at inactivating chlorine-resistant pathogens, such as *Cryptosporidium* (Clancy et al. 2000), and the potential to minimize halogen-containing DBP formation with its lack of chemical inputs. In North America, however, UV needs to be used in combination with a secondary disinfectant, such as chlorine or chloramine, to provide a residual for distribution. Low pressure (LP, monochromatic output at 253.7 nm) and medium pressure (MP, polychromatic output 200-400 nm) are the two commonly used lamp types for UV treatment. Most of the research investigating DBP formation from UV-chlorine/chloramine treatment has focused on the regulated THM4 and HAA5 (Malley et al. 1995; Liu et al. 2002; Dotson et al. 2010), rather than emerging, unregulated DBPs, some of which are thought to be more geno- and cytotoxic. Studies that have looked at effects on nitrogen-containing DBPs showed that MP UV at disinfection doses (40-186 mJ/cm²), in combination with chlorine or chloramine, could increase the formation of halonitromethanes in waters containing nitrate (1-10 mg N/L) (Reckhow et al. 2010; Shah et al. 2011).

In addition to DBP analysis, toxicological studies are an important aspect of evaluating and comparing alternative treatment processes. Commonly studied health endpoints in DBP toxicity studies include cytotoxicity (cell death); mutagenicity (changes in DNA sequence); genotoxicity (includes mutagenicity as well as DNA damage); and carcinogenicity (causes cancer). While the value and necessity of *in vivo* animal studies for estimating human health risk to DBPs through multiple exposure routes and different endpoints is recognized, these types of experiments are very labor-intensive, costly, and lengthy. *In vitro* assays allow for lower cost, shorter time-frame, and higher throughput experiments that are well-suited for comparative studies. Additionally, *in vitro* experiments can be carried out using human cells, while corresponding *in vivo* studies clearly could not be performed on human subjects. *In vitro* assays that are commonly used for DBP toxicity studies to test the above-mentioned endpoints include the Ames mutagenicity assay; the single cell gel electrophoresis (“comet”) genotoxicity assay; and a microplate-based cytotoxicity assay. A study that looked at mutagenicity in *Salmonella* for organic extracts of treated waters showed that those treated with ozone and post-chlorination were less mutagenic than those treated with chlorine (DeMarini et al. 1995). A similar experiment confirmed this finding using chlorine doses adjusted to leave similar target residuals (Claxton et al. 2008). Backlund (1995) observed an increase in *Salmonella* mutagenicity for a concentrated extract of a surface water treated with 10-60 mJ/cm² LP UV prior to chlorination, compared to the same water treated with only chlorine at the same dose. One disadvantage to the Ames mutagenicity assay is that the test subject is bacteria, which makes results difficult to extrapolate to humans. The comet genotoxicity assay has been applied to DBP studies using mammalian and even human

cells (Landi et al. 2003), so the results obtained from this assay are thought to be more relevant for human health. However, the majority of these studies have only tested single compounds rather than DBP mixtures, and research that has taken place on mixtures has typically used simple, defined mixtures that are not representative of a real disinfected water that consumers would be exposed to on a regular basis.

Most toxicological assays require sample concentration to induce a measurable response. A common technique for concentrating treated water samples is the use of XAD resins followed by elution with an organic solvent such as ethyl acetate (Loper et al. 1978; DeMarini et al. 1995). While this process allows for the application of complex mixtures to an assay, the concentration method itself may result in the loss of volatile DBPs and unidentified byproducts, and thereby, part of the toxicological fraction. For this reason, an approach in which the sample is pre-concentrated using reverse osmosis (RO) before disinfection has been developed (Pressman et al. 2010) and was used in this current work.

This work aimed to evaluate the DBP findings presented in previous chapters in the context of potential human health implications, while filling some of the research gaps described above. These include: a lack of toxicity studies on DBP mixtures, particularly those produced during alternative treatment processes, biological systems that are difficult to extrapolate to humans (e.g. bacteria), and concentration methods that may not conserve known and unknown volatile DBPs. Accordingly, the objective of this study was to use an *in vitro* chronic cytotoxicity assay in combination with DBP and total organic halogen analysis to evaluate the relative toxicity of byproducts produced during UV-chlorine/chloramine treatment of waters containing pre-concentrated organic carbon.

This approach was used so that no further concentration steps were required after disinfectant addition, limiting the loss of volatile DBPs. The assay used normal human colon cells, a relevant target cell for investigating human health effects from DBPs. The results were compared to the same waters treated with only chlorine or chloramine at a dose adjusted to provide a similar residual. A subset of samples were spiked with nitrate and iodide to investigate the impact of inorganic precursors on byproduct formation and toxicity.

5.2 Materials and Methods

Sample Preparation

Nordic Reservoir NOM was obtained as an RO isolate from the International Humic Substance Society (St. Paul, MN, USA). Initially, the aim was to use RO concentrate prepared from Orange County Water and Sewer Authority (OWASA) Drinking Water Treatment Plant raw water (Carrboro, NC, USA) to be consistent with the experiments in previous chapters. However, preliminary studies showed that the OWASA RO matrix alone inhibited cell growth at dissolved organic carbon (DOC) concentrations above 20 mg C/L (data shown in Appendix 7), which may have resulted from high levels of inorganics that were concentrated along with the organic precursors. The commercially available NOM isolates undergo additional desalting steps during their preparation, and cell growth inhibition at lower DOC concentrations was not observed for Nordic Reservoir NOM. In the solutions that were applied to cells for preliminary tests, the OWASA RO concentrate contained chloride and sulfate at 160 mg Cl⁻/L and 145 mg SO₄²⁻/L, compared to 15 mg Cl⁻/L and 38 mg SO₄²⁻/L in the Nordic Reservoir NOM. It was determined through preliminary tests that a Nordic Reservoir DOC concentration of

100 to 120 mg C/L was ideal for generating enough DBPs upon chlorination or chloramination to induce a measurable response in the cytotoxicity assay but would not itself nor the target residuals affect the cell growth prior to disinfection. Characteristics of the sample prior to UV-chlorine/chloramine treatment are shown in Table 5-1.

Aqueous solutions of Nordic Reservoir NOM were prepared by weighing out the solid NOM isolate and dissolving in laboratory grade water (LGW). LGW was prepared in-house from a Dracor system (Durham, NC, USA), which pre-filters inlet 7 M Ω deionized water to 1 μ m, removes residual disinfectants, reduces total organic carbon to less than 0.2 mg C/L with an activated carbon cartridge, and removes ions to 18 M Ω with mixed bed ion-exchange resins. Samples were filtered (0.45 μ m) and DOC and total dissolved nitrogen (TDN) were measured using a Shimadzu TOC-V_{CPH} Total Organic Carbon Analyzer with a TNM-1 Total Nitrogen Measuring Unit (Shimadzu Corporation, Atlanta, GA, USA) following Standard Method 5310 (APHA 1999). Samples were stored in amber glass bottles at 4°C until use. Prior to chlorination/chloramination, samples were buffered with 20 mM phosphate buffer at pH 7.1 (ideal pH for the cells used in this work). A subset of samples were spiked with nitrate (100 mg N/L) and iodide (5 mg/L), administered in the sodium and potassium salt form, respectively. These spiking amounts were chosen to correspond with a high level of nitrate or iodide correspondingly scaled-up with the DOC (approximately 50-fold) compared to a typical surface water, and it was confirmed that the phosphate buffer and nitrate/iodide levels did not affect cell growth through preliminary tests (results shown in Appendix 7).

Table 5-1. Characteristics of Nordic Reservoir NOM solution prior to UV/chlorine-chloramine treatment and application to cytotoxicity assay.

parameter	unit	concentration
DOC	mg C/L	112
TDN	mg N/L	4.2
SUVA ₂₅₄	(L /mg C·m)	4.5
chloride	mg/L	17.8
nitrate	mg N/L	0.20
bromide	mg/L	<0.04
iodide	mg/L	<0.08

DOC = dissolved organic carbon

TDN = total dissolved nitrogen

SUVA₂₅₄ = specific UV absorbance (UV absorbance at 254 nm normalized to dissolved organic carbon)

UV Treatment

UV treatment was performed using quasi-collimated irradiation from a custom-built unit containing a 550 W MP lamp (Ace-Hanovia, Vineland, NJ, USA) with a 4-inch aperture. Samples were retained in a 250-mL capacity Pyrex crystallization dish and stirred during irradiation. Constant sample temperature was maintained at 20-25°C by placing the dish in a copper coil which was connected to a programmable refrigerated recirculating water unit. A manual shutter was used to rapidly begin or end the irradiation. An MP UV dose of 500 mJ/cm² was applied and determined using calculation techniques described by Bolton and Linden (2003)⁴. Briefly, UV irradiance was measured at the water surface using an SED240 detector with a W diffuser connected to an IL1400A radiometer (International Light, Peabody, MA, USA). The irradiance between 200 to 300 nm was multiplied by a Petri factor (0.92), water factor, radiometer sensor factor, reflection factor, and germicidal factor to obtain a germicidal irradiance in

⁴It is recognized that 500 mJ/cm² is a higher dose than those typically used for disinfection (40-186 mJ/cm²), but it was chosen to enhance trends and to determine which treatment conditions were of interest for further investigation.

mW/cm². The irradiation time (s) was then determined by dividing the desired UV dose (mJ/cm² or mW·s/cm²) by the germicidal irradiance. Uridine actinometry was used to confirm UV irradiance following the procedure described by Jin et al. (2006). The MP UV system operating procedure is provided in Appendix 3. UV/visible absorbance was measured using a Hewlett Packard 8452A Diode Array spectrophotometer (Agilent, Santa Clara, CA, USA).

Chlorination and Chloramination

It was determined through preliminary experiments that ascorbic acid, which is typically used to quench residual disinfectants before DBP analysis, as well as the byproducts of this quenching reaction, significantly increased cell growth. However, chlorine or monochloramine residuals up to 10 mg/L as Cl₂ did not impact cell growth in these preliminary tests (data shown in Appendix 7), so treated samples were applied to the assay without quenching and with a target residual of 3.0 mg/L as Cl₂ after 24 hours. After UV irradiation, samples were immediately dosed with chlorine from a concentrated sodium hypochlorite stock solution (laboratory grade, 5.6-6%, ThermoFisher Scientific, Waltham, MA, USA) or pre-formed monochloramine. Samples were then transferred to headspace-free amber glass bottles with caps and polytetrafluoroethylene (PTFE)-lined septa and held for 24 hours at 25°C, at which point chlorine or monochloramine residuals were measured and samples were applied to the cytotoxicity assay. Free chlorine residuals were measured in duplicate using the *N,N*-diethyl-*p*-phenylenediamine (DPD) colorimetric method following Standard Method 4500-Cl G (APHA 1999). A pre-formed monochloramine solution was prepared by adding free chlorine drop-wise to an

ammonium chloride (ACS grade, Mallinckrodt, St. Louis, MO, USA) solution that was adjusted to pH 8.5 with NaOH at a 1:1.2 Cl:N molar ratio (standard operating procedure is provided in Appendix 4). Monochloramine is referred to as chloramine throughout this paper for the purpose of discussion, but the pre-formed chloramine solution was prepared such that monochloramine was the primary species formed (dichloramine negligible) and ammonium chloride was present in excess so that no free chlorine remained. Chloramine speciation and concentration in the pre-formed solution were verified by UV spectrometry and solving simultaneous Beer's Law equations as described by Schreiber and Mitch (2005). Chloramine residuals in samples were analyzed in duplicate using an adaption of the indophenol method (Hach Method 10171) with MonochlorF reagent (Hach Company, Loveland, CO, USA). In order to determine the appropriate chlorine or monochloramine dose required to achieve the target residual, demand tests were carried out by applying a range of chlorine or monochloramine doses to 25 mL aliquots of each sample. After these samples were held headspace-free for 24 hours at 25°C, the chlorine or monochloramine residuals were measured and plotted against disinfectant dose, and the appropriate dose to achieve the target residual was selected.

Chronic Cytotoxicity Assay

An adaption of the microplate cytotoxicity assay described by Plewa et al. (2004) was used for this study, employing normal human colon cells (NCM460, INCELL Corporation, San Antonio, TX, USA) instead of Chinese hamster ovary (CHO) cells. Plewa and colleagues (2002) demonstrated that CHO chronic cytotoxicity was significantly and highly correlated with CHO genotoxicity for a range of DBPs, while the

same was not true for *Salmonella*, suggesting that mammalian cell chronic cytotoxicity is a useful predictive endpoint. NCM460 cells were added to flat bottom tissue culture 96-well plates at a density of 10,000 cells (in 200 μ L INCELL M3:10 media) per well, and held overnight in a 37°C incubator under a 5% CO₂ and water vapor atmosphere. 8 wells were kept empty as a blank control. Concentrated media was prepared by dissolving Minimal Essential Medium (MEM, Gibco, Carlsbad, CA, USA) and sodium bicarbonate (9.5 and 2.2 g/L final concentration, respectively) in fetal bovine serum and INCELL 10x SMX growth factor concentrate (both 10% final concentration by volume). The pH was adjusted to 7.1-7.2 (ideal pH for NCM460 cells) using sodium hydroxide and then this solution was sterile filtered (0.22 μ m, Millipore, Billerica, MA, USA). The disinfected sample was then added to the concentrated media solution at a volume ratio of 4:1. Each plate was dosed with serial dilutions of the sample (8 replicate rows for each dilution), with 8 control cell wells receiving only media (same MEM solution prepared with LGW instead of disinfected sample). The first and last columns were left empty. After sample application, plates were covered with sterile AlumnaSeal (RPI Corporation, Mt. Prospect, IL, USA), incubated for 72 hours, and processed as described by Plewa et al. (2004). Plates were read with a Wallac Victor 1420 Multilabel Counter at 600 nm (PerkinElmer Wallac Inc., Gaithersburg, MD, USA). Duplicate plates were run for each sample. A standard operating procedure for the assay is shown in Appendix 8. Data was analyzed using SigmaPlot 11.0 with integrated SigmaStat (Systat Software, Chicago, IL, USA). Three-parameter sigmoidal curves were fit to the data to calculate IC₅₀ and IC₂₀ values (inhibitory concentration at which 50 or 20% cell death occurs). A one-way analysis of variance test (ANOVA) was carried out on each sample to determine if a significant

cytotoxic response was induced by the sample, compared to the control. Confidence intervals (95%) and statistical significance ($P < 0.01$) between sample IC_{50} values (or IC_{20} and IC_{10} if 50% cell death was not achieved) were determined using R Statistical Software with the “boot” package (R Foundation for Statistical Computing, Vienna, Austria). The R code used for these analyses is provided in Appendix 7.

DBP and Total Organic Halogen Analysis

After the 24-hour holding time, chlorine/chloramine residuals were measured and an aliquot of the sample was transferred to an amber glass vial and immediately applied to the chronic cytotoxicity assay. The remaining samples were diluted 5x (chloraminated samples) or 10x (chlorinated samples) in LGW so that the analyte concentrations would be within the instrumental detection range. Samples were then transferred to vials containing quenching agent (ammonium sulfate for HAAs and ascorbic acid for all other compounds) and stored headspace-free at 4°C until DBP and total organic halogen analysis, which was carried out as five separate extractions: (1) THM10 (10 chlorine-, bromine-, and iodine-containing species), 4 haloacetonitriles (trichloro-, dichloro-, bromochloro-, and dibromo-acetonitrile), two haloketones (1,1-dichloro- and 1,1,1-trichloro-propanone), two halonitromethanes (trichloro- and tribromo-nitromethane), chloral hydrate, and 11 haloacetamides (bromo-, dichloro-, bromochloro-, trichloro-, dibromo-, chloriodo-, bromodichloro-, bromiodo-, dibromochloro-, tribromo-, and diiodo-acetamide); (2) cyanogen chloride; (3) nine chlorine- and bromine-containing HAAs (HAA9); (4) total organic halogen; and (5) total organic halogen speciation into total organic chlorine, bromine, and iodine. All analyses were carried out within two

weeks of quenching, except for the first suite of DBPs, which were extracted within 24 hours of quenching. DBPs were liquid-liquid extracted with methyl tert-butyl ether (MtBE) and analyzed on a Hewlett-Packard 5890 gas chromatograph with ^{63}Ni electron capture detector (GC-ECD) following the procedures described by Scilimenti et al. (1994) for cyanogen chloride, Brophy et al. (2000) for HAAs, and Weinberg et al. (2002) for the remaining DBPs. Standard operating procedures for these extractions are provided in Appendices 5A-5C. THM4, HAA9, chloral hydrate, chloropicrin (trichloronitromethane), haloacetonitrile, haloketone, and bromo-, dichloro- and trichloro-acetamide standards were obtained from Supelco and Sigma-Aldrich (Sigma Chemical Co., St. Louis, MO, USA). Bromopicrin (tribromonitromethane), iodo-THM, and remaining haloacetamide standards were obtained from Orchid Cellmark (New Westminster, BC, Canada). Cyanogen chloride was obtained from SPEX Certiprep (Metuchen, NJ, USA). A Zebron (Phenomenex, Torrance, CA, USA) ZB-1 capillary column (30 m length, 0.25 mm inner diameter, 1.0- μm film thickness) was used for chromatographic separation of compounds, except for cyanogen chloride which was analyzed on a ZB-1701 capillary column (30 m length, 0.25 mm inner diameter, 1.0- μm film thickness). Chromatographic conditions for DBP analysis are described in Chapter 2. All samples were analyzed in duplicate and 1,2-dibromopropane was used as an internal standard. The minimum reporting limit (MRL) for all compounds except HAAs was 0.5 or 1 $\mu\text{g/L}$ (based on sample dilution). The MRL for HAAs ranged from 0.5 to 15 $\mu\text{g/L}$ for individual species. Total organic halogen was measured on a Rosemount Dohrmann DX-2000 organic halide analyzer using adsorption, pyrolysis, and titration as described in Standard Method 5320 (APHA 1999). Total organic halogen was further

separated into total organic chlorine, bromine, and iodine, using an adaption of Standard Method 5320 as described by Hua and Reckhow (2006). Samples were adsorbed and pyrolyzed, but instead of titrating the hydrogen halides formed during pyrolysis, they were collected in 10 mL LGW and measured as chloride, bromide, and iodide by ion chromatography. Analysis was carried out with a Dionex ion chromatography system comprised of a GPM-2 Gradient pump, CDM-II Conductivity Detector, and Dionex eluent degas module with an IonPac AS22 analytical column, AG22 Guard column, and AMMS-III 4 mm ion suppressor (Dionex, Sunnyvale, CA, USA) using 5 mM sodium carbonate/1.4 mM sodium bicarbonate eluent.

5.3 Results

DBP Formation

A summary of DBP and total organic halogen formation compared to IC₂₀ and IC₅₀ values (inhibitory concentrations at which 20 and 50% cell death occurs, respectively, compared to control cells) is shown in Table 5-2. For comparison across samples, a lower IC₂₀ or IC₅₀ value indicates a higher relative toxicity (i.e. sample becomes more cytotoxic at a lower concentration). THM4 formation was increased 33% with the use of 500 mJ/cm² MP UV prior to chlorination in ambient Nordic Reservoir samples, compared to chlorination alone, similar to the 30-40% increases observed with 1000 mJ/cm² MP UV followed by chlorination in samples presented in Chapter 2. Total organic halogen, THM4, and HAA9 formation were higher during chlorination compared to chloramination, as expected based on past work (Brodtsmann & Russo 1979; Lykins et al. 1986) and consistent with findings presented in previous chapters. During

chloramination, however, there was a greater fraction of unknown total organic halogen (82-87%, percentage of measured total organic halogen that could not be accounted for by chlorine equivalents of individually measured DBPs) compared to chlorination (30-42%), which is also consistent with previous research (Hua & Reckhow 2007; Diehl et al. 2000). Regardless of treatment condition, the total organic halogen formation accounted for 10-13% of the consumed chlorine/chloramine (demand) in all samples. This suggests that while the chloramine demand of this water was lower compared to the chlorine demand on a Cl_2 :DOC basis, the chloramine that did react under the experimental conditions used here had the same ability as chlorine to become incorporated into halogenated organics.

Table 5-2. Effect of treatment conditions on DBP formation and cell growth inhibition (IC₂₀ and IC₅₀ values).

Spiking ^a	MP UV dose (mJ/cm ²)	Secondary disinfectant	Demand ^b (µM Cl)	THM4 (µM)	THM10 ^c (µM)	HAA9 (µM)	Total organic halogen (µM as Cl)	Unknown total organic halogen ^d	DOC mg C/L ^e		Total organic halogen M as Cl	
									IC ₂₀	IC ₅₀	IC ₂₀	IC ₅₀
ambient	0	HOCl	6030	67.3	67.3	77.2	684	36%	30±3	66±3	(1.8±0.2)×10 ⁻⁴	(3.9±0.2)×10 ⁻⁴
ambient	500	HOCl	6450	89.5	89.5	81.1	859	39%	34±5	72±4	(2.6±0.4)×10 ⁻⁴	(5.6±0.3)×10 ⁻⁴
nitrate	0	HOCl	6250	82.6	82.6	75.8	831	42%	27±5	76±5	(1.9±0.3)×10 ⁻⁴	(5.6±0.4)×10 ⁻⁴
nitrate	500	HOCl	7330	78.6	78.6	75.8	763	31%	32±4	63±3	(2.2±0.3)×10 ⁻⁴	(4.3±0.2)×10 ⁻⁴
iodide	0	HOCl	6540	85.7	85.7	91.0	784	33%	47±5	81±4	(3.3±0.3)×10 ⁻⁴	(5.7±0.3)×10 ⁻⁴
ambient	0	NH ₂ Cl	820	0.8	0.8	3.6	94.6	87%	NA ^f	NA	NA	NA
ambient	500	NH ₂ Cl	1200	1.3	1.3	6.9	140	85%	29±7	70±4	(3.7±0.8)×10 ⁻⁵	(8.7±0.4)×10 ⁻⁵
iodide	0	NH ₂ Cl	1050	0.6	1.3	3.4	124	88%	60±6	NA	(6.6±0.7)×10 ⁻⁵	NA
iodide	500	NH ₂ Cl	1420	1.0	1.9	6.3	143	82%	39±4	63±3	(5.0±0.5)×10 ⁻⁵	(8.0±0.3)×10 ⁻⁵

^aAmbient = unspiked. Nitrate and iodide spiking amounts were 100 mg N/L and 5 mg I/L, respectively.

^bDemand is the difference between chlorine/chloramine dose and residual after 24 hour holding time.

^cTHM10 = sum of 10 chlorine-, bromine-, and iodine-containing species.

^dUnknown = difference between measured total organic halogen value and sum of chlorine equivalents from individually measured DBPs.

^eIC₂₀ and IC₅₀ values are reported as DOC concentration or total organic halogen formation in the Nordic Reservoir sample (average of n = 16 replicates) with 95% confidence interval shown as ± value.

^fNA = not applicable, could not be calculated because 20 or 50% cell growth inhibition was not observed in this sample. IC₁₀ values for the ambient and iodide-spiked NH₂Cl samples were 83±6 and 60±6 mg C/L, respectively, on a DOC basis and (1.6±0.8)×10⁻⁵ and (3.6±0.6)×10⁻⁵ M as Cl, respectively, on a total organic halogen basis.

Cytotoxicity

All treated samples passed a one-way analysis of variance test (ANOVA) test ($P < 0.01$), meaning that cell growth inhibition was statistically significant compared to control cells. R^2 values for all sample curves were 0.98-0.99, except for ambient and iodide-spiked chloramine alone samples (0.78 and 0.93, respectively), which were the least cytotoxic samples on a DOC basis. Although it is tempting to make assumptions about statistical significance by just looking at standard deviation error bars or confidence intervals, this can lead to mistaken conclusions when interpreting the type of data presented in this chapter (Schenker and Gentleman 2001). Most samples discussed in Chapters 2, 3, and 4 (and DBP results discussed in this chapter), were only analyzed in duplicate due to limited available sample volume and labor-intensive extraction procedures. “Significance” of findings between different treatments in those cases was more generally defined as whether the range of values between two replicates overlapped with that of another sample. The toxicity data presented in this chapter contained enough replicates to carry out statistical tests for significance, the results of which are summarized in Table 5-3.

Figures 5-1 and 5-2 show the dose-response curves for chlorine and MP UV-chlorine treatment of ambient (Figure 5-1) and nitrate-spiked (Figure 5-2) samples, as a function of DOC in the serially diluted samples of treated Nordic Reservoir NOM. Cytotoxicity induced by the ambient chlorinated sample was not statistically different than that of the MP UV + chlorine sample. The use of MP UV prior to chlorination in nitrate-spiked samples resulted in a greater cytotoxicity that was statistically different than that of the nitrate-spiked chlorinated sample (76 ± 5 and 63 ± 3 mg DOC/L for chlorine

and MP UV + chlorine, respectively), shown in Figure 5-2. Treatment with MP UV prior to chloramination resulted in a higher cytotoxicity compared to chloramination alone, and this was further increased in the presence of iodide, shown in Figure 5-3. Cell growth inhibition of 50% was not obtained by either the ambient or iodide-spiked chloramine alone samples, but was in the corresponding MP UV-treated samples. Cytotoxicity was slightly higher in the iodide-spiked compared to the ambient MP UV + chloramine samples. The cytotoxicity curves for all treated samples are shown on the same plot in Figure 5-4. Figure 5-5 shows the dose response curve for iodide-spiked samples as a function of total organic halogen formation rather than DOC of the sample that was shown in Figures 5-1 to 5-4. While the overall total organic halogen produced in the chlorinated samples (684-859 μM as Cl) was higher than that of chloraminated samples (95-143 μM as Cl), the organic halogens formed during chloramination were more cytotoxic on a molar basis, shown in Figure 5-5 and Table 5-2.

Table 5-3. Results of statistical comparison for IC₅₀ values (on a DOC basis) between each sample. If cytotoxicity was statistically different (P<0.01), it is denoted by Y (yes) and > sign shows which sample was more cytotoxic. If not statistically different (P>0.01), it is denoted by N (no).

Sample ^a	1	2	3	4	5	6 ^b	7	8 ^c	9
1		N	Y, 1>3	N	Y, 1>5	Y, 1>6	N	Y, 1>8	N
2			N	Y, 4>2	Y, 2>5	Y, 2>6	N	Y, 2>8	Y, 9>2
3				Y, 4>3	N	Y, 3>6	N	Y, 3>8	Y, 9>3
4					Y, 4>5	Y, 4>6	N	Y, 4>8	N
5						Y, 5>6	Y, 7>5	Y, 5>8	Y, 9>5
6							Y, 7>6	Y, 8>6	Y, 9>6
7								Y, 7>8	Y, 9>7
8									Y, 9>8
9									

^aSample legend:

1 = ambient, HOCl; 2 = ambient, MP UV + HOCl;

3 = nitrate-spiked, HOCl; 4 = nitrate-spiked, MP UV + HOCl; 5 = iodide-spiked, HOCl;

6 = ambient, NH₂Cl; 7 = ambient, MP UV + NH₂Cl;

8 = iodide-spiked, NH₂Cl; 9 = iodide-spiked, MP UV + NH₂Cl

Table is read by comparing top legend (left to right) samples with left sidebar samples (top to bottom) in corresponding cell.

^bIC₁₀ values of sample 6 were compared with IC₁₀ values of other samples because 50 and 80% cell growth inhibition were not obtained.

^cIC₂₀ values of sample 8 were compared with IC₂₀ values of other samples because 50% cell growth inhibition was not obtained.

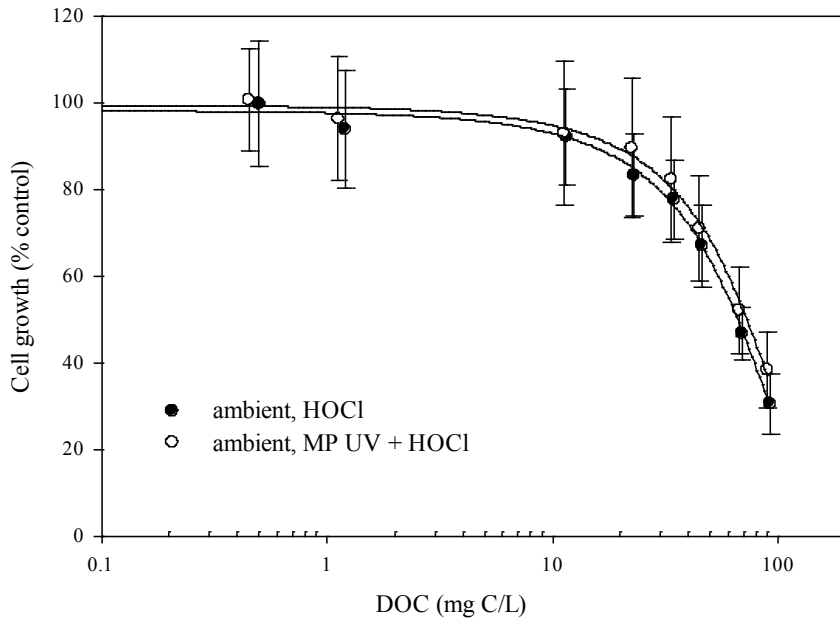


Figure 5-1. Dose-response curves for chlorine and MP UV-chlorine treatment of ambient Nordic Reservoir samples. MP UV dose was 500 mJ/cm². Error bars represent standard deviation for n = 16 replicates.

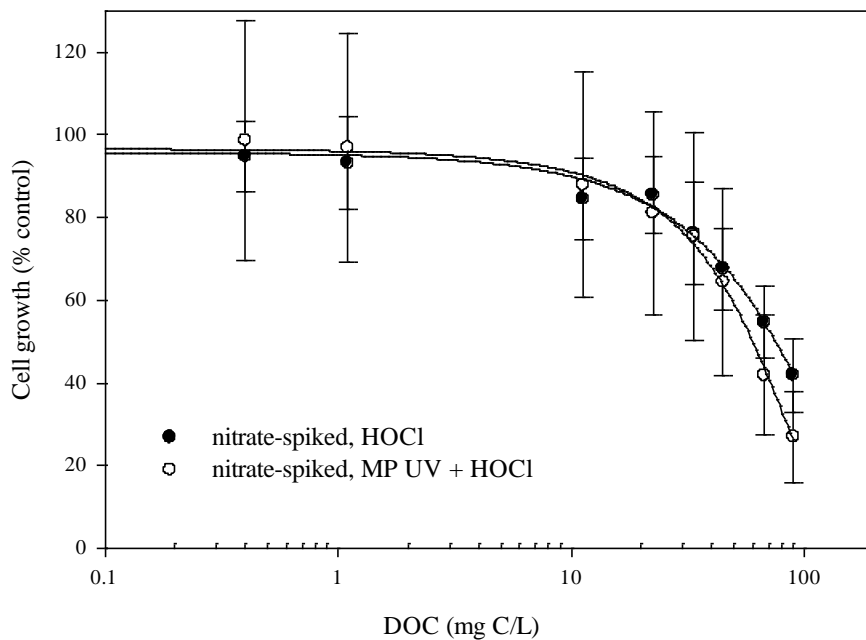


Figure 5-2. Dose-response curves for chlorine and MP UV-chlorine treatment of nitrate-spiked Nordic Reservoir samples. MP UV dose was 500 mJ/cm², and nitrate spiking amount was 100 mg N/L. Error bars represent standard deviation for n = 16 replicates.

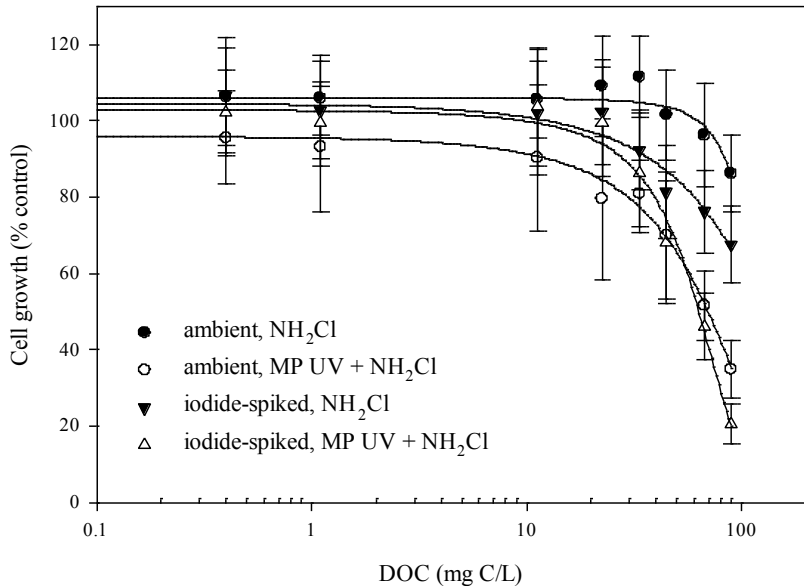


Figure 5-3. Dose-response curves for chloramine and MP UV-chloramine treatment of ambient and iodide-spiked Nordic Reservoir samples. MP UV dose was 500 mJ/cm², and iodide spiking amount was 5 mg/L. Error bars represent standard deviation for n = 16 replicates.

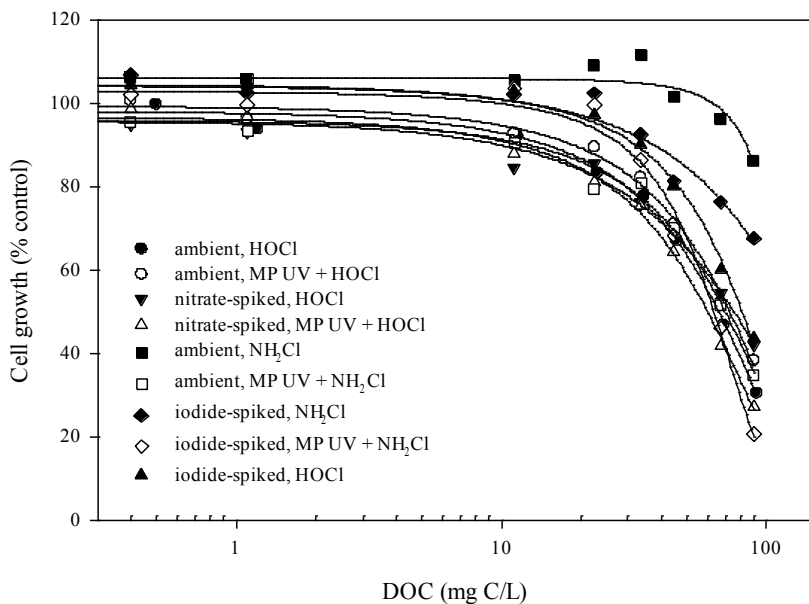


Figure 5-4. Dose-response curves for all treated Nordic Reservoir samples on a DOC basis. MP UV dose was 500 mJ/cm², and spiking amounts were 100 mg N/L nitrate and 5 mg/L iodide. Each point represents n = 16 replicates, standard deviation error bars not shown here to keep plot legible.

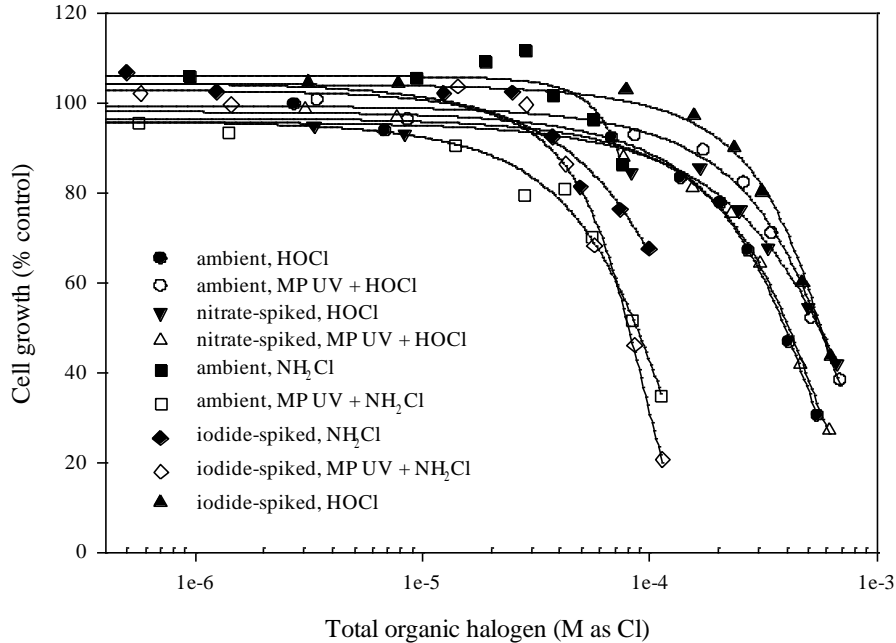


Figure 5-5. Dose-response curves for all treated Nordic Reservoir samples on a total organic halogen formation basis. MP UV dose was 500 mJ/cm², and spiking amounts were 100 mg N/L nitrate and 5 mg/L iodide. Each point represents n = 16 replicates, standard deviation error bars not shown here to keep plot legible.

Emerging DBP Formation

Table 5-4 shows the formation of several unregulated DBPs

(trichloronitromethane, chloral hydrate, and cyanogen chloride) that have been previously shown to be impacted by MP UV irradiation in sequence with chlorine or chloramine (Liu et al. 2006; Reckhow et al. 2010) and are discussed in more detail in Chapter 2.

Trends observed under different treatment conditions in this study were generally consistent with results presented in previous chapters. In nitrate-spiked samples, trichloronitromethane formation was greater in samples treated with MP UV followed by chlorine (15.3 µM, 2.5 mg/L), compared to chlorine alone (0.1 µM, 0.017 mg/L).

Without UV, trichloronitromethane yield (concentration normalized to DOC) in ambient

samples was similar to results presented in Chapter 2 (0.8 and 0.7 nmol/mg C for Nordic Reservoir and Utility C samples, respectively, treated with chlorine alone). In those ambient samples, trichloronitromethane formation with 500 mJ/cm² (Nordic Reservoir) or 1000 mJ/cm² (Utility C) MP UV followed by chlorine was 1.0 and 1.5 nmol/mg C, respectively. The nitrate-spiked Nordic Reservoir sample treated with 500 mJ/cm² MP UV followed by chlorine, however, had a higher trichloronitromethane yield (136 nmol/mg C) compared to the nitrate-spiked Utility C sample treated with 1000 mJ/cm² MP UV and chlorine (22 nmol/mg C). A comparison of DBP formation between concentrated and dilute Nordic Reservoir samples is discussed later in this chapter.

Chloral hydrate formation was increased 70-90% with the use of 500 mJ/cm² MP UV prior to chlorination compared to samples treated with chlorine alone, in both ambient and nitrate-spiked samples. Consistent with results presented in Chapter 2, spiking with nitrate did not affect chloral hydrate formation during chlorination or MP UV/chlorine treatment. For samples treated with chloramine alone, chloral hydrate was below detection limit (<0.003 μM, <0.5 μg/L), but was detected in samples treated with 500 mJ/cm² MP UV prior to chloramination (0.02-0.07 μM, 3.3-11 μg/L).

Cyanogen chloride is generally observed as a chloramination byproduct (Krasner et al. 1989), which is consistent with the higher levels formed in chloraminated compared to chlorinated samples presented here and in previous chapters. Its formation increased three- to four-fold with the use of 500 mJ/cm² MP UV followed by chloramination in ambient (0.61 μM, 38 μg/L) and iodide-spiked samples (0.58 μM, 36 μg/L), compared to chloramination alone (0.16 and 0.20 μM, 10 and 13 μg/L, for ambient and iodide-spiked samples, respectively). However, even at these levels obtained from high disinfectant

doses and concentrated NOM, cyanogen chloride concentrations remained below the World Health Organization guideline value of 70 µg/L (1.1 µM) for the sum of all cyanide species in water (WHO 1993). In comparison to cyanogen chloride yield from chloramine and MP UV + chloramine treatment of two different source waters presented in Chapter 2, its formation in ambient Nordic Reservoir NOM was between that of Utility B and C samples. Cyanogen chloride yield was 1.5, <0.005, and 2.3 nmol/mg C for ambient Nordic Reservoir, Utility B, and Utility C samples, respectively, following chloramination alone. For samples treated with 500 mJ/cm² MP UV (Nordic Reservoir) or 1000 mJ/cm² (Utilities B and C) followed by chloramination, cyanogen chloride yield was 5.5, 14.9, and 4.5 nmol/mg C, respectively. Utility B samples had higher ambient nitrate concentration (N:DOC ratio of 0.56) compared to Nordic Reservoir and Utility C (N:DOC ratios of 0.002 and <0.007, respectively) and nitrate was shown to enhance cyanogen chloride formation with MP UV + chloramine treatment, which is likely why Utility B had the higher cyanogen chloride yield compared to the other source waters.

Chloral hydrate and tribromonitromethane were also evaluated as individual standards with the chronic cytotoxicity assay; the calculated IC₅₀ values for these compounds were 5.4×10⁻⁵ M and 2.1×10⁻⁵ M, respectively (data shown in Appendix 7). Tribromonitromethane was chosen over trichloronitromethane because the latter was not available as an individual standard (sold in a mixture with other DBPs). As these samples were not spiked with bromide, tribromonitromethane was below detection limit (<1.7 or 3.4 nM, <0.5 or 1.0 µg/L) in all samples except the nitrate-spiked, MP UV + chlorine treated sample (3.9 nM, 1.2 µg/L).

In comparison to another cell type, Plewa and colleagues (2004) reported a cytotoxicity IC_{50} value of 8.57×10^{-6} M for tribromonitromethane in CHO cells, which means that tribromonitromethane was more cytotoxic for CHO cells than for human colon cells. A range of DBPs have been individually evaluated using this assay with NCM460 human colon cells and compared to results in CHO cells (DeAngelo et al. 2007, DeAngelo unpublished data). The cytotoxicity of DBP classes and speciation show similar trends between the two cell types but the magnitude of specific DBP IC_{50} values varied for some compounds. Different toxicity responses between the two cell lines would be expected because CHO cells are not metabolically active, while the human colon cells can undergo metabolism (DeAngelo et al. 2007). The difference in toxicity of the same compound between different cell types would depend on its mode of action and associated cellular functions of the target cell. Toxicity of some chemicals is activated by metabolism (e.g. nitrosamines), while others can be processed through metabolism into less toxic compounds (Wagner et al. 2012).

UV had little effect on the formation of haloacetamides during chlorination, as previously observed with samples described in Chapter 2. Dichloro- and trichloroacetamide were the only haloacetamide species detected in ambient samples, while chloriodo- and diiodoacetamide were also detected in iodide-spiked chloraminated samples. Dichloroacetamide was the main species formed during chloramination with very little trichloroacetamide formation, similar to what is typically observed with haloacetic acids and further supporting the hypothesis that di- and trihalogenated DBPs are formed through different mechanisms (Hua & Reckhow 2007). Dichloro- and trichloroacetamide formation were increased 82-83% with the use of MP

UV prior to chloramination, compared to chloramination alone. These compounds were not evaluated as individual standards with the human colon cells in this work, but Plewa et al. (2008) reported CHO chronic cytotoxicity IC_{50} values of 1.92×10^{-3} and 2.05×10^{-3} M for dichloro- and trichloroacetamide, respectively. In the same study, chloriodo- and diiodoacetamide were three to four orders of magnitude more cytotoxic to CHO cells (chloriodo- and diiodoacetamide IC_{50} values of 5.97×10^{-6} and 6.78×10^{-7} M, respectively) compared to the di- and trichlorinated species. In the current study, formation of chloriodo- and diiodoacetamide were increased 53% and 31%, respectively, in iodide-spiked samples treated with MP UV prior to chloramination, compared to chloramination alone, shown in Table 5-4.

Diiodoacetamide was evaluated as an individual standard for cytotoxicity in human colon cells, and an IC_{50} value of 6.1×10^{-6} M was determined. This is higher (less cytotoxic) compared to the CHO cytotoxicity IC_{50} , consistent with what was observed for tribromonitromethane cytotoxicity between the two cell types. Assuming a similar relative difference between human colon cell and CHO cytotoxicity IC_{50} responses for chloriodo- and diiodo-acetamide, a human colon cell cytotoxicity IC_{50} of 5.4×10^{-5} M can be estimated for chloriodoacetamide (which was not evaluated as an individual standard for the current study). The formation of iodine-containing acetamides in iodide-spiked samples treated with chloramine and MP UV + chloramine were 1.3×10^{-7} and 2.0×10^{-7} M, respectively, for chloriodoacetamide and 8.0×10^{-8} and 1.1×10^{-7} M, respectively, for diiodoacetamide, which is one to two orders of magnitude less than the calculated (or estimated) IC_{50} values for these compounds.

Iodine Incorporation

Also shown in Table 5-4 is the iodine speciation into THMs, which is of importance because iodine-substituted DBPs are thought to be more toxic than their corresponding chlorine-containing byproducts (Richardson et al. 2008). This study focused on iodine rather than bromine incorporation, due to the higher relative toxicity of iodine-substituted DBPs. Iodine incorporation into DBPs can occur when iodide is present in source waters, which can result from rainfall, rock weathering, and saltwater intrusion in surface and groundwaters, with concentrations typically in the low $\mu\text{g/L}$ range (Fuge & Johnson 1986). Its incorporation is favored during chloramination rather than chlorination because hypiodous acid (HOI, $\text{pK}_a=10.6$), the reactive iodine species, is quickly oxidized to inert iodate when free chlorine is present. However, in the presence of monochloramine, the kinetics of iodate formation is much slower giving HOI a chance to react with NOM (Bichsel & von Gunten 2000). An iodine incorporation factor (IIF) can be calculated among a class of halogenated DBPs using the following equation (Gould et al. 1981; Obolensky & Singer 2005):

$$\text{IIF} = \frac{\sum(\text{molar conc.} \times \# \text{I atoms})}{\sum(\text{molar conc.}) \times (\# \text{halogen atoms})}$$

As expected, iodine incorporation into THMs only occurred in iodide-spiked, chloraminated samples. Treatment with MP UV prior to chloramination slightly decreased the IIF, but increased the overall THM10 formation by 50% on a molar basis. Organic iodine was detected in all iodide-spiked samples, including the chlorinated sample even though no individually-measured iodine-containing DBPs were detected in that case. The total organic iodine values for chlorine alone, chloramine alone, and MP

UV (500 mJ/cm²) followed by chloramine treatment in iodide-spiked samples were: 4.7, 22.7, and 19.6 μM (0.59, 2.88, and 2.49 mg/L), respectively. This represents 50-58% incorporation of the spiked iodide (39 μM, 5 mg/L) into iodinated organics during chloramination, although only 9-13% of this total organic iodine could be accounted for by the individually measured iodine-containing THMs and haloacetamides. Kristiana and colleagues (2009) reported similar incorporation of spiked iodide into total organic iodine during chloramination of NOM isolates, with a maximum around 60%. This is much higher than the percentage incorporation of chloramine into chlorinated organics, which was just 10% and 6% (as Cl₂) of the chloramine dose applied in the current study, for ambient and iodide-spiked samples, respectively. This suggests a greater reactivity of HOI with NOM and/or competitive kinetics between HOI and NH₂Cl with organic precursors or other water constituents. Rate constants of 0.1 to 0.4 M⁻¹ s⁻¹ for the reaction of HOI with surface water NOM (in the presence of NH₂Cl) were determined by Bichsel and von Gunten (2000). In comparison, rate constants for the reaction of monochloramine with a range of NOM isolates were reported by Duirk and colleagues (2005) to be 2.9 to 9.6 M⁻¹ s⁻¹, but these were not measured in the presence of iodide or HOI and, thus, would not take into account any competitive reactions. Bromine incorporation is not reported here since samples were not spiked with additional bromide and overall incorporation was very low (bromine incorporation factor into THM10 ranged from 0.001 to 0.002 for all samples).

Table 5-4. Effect of treatment conditions on emerging DBP formation in Nordic Reservoir samples. Detection limits vary due to different dilutions.

Spiking	MP UV dose (mJ/cm ²)	Secondary disinfectant	CH ^a (µM)	CNCl ^b (µM)	TCNM ^c (µM)	CIAM ^d (µM)	DIAM ^e (µM)	Total organic iodine (µM)	THM10 IIF ^f
ambient	0	HOCl	6.7	0.07	0.09	<0.005	<0.003	<2.5	<1.7×10 ⁻⁵
ambient	500	HOCl	11.2	0.07	0.11	<0.002	<0.002	<3.8	<1.2×10 ⁻⁵
nitrate	0	HOCl	6.4	0.07	0.10	<0.005	<0.003	<3.8	<1.3×10 ⁻⁵
nitrate	500	HOCl	12.0	0.07	15.3	<0.005	<0.003	<3.8	<1.4×10 ⁻⁶
iodide	0	HOCl	5.8	0.02	0.12	<0.005	<0.003	4.7	<6.5×10 ⁻⁶
ambient	0	NH ₂ Cl	<0.003	0.16	0.01	<0.002	<0.002	<3.8	<6.9×10 ⁻⁴
ambient	500	NH ₂ Cl	0.07	0.61	0.01	<0.002	<0.002	<2.5	<4.3×10 ⁻⁴
iodide	0	NH ₂ Cl	<0.003	0.20	0.01	0.13	0.08	22.7	0.43
iodide	500	NH ₂ Cl	0.02	0.58	0.02	0.20	0.11	19.6	0.38

^aCH = chloral hydrate

^bCNCl = cyanogen chloride

^cTCNM = trichloronitromethane (chloropicrin)

^dCIAM = chloroiodoacetamide

^eDIAM = diiodoacetamide

^fIIF = iodine incorporation factor; detection limit was calculated using Br₂ICH detection limit (0.5 or 1.0 µg/L, 1.7 or 3.3 nM) for each specific sample

Comparison to DBP Formation in Diluted Samples

The use of *in vitro* assays in the evaluation of water quality requires concentrated samples to obtain measurable responses. However, it is important to consider how this scaling-up could alter reactions during UV-chlorine/chloramine treatment in comparison to those that would occur in waters containing lower DOC levels. The formation of a subset of DBPs in four of the concentrated Nordic Reservoir NOM samples were compared to their formation in samples that were treated with UV/chlorine-chloramine after dilution in LGW to a lower DOC concentration of 3 mg C/L (for comparison to results presented in Chapter 2), with the results shown in Table 5-5. Diluted samples were buffered with 0.5 mM phosphate buffer at pH 7.1. Nitrate-spiking concentrations and chlorine/chloramine doses were correspondingly scaled-down in the dilute samples to achieve the same N:DOC and Cl₂:DOC ratios as the concentrated samples. Chlorine and chloramine demands were higher per mg DOC in the concentrated compared to the dilute samples and to a greater extent for chloramine. DBP and total organic halogen formation in the concentrated samples (after correcting for 37.3x factor) ranged from 0 to 100% higher compared to the dilute treated samples, except for THM4 formation in ambient chloraminated samples, which was 5 to 12 times higher in the concentrated compared to diluted samples. Comparing the relative changes observed with the use of MP UV prior to chlorination (or chloramination for cyanogen chloride), there was a greater relative increase in trichloronitromethane formation and lower relative increases in chloral hydrate and cyanogen chloride for the concentrated sample. These findings are further discussed in the following section in relation to their proposed UV-induced formation mechanisms.

Table 5-5. Comparison of 24-hour chlorine/chloramine demand and DBP/total organic halogen yield (molar concentration normalized to DOC) in dilute vs. concentrated (conc.) samples. Chlorine/chloramine doses and nitrate-spiking amounts were applied at the same Cl₂:DOC and N:DOC ratios to both conc. and dilute samples. Detection limits vary due to different dilution factors.

Spiking ^a	MP UV dose (mJ/cm ²)	Secondary disinfectant	Demand ($\mu\text{mol Cl/mg C}$)		THM4 ($\mu\text{mol/mg C}$)		HAA9 ($\mu\text{mol/mg C}$)		CH (nmol/mg C)		CNCI (nmol/mg C)		TCNM (nmol/mg C)		Total organic halogen ($\mu\text{mol Cl/mg C}$)	
			conc. ^d	dilute	conc.	dilute	conc.	dilute	conc.	dilute	conc.	dilute	conc.	dilute	conc.	dilute
ambient	0	NH ₂ Cl ^b	7.3	2.3	7.2	0.6	32	24	<0.03	0.4	1.5	0.7	0.07	<0.2	0.8	0.4
ambient	500	NH ₂ Cl	11	5.4	9.0	1.7	62	65	0.6	0.5	5.5	3.2	0.1	<0.2	0.9	0.6
nitrate	0	HOCl ^c	56	40	737	492	677	425	57	35	0.6	<0.5	0.9	0.9	6.2	3.9
nitrate	500	HOCl	65	55	702	499	677	450	107	87	0.6	<0.5	136	103	7.7	4.4

^aNitrate spiking amounts were 100 and 2.7 mg N/L (7.1 and 0.2 mM as N) in the conc. and dilute samples, respectively.

^bNH₂Cl doses were 32 and 47 mg/L as Cl₂ (0.9 and 1.3 mM Cl) in the no UV and 500 mJ/cm² MP UV conc. samples, respectively. NH₂Cl doses were 0.9 and 1.3 mg/L as Cl₂ (0.024 and 0.036 mM Cl) in the no UV and 500 mJ/cm² MP UV dilute samples, respectively.

^cHOCl doses were 224 and 262 mg/L as Cl₂ (6.3 and 7.4 mM Cl) in the no UV and 500 mJ/cm² MP UV conc. samples, respectively. HOCl doses were 6.0 and 7.0 mg/L as Cl₂ (0.17 and 0.20 mM Cl) in the no UV and 500 mJ/cm² MP UV dilute samples, respectively.

^dDOC concentrations were 112 and 3 mg C/L in conc. and dilute samples, respectively.

5.4 Discussion

A combination of factors appears to be accounting for the observed cytotoxicity in treated NOM samples. In ambient and iodide-spiked waters, chlorinated samples were more cytotoxic than corresponding chloraminated samples per mg of DOC treated. However, byproducts produced during chloramination, regardless of UV dose, were more cytotoxic than those produced during chlorination on a total organic halogen formation basis (Table 5-2). The formation of iodine-substituted DBPs during chloramination resulted in an increased cytotoxicity compared to the same sample without iodide-spiking, as expected based on past work that has shown iodinated DBPs to be more cytotoxic than their chlorinated counterparts (Richardson et al. 2008). Additionally, this increased cytotoxicity was not observed when samples were spiked with iodide during chlorination, which is consistent with the lack of iodine incorporation into DBPs in the presence of free chlorine (Bichsel & von Gunten 2000).

The use of MP UV prior to chloramination also increased cytotoxicity compared to samples treated with chloramine alone, to the extent that UV + chloramine treatment resulted in a similar cytotoxicity as samples treated with chlorine. This was not due to greater bromine or iodine incorporation. The formation of chloral hydrate or trichloronitromethane alone could not account for this increase based on the individually measured (chloral hydrate) or estimated (trichloronitromethane) IC_{50} values for these compounds. Although a full dose-response curve was not obtained for cyanogen chloride, a range of concentrations was analyzed with this assay (8×10^{-8} to 2.2×10^{-5} M). The cell growth remained greater than 90% at the concentration that was formed from MP UV treatment during chloramination (5.8×10^{-7} to 6.1×10^{-7} M), so cyanogen chloride

alone would also not be able to explain the observed cytotoxicity changes. These results suggest that there could be a synergistic cytotoxicity effect among the byproducts generated from MP UV + chloramine treatment. The percentage of unknown total organic halogen was not significantly changed by UV, although the compounds within this unknown fraction could have been more cytotoxic relative to those produced with chloramination alone. As noted in the background section, there have been relatively few studies investigating the toxicity of DBP mixtures generated from different drinking water treatment processes, and, therefore, the effect of these mixtures of DBPs at low concentrations on toxicity is not well understood.

There was a small but statistically meaningful increase in cytotoxicity for nitrate-spiked samples that were treated with MP UV prior to chlorination, compared to chlorination alone. This was not observed in ambient samples, which suggests that nitrate was responsible for the production of cytotoxic DBPs during MP UV treatment and subsequent chlorination. Trichloronitromethane was increased 150-fold with the use of MP UV in these samples. The change in trichloronitromethane concentration between these samples (1.5×10^{-5} M) was about 4-fold lower, but on the same order of magnitude, as its individually measured IC_{50} value of 6.3×10^{-5} M (DeAngelo unpublished data). The increase in tribromonitromethane with the use of MP UV prior to chlorination in nitrate-spiked samples was 4×10^{-9} M, four orders of magnitude lower than its measured IC_{50} value of 2.1×10^{-5} M. The change in chloral hydrate formation between the nitrate-spiked chlorinated and MP UV + chlorine treated samples was 5.6×10^{-6} M, one order of magnitude less than its measured IC_{50} value (5.4×10^{-5} M). The same increase in chloral hydrate formation occurred in the corresponding ambient samples, where an increased

cytotoxicity was not observed. It is difficult to conclude that a single DBP was responsible for the increase in cytotoxicity observed when MP UV was used prior to chlorination in nitrate-spiked samples, because little is known about the effect of DBP mixtures at low concentrations in real waters. However, based on the analyzed DBPs, their measured IC₅₀ values, and the lack of cytotoxicity change in ambient samples, trichloronitromethane was the most likely compound to have contributed to the cytotoxicity increase in this case.

The findings presented here demonstrate the value of evaluating DBP mixtures, particularly when comparing toxicity of byproducts produced from different treatments. For example, based on the IC₅₀ cytotoxicity values of single compounds that were found to be increased by MP UV treatment during chloramination, the significant increase in cytotoxicity that was observed compared to that of samples treated with chloramine alone would not have been predicted. Furthermore, even if general predictions could be made based on single compound toxicity data, it is not feasible to test every individual DBP of interest or possible combinations of simple, defined mixtures, and these studies would not provide any information on the unknown fraction.

The need to use concentrated samples for this type of cytotoxicity assay is unavoidable, so there are inherent limitations that need to be recognized. The approach of treating pre-concentrated samples was used so that known and unknown volatile DBPs would be conserved, but some differences in DBP formation were observed between treated dilute and concentrated samples (when normalized by the concentration factor). Despite these limitations, the comparison of concentrated and dilute samples provided additional evidence for the proposed pathways of DBP formation resulting from UV-

chlorine/chloramine processes. The proposed mechanism for enhanced halonitromethane formation following MP UV irradiation and subsequent chlorination/chloramination is discussed in previous chapters and $\cdot\text{NO}_2$ is thought to be the primary reactive species responsible (Reckhow et al. 2010, Shah et al. 2011). The availability of $\cdot\text{NO}_2$ is limited by its recombination with $\cdot\text{OH}$, which is also produced during nitrate photolysis. NOM and inorganic carbon species are known to act as $\cdot\text{OH}$ scavengers (Mack & Bolton 1999; Sharpless & Linden 2001; Chiron et al. 2009), thus, the increased background levels of these components in the concentrated samples could be responsible for increased $\cdot\text{NO}_2$ reaction and subsequent trichloronitromethane formation compared to the more dilute samples. Furthermore, the opposite trend for chloral hydrate and cyanogen chloride production with the addition of MP UV prior to chlorination or chloramination (lower relative increase in concentrated compared to diluted samples) suggests that their formation is $\cdot\text{OH}$ -mediated. The formation of aldehydes from UV photolysis of NOM (Malley et al. 1995; Liu et al. 2002), which can further react with chlorine or chloramine to produce chloral hydrate or cyanogen chloride (McKnight & Reckhow 1992; Pedersen et al. 1999), are proposed pathways for the observed increase in these DBPs with the addition of MP UV. Aldehydes are also known to be produced during ozonation (Yamada & Somiya 1989), a process which uses $\cdot\text{OH}$ as the primary oxidant.

5.5 Conclusions

This study demonstrated the use of an *in vitro* cytotoxicity assay in combination with DBP analysis and its potential for process evaluation in drinking water treatment. It is important to understand the implications of processes that are being used as an integral

part of drinking water treatment, particularly for different water types and as source waters become increasingly impacted by anthropogenic activity. The observed increase in cytotoxicity with the use of MP UV prior to chloramination warrants further research into the byproduct mixtures produced under these scenarios. Since the UV doses used in this study (500 mJ/cm²) were higher than those typically applied for disinfection (40-186 mJ/cm²), future experiments should look at lower disinfection doses. Additional assays (e.g. genotoxicity, carcinogenicity) should also be included for future work as human health endpoints of interest for DBP exposure. While Plewa and colleagues (2002) demonstrated that mammalian cell cytotoxicity was a good predictor of genotoxicity for a range of byproducts, DBP mixtures and unknown DBPs may have different modes of action that are important to consider when evaluating treatment processes.

A number of the findings presented here were consistent with what would be expected based on prior knowledge of the relative toxicity and formation conditions for different byproducts; however, there was not a clear correlation between cytotoxicity and any specific DBP, class of DBPs, or total organic halogen formation. As a result, no single parameter was identified (total organic halogen, for example) that could be monitored to predict the overall cytotoxicity of treated waters. Rather, this work demonstrated the application of a complementary tool for evaluating treatment processes under different conditions and interpreting DBP findings in the context of public health implications.

Sources Cited for Chapter 5

- APHA (American Public Health Association), American Water Works Association, and Water Environment Federation, 1999. *Standard Methods for the Examination of Water and Wastewater*. 20th Edition, American Public Health Association: Washington, DC.
- Backlund, P., 1995. Introduction and removal of disinfection byproducts and mutagenic activity by chemical and photolytic treatments. *Revue des Sciences de L'eau*, 8(3), pp.387-401.
- Bellar, T.A. et al., 1974. The occurrence of organohalides in chlorinated drinking waters. *Journal American Water Works Association*, 66(12), pp.703-706.
- Bichsel, Y. & von Gunten, U., 2000. Formation of iodo-trihalomethanes during disinfection and oxidation of iodide-containing waters. *Environmental Science & Technology*, 34(13), pp.2784-2791.
- Bolton, J.R. & Linden, K.G., 2003. Standardization of methods for fluence (UV dose) determination in bench-scale UV experiments. *Journal of Environmental Engineering*, 129(3), pp.209-216.
- Bove, F.J. et al., 1995. Public Drinking Water Contamination and Birth Outcomes. *American Journal of Epidemiology*, 141(9), pp.850-862.
- Brodthmann, N.V. & Russo, P.J., 1979. The use of chloramine for reduction of trihalomethanes and disinfection of drinking water. *Journal American Water Works Association*, 71(1), pp.40-42.
- Brophy, K.S. et al., 2000. Quantification of nine haloacetic acids using gas chromatography with electron capture detection. In *Natural Organic Matter and Disinfection By-Products, ACS Symposium Series 761*. American Chemical Society, pp.343-355.
- Bull, R.J. et al., 2001. *Health Effects and Occurrence of Disinfection By-Products*, American Water Works Association and Water Research Foundation: Denver, Colorado.
- Cantor, K.P. et al., 1998. Drinking water source and chlorination byproducts I. Risk of bladder cancer. *Epidemiology*, 9(1), pp.21-28.
- Chiron, S. et al., 2009. Bicarbonate-enhanced transformation of phenol upon irradiation of hematite, nitrate, and nitrite. *Photochemical & Photobiological Sciences*, 8(1), pp.91-100.

- Clancy, J.L. et al., 2000. Using UV to inactivate *Cryptosporidium*. *Journal American Water Works Association*, 92(9), pp.97-104.
- Claxton, L.D. et al., 2008. Integrated disinfection by-products research: salmonella mutagenicity of water concentrates disinfected by chlorination and ozonation/postchlorination. *Journal of Toxicology and Environmental Health, Part A*, 71(17), pp.1187-1194.
- DeAngelo, A.B., et al., 2007. Development of normal human colon cell cultures to identify priority unregulated disinfection by-products with a carcinogenic potential. *Water Science & Technology*, 56(12), pp.51-55.
- DeMarini, D.M. et al., 1995. Mutation spectra in salmonella of chlorinated, chloraminated, or ozonated drinking water extracts: comparison to MX. *Environmental and Molecular Mutagenesis*, 26(4), pp.270-285.
- Diehl, A.C. et al., 2000. DBP formation during chloramination. *Journal American Water Works Association*, 92(6), pp.76-90.
- Dotson, A.D. et al., 2010. UV/H₂O₂ treatment of drinking water increases post-chlorination DBP formation. *Water Research*, 44(12), pp.3703-3713.
- Duirk, S.E. et al., 2005. Modeling monochloramine loss in the presence of natural organic matter. *Water Research*, 39(14), pp.3418-3431.
- Fuge, R. & Johnson, C.C., 1986. The geochemistry of iodine - a review. *Environmental Geochemistry and Health*, 8(2), pp.31-54.
- Gould, J.P. et al., 1981. Formation of brominated trihalomethanes-extent and kinetics. In: *Proceedings of the 4th Conference on Water Chlorination*. Ann Arbor, Michigan.
- Hua, G. & Reckhow, D.A., 2006. Determination of TOCl, TOBr and TOI in drinking water by pyrolysis and off-line ion chromatography. *Analytical and Bioanalytical Chemistry*, 384(2), pp.495-504.
- Hua, G. & Reckhow, D.A., 2007. Comparison of disinfection byproduct formation from chlorine and alternative disinfectants. *Water Research*, 41(8), pp.1667-1678.
- Jin, S. et al., 2006. Polychromatic UV Fluence Measurement Using Actinometry, Biodosimetry, and Mathematical Techniques. *Journal of Environmental Engineering*, 132(8), pp.831-842.
- Krasner, S.W. et al., 1989. The occurrence of disinfection by-products in US drinking water. *Journal American Water Works Association*, 81(8), pp.41-53.

- Krasner, S.W. et al., 2006. Occurrence of a new generation of disinfection byproducts. *Environmental Science & Technology*, 40(23), pp.7175-7185.
- Kristiana, I. et al., 2009. The formation of halogen-specific TOX from chlorination and chloramination of natural organic matter isolates. *Water Research*, 43(17), pp.4177-4186.
- Landi, S. et al., 2003. Induction of DNA strand breaks by trihalomethanes in primary human lung epithelial cells. *Mutation Research*, 538(1-2), pp.41-50.
- Liu, W. et al., 2002. Comparison of disinfection byproduct (DBP) formation from different UV technologies at bench scale. *Water Science & Technology: Water Supply*, 2(5-6), pp.515-521.
- Liu, W. et al., 2006. THM, HAA and CNCl formation from UV irradiation and chlor(am)ination of selected organic waters. *Water Research*, 40(10), pp.2033-2043.
- Loper, J.C. et al., 1978. Residue organic mixtures from drinking water show in vitro mutagenic and transforming activity. *Journal of Toxicology and Environmental Health, Part A*, 4(5-6), pp.919-938.
- Lykins, B.W. et al., 1986. Chemical products and toxicologic effects of disinfection. *Journal American Water Works Association*, 78(11), pp.66-75.
- Mack, J. & Bolton, J.R., 1999. Photochemistry of nitrite and nitrate in aqueous solution: a review. *Journal of Photochemistry and Photobiology A: Chemistry*, 128(1-3), pp.1-13.
- Malley, J.P. et al., 1995. *Evaluation of the Byproducts Produced from the Treatment of Groundwaters with Ultraviolet Irradiation*. American Water Works Association and Water Research Foundation: Denver, Colorado.
- McKnight, A. & Reckhow, D.A., 1992. Reactions of ozonation by-products with chlorine and chloramines. In: *Proceedings of the Annual AWWA Conference*. Vancouver, British Columbia.
- National Cancer Institute, 1976. *Report on the Carcinogenesis Bioassay of Chloroform (CAS No. 67-66-3)*, National Cancer Institute: Bethesda, Maryland.
- Obolensky, A. & Singer, P.C., 2005. Halogen substitution patterns among disinfection byproducts in the information collection rule database. *Environmental Science & Technology*, 39(8), pp.2719-2730.

- Pedersen, E.J. et al., 1999. Formation of cyanogen chloride from the reaction of monochloramine with formaldehyde. *Environmental Science & Technology*, 33(23), pp.4239-4249.
- Plewa, M.J. et al., 2002. Mammalian cell cytotoxicity and genotoxicity analysis of drinking water disinfection by-products. *Environmental and Molecular Mutagenesis*, 40(2), pp.134-142.
- Plewa, M.J. et al., 2004. Halonitromethane drinking water disinfection byproducts: chemical characterization and mammalian cell cytotoxicity and genotoxicity. *Environmental Science & Technology*, 38(1), pp.62-68.
- Plewa, M.J. et al., 2008. Occurrence, synthesis, and mammalian cell cytotoxicity and genotoxicity of haloacetamides: an emerging class of nitrogenous drinking water disinfection byproducts. *Environmental Science & Technology*, 42(3), pp.955-961.
- Pressman, J.G. et al., 2010. Concentration, chlorination, and chemical analysis of drinking water for disinfection byproduct mixtures health effects research: U.S. EPA's Four Lab Study. *Environmental Science & Technology*, 44(19), pp.7184-7192.
- Reckhow, D.A. et al., 2010. Effect of UV treatment on DBP formation. *Journal American Water Works Association*, 102(6), pp.100-113.
- Richardson, S.D. et al., 2007. Occurrence, genotoxicity, and carcinogenicity of regulated and emerging disinfection by-products in drinking water: a review and roadmap for research. *Mutation Research*, 636, pp.178-242.
- Richardson, S.D. et al., 2008. Occurrence and mammalian cell toxicity of iodinated disinfection byproducts in drinking water. *Environmental Science & Technology*, 42(22), pp.8330-8338.
- Rook, J.J., 1974. Formation of haloforms during chlorination of natural waters. *Water Treatment and Examination*, 23(2), pp.234-243.
- Sawada, M. & Kamataki, T., 1998. Genetically engineered cells stably expressing cytochrome P450 and their application to mutagen assays. *Mutation Research*, 411(1), pp.19-43.
- Schenker, N. and Gentleman, J.F., 2001. On judging the significance of differences by examining the overlap between confidence intervals. *The American Statistician*, 55(3), pp.182-186.

- Schreiber, I.M. & Mitch, W.A., 2005. Influence of the order of reagent addition on NDMA formation during chloramination. *Environmental Science & Technology*, 39(10), pp.3811-3818.
- Sclimenti, M.J. et al., 1994. The simultaneous determination of cyanogen chloride and cyanogen bromide in chloraminated waters by a simplified microextraction GC/ECD technique. In: *Proceedings of the AWWA Water Quality Technology Conference*. Charlotte, North Carolina, pp.489-506.
- Shah, A.D. et al., 2011. Impact of UV disinfection combined with chlorination/chloramination on the formation of halonitromethanes and haloacetonitriles in drinking water. *Environmental Science & Technology*, 45(8), pp.3657-3664.
- Sharpless, C.M. & Linden, K.G., 2001. UV photolysis of nitrate: effects of natural organic matter and dissolved inorganic carbon and implications for UV water disinfection. *Environmental Science & Technology*, 35(14), pp.2949-2955.
- U.S. EPA (Environmental Protection Agency), 2006. National Primary Drinking Water Regulations: Stage 2 Disinfectants and Disinfection Byproducts Rule. *Federal Register*, 71(2), pp.387-493.
- Wagner, E.D. et al., 2012. Comparative genotoxicity of nitrosamine drinking water disinfection byproducts in *Salmonella* and mammalian cells. *Mutation Research* 741(1-2), pp.109-115.
- WHO (World Health Organization), 1993. *Guidelines for Drinking-Water Quality*. 2nd Edition, World Health Organization: Geneva.
- Weinberg, H.S. et al., 2002. *The Occurrence of Disinfection By-Products (DBPs) of Health Concern in Drinking Water: Results of a Nationwide DBP Occurrence Study*. EPA/600/R-02/068, U.S. EPA: Athens, Georgia.
- Yamada, H. & Somiya, I., 1989. The determination of carbonyl compounds in ozonated water by the PFBOA method. *Ozone: Science & Engineering*, 11(2), pp.127-141.

Chapter 6: Conclusions and Implications

6.1 Summary of Results

This dissertation presents results from an investigation into the impacts of UV irradiation on finished drinking water quality when used in combination with post-chlorination or chloramination. The main objectives of this research were to determine the effect of UV photolysis followed by chlorination or chloramination on organic and inorganic water constituents involved in the formation and speciation of disinfection byproducts (DBPs) and to use a toxicological assay as a complimentary tool to DBP analysis and precursor characterization studies to compare the relative toxicity of various drinking water treatments involving UV irradiation. These objectives were carried out through the measurement of a range of regulated and unregulated DBPs following treatment of surface waters containing different organic and inorganic precursors and through the application of an *in vitro* human cell chronic cytotoxicity assay to concentrated synthetic model waters that were treated with UV, chlorine, and chloramine. Two organic precursor characterization techniques, fluorescence spectroscopy and dissolved organic matter (DOM) fractionation by polarity on XAD resins, were used to gain a better understanding of the mechanisms by which DBPs and their precursors are affected by UV irradiation and combined UV-chlorine/chloramine treatment. With the exception of the fractionation study, where samples were compared on an equivalent

chlorine/chloramine dose basis, results were compared to the same waters treated with only chlorine or chloramine, at a dose adjusted to achieve equivalent chlorine or chloramine residual.

While past work demonstrated that the use of UV at disinfection doses prior to chlorination or chloramination has little effect on the formation of regulated trihalomethanes (THMs) and haloacetic acids (HAAs), the literature is lacking in comprehensive studies evaluating the impacts of UV on emerging, unregulated DBPs that are thought to be more toxicologically potent than the currently regulated byproducts. In addition, toxicological tools for assessing the potential human health impacts of drinking water disinfection byproducts have not fully addressed the effects of DBP mixtures, particularly those produced by alternative treatment processes such as combined UV-chlorine/chloramine. This study aimed to fill some of these research gaps through the objectives described above.

Results presented in Chapter 2 confirmed that disinfection doses (40-186 mJ/cm²) of low and medium pressure (LP and MP) UV did not significantly affect the formation of regulated THMs and HAAs with subsequent chlorination or chloramination under a range of organic and inorganic precursor conditions. With higher doses of MP UV (1000 mJ/cm²) followed by chlorination, THM formation was increased up to 40% compared to samples treated with chlorine alone. This finding, along with the corresponding increase in chlorine demand and decrease in fluorescence intensity for two DOM components (results described in Chapter 4), suggests that at high doses, UV generates precursors that are more amenable to reaction with chlorine. In the presence of nitrate (1-10 mg N/L), chloropicrin (trichloronitromethane) formation was increased by MP UV, even at

disinfection doses. LP UV did not affect chloropicrin formation, which is consistent with previous research. However, past UV studies have not analyzed for bromopicrin (tribromonitromethane) formation and results presented here showed that it was influenced to a greater extent by UV (both LP and MP) than chloropicrin. In samples containing bromide and nitrate, bromopicrin formation increased 30-60% with 40 mJ/cm² LP UV and 4- to 10-fold with 40 mJ/cm² MP UV, after subsequent chlorination. There are currently no regulations or guidelines for chloropicrin or bromopicrin in drinking water, but single-compound toxicological studies have suggested that halonitromethanes are among the most geno- and cytotoxic DBPs for mammalian cells (Plewa et al. 2004). Chloral hydrate and cyanogen chloride formation were increased by the use of MP UV prior to chlorination or chloramination, and nitrate further enhanced this effect for cyanogen chloride but not for chloral hydrate. The World Health Organization guideline value of 10 µg/L for chloral hydrate (WHO 1993) was exceeded in samples treated with 1000 mJ/cm² LP or MP UV followed by chlorination and with lower doses of MP UV for waters that formed 7-8 µg/L chloral hydrate with chlorine alone. Cyanogen chloride formation did not exceed the World Health Organization guideline value of 70 µg/L (WHO 1993) in any samples. When followed by chlorination or chloramination, UV treatment was not found to increase bromine or iodine incorporation into individually measured DBPs or total organic halogens, a surrogate measure which captures both known and unknown byproducts.

The organic precursor characterization techniques described in Chapters 3 and 4 provided insight into the types of precursors responsible for formation of specific DBPs or DBP classes, and how these were affected by UV. The use of fluorescence

spectroscopy allowed for observation of changes in specific DOM components following UV, chlorine, and chloramine treatment that were not detectable by UV/visible absorbance spectroscopy or dissolved organic carbon (DOC) analysis. Consistent with past work, hydrophobic precursors in the XAD fractionation study contributed to the majority of THM and HAA formation during chlorination, while chloral hydrate and chloropicrin precursors were more hydrophilic. The intensities of two components (one terrestrial humic-like and the other protein/tryptophan-like) were decreased by UV irradiation, suggesting that the UV-induced precursors responsible for chloral hydrate and cyanogen chloride formation with subsequent chlorination/chloramination originated from one or both of these components. The fluorescence intensities of all four components were affected similarly with UV irradiation in the presence of nitrate, so it is difficult to draw any conclusions from the fluorescence results about which components were most responsible for halonitromethane formation. The low mass balance (comparison of DBP formation in hydrophilic and hydrophobic acids XAD fractions to unfractionated water) observed for chloral hydrate and chloropicrin suggests that the reactivity of hydrophilic precursors may be altered through the XAD resin fractionation procedure. Differences between SRNOM reactivity compared to OWASA, even though similar hydrophilic/hydrophobic acid distribution.

Results presented in Chapter 5 showed no significant changes in cytotoxicity when 500 mJ/cm^2 MP UV was used prior to chlorination in ambient Nordic Reservoir samples. However, a small increase in cytotoxicity was observed when samples were spiked with nitrate and treated with 500 mJ/cm^2 MP UV followed by chlorination (compared to the same sample without UV treatment), where enhanced chloropicrin and

chloral hydrate formation was observed. Without UV, samples treated with chlorine showed greater cytotoxicity than those treated with chloramine. Spiking with iodide increased the cytotoxicity of chloraminated samples, but those treated with chlorine (both with and without iodide spiking) were still more cytotoxic. When MP UV treatment was included prior to chloramination, cytotoxicity was increased and to a greater extent in samples containing iodide.

6.2 Examination of Individual Hypotheses

Hypothesis 1: The formation of reactive chemical species from UV photolysis of waters containing nitrate, bromide, and/or iodide will influence nitrogen- and halogen-containing DBP formation with subsequent chlorination or chloramination and, thereby, the toxicity of the treated water.

The findings of this study showed that nitrate had the most significant effect on DBP formation during UV-chlorine/chloramine treatment, in comparison to the other inorganic species (bromide and iodide). The presence of nitrate during UV treatment and subsequent chlorination/chloramination resulted in increased halonitromethane formation. This is thought to be due to the formation of reactive nitrogen species from the photolysis of nitrate, such as $\cdot\text{NO}_2$, which can act as nitrating agents toward organic precursors. These nitrated organics can then produce halonitromethanes upon chlorination/chloramination. Small changes in cytotoxicity were observed when concentrated synthetic waters spiked with nitrate were pre-treated with 500 mJ/cm² MP UV prior to chlorination, compared to the same sample treated with chlorine alone. However, the most significant change in cytotoxicity was with 500 mJ/cm² MP UV treatment prior to chloramination, compared to chloramination alone. The increased

formation of specific byproducts (halonitromethanes, haloacetamides, cyanogen chloride, chloral hydrate) in the UV + chloramine-treated sample would not be expected to account for these observed changes based on their individually measured cytotoxicity, suggesting that the mixture of these compounds may have had an synergistic effect on cytotoxicity.

In general, spiking with bromide resulted in a shift to bromine-containing DBPs upon chlorination/chloramination, but UV treatment did not further affect the bromine incorporation. Likewise, iodine incorporation into THMs, haloacetamides, and total organic iodine was observed when samples were spiked with iodide prior to chloramination, but this was not affected by pre-treatment with UV. Thus, the significant increase in cytotoxicity that was observed with MP UV treatment prior to chloramination compared to chloramination alone in iodide-spiked samples was not due to increased iodine incorporation. A similar increase in cytotoxicity was observed with MP UV pre-treatment followed by chloramination of samples that were not spiked with iodide, compared to samples treated with chloramine only.

Hypothesis 2: UV irradiation changes the molecular weight distribution of NOM, which will impact its reactivity towards disinfectants (chlorine, chloramine) and the speciation of DBPs.

The increased chlorine demand that was observed with the use of high MP UV doses (1000 mJ/cm^2) in ambient samples supports the hypothesis that UV impacts the reactivity of NOM with chlorine. Chloramine demand was not affected to the same extent by UV. Results presented in Chapter 4 showed that pre-treatment with any dose of MP UV resulted in a greater reduction of fluorescence intensity for a humic-like component with subsequent chlorination, compared to the reduction of its fluorescence

intensity from chlorination or MP UV alone, suggesting that MP UV made this precursor more amenable to reaction with chlorine. While there were no experiments that looked directly at NOM molecular weight distribution (UV/visible absorbance spectral slope approach was not sensitive enough under the experimental conditions used), the findings presented in Chapter 4 suggest a shift in DOM composition from MP UV treatment without complete mineralization. It was hypothesized that production of smaller, more hydrophilic precursors by UV would result in increased bromine and iodine incorporation into DBPs and total organic halogen when bromide and iodide were present during subsequent chlorination or chloramination, but this was not observed, as described in Chapters 2 and 5.

6.3 Implications

The use of UV for drinking water treatment offers advantages to traditional processes, including inactivation of chlorine-resistant pathogens and reducing dependence on chemical disinfectants, which require handling, transport, and storage of dangerous chemicals. At the same time, it is important to understand the implications of a process that is being used as an integral part of drinking water treatment. This research will add to the limited literature that has evaluated potential impacts of UV on finished drinking water quality, which can be used to help in the design and optimization of combined UV-chlorine/chloramine processes for drinking water treatment.

Although the most significant changes in DBP formation were observed for samples treated with high doses of UV and elevated inorganic precursor concentrations, there were notable effects observed with disinfection doses of UV and lower nitrate

levels. The greater potential toxicity of byproducts that were found to be affected by UV (chloral hydrate, halonitromethanes, cyanogen chloride) compared to the regulated THMs and HAAs warrants consideration of practices that could reduce their formation. Chloral hydrate and halonitromethanes are primarily produced from hydrophilic precursors, which are not easily removed through coagulation/flocculation (Collins et al. 1986). If UV, and in particular MP UV, is being implemented on source waters containing nitrate concentrations greater than 1 mg N/L, utilities should consider options for nitrate reduction upstream from UV processes. Methods that have been shown to be effective for nitrate removal include ion exchange, electrodialysis, and reverse osmosis (Clifford and Liu 1993; Hell et al. 1998; Bohdziewicz et al. 1999). If the addition of these processes is not feasible, the use of LP over MP UV would help limit the formation of halonitromethanes.

Formation of cyanogen chloride did not exceed the World Health Organization guideline value of 70 $\mu\text{g/L}$, even with the addition of 1000 mJ/cm^2 MP UV prior to chloramination. However, the enhanced cytotoxicity that was observed for samples treated with MP UV followed by chloramination, for which cyanogen chloride was one of the most impacted byproducts, compared to chloramination alone, suggests that further toxicological evaluation of the byproducts formed under these conditions and potential synergistic effects needs to be carried out. Future work should determine if increased toxicity is also observed with lower UV doses and LP UV (only MP UV treatment was evaluated for toxicity work) and should include assays with other toxicological endpoints, such as genotoxicity and carcinogenicity.

The scope of this project only included evaluation of UV with post-chlorination and chloramination. While a recent survey showed that the majority (68%) of utilities employing UV did not apply chlorine or chloramine upstream of UV processes (Linden et al. 2012), one-third did and future work should investigate the impact of UV when used after chlorination/chloramination. Photolysis products of free chlorine and chloramine could potentially add more precursors and pathways for DBP formation. Limited research has evaluated different UV/chlorine/chloramine sequences, but again, most work has focused on the regulated byproducts and not DBPs that are thought to be more geno- and cytotoxic. Additional experimental design considerations are necessary for evaluating UV after chlorine/chloramine addition to prevent loss of DBPs formed prior to irradiation.

Finally, while the focus of this research was on UV for drinking water disinfection, these findings may have implications for UV advanced oxidation processes (e.g. UV/H₂O₂, UV/O₃), where higher UV doses than those used for disinfection are applied. The formation of regulated THMs and HAAs could exceed maximum contaminant levels if advanced oxidation processes are used in combination with chlorine for residual disinfection. The effect of UV/H₂O₂ treatment on THMs and HAAs has been studied and the use of H₂O₂ further increased THM₄ formation with high MP UV doses and post-chlorination (Dotson et al. 2010). Future research on UV advanced oxidation processes should consider additional DBPs, including those that were affected by UV in this study. The impacts on chloral hydrate, halonitromethanes, and cyanogen chloride would be more significant with these higher UV doses, and the presence of nitrate would further enhance the halonitromethanes and cyanogen chloride formation. The results

presented here should be taken into consideration when implementing UV advanced oxidation processes.

Appendix 1: Reverse Osmosis (RO) Concentration Standard Operating Procedure (SOP)

Prepared by: Bonnie Lyon

Procedure is carried out at OWASA (Orange County Water & Sewer Authority) using custom-built portable unit. Contact Rachel Monschein (RMonschein@owasa.org, (919-537-4227) to let her know when you will be coming in to do RO concentration. It needs to be on a Saturday or Sunday when they are not working in the laboratory.

Materials:

- RO Concentration unit with tubing (stored at OWASA)
- Two big blue bins for collecting water (stored at OWASA)
- Yard stick (stored at OWASA)
- Graduated cylinder (500 mL or 1 L)
- Amber glass bottles for collecting final RO concentrate (4 L, acid washed, dried)
- 40 mL vials with caps for collecting samples throughout process
- Power strip
- Gloves
- Label tape and marker
- Ear plugs (filtering pump is very loud)

Clean filters

1. Collect finished water in big blue bin labeled #1 using short green tubing. Collect about 10 cm of finished water for cleaning filters. Remove shorter green tubing and put aside.
2. Place one end of longer green tubing into bin #1 and connect other end to inlet of pump #1 (when looking at back of unit, older pump on the right and inlet is fitting on the left front side of pump – “In” is written there). Place end of black tubing that is connected to outlet of filters into sink for waste.

3. Plug filter pump power cord into power strip and turn power strip on. Let waste from first 30 seconds of cleaning drain into sink, then put outlet into bin #1 and let pump run ~ 5 minutes. *Be careful to keep pump inlet tubing submerged so no air is pulled through pump and filters*
4. To drain rinse water from bin before shutting off pump (since it is heavy when filled with water and hard to dump out), put outlet of filters into sink and pump almost all of water out of bin.
5. Empty remaining rinse water from bin #1 and wipe dry with paper towels.
6. If desired, collect some rinse water in 40 mL vials for analyses back at UNC.

Filter water to be RO concentrated

7. Collect water to be concentrated (could be raw or settled water depending on experimental objectives) in bin #1 using black tubing with metal fitting and green tape on it. Connect end of tubing without metal fitting to outlet of desired OWASA water spout and place other end into bin #1.
8. Fill bin until almost full – past 180L mark because some will leak during filtering.
9. Carefully remove tubing from water outlet and bin and drain excess water in tubing into sink.
10. Collect some of the water that will be concentrated in 40 mL vials for UNC analyses.
11. Put end of long green tubing into bin #1 which is filled with raw or settled water (other end is still connected to filtering pump).
12. Put outlet of filters (black tubing) into bin #2.
13. Turn on filtering pump and filter collected water until bin #2 is filled to 180 L mark.
14. Empty any remaining water from bin #1 into sink. Set bin #1 and filtering tubing aside.
15. Unplug filtering pump from power strip.

RO concentration

16. Place clear (criss-crossy inside pattern) tubing that is connected to RO pump inlet into bin #2 which contains the filtered water to be RO concentrated. Also place black tubing that is connected to outlet of RO membrane into bin #2. Use this heavier tube to hold down the clear tubing which tends to float up to surface. Use tape to hold down tubing if necessary. *Be careful to keep pump inlet tubing submerged so no air is pulled through pump and membrane*
17. Open red valve next to inlet of RO membrane – turn parallel to tubing to open. During storage, valve should be in the perpendicular position which is closed.
18. Connect clear tubing to outlet at top of RO membrane (tubing has a male fitting). Turn the grey valve $\sim 30^\circ$ to the left to open slightly. During storage valve will be pointing straight up in the closed position. Place other end of this tubing into sink. The RO permeate will come out of this tubing.
19. Open round red valve at the outlet of RO membrane completely.
20. Plug in RO pump cord to power strip, turn on.
21. Permeate will start to come out of clear tubing.
22. Slowly turn the round red valve to the right until pressure is increased to 200 psi, watching the pressure gauge on the front of RO unit (labeled “pump pressure”). DO NOT let pressure go above 200 psi during RO concentration.
23. Run RO pump until desired concentration factor is obtained – for example, until ~ 4 L remain.
24. Take periodic samples of RO concentrate and permeate for UNC analyses – record water height by measuring with yard stick.
25. When ready to collect final RO concentrate, stop motor. Remove permeate tubing by pressing thing grey ring and close valve (perpendicular to tubing). Leave other two valves open.
26. Place outlet of RO concentrate into collection bottles (put bottles in secondary container to catch spilled water and be able to account for total final volume). Turn pump back on and collect RO concentrate. Again, be careful not to let air into RO pump tubing inlet. Turn pump off and measure any remaining water to account for final volume.

Clean filters

27. Collect finished water in bin #1 for rinsing filters and RO membrane.
28. Clean filters as done in steps 2 and 3. Turn off filter pump.
29. Put RO inlet tubing in bin #1, put outlet tube into sink. Run RO pump ~1 minute or until water leaving RO concentrate tubing is clear. Turn off RO pump.
30. Turn red RO inlet valve perpendicular to tubing (closed) and close round red outlet valve immediately, to keep RO membrane sealed in clean water for storage.
31. Clean up any spilled water on floor, benches.
32. Empty bins #1 and #2 and wipe dry with paper towels. Put black lids loosely on bins. CAREFULLY roll RO unit back into storage closet. Place bins and tubing in storage closet.
33. Leave OWASA lab exactly as you found it – the lab staff are very kind to let us store the RO unit there and use their facility, so be respectful.

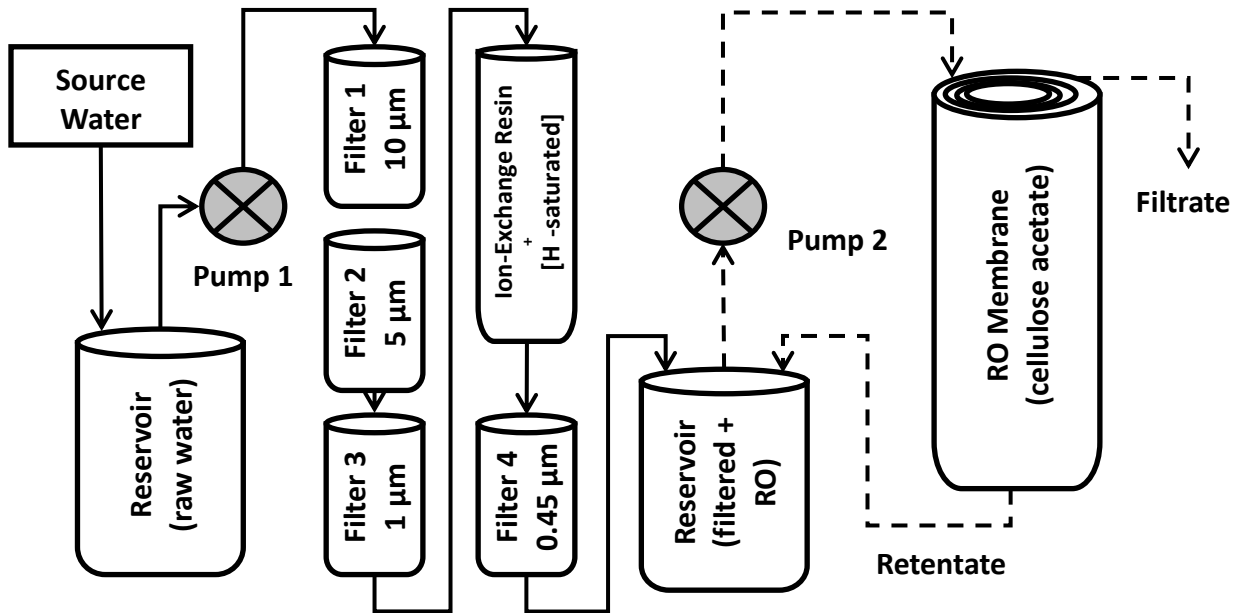


Figure A1-1. Schematic of RO concentration procedure.

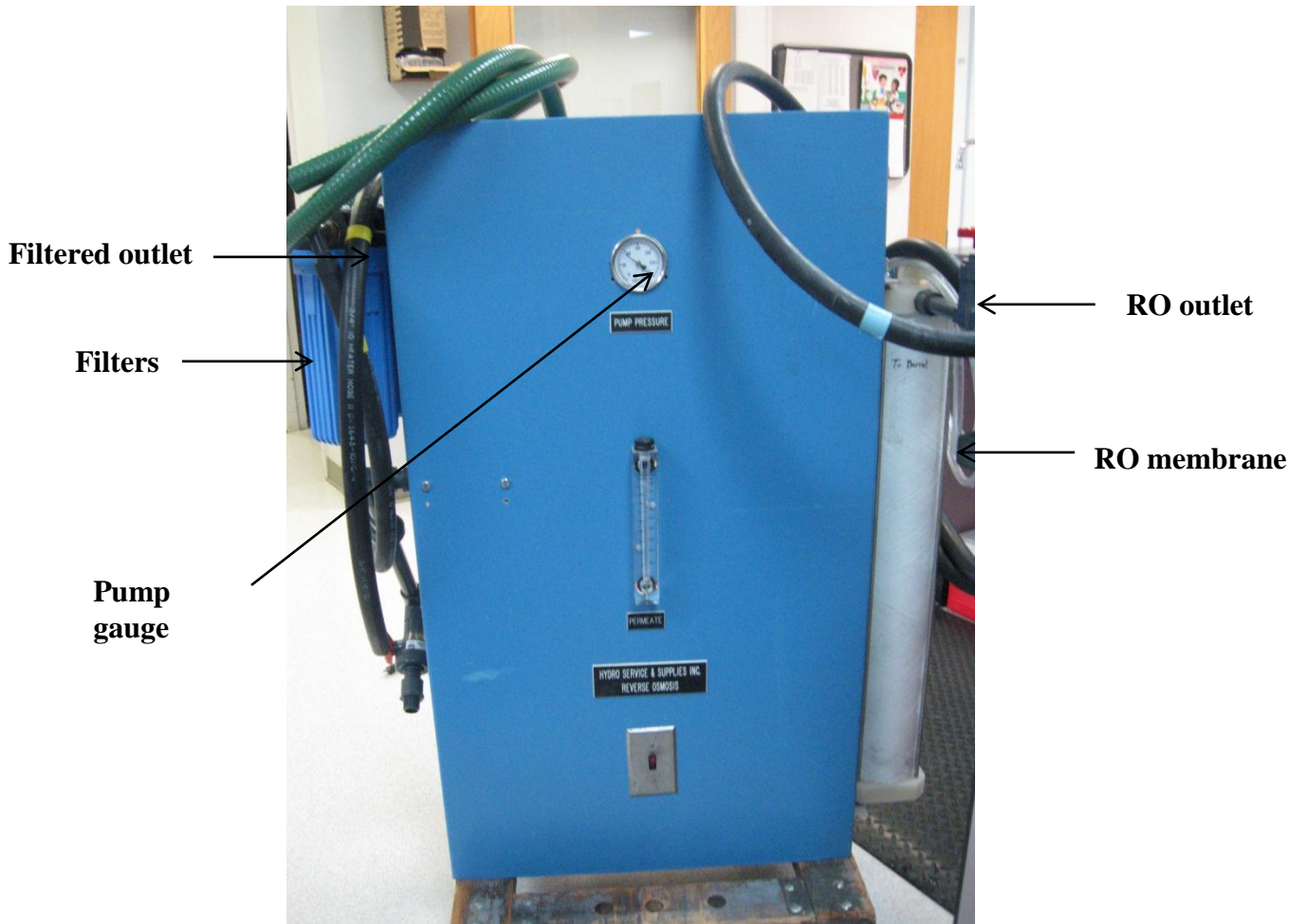


Figure A1-2. Front of RO concentration unit.

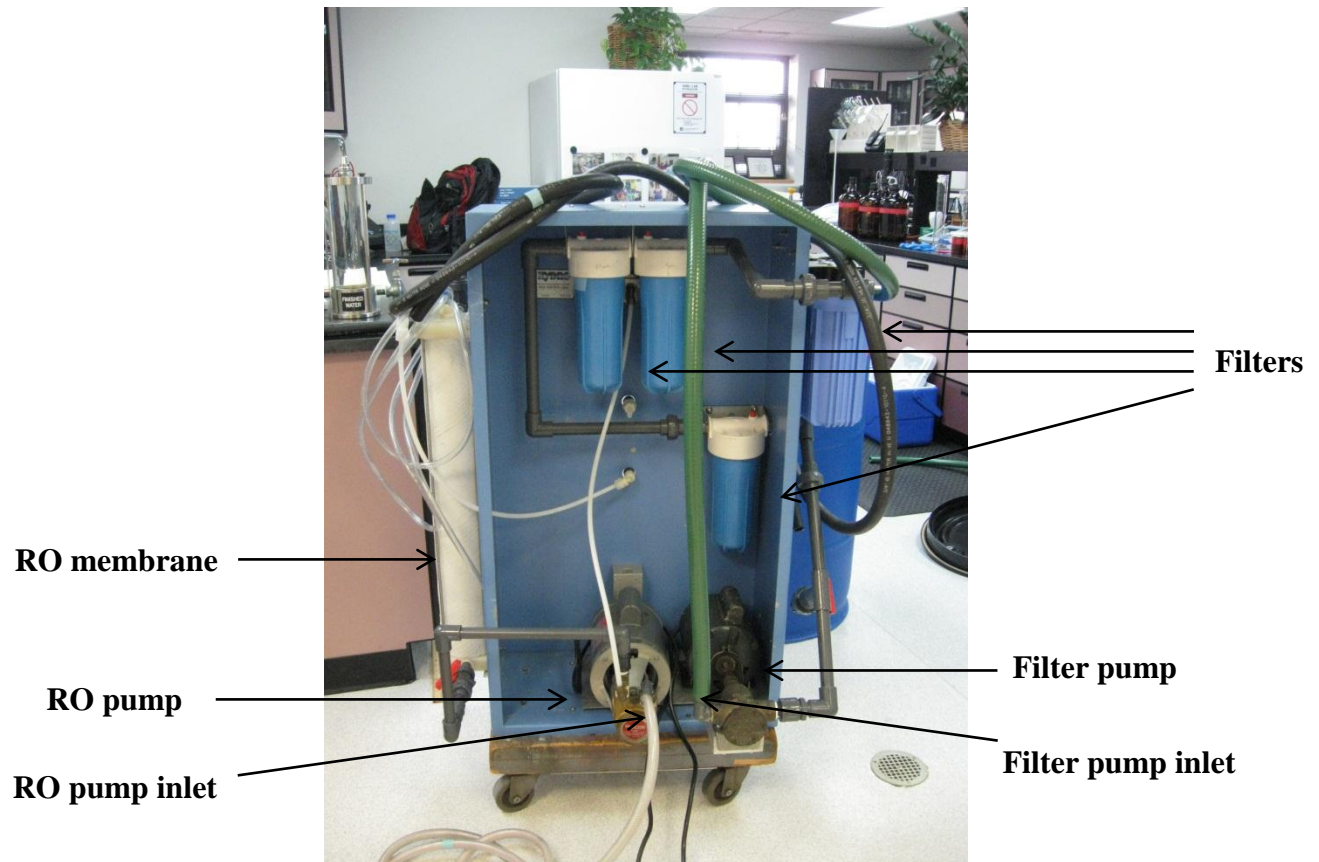


Figure A1-3. Back of RO concentration unit.

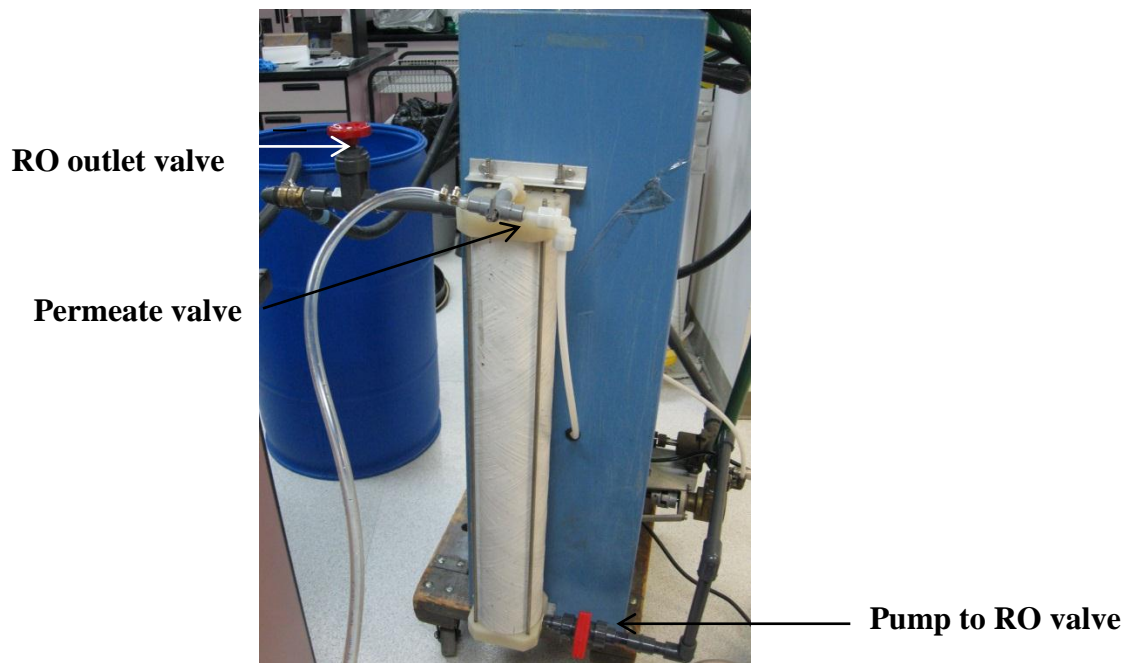


Figure A1-4. RO membrane enclosure.

Appendix 2: Supplemental Information for Chapter 2

Table A2-1. Reverse osmosis (RO) feed and RO concentrate (conc.) characteristics for Orange County Water and Sewer Authority (OWASA) drinking water treatment plant raw and settled waters.

parameter (units)	raw water ^a		settled water	
	feed	RO conc. ^b	feed	RO conc.
dissolved organic carbon (mg C/L)	5.1	120	2.0	28.4
total dissolved nitrogen (mg N/L)	0.48	9.17	0.13	2.17
nitrate (mg N/L)	0.2	3.0	0.03	0.3
bromide (µg/L)	<0.02	0.3	0.02	0.2
SUVA ₂₅₄ (L/mg C·m)	2.6	2.4	1.2	1.4

^aThis was concentrated and characterized on a different day from the RO used for Chapter 3 experiments, but the same operating conditions were used so the concentration factors are expected to be similar.

^bConcentration factors by volume were: 32× for the raw water and 15× for the settled water.

Table A2-2. Effect of MP UV (dose is in mJ/cm²) followed by chlorination and chloramination on THMs in ambient and iodide-spiked Utility C samples. Values shown are averages between experimental duplicates in µg/L. Br₂ICH and BrI₂CH were below detection limit (<0.1 µg/L) in all samples.

spiking	treatment	Cl ₃ CH	BrCl ₂ CH	Br ₂ ClCH	Cl ₂ ICH	Br ₃ CH	BrClICH	Cl ₂ CH	I ₃ CH	ΣTHM4	ΣTHM10
ambient	HOCl alone	67	14	2.9	<0.1	0.2	<0.1	<0.1	<0.1	84	84
	MP 40 + HOCl	71	15	2.9	<0.1	0.2	<0.1	<0.1	<0.1	88	88
	MP 186 + HOCl	82	16	2.9	<0.1	0.2	<0.1	<0.1	<0.1	100	100
	MP 1000 + HOCl	94	16	3.0	<0.1	0.2	<0.1	<0.1	<0.1	114	114
I ⁻ spiked (0.5 mg/L)	HOCl alone	67	15	3.1	<0.1	0.2	<0.1	<0.1	<0.1	85	85
	MP 40 + HOCl	70	15	3.1	<0.1	0.2	<0.1	<0.1	<0.1	88	88
	MP 186 + HOCl	77	16	3.2	<0.1	0.2	<0.1	<0.1	<0.1	96	96
	MP 1000 + HOCl	93	16	3.1	<0.1	0.2	<0.1	<0.1	<0.1	112	112
ambient	NH ₂ Cl alone	0.5	0.1	<0.1	<0.1	<0.1	<0.1	<0.1	<0.1	0.6	0.6
	MP 40 + NH ₂ Cl	0.6	0.1	<0.1	<0.1	<0.1	<0.1	<0.1	<0.1	0.7	0.7
	MP 186 + NH ₂ Cl	0.6	0.1	<0.1	<0.1	<0.1	<0.1	<0.1	<0.1	0.8	0.8
	MP 1000 + NH ₂ Cl	0.6	0.1	<0.1	<0.1	<0.1	<0.1	<0.1	<0.1	0.7	0.7
I ⁻ spiked (0.5 mg/L)	NH ₂ Cl alone	0.2	0.1	<0.1	0.4	<0.1	0.4	1.9	11	0.4	14
	MP 40 + NH ₂ Cl	0.3	0.1	<0.1	0.4	<0.1	0.5	1.9	13	0.4	15
	MP 186 + NH ₂ Cl	0.3	0.1	<0.1	0.3	<0.1	0.5	1.8	14	0.4	17
	MP 1000 + NH ₂ Cl	0.2	0.1	<0.1	0.2	<0.1	0.3	2.1	10	0.3	13

Kinetics Experiment

Utility C samples were spiked with nitrate (10 mg N/L) or nitrate and bromide (10 mg N/L and 1 mg Br/L) and treated with chlorine and chloramine, with and without 1000 mJ/cm² MP UV pre-treatment. The objective of this experiment was to determine the kinetics of cyanogen chloride and halogenated volatile DBP formation with varying chlorine and chloramine contact times (2 min to 67 hours) following MP UV irradiation. A residual of 1 mg/L as Cl₂ after 72 hours was targeted so samples could be compared on an equivalent residual basis, however, actual residuals ranged from 0.9 to 3.7 mg/L as Cl₂. Aside from the different chlorine/chloramine contact times, samples were prepared and treated according to the same methods described in Chapter 2. Table A5-3 shows the measured chlorine/chloramine residuals at each time point. Tables A5-4 and A5-5 shows the formation of cyanogen chloride and halogenated volatiles for chlorinated and chloraminated samples, respectively.

Table A2-3. Chlorine/chloramine residuals at specified time points for kinetics study (mg/L as Cl₂) in spiked Utility C samples.

spiking	treatment	2 min	1 hr	6 hr	21 hr	67 hr
NO ₃ ⁻ spiked*	HOCl alone	2.9	2.5	2.4	1.7	1.1
	MP 1000 + HOCl	4.7	3.6	3.5	2.6	1.8
NO ₃ ⁻ + Br ⁻ spiked	HOCl	3.3	3.0	2.6	1.9	1.0
	MP 1000 + HOCl	7.8	6.9	6.1	4.8	3.7
NO ₃ ⁻ spiked	NH ₂ Cl	1.4	1.3	1.2	1.1	0.9
	MP 1000 + NH ₂ Cl	3.7	3.5	3.2	2.4	1.6
NO ₃ ⁻ + Br ⁻ spiked	NH ₂ Cl	1.5	1.4	1.3	1.1	0.9
	MP 1000 + NH ₂ Cl	4.6	4.4	3.8	2.9	1.9

* Spiking amounts were 10 mg N/L nitrate and 1 mg/L bromide.

Table A2-4. Formation of cyanogen chloride and halogenated volatile species in nitrate- and nitrate- & bromide-spiked Utility C samples following chlorination and 1000 mJ/cm² MP UV + chlorine treatment, with different chlorine contact times. Values shown are averages between experimental duplicates in µg/L. Iodo-THMs were below detection limit (<0.1 µg/L) in all samples.

spiking/treatment	time	CNCl	Cl ₂ CH	TCAN	DCAN	BrCl ₂ CH	CH	11DCP	TCNM	Br ₂ CICH	BCAN	111TCP	Br ₃ CH	DBAN	TBNM	ΣTHM4
NO ₃ ⁻ spiked*, HOCl	2 min	<0.1	3.7	0.3	0.3	0.8	0.5	0.4	0.1	0.2	0.2	1.2	<0.1	<0.1	0.2	4.7
	1 hr	<0.1	21	0.4	1.4	6.2	1.7	0.3	0.1	1.3	0.7	2.5	<0.1	0.2	0.2	28
	6 hr	<0.1	34	0.4	2.0	9.0	2.9	0.2	0.2	1.7	0.8	3.1	0.1	0.2	0.1	44
	21 hr	<0.1	68	0.4	2.8	14	6.5	0.2	0.3	2.4	1.1	2.5	0.2	0.3	0.1	85
	67 hr	<0.1	101	0.4	2.6	18	14	0.1	0.3	2.9	1.0	0.9	0.2	0.3	0.1	123
NO ₃ ⁻ spiked, MP UV + HOCl	2 min	1.6	4.0	0.4	0.7	1.1	1.7	0.8	3.7	0.3	0.3	2.9	<0.1	<0.1	0.4	5.3
	1 hr	0.1	25	0.5	1.8	7.0	18	1.0	7.5	1.2	0.7	7.2	<0.1	0.1	0.6	33
	6 hr	<0.1	43	0.5	2.4	9.7	24	0.6	8.2	1.5	0.8	11	<0.1	0.2	0.5	54
	21 hr	<0.1	98	0.5	2.9	15	31	0.2	11	2.0	0.9	7.6	0.1	0.2	0.5	116
	67 hr	<0.1	147	0.5	2.1	19	39	0.2	13	2.5	0.7	1.9	0.1	<0.1	0.5	169
NO ₃ ⁻ + Br ⁻ spiked, HOCl	2 min	<0.1	1.0	0.4	0.2	2.1	0.3	0.3	<0.1	3.7	0.4	0.5	3.7	0.9	0.6	11
	1 hr	<0.1	2.8	0.4	0.3	9.2	0.5	0.2	<0.1	22	1.4	0.6	29	4.3	0.7	64
	6 hr	<0.1	3.6	0.3	0.3	13	0.7	0.1	<0.1	32	1.9	0.6	43	6.0	0.6	93
	21 hr	<0.1	5.8	0.3	0.4	23	0.9	<0.1	<0.1	62	2.7	0.1	86	9.0	0.8	177
	67 hr	<0.1	6.8	0.3	0.3	29	0.7	<0.1	<0.1	95	3.1	<0.1	139	12	1.1	269
NO ₃ ⁻ + Br ⁻ spiked, MP UV + HOCl	2 min	0.9	0.5	0.4	0.2	1.8	0.9	0.4	<0.1	5.4	0.8	0.4	5.5	1.3	15	13
	1 hr	<0.1	2.2	0.5	0.4	11	3.2	0.4	<0.1	30	1.8	1.0	25	3.8	22	69
	6 hr	<0.1	3.9	0.4	0.5	21	3.6	0.3	<0.1	47	2.2	1.8	37	5.2	24	109
	21 hr	<0.1	9.1	0.4	0.6	46	4.1	<0.1	<0.1	90	2.9	1.0	67	7.0	28	213
	67 hr	<0.1	17	0.4	0.4	70	4.4	<0.1	<0.1	139	2.4	0.2	95	6.4	31	322

* Spiking amounts were 10 mg N/L nitrate and 1 mg/L bromide.

Table A2-5. Formation of cyanogen chloride and halogenated volatile species in nitrate- and nitrate- & bromide-spiked Utility C samples following chloramination and 1000 mJ/cm² MP UV + chloramine treatment, with different chloramine contact times. Values shown are averages between experimental duplicates in µg/L. 111TCP and iodo-THMs were below detection limit (<0.1 µg/L) in all samples.

spiking/treatment	time	CNCl	Cl ₃ CH	TCAN	DCAN	BrCl ₂ CH	CH	11DCP	TCNM	Br ₂ CICH	BCAN	Br ₃ CH	DBAN	TBNM	∑THM4
NO ₃ ⁻ spiked*, NH ₂ Cl	2 min	<0.1	0.1	0.3	0.1	<0.1	0.2	0.1	<0.1	0.1	<0.1	<0.1	<0.1	<0.1	0.2
	1 hr	<0.1	0.1	0.3	0.1	<0.1	0.2	0.6	<0.1	0.1	<0.1	<0.1	<0.1	<0.1	0.2
	6 hr	<0.1	0.2	0.3	0.1	<0.1	0.2	0.7	<0.1	0.1	<0.1	<0.1	<0.1	<0.1	0.3
	24 hr	0.1	0.4	0.3	0.2	<0.1	0.2	0.8	<0.1	0.1	<0.1	<0.1	<0.1	<0.1	0.5
	72 hr	0.3	1.0	0.3	0.2	<0.1	0.2	0.8	<0.1	<0.1	<0.1	<0.1	<0.1	<0.1	1.0
NO ₃ ⁻ spiked, MP UV + NH ₂ Cl	2 min	1.3	<0.1	0.4	0.1	<0.1	0.2	0.2	<0.1	<0.1	<0.1	<0.1	<0.1	<0.1	0.0
	1 hr	2.8	<0.1	0.4	0.2	<0.1	0.2	1.6	<0.1	<0.1	<0.1	<0.1	<0.1	<0.1	0.0
	6 hr	3.2	0.2	0.4	0.3	<0.1	0.3	2.3	0.3	<0.1	<0.1	<0.1	<0.1	0.1	0.2
	24 hr	3.0	0.6	0.4	0.5	0.1	0.4	2.7	1.6	<0.1	<0.1	<0.1	<0.1	0.1	0.7
	72 hr	2.3	1.2	0.4	0.5	0.2	0.4	2.6	3.3	<0.1	<0.1	<0.1	<0.1	0.1	1.5
NO ₃ ⁻ + Br ⁻ spiked, NH ₂ Cl	2 min	<0.1	0.1	0.3	<0.1	<0.1	<0.1	<0.1	<0.1	0.1	<0.1	<0.1	<0.1	<0.1	0.2
	1 hr	<0.1	0.1	0.4	0.1	<0.1	<0.1	0.6	<0.1	0.1	0.1	<0.1	<0.1	<0.1	0.2
	6 hr	<0.1	0.2	0.3	0.1	<0.1	<0.1	0.7	<0.1	0.1	0.1	<0.1	<0.1	<0.1	0.3
	24 hr	0.1	0.3	0.3	0.1	0.2	<0.1	0.7	<0.1	0.1	0.2	<0.1	<0.1	0.1	0.7
	72 hr	0.1	0.6	0.3	0.2	0.9	<0.1	0.5	<0.1	0.4	0.2	0.2	<0.1	0.1	2.1
NO ₃ ⁻ + Br ⁻ spiked, MP UV + NH ₂ Cl	2 min	1.3	<0.1	0.4	0.1	<0.1	<0.1	0.2	<0.1	<0.1	<0.1	<0.1	<0.1	<0.1	0.0
	1 hr	2.8	<0.1	0.4	0.2	<0.1	<0.1	1.0	<0.1	0.1	0.3	<0.1	0.1	1.8	0.1
	6 hr	3.2	<0.1	0.4	0.2	0.6	<0.1	0.9	0.1	0.9	0.4	0.8	0.3	4.1	2.4
	24 hr	3.0	<0.1	0.4	0.2	2.8	<0.1	0.2	0.2	4.0	0.6	5.1	0.7	7.6	12
	72 hr	2.3	0.2	0.4	0.2	4.3	<0.1	<0.1	0.4	7.7	0.6	11	1.1	8.1	23

* Spiking amounts were 10 mg N/L nitrate and 1 mg/L bromide.

Appendix 3: SOP for Medium Pressure (MP) UV System

Prepared by Bonnie Lyon

Materials:

- Laboratory grade water (LGW), purified using a secondary water purification system (Dracor Water Systems, Durham, NC, USA). Water pretreated with an general in-house purification system was pre-filtered (1 μ m filter), treated to remove chlorine or chloramine residuals, passed through an activated carbon cartridge to reduce the total organic carbon content to less than 0.2 mg/L and passed through mixed-bed ion exchange resins to reduce the ion content to less than 18 M Ω .
- Uridine (Sigma catalog #U3750, Sigma Chemical Co., St. Louis, MO, USA)
- Disodium phosphate heptahydrate (Fisher catalog #S373, ThermoFisher Scientific, Waltham, MA, USA)
- Monosodium phosphate monohydrate (Fisher catalog #S369)
- Crystallization dish (Pyrex, Corning Inc., Corning, NY, USA)
- Stir bar
- 2 quartz cuvettes
- Kimwipes
- Disposable Pasteur pipets and rubber bulb
- Lens paper
- MP UV lamp system
- Timer/Stopwatch
- Copper coil connected to recirculating water bath to maintain sample temperature during irradiation
- 25 mL amber glass vials
- “MP UV dose calculation.xls” spreadsheet for calculating UV irradiance and time required to achieve target doses

Solutions:

Phosphate buffer stock – prepare a 100 mM buffer stock at pH 7 by adding 1.04 g disodium phosphate heptahydrate and 0.85 g monosodium monohydrate to a 100 mL volumetric flask containing LGW. Fill to line with LGW.

Uridine stock – prepare a 12 mM uridine stock solution by adding approximately 0.293 g solid uridine a 100 mL volumetric flask containing LGW. Fill to line with LGW.

Uridine dilution – prepare a 0.012 mM dilution of the uridine stock solution by adding 1 mL of the uridine stock solution and 10 mL of the phosphate buffer stock to a 1 L volumetric flask containing LGW. Fill to line with LGW. Store at 4°C. Let come to room temperature before use.

Notes:

*Wear UV-protective goggles while operating lamp (most of our lab goggles are UV-A and B protective)

*Never open the sample compartment door while the shutter is open and lamp is on.

Procedure:

Uridine Actinometry

1. Turn on MP UV lamp—plug into power source, switch lamp to “on,” turn on fan (at 100%), and turn on temperature probe. Be sure to turn on lamp before turning on fan – if it is too cool in the lamp compartment, the lamp will not turn on. **Make sure that the shutter is shut before turning lamp on.** Allow to warm up for at least 30 minutes. Be sure to either note the time you turn the lamp on or use stopwatch to record this time. Total lamp hours are recorded in the logbook located next to the system, and the lamp needs to be replaced around 1000 hours.
2. Shortly after turning on the MP UV lamp to warm up, turn on UV/vis spectrometer. These lamps also need to warm up for 30 minutes prior to use.
3. While lamps are warming up, transfer about 10 mL of the sample(s) you will be irradiating into 25-mL amber glass vials with caps and PTFE-lined septa. If these are very concentrated samples you may need to dilute (a surface water with <5 mg N/L nitrate and DOC <10 mg C/L will likely not need dilution). If it has a high DOC or >5 mg N/L nitrate, make a dilution in LGW. Note the dilution you make so you can correct the absorbance spectra later.
4. Once MP UV lamp has warmed up for 30 minutes, measure out uridine dilution (use same volume that will be used for sample treatment) and pour into crystallization dish. Temperature (reading on probe) typically stabilizes around 325-330°C. Also fill a 25-mL amber glass vial with uridine dilution for “t=0” sample.
5. Place stir bar in dish and measure sample depth (distance from bottom of crystallization dish to top of water line). Input this value (in cm) into MP UV dose calculation spreadsheet (Tab 3 “Actinometry”, Cell B12).
6. Place crystallization dish on stir plate in sample compartment and adjust jack stand to desired height (note this height – measured from the bottom of the compartment to the top of the aqueous sample). Place cooling coils around crystallization dish and turn on recirculating water bath. Temperature is set at 20°C on unit, which was determined to be sufficient to keep sample temperature around 25°C during irradiation. Make sure dish is centered and sitting flat on stir plate. Adjust stir plate to desired mixing speed (usually around setting 1-2, depending on the volume being used).
7. Close the lamp door. Set timer for desired irradiation time (typically use 3-8 minutes for uridine measurement). Simultaneously open lamp shutter and start timer. When lamp has been on for a while, the shutter door gets hot. Be careful - use gloves or ruler to open without burning your hand.
8. When desired time has elapsed, stop irradiation by closing shutter.

9. Carefully remove irradiated uridine solution and transfer to a 25-mL amber glass vial, filling and then discard remaining uridine solution. This will be the $t=x$ sample, where x = minutes irradiated. Input the value of x (minutes) into the MP UV dose calculation spreadsheet (Tab 3-Actinometry, Cell B11).
10. Keep MP UV lamp on.
11. Bring two uridine samples, two quartz cuvettes, Kimwipes, lens paper, disposable Pasteur pipets, and LGW to the UV/vis spectrometer.
12. Turn on laptop attached to spectrometer and open UV/vis software (it usually opens automatically when computer is turned on).
13. Wear gloves while handling quartz cuvettes. Rinse cuvettes thoroughly with LGW and then fill both with LGW using a Pasteur pipet. Use a Kimwipe to dry outside of cuvette and then clean with a lens paper.
14. Place reference cuvette containing LGW in the back cuvette compartment of UV/vis spectrometer and second cuvette containing LGW in the front (sample) compartment. Be sure to note the orientation and if cuvette has two frosted sides, make sure that clear (“unfrosted”) side is facing the path of the UV beam.
15. Run LGW blank baseline.
16. Discard and replace contents of cuvette in sample compartment with $t=0$ uridine sample using a Pasteur pipet. Dry and clean outside of cuvette using a Kimwipe and lens paper. Measure absorbance from 200-400 nm. The spectrum should have a maxima around 262 nm, and for the $t=0$ sample, the absorbance at 262 nm should be around 0.12. See Figure A1-1 for typical uridine spectra.
17. Discard and refill cuvette with $t=x$ uridine sample, rinsing twice with the sample prior to filling. Dry and clean outside of cuvette using a Kimwipe and lens paper.
18. Measure absorbance from 200-400 nm. Next you will measure the absorbance of each sample you will be irradiating.
19. Discard uridine sample and rinse at least three times with LGW.
20. Rinse with your sample. Fill with sample and measure absorbance
21. Save your absorbance files in excel format (Print Report, File→save as→then save your file as an .xls file) and email files to yourself (no flash drive on this computer).
22. Shut down software, turn off UV/vis lamps, and turn off laptop attached to spectrometer.
23. Make sure to record total time UV/vis lamps on in logbook.

Dose Calculations

24. Input uridine and sample absorbance spectra into MP UV dose calculation spreadsheet. (Input directions are listed in Tab 1-Instructions).
25. Determine time required to achieve desired dose for the samples you will be irradiating, e.g. 40 mJ/cm^2 , 1000 mJ/cm^2 . You will need to paste in the absorbance spectra and determine the irradiation time for each individual sample. If you made a dilution to any sample, multiply the absorbance at each wavelength by the dilution factor. Save the MP UV dose calculation spreadsheet under a new filename so that you can refer back to the values you calculated.

Sample Irradiation

26. Measure out and transfer sample to be irradiated into clean crystallization dish. Add clean stir bar. Measure sample depth (if using same volume as uridine solution, this should be the same depth)
27. Place sample on center of stir plate with copper cooling coils surrounding dish. Adjust stand height so sample water line is at the same height that the uridine solution water line was at. If using same sample volume as was used for uridine, you should not need to adjust stand.
28. Turn on recirculating water bath. Make sure dish is centered and sitting flat on stir plate. Adjust stir plate to desired mixing speed (usually around setting 1-2, depending on the volume being used).
29. Close door to sample compartment. Set timer for desired irradiation time and simultaneously open shutter and start timer.
30. When desired time has elapsed, stop irradiation by closing shutter.
31. Repeat for remaining samples.
32. When all samples are finished, turn off lamp and unplug from power source. Record total time lamp was on in logbook. Leave fan on for ~30 minutes to cool the lamp and then turn off fan.

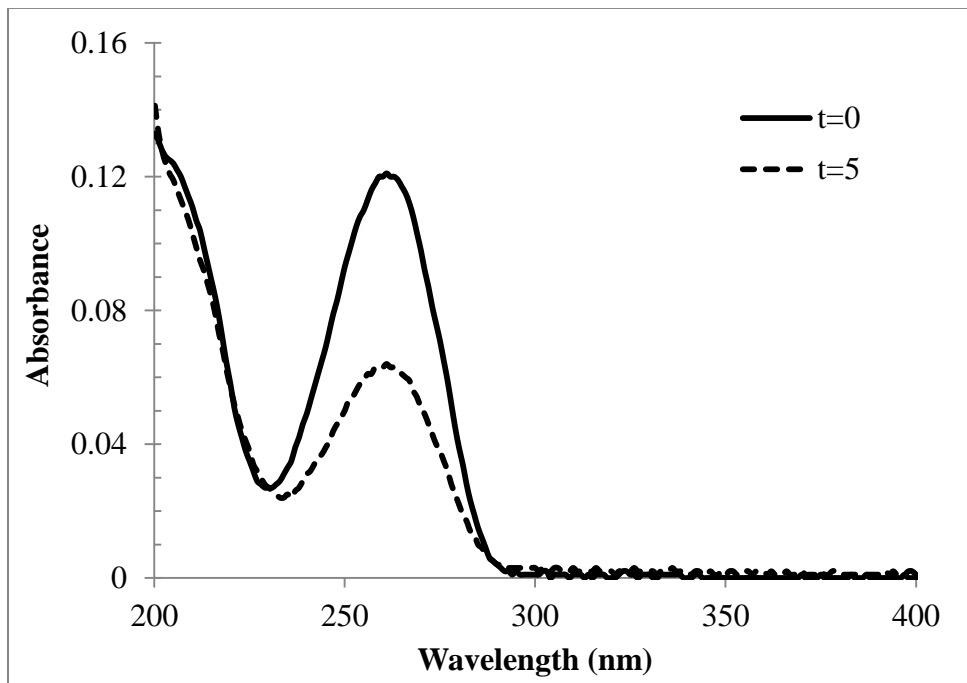


Figure A3-1. Typical uridine UV/vis absorbance spectra for t=0 and t=5 min. Irradiated uridine solution volume was 75 mL.

Appendix 4: Preparation of Monochloramine Dosing Solution

Prepared by Katja Kritsch and updated by Bonnie Lyon

This procedure describes the preparation of 100 mL of a 1400 mg Cl₂/L monochloramine dosing solution. The sodium hypochlorite stock should be titrated monthly according to Standard Method 4500-B (APHA 1999). The monochloramine dosing solution should be prepared fresh daily.

Materials:

Reagents

- Laboratory grade water (LGW), purified using a secondary water purification system (Dracor Water Systems, Durham, NC, USA). Water pretreated with an general in-house purification system was pre-filtered (1 µm filter), treated to remove chlorine or chloramine residuals, passed through an activated carbon cartridge to reduce the total organic carbon content to less than 0.2 mg/L and passed through mixed-bed ion exchange resins to reduce the ion content to less than 18 MΩ.
- Sodium hypochlorite solution, 5.6 - 6% as Cl₂ (Fisher, ThermoFisher Scientific, Waltham, MA, USA)
- Ammonium chloride, granular, ≥99%, certified ACS (Fisher Scientific)
- Sodium hydroxide, 50% w/w certified (Fisher Scientific)

Glassware

All glassware should be washed in a detergent (Alconox) solution, rinsed with tap water and LGW, soaked in a 10% nitric acid solution overnight, rinsed three times with LGW and dried in an 80°C oven designated for glassware drying. Volumetric glassware cannot be dried in the oven; instead it is rinsed three times with methanol and dried in a clean bin on a clean Kimwipe, covered with another Kimwipe and dried on the bench top. Caps and PTFE (Teflon)-lined septa cannot be acid washed. They are washed in a soap solution separate from glassware, rinsed three times with LGW and three times with methanol. To dry, caps and liners are placed in a clean bin on a clean Kimwipe, covered with another Kimwipe and dried on the bench top.

- 125 mL amber Boston round bottle with open-top caps and PTFE-lined septa
- 10 mL and 100 mL clear glass volumetric flasks with ground glass stoppers for ammonium chloride stock solution preparation and UV measurement dilution
- Clear 250-mL Erlenmeyer flask
- Volumetric glass pipettes with rubber bulb
- Disposable Pasteur pipettes and rubber bulbs
- 25 mL glass burette (Pyrex, Corning Inc., Corning, NY, USA)

Instruments and Additional Materials

- Analytical balance
- UV/vis spectrometer
- 2 quartz cuvettes
- Kimwipes
- Lens wipes
- Burette stand
- Stir plate and PTFE-coated stir bar for titration
- Hexagonal polystyrene weighing dishes
- Intermediate range pH test strips, pH 5 – 10, EMD colorpHast

Solution Preparation:

NaOH solution (1 M) for pH adjustment

Prepare a 1 M solution in LGW from 50% w/w NaOH (specific gravity = 1.53). Add 1.3 mL to a 25 mL volumetric flask containing LGW. Fill to line with LGW.

Transfer to a polypropylene vial for storage. Solution is stored in cabinet marked for bases at room temperature.

Free Chlorine Stock Solution

The hypochlorite stock solution comes ready to use and does not need to be diluted.

However, the hypochlorite stock concentration needs to be determined prior to use according to Standard Method 4500-B (APHA 1999). If the concentration was determined within the past 4 weeks, it is acceptable to use a previously titrated solution.

Ammonium Chloride Solution

To prepare a monochloramine solution, free chlorine is added to an ammonium chloride solution at a 1.2:1 N:Cl molar ratio.

1. Prepare a 24 mM ammonium chloride solution by adding 0.128 g ammonium chloride to a 100 mL volumetric flask containing LGW. Fill to line with LGW.
2. Adjust to pH 8 with 1 M NaOH (typically ~5 drops). Test pH with pH paper.

Chloramine Dosing Solution Preparation and Analysis:

Chloramine Dosing Solution Preparation

3. Transfer ammonium chloride solution to a 250 mL Erlenmeyer flask. Place stir bar in flask and place on stir plate. Turn on stir plate and mix solution slowly.
4. Determine the volume of hypochlorite stock solution to add to the ammonium chloride solution using the following equation:

$$\text{Volume (mL)} = \frac{1400 \text{ mg} \frac{\text{Cl}_2}{\text{L}} \times 100 \text{ mL}}{[\text{Cl}_2] \left(\frac{\text{mg} \text{Cl}_2}{\text{L}} \right)}$$

where volume = the amount of hypochlorite stock to add, 1400 mg Cl₂/L is the target stock concentration, 100 mL is the volume of ammonium chloride solution, and

[Cl₂] is the measured hypochlorite stock solution in mg/L as Cl₂ (a fresh bottle of 5.6-6% hypochlorite = 62-66 mg Cl₂/mL).

5. Measure out this amount with a glass volumetric pipette and add to the glass burette.
6. Open the burette VERY slowly and add the hypochlorite stock drop-wise to the flask (which is on the stir plate, with stirring).
7. When all hypochlorite has been added, transfer monochloramine solution to a 125 mL amber glass bottle with cap and PTFE-lined septa. If using the monochloramine dosing solution immediately, proceed to next step. If not using dosing solution immediately, store at 4°C and measure UV/vis absorbance (described below) for concentration calculation just before use.

Determination of the Chloramine Concentration in the Dosing Solution

8. Turn on the UV/vis spectrometer at least 30 minutes prior to use to warm up the lamps (recommend turning on just before starting chloramine solution preparation so it will be ready when dosing solution is prepared).
9. Prepare a 1:20 dilution of the dosing solution by transferring 0.5 mL of the dosing solution into a 10 mL volumetric flask using a glass pipette and fill to the line with LGW.
10. Stopper the flask and invert three times to mix.
11. Zero the instrument with LGW.
12. Transfer an appropriate volume of diluted dosing solution into a cuvette and measure the absorbance at the 245 and 295 nm wavelengths to determine the monochloramine and dichloramine concentrations by solving simultaneous Beer's Law equations, as described by Schreiber and Mitch (2005).

$$c_{di} = M_{Cl_2} \times 10 \times 1000 \times \left(\frac{\left(A_{295} - \left(\frac{A_{245}}{\epsilon_{m,245}} \times \epsilon_{m,295} \right) \right)}{\left(\frac{\epsilon_{di,295} - \left(\epsilon_{di,245} \times \epsilon_{m,295} \right)}{\epsilon_{m,245}} \right)} \right)$$

$$c_m = M_{Cl_2} \times 10 \times 1000 \times \left(\frac{A_{245}}{\epsilon_{m,245}} - c_{di} \times \frac{\epsilon_{di,245}}{\epsilon_{m,245}} \right)$$

- c_{di} = concentration dichloramine (mg Cl₂/L)
- c_m = concentration monochloramine (mg Cl₂/L)
- M_{Cl₂} = molar mass of Cl₂ (g/mol)
- A₂₄₅ = absorbance measured at 245 nm
- A₂₉₅ = absorbance measured at 295 nm
- ε_{di,245} = 208 = extinction coefficient of dichloramine at λ = 245 nm
- ε_{di,295} = 267 = extinction coefficient of dichloramine at λ = 295 nm
- ε_{m,245} = 445 = extinction coefficient of monochloramine at λ = 245 nm
- ε_{m,295} = 14 = extinction coefficient of monochloramine at λ = 295 nm

Use the calculated concentration c_m to for dosing calculations. Be sure that the results give a low (single digit or sometimes negative due to the error range of the method) number for dichloramine if a “pure” monochloramine dosing solution is desired.

Free chlorine may be determined using the Hach colorimeter and the appropriate procedures. A dosing solution with a monochloramine concentration close to 1400 mg Cl_2/L and negligible dichloramine indicates that the preparation of pure monochloramine was successful.

Sources Cited

APHA (American Public Health Association), American Water Works Association, and Water Environment Federation, 1999. Standard Methods for the Examination of Water and Wastewater. 20th Edition, American Public Health Association: Washington DC.

Schreiber, I.M. & Mitch, W.A., 2005. Influence of the order of reagent addition on NDMA formation during chloramination. *Environmental Science & Technology*, 39(10), pp.3811-3818.

Appendix 5: DBP Extractions

5.A Halogenated Volatiles/Haloacetamides Extraction SOP

Prepared by: Bonnie Lyon

Halogenated Volatiles

Abbreviation	Compound	CAS #	mol. wt. (g/mol)
Cl ₃ CH	chloroform	67-66-3	119.4
BrCl ₂ CH	bromodichloromethane	75-27-4	163.8
Br ₂ ClCH	dibromochloromethane	124-48-1	208.3
Br ₃ CH	bromoform	75-25-2	252.7
Cl ₂ ICH	dichloriodomethane	594-04-7	210.8
ClI ₂ CH	chlorodiiodomethane	638-73-3	302.3
Br ₂ ICH	dibromiodomethane	593-94-2	299.7
BrI ₂ CH	bromodiiodomethane	557-95-9	346.7
BrClICH	bromochloriodomethane	3490-00-8	255.3
I ₃ CH	iodoform	75-47-8	393.7
DCAN	dichloroacetonitrile	3018-12-0	109.9
TCAN	trichloroacetonitrile	545-06-2	144.4
BCAN	bromochloroacetonitrile	83463-62-1	154.4
DBAN	dibromoacetonitrile	3252-43-5	198.9
CH	chloral hydrate	302-17-0	165.4
11DCP	1,1-dichloropropanone	513-88-2	127.0
111TCP	1,1,1-trichloropropanone	918-00-3	161.4
TCNM	Trichloronitromethane (chloropicrin)	76-06-2	164.4
TBNM	Tribromonitromethane (bromoopicrin)	76-06-2	297.8

Haloacetamides

Abbreviation	Compound	CAS #	mol. wt. (g/mol)
DCAM	dichloroacetamide	683-72-7	128.0
TCAM	trichloroacetamide	594-65-0	162.4
BAM	bromoacetamide	683-57-8	138.0
DBAM	dibromoacetamide	598-70-9	216.9
TBAM	tribromoacetamide	594-47-8	295.8
BCAM	bromochloroacetamide	62872-34-8	172.4
DBCAM	dibromochloroacetamide	855878-13-6	251.3
BDCAM	bromodichloroacetamide	98137-00-9	206.9
CIAM	chloroiodoacetamide	62872-35-9	219.4
BIAM	bromoiodoacetamide	62872-36-0	263.9
DIAM	diiodoacetamide	5875-23-0	310.9

Materials

- Clear 60-mL glass screw cap sample vials with polytetrafluoroethylene (PTFE)-lined silicone septa and open top caps
- 50-250 μ L Dade Model J micropipetter fitted with clean glass capillary tips
- 100-mL glass volumetric flasks with glass stoppers
- 1-L amber bottle mounted with 10-mL pump pipetting dispenser containing PFTE transfer line
- Disposable glass Pasteur pipettes and rubber bulbs
- pH indicator strips pH 0-6 – colorpHast, EMD Chemicals, (Fisher Scientific catalog #M95863, ThermoFisher Scientific, Waltham, MA, USA)
- GC vials - 12x32 mm 1.8-mL amber glass vials (Laboratory Supply Distributors catalog #20211ASRS-1232, Mt. Laurel, NJ, USA)
- GC Caps - 11 mm seal w/ Red Teflon[®] faced silicone septa, 40 Mils thick, (Supelco catalog #27360-U, Sigma Chemical Co., St. Louis, MO, USA)
- GC vial inserts – 5x30 mm Flat Bottom LVI (Laboratory Supply Distributors catalog #20870-530)
- Hand crimper for sealing gas chromatography autosampler vials
- Vortexer
- Teflon tape
- Stainless steel scupula

Instrumentation

Gas Chromatograph

- Hewlett-Packard GC5890 Series II with electron capture detector
- Capillary Column: Zebron-1 (Phenomenex, Torrance, CA, USA) 30 m length, 0.25 mm inner diameter, 1.0- μ m film thickness
- Data System: Hewlett-Packard ChemStation

GC Gases

- Carrier Gas-Ultra High Purity helium (National Welders catalog #325042, Morrisville, NC, USA)
- Makeup Gas-Ultra High Purity nitrogen (National Welders catalog #475041)

GC Supplies

- 11-mm diameter Thermolite septa (Restek catalog #27142, Bellafonte, PA, USA)
- Split/splitless injector liner sleeve with deactivated glass wool, 4 mm inner diameter (Restek catalog #439542)
- Graphite/vespel 0.5 mm ferrules (Chromatography Research Supplies catalog #213164, Louisville, KY, USA)
- 10 μ L tapered needle syringe (Hamilton catalog #80390, Reno, NV, USA)

Reagents

- Laboratory grade water (LGW), purified using a secondary water purification system (Dracor Water Systems, Durham, NC, USA). Water pretreated with an general in-house purification system was pre-filtered (1 µm filter), treated to remove chlorine or chloramine residuals, passed through an activated carbon cartridge to reduce the total organic carbon content to less than 0.2 mg/L and passed through mixed-bed ion exchange resins to reduce the ion content to less than 18 MΩ.
- OmniSolv Methyl-t-Butyl Ether (extraction solvent) (EMD Chemicals, Fisher catalog #MX08266)
- Sodium sulfate (Na₂SO₄), granular ACS grade (Mallinckrodt catalog #8024, St. Louis, MO, USA). Bake at 400°C in muffle furnace for 24 hours in a shallow, porcelain dish covered with aluminum foil. Store in desiccator.
- L-Ascorbic Acid (chlorine/chloramine quenching agent), certified ACS grade (Fisher catalog #A61-25)
- Sulfuric Acid (for pH adjustment), certified ACS Plus (Fisher catalog #A300-212)

Standards

- THM Calibration Mix, 2000 µg/mL each in methanol. (Supelco catalog #48140-U)
- EPA 551B Halogenated Volatiles Mix, 2000 µg/mL each in methanol (Supelco catalog #4-8046)
- Chloral Hydrate, 1000 µg/mL in acetonitrile (Supelco catalog # 47335-U)
- Internal Standard (IS): 1,2-dibromopropane neat standard, 99+%, (Aldrich catalog #14,096-1)
- Bromoacetamide (98%), (Acros Organics catalog #291100050, ThermoFisher Scientific)
- Dichloroacetamide (98%), (Acros Organics catalog #113050100)
- Trichloroacetamide (99%), (Acros Organics catalog #202920250)
- Triiodomethane (iodoform), 99%, (Aldrich catalog #109452)

The following standards are obtained from Orchid Cellmark, New Westminster, British Columbia, Canada):

- Tribromonitromethane, 95+% (catalog #HNM005)
- Bromochloroacetamide, (catalog #HAM001)
- Bromodichloroacetamide, (catalog #HAM001)
- Tribromoacetamide, (catalog #HAM003)
- Chloroiodoacetamide, (catalog #HAM004)
- Dibromochloroacetamide, (catalog #HAM005)
- Dibromoacetamide, (catalog #HAM006)
- Diiodoacetamide, (catalog #HAM007)
- Bromoiodoacetamide, (catalog #HAM008)
- Bromodiiodomethane, (catalog #HM002)
- Bromochloroiodomethane, (catalog #HM003)
- Chlorodiiodomethane, (catalog #HM004)
- Dibromiodomethane, (catalog #HM005)
- Dichloroiodomethane, (catalog #HM006)

Samples

Samples should be collected headspace-free in pre-cleaned 60 mL glass vials with screw caps and PTFE-lined silicone septa containing ascorbic acid. Prepare a solution of ascorbic acid in LGW so that 100 μL can be added to the 60 mL vial to provide the correct amount of ascorbic acid at the stoichiometric ratio (2.48 mg ascorbic/mg Cl_2 , multiplied by 2 for a safety factor) for the expected chlorine residual. This ascorbic acid solution needs to be made fresh daily. Samples should be filled head-space free and holding vial at an angle so halogenated volatiles do not escape through volatilization. Store samples in fridge at 4°C. Samples should be extracted within 24 hours of quenching.

Procedure

Internal Standard

Stock solution of Internal Standard (IS) at $\sim 2000 \mu\text{g/mL}$ in MtBE: prepared by injecting 10 μL of the neat standard and injecting into a 5 mL volumetric flask containing MtBE, fill to line with MtBE.

Primary dilution at 100 $\mu\text{g/mL}$: prepared by injecting 250 μL of IS stock solution using a micropipette into a 5 mL volumetric flask containing MtBE, fill to line with MtBE.

Extracting solution at 50 $\mu\text{g/L}$ or 100 $\mu\text{g/L}$ (depending on what expected concentration of analytes in samples): calculate how much extracting solvent will be needed for all of your samples and calibrations (3 mL for each sample and calibration). Make from primary dilution, and prepare more than needed because there may be bubbles in the dispenser that you need to clear, and will need to pump a few times to start out.

Halogenated Volatiles Calibration Standards

These are prepared as a mix of all halogenated volatile compounds

Prepare individual stock solutions of tribromonitromethane and iodo-THMs at approximately 2000 $\mu\text{g/mL}$ in MtBE by weighing out 20 mg each compound and add to 10 mL volumetric flask containing MtBE. Fill to line with MtBE.

Calibration Standard #1: 100 $\mu\text{g/mL}$, Add 100 μL of each THM4, EPA551B, iodo-THMs, and tribromonitromethane stock calibration mix and 200 μL of chloral hydrate to 2 mL volumetric flask containing MtBE, fill to line with MtBE.

Calibration Standard #2: 1 $\mu\text{g/mL}$, Add 20 μL of Calibration Standard #1 into 2 mL volumetric flask containing MtBE, fill to line with MtBE.

(These calibration standard concentrations can be changed if range of calibration curve is different.)

Haloacetamide Stock & Calibration Standards

Stock concentration: 2000 µg/mL. Prepared from solid standards of each haloacetamide. Weigh out 20 mg of each compound, dissolve in 10 mL high purity MtBE.

Calibration Standard #1: 20 µg/mL. Add 20 µL of primary dilution stock into 2 mL volumetric flask containing MtBE, fill to line with MtBE.

Calibration Standard #2: 1 µg/mL. Add 100 µL of Calibration standard #1 into 2 mL volumetric flask containing MtBE, fill to line with MtBE.

1. Transfer standards to a 2-mL amber glass vial and store in laboratory standards freezer at -15°C.
2. Check calibration standards a few days before extraction. Make up two dilutions (50 µg/L and 1 µg/L) in MtBE containing internal standard. Standards should be monitored for degradation and contamination by comparing standard chromatographic peak area values obtained on the performance evaluated designated GC to those obtained during initial calibration of standard. The responses obtained on the same instrument are normalized relative to the freshly prepared internal standard to account for instrument detector drift and the values for each compound stored on a spreadsheet on the GC computer and backed-up to the external hard drive. New standards should be made from the stock solution if check exceeds 20% drift. If the drift persists, purchase new stock solutions from two suppliers and compare the responses making a note of the stock batch number.
3. Prepare a laboratory reagent blank (the level 1 calibration standard - see step 6) and the laboratory fortified blank (level 3 calibration standard – see step 6) at the beginning of each day and analyze on the GC before extracting samples. If QC criteria fail, troubleshoot and correct the problem, reanalyzing these check standards before proceeding to the next step.
4. Prepare calibration standards in 100 mL LGW according to the range of concentrations expected in the samples. Examples for halogenated volatiles and haloacetamides are shown below.

Example of Halogenated Volatile Calibrations

Level	Concentration (µg/L)	Calibration standard	Volume cal. std. added (µL) to 100 mL LGW
1	0	--	0
2	0.1	1 µg/mL	10
3	1	1 µg/mL	100
4	10	100 µg/mL	10
5	20	100 µg/mL	20
6	50	100 µg/mL	50
7	100	100 µg/mL	100

Example of Haloacetamide Calibrations

Level	Concentration ($\mu\text{g/L}$)	Calibration standard	Volume cal. std. added (μL) to 100 mL LGW
1	0	--	0
2	0.1	1 $\mu\text{g/mL}$	10
3	0.5	1 $\mu\text{g/mL}$	50
4	5	20 $\mu\text{g/mL}$	25
5	10	20 $\mu\text{g/mL}$	50
6	25	20 $\mu\text{g/mL}$	125
7	50	20 $\mu\text{g/mL}$	250

5. Prepare matrix spike (MS) and matrix spike duplicate (MSD) in 30mL samples → should be ~2-3 times halogenated volatile levels in samples.
6. Measure 30 mL from all calibration standards using a 50mL measuring cylinder starting from lowest to highest concentration and then follow with the samples all in duplicate and transfer into 60 mL vials. Rinse cylinder 3 times with LGW and once with sample to be measured next between each. Pour at an angle so halogenated volatiles are not lost through volatilization.
7. Adjust all samples and calibrations to approximately pH 3.5 with 0.2 N H_2SO_4 . (Amount required for pH adjustment will likely be different for calibrations compared to samples. Use remaining 30 mL aliquot from 60 mL vial to determine how much H_2SO_4 will be needed.)
8. Add 3 mL extracting solvent from a solvent dispenser bottle to each 30 mL aliquot. Make sure there are no bubbles in the dispenser addition line.
9. Add ~6 g pre-baked sodium sulfate to each 30 mL sample/calibration standard. (6 g can be measured out in pre-measured marked 10 mL glass beaker) Vortex samples for 1 minute immediately after adding sodium sulfate to avoid clumping. Let samples settle for 5 minutes.
10. Using a disposable 23-cm glass Pasteur transfer ~1.5 mL from the middle of the MtBE layer (top layer) to a GC autosampler vial. Do not transfer any sodium sulfate crystals as they will clog the GC. Cap and crimp vial. Fill three GC vials for each sample (one for halogenated volatile analysis, one for haloacetamide analysis, and one backup), and two GC vials with each calibration (since you will have separate halogenated volatile and haloacetamides calibrations – need one for analysis and one backup). Use GC vial inserts. Store in the laboratory freezer at -15°C in a tray covered in aluminum foil if not analyzed immediately. Also fill two autosampler vials with MtBE and 2 vials of extracting solvent containing MtBE + IS. Analyze within 4 weeks.
11. Analyze according to specified GC method (see GC temperature programs below) on the designated GC.

Quality Control

- Precision is measured as the average and relative percent difference (RPD) of the duplicate analyses of each sample. RPD should be less than 10% otherwise sample has to be flagged as suspect. The coefficient of variation of all the internal standard responses for the complete set of samples must be less than 15%. Individual samples responsible for elevating this value above the threshold should be flagged and considered suspect.
- A calibration check standard is prepared in the mid-range of the standard calibration curve and is injected every 10 samples. If the detector response for this sample varies more than 10% from the previous injection, all samples analyzed between the two injections are flagged for investigation.
- Each sample bottle set should be accompanied by replicate field and travel blanks.

GC-ECD analysis on Hewlett-Packard GC5890 Series II:

Syringe size = 10 μ L; Injection volume = 2 μ L

Wash solvent = MtBE

Pre-injection washes = 3; Post-injection washes = 3; Pumps = 3

Injector Temperature = 200°C; Injection splitless (split after 0.5 min)

Oven equilibration time = 3 min; Oven max °C = 300°C

Gas = He; Column flow = 1 mL/min

Column type = ZB1 (Agilent), 30.0 m length, 0.25 mm inner diameter, 1 μ m film thickness

Split flow = 1 mL/min; Split ratio = 1:1

Halogenated Volatiles Oven Temperature program (Total time = 55.75 min)

	°C/min	Temperature (°C)	Time (min)
Initial	-	35	22
Level 1	10	145	2
Level 2	20	225	10
Level 3	20	260	5

Detector temperature = 290°C, Injector temp: 117°C

Haloacetamides Oven Temperature program (Total time = 59.60 min)

	°C/min	Temperature (°C)	Time (min)
Initial	-	37	1
Level 1	5	110	10
Level 2	5	280	0

Detector temperature = 300°C, Injector temp: 200°C

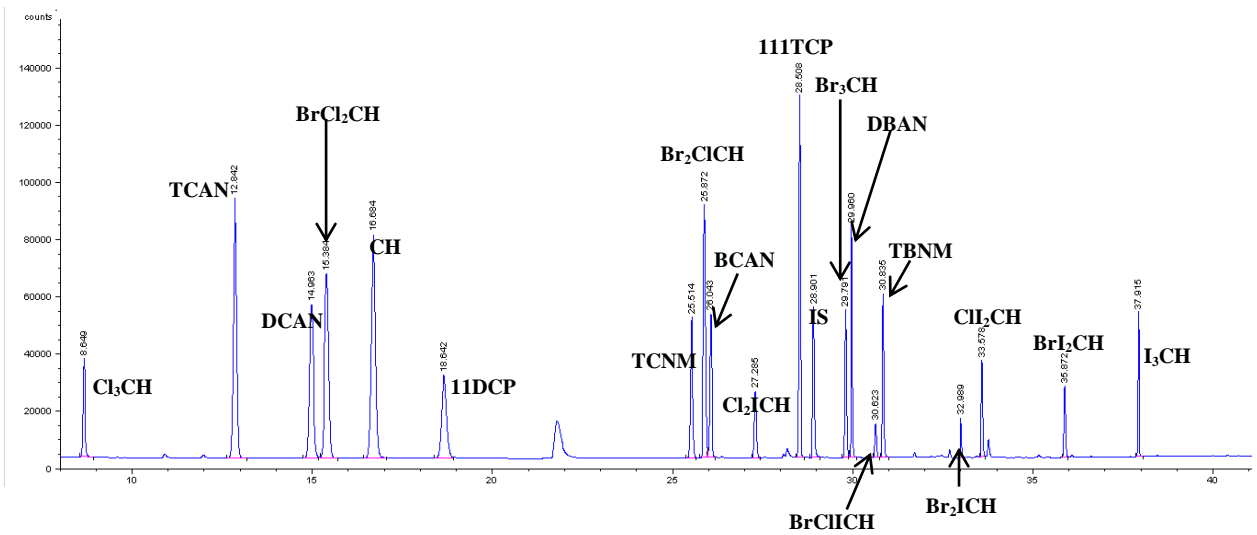


Figure A5-1. Chromatogram of halogenated volatile species for a 100 µg/L calibration point.

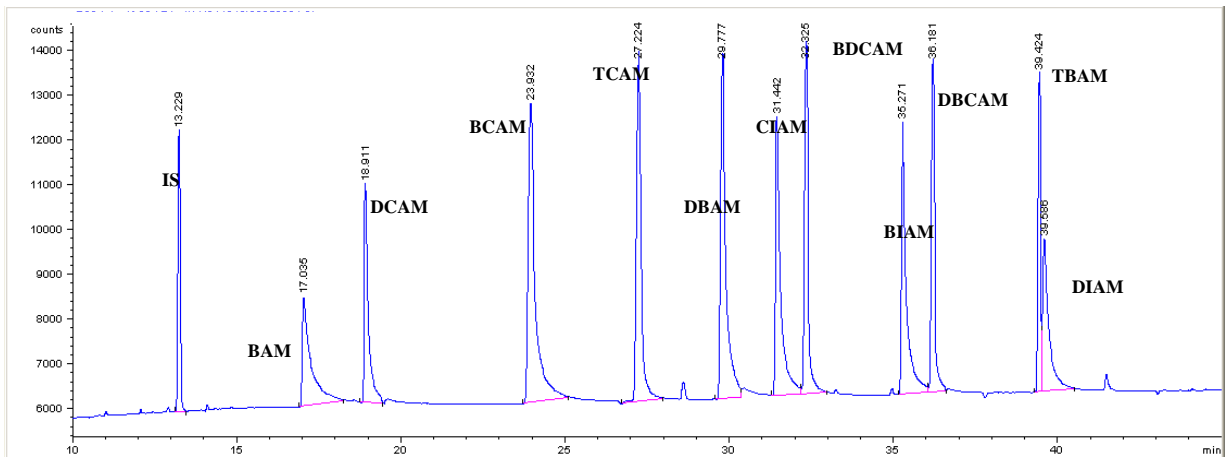


Figure A5-2. Chromatogram of haloacetamide species for a 200 µg/L calibration point.

5.B Cyanogen Chloride Extraction SOP

Prepared by: Bonnie Lyon

Materials

Equipment

- Clear 60 mL clean glass screw cap sample vials with PTFE-lined silicone septa
- 10-50 μ L and 50-250 μ L micropipetter and glass capillary tips
- 100 mL and 10 mL volumetric flasks with glass stoppers, 2 mL volumetric flask with screw cap and PTFE-lined silicone septa
- 50 mL graduated cylinder
- 1-L amber bottle mounted with 10 mL pump pipetting dispenser
- 23 cm disposable glass Pasteur pipettes and rubber bulb
- pH indicator strips pH 0-6: colorpHast (Fisher Scientific, catalog # 9586, ThermoFisher Scientific, Waltham, MA, USA).
- 1.8 mL amber glass autosampler vials with rubber/PTFE aluminum seals
- Hand crimper for sealing autosampler vials
- Vortexer
- Teflon tape
- Stainless steel scupula

Instrumentation

Gas Chromatograph

- Hewlett-Packard 6890 Series GC with autosampler/autoinjector tower and electron capture detector (ECD)
- Column: Zebron ZB-1701 (Phenomenex, Torrance, CA, USA)
- Data System: Hewlett Packard ChemStation

GC Gases

- Carrier Gas-Ultra High Purity helium (National Welders catalog #325042, Morrisville, NC, USA)
- Makeup Gas-Ultra High Purity nitrogen (National Welders catalog #475041)

GC Supplies

- 11-mm diameter Thermolite septa (Restek catalog #27142, Bellafonte, PA, USA)
- Split/splitless injector liner sleeve with deactivated glass wool, 4 mm inner diameter (Restek catalog #439542)
- Graphite/vespel 0.5 mm ferrules (Chromatography Research Supplies catalog #213164, Louisville, KY, USA)
- 10 μ L tapered needle syringe (Hamilton catalog #80390, Reno, NV, USA)

Reagents

- Laboratory grade water (LGW), purified using a secondary water purification system (Dracor Water Systems, Durham, NC, USA). Water pretreated with an general in-house purification system was pre-filtered (1 μm filter), treated to remove chlorine or chloramine residuals, passed through an activated carbon cartridge to reduce the total organic carbon content to less than 0.2 mg/L and passed through mixed-bed ion exchange resins to reduce the ion content to less than 18 M Ω .
- Cyanogen chloride stock standard 2000 $\mu\text{g}/\text{mL}$ SPEX CertiPrep (Metuchen, NJ, USA)
- Internal Standard (IS): 1,2-dibromopropane neat standard, 99+%, (Aldrich catalog #14,096-1, Sigma Chemical Co., St. Louis, MO, USA)
- Sodium sulfate, granular ACS grade (Mallinckrodt, catalog #8024, St. Louis, MO, USA) baked at 400° for 24 hours, stored in dessicator
- Extraction solvent: OmniSolv Methyl-t-Butyl Ether (Fisher catalog #MX08266)
- Solvent for dilution of standards and working solutions: Purge & Trap grade methanol (Sigma catalog # 414816)
- HPLC grade methanol (for rinsing glassware)
- L-ascorbic acid (for quenching residuals) Certified ACS grade (Sigma catalog #A5960)
- Sulfuric acid (for pH adjustment) Certified ACS Plus (Fisher catalog #A300-212)

Procedure

Internal Standard – 1,2 dibromopropane

Stock solution of IS at $\sim 2000 \mu\text{g}/\text{mL}$ in MtBE – prepared by injecting 10 μL of neat standard into a 5 mL volumetric flask containing 5 mL MtBE.

Primary dilution at 100 $\mu\text{g}/\text{mL}$: prepared by injecting 250 μL of IS stock solution using a micropipette, into a 5 mL volumetric flask containing 5 mL of MtBE.

Extracting Solution at 100 $\mu\text{g}/\text{L}$ in MtBE. Volume depends on number of samples (4 mL x # samples, be sure to make extra, as some will be used to clear bubbles in dispensing line)

Sample collection

Collect samples in 60-mL glass vials with PTFE-lined septa and screw caps, containing ascorbic acid for quenching. The amount of ascorbic acid will depend on expected chlorine residual – the stoichiometric ratio is 2.48 mg ascorbic acid/mg Cl_2 , and a safety factor of 2 is typically used. Use 1M sulfuric acid to adjust the sample pH to 2-3 to stabilize cyanogen chloride. Fill vials headspace-free and store at 4°C until analysis.

Working Solutions

Prepare one or two intermediate concentrations in high-purity methanol from the 2000 $\mu\text{g}/\text{mL}$ stock solutions in order to make calibrations.

Calibration Standards

Prepare a range of calibrations based on levels expected in samples. Working solutions and calibration standards are kept on ice at all times when not being used.

Extraction procedure

***Samples and Calibrations must be kept on ice during extraction procedure. CNCl and CNBr have very low boiling points and can be volatilized easily. ***

1. Measure out 30 mL of each calibration and sample to using a graduated cylinder and tilting the cylinder to prevent volatilization.
2. Adjust the pH of all standards to pH 2-2.5 pH using 2 drops of 1M sulfuric acid (amount may vary for different types of samples, so test with pH strips)
3. Add 4 mL of MtBE with IS extracting solution via pump dispenser to each vial.
4. Add ~10 g of baked sodium sulfate, cap, and vortex for one minute.
5. Transfer the organic layer via disposable Pasteur pipette to 2 mL amber autosampler vials. Use two autosampler vials per sample for backup. Store in freezer until ready for analysis.

GC-ECD analysis on Hewlett-Packard GC6890:

Injector:

Syringe size = 10 μ L; Injection volume = 1 μ L

Wash solvent = MtBE; Pre-injection washes = 3; Post-injection washes = 3; Pumps = 3

Injector Temperature = 120°C; Splitless injection

Oven equilibration time = 3 min; Oven max °C = 300°C

Gas = He; Flow column = 1mL/min; Column Pressure= 11.3 psi

Column type = 1701 (Zebron), 30.0m length, 0.25mm diameter, 1.0 μ m film thickness

CNX Oven Temperature program (Total time = 38.5 min)

	°C/min	Temp. (°C)	Time (min)
Initial	-	35	9
Level 1	10	200	10

Detector temperature = 300°C

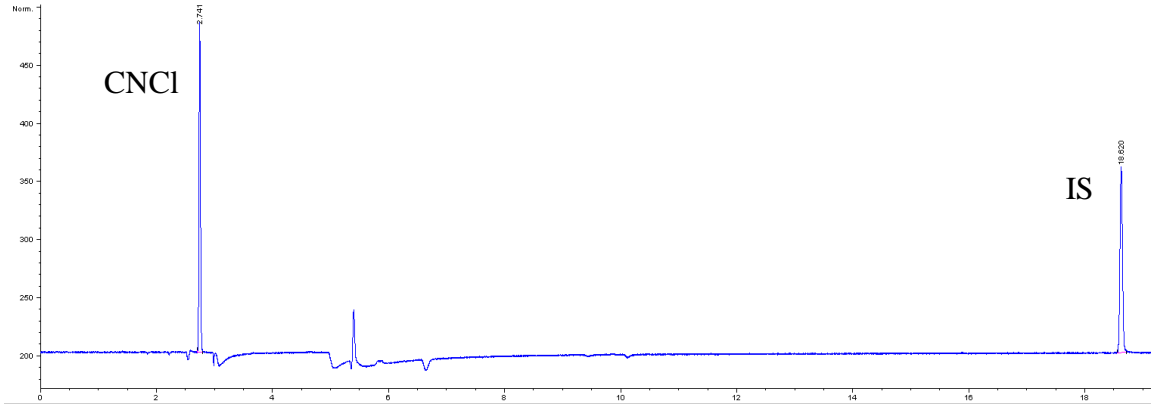


Figure A5-3. Cyanogen chloride chromatogram for a 100 µg/L calibration point.

5.C Haloacetic Acids Extraction SOP

Prepared by: Jennifer Chu

Adapted from EPA Method 552.2

Materials

- Several clear 40 mL glass vials with open-top screw caps and Teflon-lined septa
- 10-50 μL micropipetter with clean glass capillary tips
- 50-250 μL micropipetter with clean glass capillary tips
- 23-cm disposable glass Pasteur pipettes
- Rubber Pasteur pipette bulb
- 25 mL, 100 mL, 2 mL volumetric flasks with glass stoppers
- 25 mL glass graduated cylinder
- 10 mL glass beaker
- 1 L glass bottle with 10 mL pump pipetting dispenser containing PTFE transfer line
- 500 mL amber bottle mounted with 5 mL pump pipetting dispenser containing PTFE transfer line
- 5 mL amber glass standard storage vials with open top screw caps and PTFE-lined septa
- 1.8 mL glass GC autosampler vials with PTFE aluminum seals
- Hand crimper for sealing GC autosampler vials
- Thermolyne Type 16700 Mixer-MaxiMix I vortexer
- 1/2-inch Teflon tape
- Stainless steel scupula
- Plastic tub for ice bath

Reagents

- Laboratory Grade Water (LGW)
- Extraction solvent & standard solvent: OmniSolv Methyl-t-butyl ether (EMD Chemicals, Fisher catalog #MX08266, ThermoFisher Scientific, Waltham, MA, USA)
- Sodium sulfate (Na_2SO_4), granular ACS grade (Mallinckrodt, catalog #8024, St. Louis, MO, USA) Bake at 400°C in muffle furnace for 24 hours in a shallow, porcelain dish covered with aluminum foil. Store in desiccator.
- Sulfuric acid (H_2SO_4), concentrated ACS grade, for pH adjustment (Fisher catalog #A300-212)
- Anhydrous magnesium sulfate (MgSO_4), 99+%, (Acros Organics catalog #423905000, ThermoFisher Scientific)
- Silicic Acid ($\text{SiO}_2 \cdot n\text{H}_2\text{O}$), (JT Baker catalog #0324-01, Phillipsburg, NJ, USA)
- HPLC grade methanol (for rinsing glassware)
- Preservation agent/biocide: sodium azide (NaN_3), 99.99+% (Acros Organics, catalog #19038) Prepared as preservation agent at 80 mg/L by adding 400 mg solid NaN_3 to a 5 mL volumetric flask containing just under 5mL of LGW. Fill flask to 5 mL mark, invert 3 times. Transfer solution to 40mL amber vial, capped

with an open top screw cap and PTFE-lined septa. Seal cap with Teflon tape and store in lab refrigerator. This solution should be prepared every 3 months.

- Quenching agent: ammonium sulfate ((NH₄)₂SO₄), ACS grade, granular (Mallinckrodt catalog #3512, St. Louis, MO, USA)

Stock Standards

Stock standards are purchased as premixed certified solutions contained in sealed amber glass ampules. Once the glass 1 mL sealed ampule of stock solution is opened, the solution is immediately transferred to a 5 mL amber vial with a PTFE-lined screw cap. The vial should be immediately capped with the cap and neck of vial wrapped with Teflon tape. The vial should be stored in laboratory standards freezer at -15°C.

Standards should be monitored frequently for degradation by comparing standard area values to the initial calibration of the standard. Fresh standards should be prepared if this check exceeds a 20% drift. Stock standards should not be used more than 6 months after opening of sealed ampule.

- EPA 552.2 Acids Calibration Mix, (Supelco catalog #4-7787, Sigma Chemical Co., St. Louis, MO, USA)

Stock standards should be stored in 5 mL amber vials fitted with screw cap and PTFE-lined silicone septa in freezer with screw caps sealed with Teflon tape for a maximum of 3 months or until significant degradation or contamination occurs.

- Internal Standard (IS): 1,2-dibromopropane neat standard, 99+%, (Aldrich catalog #14,096-1, Sigma Chemical Co., St. Louis, MO, USA)
- Haloester Standard Stock Solution: EPA 552.2 Esters Calibration Mix at 200-2000 µg/mL in MtBE (Supelco catalog #4-7788)
- Acid Surrogate Stock Standard: 2,3-dibromopropionic acid, 99+% at 1 mg/mL in MtBE, (Supelco catalog#4-7789)

Daily working standards: primary calibration standards

- 1) HAA Standard Primary Dilution prepare at 20 µg/mL.
 - a. In the EPA 552.2 Acids Calibration Mix, each of the nine HAAs is present at a different concentration. Make this standard by tracking one of the HAA species. The following steps are written for tracking ClAA at a concentration of 600 µg/mL.
 - b. Fill a 2mL volumetric flask to just below the 2 mL mark with MtBE.
 - c. With a micropipetter, inject 67 µL of the EPA 552.2 Acids Calibration Mix into the volumetric flask. Make sure that it is injected below the MtBE surface.
 - d. Fill the flask to the 2 mL mark with MtBE. Cap the flask and invert three times.
 - e. Transfer this standard to a 5 mL amber vial with an open top screw cap lined with PTFE silicone septa. Seal cap with Teflon tape. Label and store in lab freezer at -15°C.

*Primary dilutions of HAA working standards should be routinely monitored for significant degradation by comparing standard area values to the initial

calibration of the standard. Fresh standards should be prepared if this check exceeds a 20% drift.

- 2) Internal standard primary dilution prepare at 2000 $\mu\text{g/mL}$
 - a. Weigh out 10 mg of 1,2-dibromopropane neat standard.
 - b. Inject with micropipetter into a 5 mL volumetric flask containing 5 mL of MtBE. Fill to the line with MtBE, cap, and invert 3 times.
 - c. Transfer immediately to 5 mL amber vial capped with open top screw caps lined with PTFE septa. Seal caps with Teflon tape. Label and store vial in lab freezer at -15°C .

- 3) MtBE and internal standard extraction solution prepare at approximately 50 $\mu\text{g/L}$
 - a. Using a micropipetter, directly inject 250 μL of internal standard secondary dilution standard (100 $\mu\text{g/mL}$) into a 500 mL volumetric flask containing just under 500 mL of MtBE. Standard should be directly injected into the MtBE
 - b. Fill volumetric flask to the 500 mL mark with MtBE. Cap and invert 3 times.
 - c. Transfer this standard solution and store it in 1 L amber bottle with PTFE pipetting dispenser screw top assembly.
 - d. Store in lab refrigerator at 4°C .

The volume of MtBE + IS extraction solution will vary based on the number of samples to be extracted. Each sample requires 4 mL, prepare extra so that you do not run out.

- 4) Multicomponent haloester reference standard prepare at 50 $\mu\text{g/L}$ – 500 $\mu\text{g/L}$
 - a. Fill a 10 mL glass volumetric flask with MtBE to the neck of the flask just under the 10 mL mark.
 - b. Using a micropipetter, inject 250 μL of haloester standard stock solution (200-2000 $\mu\text{g/mL}$) into MtBE.
 - c. Add MtBE to 10 mL fill line. Cap flask and invert 3 times.
 - d. Transfer this standard to a 20 mL amber vial with open top screw cap and PTFE-lined silicon septa. Seal cap with Teflon tape.
 - e. Label vial and store in lab freezer at -15°C .

- 5) Acid surrogate additive standard prepare at 20 $\mu\text{g/mL}$
 - a. Add 100 μL of 1 mg/mL acid surrogate stock standard to a 5 mL volumetric flask containing MtBE filled just under the 5 mL mark on the neck of the flask.
 - b. Fill to the 5 mL mark with MtBE. Cap and invert 3 times.
 - c. Transfer this standard to 5 mL amber vial with open top screw cap and PTFE-lined silicone septa. Seal cap with Teflon tape.
 - d. Label vial and store in lab freezer -15°C .

- 6) EPA 552.2 acids calibration mix (HAA9) matrix spike standard (MS)

- a. In the Supelco EPA 552.2 Acids Calibration Mix, each of the nine HAAs is present at a different concentration. Make this standard by tracking the HAA with the least concentration. The following steps are written for tracking ClAA at a concentration of 600 µg/mL. The final concentration of this dilution is 6 µg/mL of ClAA.*
 - b. Add 20µL of the Supelco EPA 552.2 Acids Calibration Mix to a 2mL volumetric flask filled with MtBE. Be sure to inject beneath the MtBE layer.
 - c. Fill to the 2mL mark with MtBE. Cap flask and invert 3 times.
 - d. Transfer this standard to a 5mL amber vial with an open top screw cap lined with PTFE silicone septa.
 - e. Seal cap with Teflon tape. Label and store in lab freezer at -15°C.
- *The final concentration of this solution should be around 10-20 µg/mL.

Instrumentation

- 1) Gas Chromatograph (GC)
 - a. Hewlett-Packard 5890 with electron capture detector (ECD)
 - b. Capillary Column ZB-1 (Zebron, Phenomenex) 30 m length x 0.30 mm inner diameter, 1.0 µm film thickness, or equivalent
 - c. Data System: Hewlett-Packard ChemStation
- 2) GC Gases
 - a. Carrier Gas-Ultra High Purity helium (National Welders catalog #325042, Morrisville, NC, USA)
 - b. Makeup Gas-Ultra High Purity nitrogen (National Welders catalog #475041)
- 3) Miscellaneous GC Equipment
 - a. 11-mm diameter Thermolite septa (Restek catalog #27142, Bellafonte, PA, USA)
 - b. Split/splitless injector liner sleeve with deactivated glass wool, 4 mm inner diameter (Restek catalog #439542)
 - c. Graphite/vespel 0.5 mm ferrules (Chromatography Research Supplies catalog #213164, Louisville, KY, USA)
 - d. 10 µL tapered needle syringe (Hamilton catalog #80390, Reno, NV, USA)

Samples

Samples should be collected in pre-cleaned 40 mL glass vials with open top screw caps and PTFE-lined silicone septa. Pre-preserve vials in the lab before collecting samples by pipetting 50 µL of the 80 mg/L sodium azide solution directly into the vial and adding approximately 20 mg (8 grains) of ammonium sulfate. Cap and label all vials properly. Samples should be extracted within 14 days from date of collection.

Test Mixes: Preparation & Procedure

- 1) Prepare a dilution of MtBE + IS stock solution in a 25 mL volumetric flask.
- 2) Add a dilution of MtBE stock solution to a small GC vial. Cap and label the vial.

- 3) Add the MtBE + IS from step 1 to a small GC vial. Cap and label the vial.
- 4) Add a dilution of HAA9 ester mix to a third GC vial. Cap and label the vial.
- 5) Run all three vials on a GC prior to extracting samples to ensure the purity and cleanliness of these reagents.
- 6) If these reagents are clean and the GC is functioning properly, extract samples within three weeks of the date the samples were collected.
- 7) GC data should be removed from the GC computers within one month.

Calibration Standards

- 1) Prepare all standards in 100 mL of LGW.
- 2) Label 6 separate 100 mL volumetric flasks with the concentrations to be prepared. The lowest concentration should not be below 0.1 µg/L.
- 3) Fill each 100 mL volumetric flask with LGW to just below the fill line on the neck of the flask.
- 4) With an appropriate micropipetter that uses glass capillary tips, put a measured amount of the primary calibration standard directly into LGW below the surface. The amount of primary calibration standard will vary depending on the desired concentration of the secondary calibration standards.
- 5) Fill the volumetric flask to the fill line with LGW, cap the flask, and invert three times.
- 6) Two blanks should be prepared by filling two 40 mL clear glass vials with 20 mL LGW.
 - a. Measure 20 mL LGW with a clean glass 25 mL graduated cylinder.
 - b. Label, then cap vials using open top screw caps with PTFE-lined septa.
- 7) Rinse the 25 mL graduated cylinder three times with LGW.
- 8) Using the cleaned 25 mL graduated cylinder, transfer 20 mL of the secondary calibration standards in the 100 mL volumetric flasks to 40 mL glass vials. Again, these glass vials are capped with open top screw caps and PTFE-lined septa.
 - a. Make duplicates of these 20 mL secondary calibration standards.
 - b. Make sure the vials are labeled accordingly.

Matrix Spike Addition

- 1) Matrix spike (MS) and matrix spike duplicate (MSD) samples should be prepared. These samples should be chosen randomly from the duplicates of collected samples. One set of MS and MSD samples should be prepared for each analytical batch.
- 2) Add 25 µL of the HAA9 Matrix Spike Standard to a 25 mL of the matrix spike sample.
- 3) Make a duplicate 25 mL aliquot of sample.
- 4) Measure 20mL using a graduated cylinder for each spike solution into a clean 40mL glass vial. Label each standard as a MS or a MSD.

Sample Preparation

- 1) Remove samples (stored in 40 mL glass vials) from refrigerator and let them warm to room temperature while preparing calibration standards.
- 2) Use a clean 25 mL glass graduated cylinder to measure out 20 mL of each sample.

- 3) Dispose remaining amount of sample into a waste beaker.
- 4) Pour the measured 20 mL sample back into its 40 mL glass vial. Pour samples on the side of the glass (graduated cylinder or vials) to reduce the samples' interaction with air.
- 5) Between measurements, rinse graduated cylinder 3 times with LGW. Pre-rinse graduated cylinder one time with the next sample to be transferred.

NOTE: Wash all used glassware 3 times with LGW and once with methanol.

Acid Surrogate Addition

- 1) Add 20 μL of the acid surrogate additive standard at 20 $\mu\text{L}/\text{mL}$ to all 20 mL calibration standards, samples, and matrix spike samples using a micropipetter.
- 2) Stir in the surrogate with the pipetter tip. Do NOT cap and invert samples. Change pipette tip between samples.

Acidification

- 1) Using a glass pipette, add 1.5 mL of concentrated sulfuric acid (H_2SO_4) to all 20mL of calibration standards, samples, and matrix spike samples.
- 2) Let vials cool in an ice bath for 20-30 min.
- 3) Swirl these vials gently to mix water and acid.

Internal Standard Addition

- 1) Using a pump pipette dispenser, add 4 mL of MtBE + IS to each 20 mL sample and calibration standard.
- 2) When using the pump pipette dispenser, make sure there are no bubbles in the addition line.
- 3) Two layers will be visible: an organic top layer of MtBE and an aqueous bottom layer.

Sodium Sulfate Addition and Extraction

- 1) Add about 10 g of baked sodium sulfate to each sample and calibration standard. This mass is measured out in a pre-measured glass beaker especially for this step.
- 2) Immediately after adding sodium sulfate, vortex all samples and calibration standards for 1 minute to prevent solidification of sodium sulfate.

Solvent Transfer to 2mL Volumetric Flasks

- 1) For each sample and calibration standard: With a clean, glass, 23 cm Pasteur pipette, transfer 2 mL of the top layer (MtBE + IS layer) to a clear, glass 2 mL volumetric flask capped with screw caps and PTFE-lined septa.
- 2) Use a clean pipette for each transfer. Be sure not to transfer any water and sodium sulfate crystals.

Derivatization

To all MtBE extracts in 2 mL volumetric flasks:

- 1) Add 1/2 of a small, rounded scoop of anhydrous powdered magnesium sulfate. Re-cap the flask. DO NOT MIX!

- 2) Add 225 μL cold diazomethane with a micropipette. Re-cap the flask and DO NOT MIX!
- 3) Store these flasks in the refrigerator for 15 minutes.
- 4) Check for a yellow color in all samples. Note the samples that are not yellow in color.
- 5) Allow samples to warm to room temperature (about 15 minutes).
- 6) Add a small rounded scoop of silicic acid n-hydrate powder. The extract should become colorless because silicic acid quenches residual diazomethane.
- 7) Remove enough of the extracts from the 2 mL volumetric flasks to fill GC vials about 70% full. Make sure no solids are in the vials, and then cap the vials.
- 8) Label each vial with the sample location and date.
- 9) Place these samples in a tray and wrap them in aluminum foil.
- 10) Label foil with name, date, and test. Store in the freezer before GC analysis.

GC-ECD analysis on Hewlett-Packard GC-ECD 5890:

Injector:

Syringe size = 10 μL ; Injection volume = 1 μL

Wash solvent = MtBE; Pre-injection washes = 3; Post-injection washes = 3; Pumps = 3

Injector Temperature = 180°C; Splitless injection

Oven equilibration time = 3 min; Oven max °C = 300°C

Gas = He; Flow column = 1 mL/min; Column Pressure= 11.3 psi

Column type = ZB-1, 30.0 m length, 0.25 mm diameter, 1.0 μm film thickness

Oven Temperature program (total time = 52.5 min)

	°C/min	Temp. (°C)	Time (min)
Initial	-	37	21
Level 1	5	136	3
Level 2	20	250	3

Detector temperature = 300°C

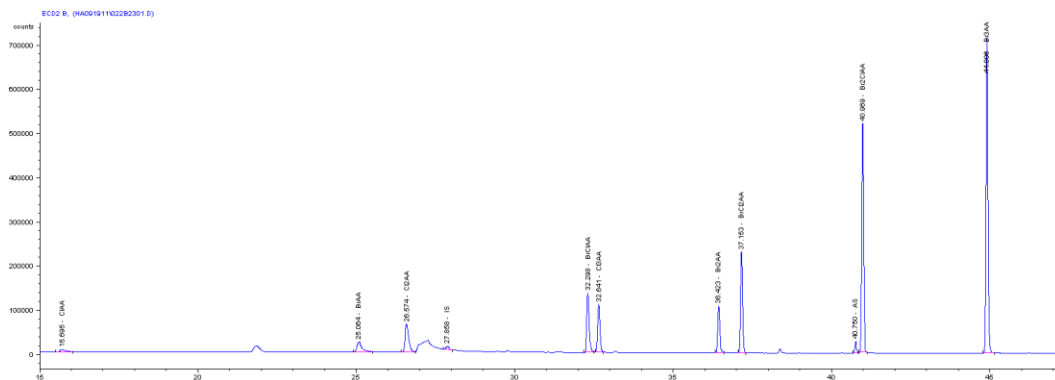


Figure A5-4. Haloacetic acid chromatogram for 500 $\mu\text{g/L}$ (as Br_3AA) calibration point.

Appendix 6: Supplemental Information for Chapter 4

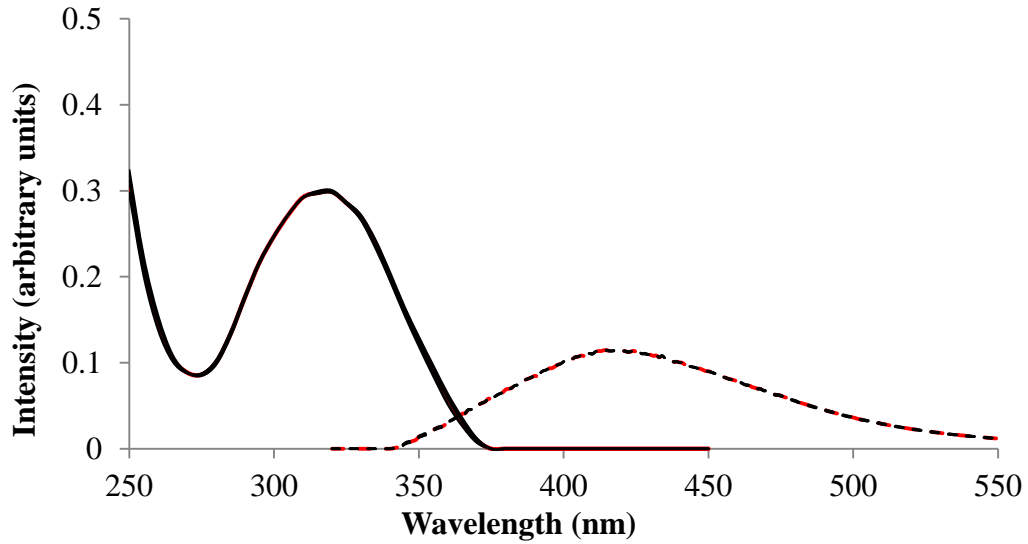


Figure A6-1. Component 1 excitation (solid line) and emission (dashed line) spectra of four validation splits compared to modeled component. Modeled spectra are shown by thicker red line, while splits are shown by thinner black lines.

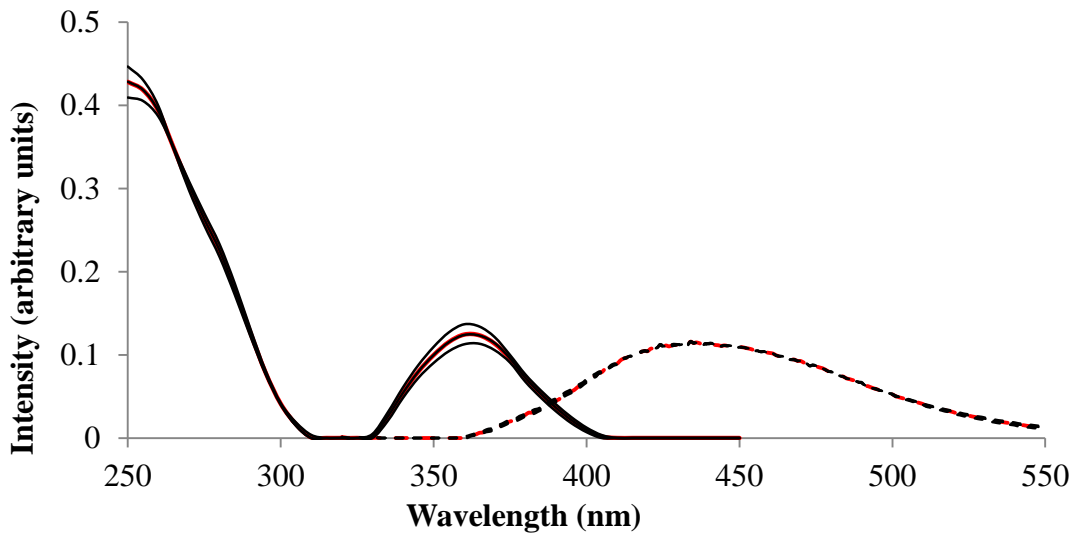


Figure A6-2. Component 2 excitation (solid line) and emission (dashed line) spectra of four validation splits compared to modeled component. Modeled spectra are shown by thicker red line, while splits are shown by thinner black lines.

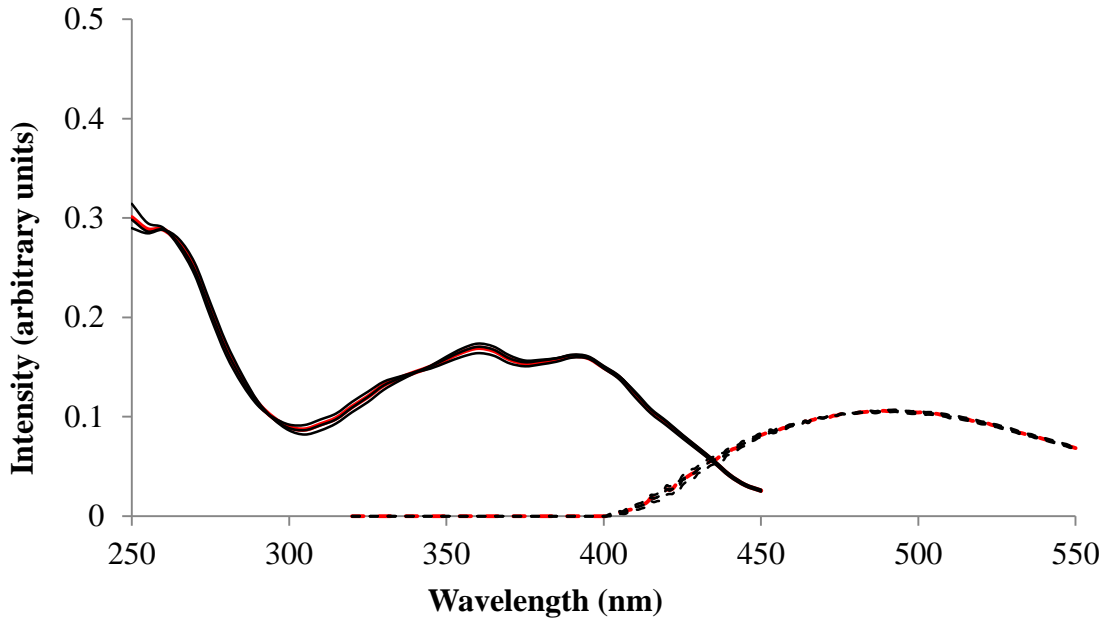


Figure A6-3. Component 3 excitation (solid line) and emission (dashed line) spectra of four validation splits compared to modeled component. Modeled spectra are shown by thicker red line, while splits are shown by thinner black lines.

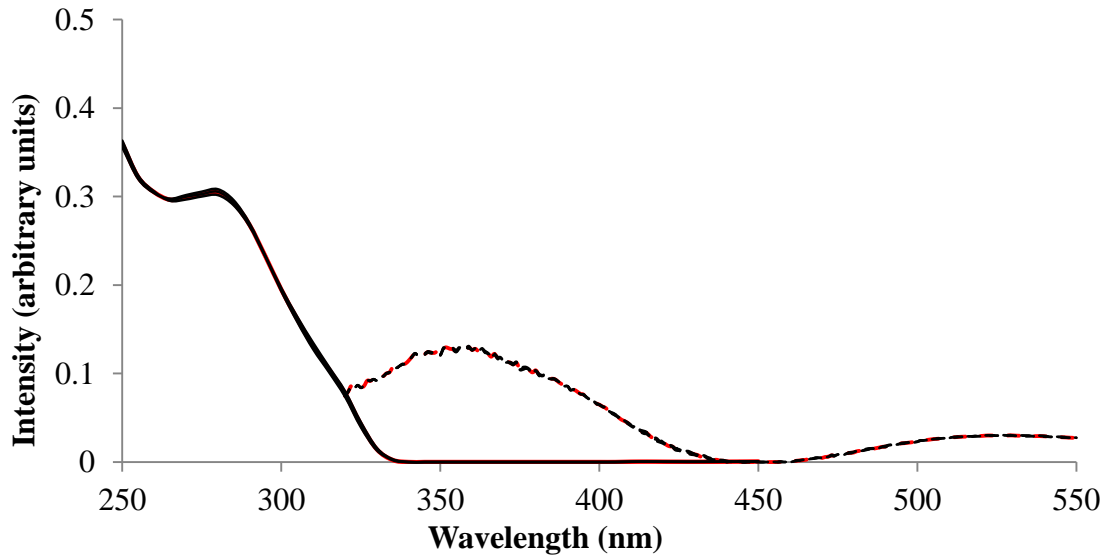


Figure A6-4. Component 4 excitation (solid line) and emission (dashed line) spectra of four validation splits compared to modeled component. Modeled spectra are shown by thicker red line, while splits are shown by thinner black lines.

Table A6-1. Effect of MP UV (dose is in mJ/cm²) followed by chlorination on the formation of halogenated volatiles in ambient and spiked samples. Values shown are averages between experimental duplicates in µg/L. TCAN and iodo-THMs were below detection limit (<0.1 µg/L) in all samples. Halogenated volatile abbreviations are defined in Appendix 5A.

spiking	treatment	Cl ₃ CH	DCAN	BrCl ₂ Cl	CH	11DCP	TCNM	Br ₂ ClCH	BCAN	111TCP	Br ₃ CH	DBAN	TBNM	ΣTHM4
ambient	HOCI alone	66.9	2.8	12.9	7.8	0.2	0.2	2.3	1.2	1.9	0.2	0.2	<0.1	82.2
	MP 40 + HOCl	69.0	2.9	13.0	9.8	0.2	0.2	2.3	1.1	2.2	0.2	0.2	<0.1	84.4
	MP 186 + HOCl	73.5	3.0	13.1	14.9	0.2	0.3	2.3	1.1	2.8	0.2	0.2	<0.1	89.1
	MP 1000 + HOCl	94.4	3.3	14.4	32.0	0.3	0.5	2.3	1.1	4.7	0.2	0.2	<0.1	111
NO ₃ ⁻ spiked (10 mg N/L)	HOCI alone	65.4	2.9	12.7	8.1	0.2	0.2	2.3	1.2	2.1	0.2	0.2	<0.1	80.6
	MP 40 + HOCl	69.4	2.9	12.9	11.1	0.2	1.3	2.2	1.1	2.5	0.2	0.2	0.2	84.7
	MP 186 + HOCl	79.4	2.9	13.1	17.9	0.2	4.0	2.0	1.0	3.4	0.2	0.1	0.3	94.7
	MP 1000 + HOCl	93.5	2.9	13.6	31.5	0.3	8.0	2.0	1.0	5.5	0.1	0.1	0.6	109
Br ⁻ spiked (1 mg/L)	HOCI alone	5.5	0.4	16.6	0.5	<0.1	<0.1	51.2	2.6	0.2	71.1	9.5	1.6	144
	MP 40 + HOCl	5.1	0.4	16.0	0.6	<0.1	<0.1	52.8	2.7	0.2	74.5	9.7	2.2	148
	MP 186 + HOCl	5.1	0.4	16.8	0.7	<0.1	<0.1	58.8	2.9	0.3	78.3	9.4	4.2	159
	MP 1000 + HOCl	5.5	0.5	21.0	1.2	<0.1	<0.1	76.1	2.7	0.3	84.7	8.3	10.0	187
Br ⁻ + NO ₃ ⁻ spiked (10 mg N/L + 1 mg Br/L)	HOCI alone	4.9	0.4	15.6	0.5	<0.1	<0.1	52.1	2.6	0.2	75.0	10.0	1.6	148
	MP 40 + HOCl	4.4	0.4	15.2	0.6	<0.1	<0.1	55.9	2.9	0.2	77.4	10.1	9.8	153
	MP 186 + HOCl	3.7	0.4	16.2	0.6	<0.1	<0.1	66.0	3.0	0.2	84.0	9.9	24.4	170
	MP 1000 + HOCl	2.9	0.4	18.2	1.0	<0.1	<0.1	81.0	3.1	0.2	91.4	9.3	39.6	193

Table A6-2. Effect of MP UV (dose is in mJ/cm²) followed by chloramination on the formation of halogenated volatiles in ambient and spiked samples. Values shown are averages between experimental duplicates in µg/L. TCAN, 111TCP, and iodo-THMs were below detection limit (<0.1 µg/L) in all samples.

Spiking	treatment	Cl ₃ CH	DCAN	BrCl ₂ CH	CH	11DCP	TCNM	Br ₂ ClCH	BCAN	Br ₃ CH	DBAN	TBNM	THM4
ambient	NH ₂ Cl alone	0.8	0.2	0.1	0.2	1.0	<0.1	<0.1	<0.1	<0.1	<0.1	0.1	1.0
	MP 40 + NH ₂ Cl	0.9	0.2	0.1	0.2	1.2	<0.1	<0.1	<0.1	<0.1	<0.1	0.2	1.0
	MP 186 + NH ₂ Cl	0.9	0.2	0.1	0.2	1.6	<0.1	<0.1	<0.1	<0.1	<0.1	0.2	1.0
	MP 1000 + NH ₂ Cl	0.7	0.3	0.1	0.2	2.7	<0.1	<0.1	<0.1	<0.1	<0.1	0.1	0.8
NO ₃ ⁻ spiked (10 mg N/L)	NH ₂ Cl alone	0.9	0.2	0.1	<0.1	1.1	<0.1	<0.1	<0.1	<0.1	<0.1	0.1	1.0
	MP 40 + NH ₂ Cl	0.8	0.2	0.1	<0.1	1.2	0.2	<0.1	<0.1	<0.1	<0.1	0.1	1.0
	MP 186 + NH ₂ Cl	0.7	0.3	0.1	<0.1	1.8	0.5	<0.1	0.1	<0.1	<0.1	0.1	0.9
	MP 1000 + NH ₂ Cl	0.4	0.3	0.1	<0.1	2.2	0.8	<0.1	0.1	<0.1	<0.1	0.2	0.6
Br ⁻ spiked (1 mg/L)	NH ₂ Cl alone	0.7	0.2	0.4	0.3	0.7	<0.1	0.2	0.2	<0.1	<0.1	0.2	1.3
	MP 40 + NH ₂ Cl	0.7	0.2	0.4	0.3	0.9	<0.1	0.2	0.2	<0.1	<0.1	0.2	1.3
	MP 186 + NH ₂ Cl	0.7	0.2	0.3	0.3	1.2	<0.1	0.2	0.2	<0.1	<0.1	0.2	1.1
	MP 1000 + NH ₂ Cl	0.4	0.2	0.2	0.4	1.8	<0.1	0.1	0.2	<0.1	<0.1	0.2	0.8
Br ⁻ + NO ₃ ⁻ spiked (10 mg N/L + 1 mg Br/L)	NH ₂ Cl alone	0.7	0.2	0.4	<0.1	0.7	<0.1	0.2	0.2	<0.1	<0.1	0.2	1.3
	MP 40 + NH ₂ Cl	0.5	0.2	0.5	<0.1	0.7	0.1	0.3	0.2	<0.1	<0.1	0.6	1.3
	MP 186 + NH ₂ Cl	0.4	0.2	0.6	<0.1	0.8	0.3	0.4	0.3	0.3	0.1	2.3	1.6
	MP 1000 + NH ₂ Cl	0.4	0.2	0.6	<0.1	0.6	0.1	0.7	0.4	1.0	0.3	6.3	2.7

Table A6-3. Nitrate concentration and nitrite formation (mg N/L) from MP UV irradiation of ambient and spiked samples.

spiking	treatment	nitrate*	nitrite
ambient	No UV	<0.02	<0.02
	MP 40 mJ/cm ²	<0.02	<0.02
	MP 186 mJ/cm ²	<0.02	<0.02
	MP 1000 mJ/cm ²	<0.02	<0.02
NO ₃ ⁻ spiked (10 mg N/L)	No UV	9.1	<0.02
	MP 40 mJ/cm ²	9.2	0.03
	MP 186 mJ/cm ²	9.1	0.10
	MP 1000 mJ/cm ²	8.7	0.35
Br ⁻ spiked (1 mg/L)	No UV	0.04	<0.02
	MP 40 mJ/cm ²	0.04	<0.02
	MP 186 mJ/cm ²	0.04	<0.02
	MP 1000 mJ/cm ²	0.02	0.03
Br ⁻ + NO ₃ ⁻ spiked (10 mg N/L + 1 mg Br/L)	No UV	9.5	<0.02
	MP 40 mJ/cm ²	9.4	0.03
	MP 186 mJ/cm ²	9.4	0.10
	MP 1000 mJ/cm ²	9.1	0.36

*Nitrate and nitrite were measured by ion chromatography. Irradiated samples were stored at 4°C in headspace-free amber glass vials with PTFE-lined septa and screw caps for 10 days before analysis.

Appendix 7: Supplemental Information for Chapter 5

Figures A7-1 through A7-5 show the results from preliminary tests that were carried out to determine experimental conditions for chronic cytotoxicity assay samples. Figure A7-5 shows the individually measured dose-response curves for tribromonitromethane, chloral hydrate, and diiodoacetamide standards. The R code for estimating confidence intervals and determining statistical significance between IC_{50} values is provided at the end of this appendix.

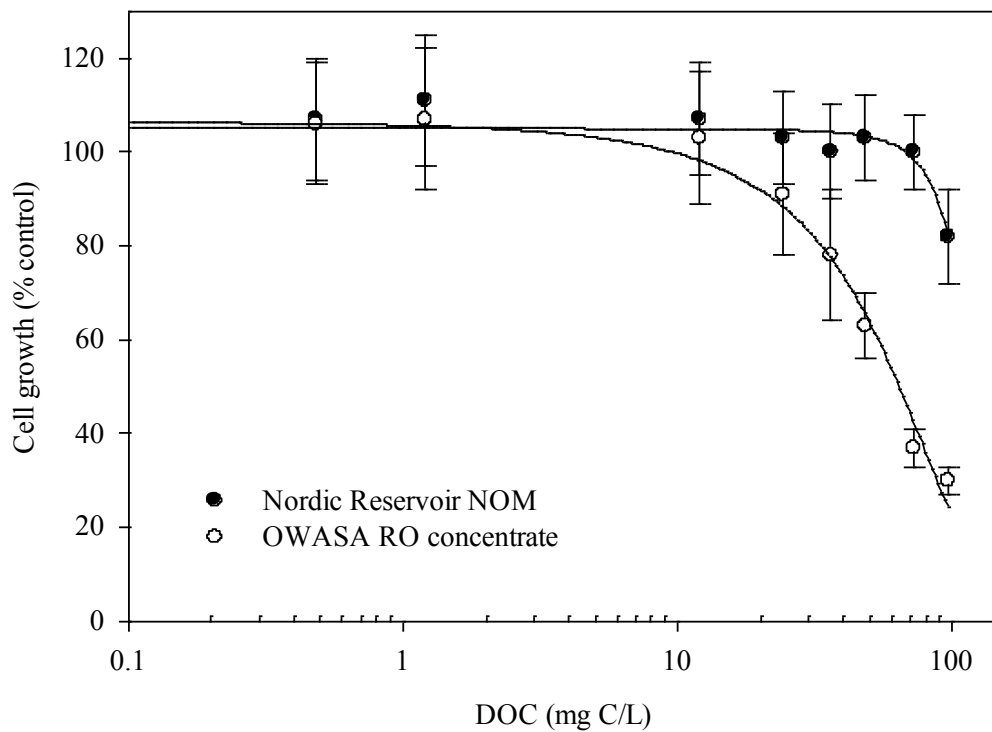


Figure A7-1. Dose-response curves for commercially available Nordic Reservoir NOM compared to Orange County Water & Sewer Authority Drinking Water Treatment Plant raw water (OWASA) reverse osmosis (RO) concentrate. Error bars represent standard deviation for n = 16 replicates.

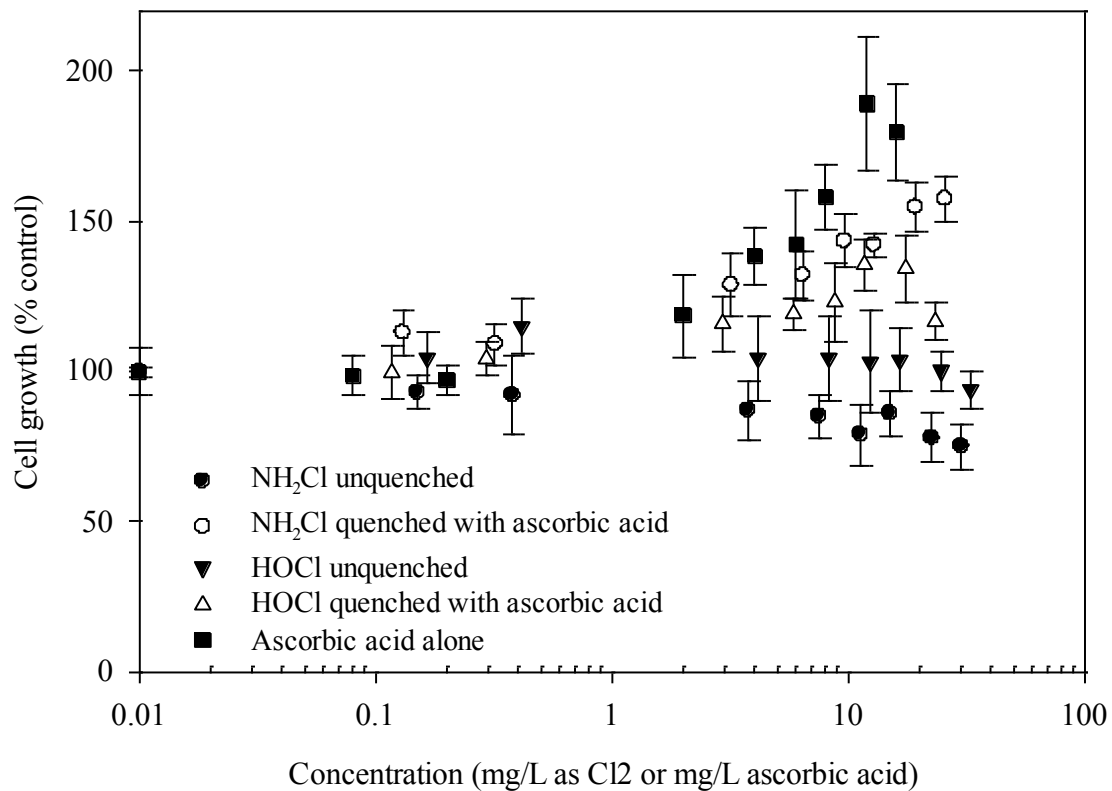


Figure A7-2. Cytotoxicity results for ascorbic acid, unquenched disinfectants and disinfectants quenched with ascorbic acid. Error bars represent standard deviation for n = 8 replicates. No curves are plotted because of poor sigmoidal curve fit to data.

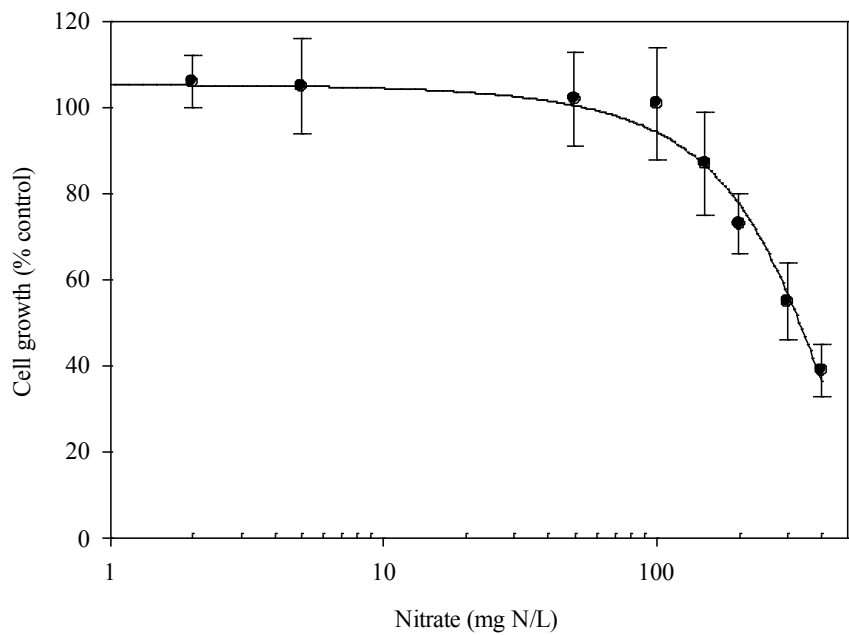


Figure A7-4. Dose-response curve for nitrate in 20 mM phosphate buffer. Spiking amount chosen for cytotoxicity studies was 100 mg N/L. Error bars represent standard deviation for n = 16 replicates.

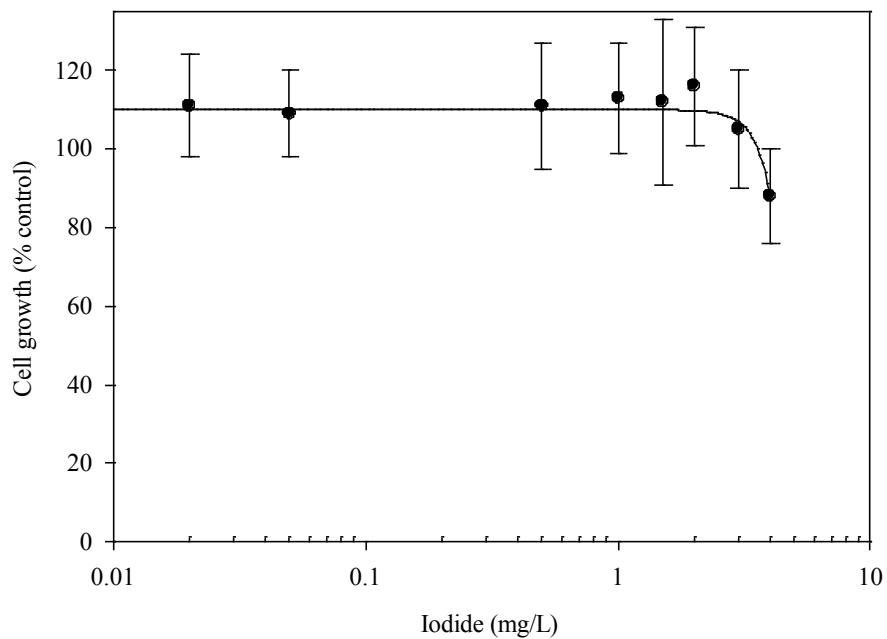


Figure A7-5. Dose-response curve for iodide in 20 mM phosphate buffer. Spiking amount chosen for cytotoxicity studies was 5 mg/L. Error bars represent standard deviation for n = 16 replicates.

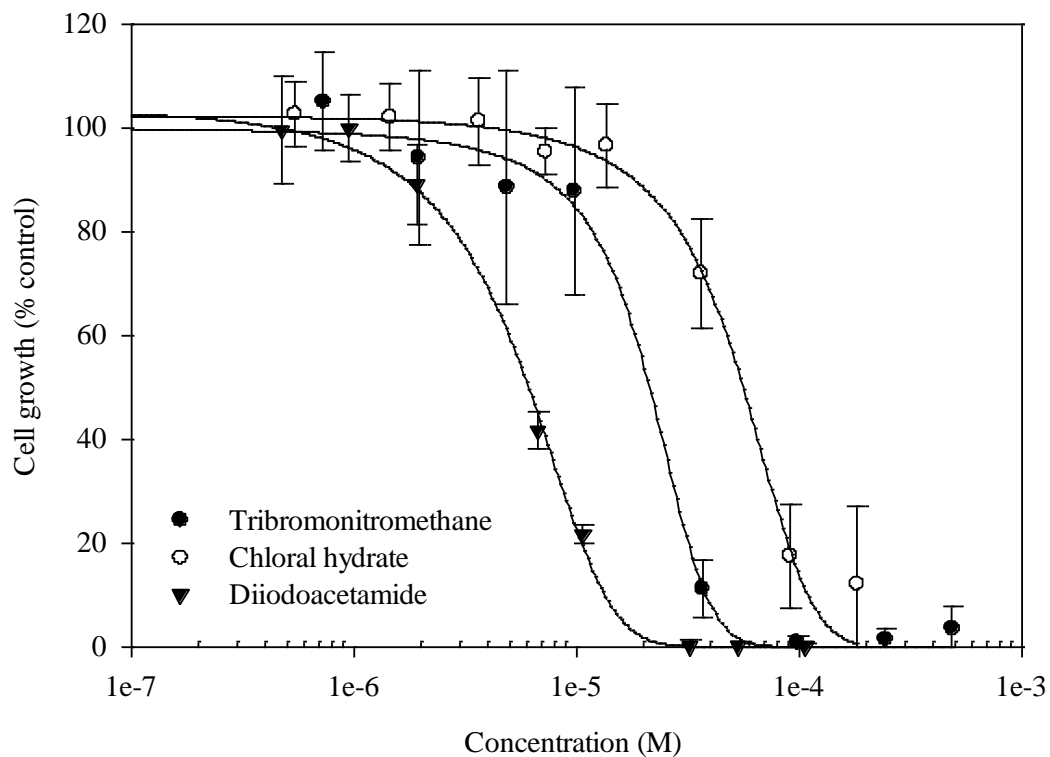


Figure A7-6. Dose-response curves for tribromonitromethane ($IC_{50} = 2.1 \times 10^{-5}$ M), chloral hydrate ($IC_{50} = 5.4 \times 10^{-5}$ M), and diiodoacetamide ($IC_{50} = 6.1 \times 10^{-6}$ M) standards.

The R code that was used for bootstrapping to estimate confidence intervals and significance between IC₅₀ values is shown here, with descriptions about what code does shown in italics below.

```
setwd("/Users/Bonnie/Research/Toxicology/DataRformat")
```

Input the path where your sample files are located.

```
doseresp1<-read.csv("Sample1.csv")
```

Imports file into R. Data should be in .csv format with two columns, the first containing concentration values (no units) and labeled with a header: "concentration" The second column will contain the corresponding cell growth % values calculated based on the plate absorbance (no units) and the header "celldensity". Example: first column – "concentration", 0, 0, 0.....highest concentration; and the second column – "celldensity", 99, 98, 99.....corresponding percentage value for highest concentration. If you have a sample which was run on two plates, you will have 144 rows of data.

```
doseresp2<-read.csv("Sample2.csv")
```

Imports your second sample.

Repeat this for all samples you are analyzing, replacing the file name and number following doseresp.

```
Fix(sigmoid)
```

Run this line, and a window will pop up. Input "x,x0,a,b" into the parentheses of function(). Then enter the equation: return(a/(1+exp(-(x-x0)/b))) between the brackets { }. This is the equation for a sigmoidal curve that will be fit to the data. Press the x button of the window and say yes when it asks you to save changes.

```
doseresp.nls<-nls(celldensity~sigmoid(concentration,x0,a,b),start=list(a=50,b=-10,x0=50),data=doseresp1)
```

Run this to fit the curve to your sample. Replace doseresp1 to run other samples.

```
summary(doseresp.nls)
```

Run this line to obtain the coefficients of the fitted curve. These should be the same coefficients obtained when a three-parameter sigmoidal curve is fit in SigmaPlot.

```
library(boot)
```

This loads the boot program.

```
fix(ic50.boot)
```

A window will pop-up after you run this line, input "indata, i" between the parentheses of function(). Enter the following equation between the brackets{ }:

```
data.star<-indata[i,]
```

```
cur.nls<-nls(celldensity~sigmoid(concentration,x0,a,b),start=list(a=50,b=-10,x0=50),data=data.star)
```

```
cur.coef<-coef(cur.nls)
```

```
return(cur.coef[3]+cur.coef[2]*(log(50)-log(cur.coef[1]-50)))
```

```
doseresp1.boot<-boot(doseresp1,ic50.boot,1000,strata=factor(doseresp1$concentration))
doseresp2.boot<-boot(doseresp2,ic50.boot,1000,strata=factor(doseresp2$concentration))
```

This will perform 1000 bootstrapping iterations to determine IC₅₀ values from your data.

```
boot.ci(doseresp1.boot)
boot.ci(doseresp2.boot)
```

This will display the estimated confidence intervals for your samples.

```
2*min(c(sum(doseresp1.boot$t>doseresp2.boot$t),sum(doseresp2.boot$t>doseresp1.boot
$t)))/1000
```

This compares the overlap of your bootstrapped values and outputs a P-value denoting the statistical significance between your IC₅₀ values. If $P < 0.01$, the values can be considered statistically different.

Appendix 8: Growth Inhibition Assay SOP

Prepared by: Rebecca Milsk

Materials/Equipment

- NCM460 Normal human colon cells (INCELL Corporation, San Antonio, TX, USA)
- M3:10A Culture Media (INCELL Corporation)
- Phosphate buffered saline solution (Ca^+ & Mg^{2+} -free, Gibco, Carlsbad, CA, USA)
- Trypsin-EDTA (Gibco)
- Isoton solution (Beckman Coulter, Fullerton, CA, USA)
- Trypan blue dye (0.4%, Sigma, St. Louis, MO, USA)
- Minimal Essential Medium (MEM, Gibco)
- 10x SMX growth factor concentrate (INCELL Corporation)
- Fungizone - Amphotericin B (Gibco)
- Fetal bovine serum (INCELL Corporation)
- Crystal violet dye (Gibco)
- Dimethyl sulfoxide (Sigma-Aldrich)
- 96 well microplates (tissue culture treated, Molecular devices, Sunnydale, CA, USA)
- 50 mL sterile culture tubes (Fisher Scientific, Fair Lawn, NJ, USA)
- 10 mL cell culture flasks (tissue culture treated, Corning, Sigma, St. Louis, MO, USA)
- Sterile, disposable 0.22 μm pore size vacuum filter unit (Nalgene, Thermo Fisher Scientific, Rochester, NY, USA)
- Sterile, disposable 0.22 μm pore size vacuum filter unit (Millipore, Billerica, MA, USA)
- Alumna-Seal foil (RPI Corporation, Mt. Prospect, IL, USA)
- 37° incubator
- Centrifuge (at least 800 rpm, that can hold 50 mL culture tubes)
- Coulter Particle Counter (Beckman Coulter)
- Hemocytometer (Hausser Scientific, Horsham, PA, USA)
- Microscope (for cell viability counting)
- Wallac Victor 1420 Multilabel Counter – plate reader at 600 nm (Perkin Elmer Wallac Inc., Gaithersburg, MD, USA)

7. Use 25 mL pipette and pipetteman to add 20 mL M3:10 to each 50 mL sterile centrifuge tube (1 tube per plate). Label one additional 50 mL sterile centrifuge tube as "cells." Check on cells using the microscope after \approx 6 minutes (one knob for the light and a switch for the power). Place flask back in incubator. Get 96-well plates from above the lab bench (behind hood). Use permanent marker to label the bottom side and top with date, initials, UNC, and sample name/#. Do not use cryogenic marker meant for freezer conditions! Label will not stay on in incubator unless it is permanent marker.
8. Once cells are detached and floating around flask (confirm using microscope), add 1 mL M3:10 medium (stops trypsin activity because trypsin inhibitor is present in fetal bovine serum in the media) to the flask (don't touch lip of flask), use rapid pipetting to mix (5-6 times, being careful not to let air in or out), and then add to tube marked "cells."
9. Turn on centrifuge (use switch on side). Press "stop/lid," place tube in centrifuge with a counterweight across from it (make sure it is filled with same volume of water as your cells vial), close the lid, and press "start." It is already programmed to run at 800 rpm and 4°C for 5 minutes.
10. In the meantime, spritz used cell flasks with alcohol or bleach and let sit (can pour down sink and discard later). Use dispenser to add 20 mL Isoton to two Coulter vials (in drawer under Coulter counter). Turn on Coulter Counter. Press button to bring platform down, remove the blue solution, and lightly blot the end of probe with a kimwipe. Place Isoton solution (1st vial) on platform and raise back up. Press "Fns," scroll right to "Flush Aperture," and press "start."
11. When centrifuging is complete, press "stop/lid" to open and remove cells (now a pellet). Place counter weight back on rack to right of centrifuge. Turn on vacuum. In the hood, tilt the tube slightly and use a pasteur pipette to remove the supernatant. Add 10 mL M3:10 (may use less or more M3:10 depending on size of pellet) to break up pellet with rapid pipetting. Vortex.
12. Add 200 μ L of cell mix to the 2nd vial of Isoton (mix with pipette, taking the liquid in and out a couple of times).
13. At the Coulter Counter, press "Set-up," then "Start" (blank is still in there to measure background). Record count. Background should be less than 100. If not, flush aperture again with fresh Isoton solution and repeat until <100 .

14. Take out blank and put vial containing cells in (inverting first). Press “Start” and record count. Press “Start” again and record count.

$$\begin{array}{l} \text{Background: } \underline{\hspace{2cm}} \\ \underline{\hspace{2cm}} \text{ cells/0.5 mL} \\ \underline{\hspace{2cm}} \text{ cells/0.5 mL} \\ \underline{\hspace{2cm}} \times 100 (\text{dilution factor (DF)}) = \underline{\hspace{2cm}} \text{ cells/mL} \end{array}$$

15. Place vial containing blue storage solution back, and raise platform up again to store probe. Shut off Coulter Counter.

16. Add 5 μL cells to 20 μL trypan blue (use non-sterile pipette, in drawer under computer, and blue tips) in a glass tube. Place 10 μL of the mixture in the hemocytometer. Count at least 100 cells, making sure to count only single cells (not clusters of 4 or more cells).

$$\begin{array}{l} \underline{\hspace{2cm}} \text{ live cells} \\ \underline{\hspace{2cm}} \text{ dead cells} \\ \underline{\hspace{2cm}} \text{ total cells} \\ \underline{\hspace{2cm}} \text{ live/ } \underline{\hspace{2cm}} \text{ total} = \underline{\hspace{2cm}} \% \text{ viable cells} \\ \text{cell concentration: } \underline{\hspace{2cm}} \times \underline{\hspace{2cm}} \% \text{ viable} = \underline{\hspace{2cm}} \text{ viable cells/mL} \end{array}$$

17. Calculate volume of suspension to obtain 1×10^6 cells for each 96 well plate.

$$1 \times 10^6 \text{ cells per plate/} \underline{\hspace{2cm}} \text{ viable cells/mL} = \underline{\hspace{2cm}} \text{ mL/plate}$$

18. Vortex cell suspension and transfer calculated volume into the 50 mL centrifuge tubes containing 20 mL M3:10. Mix well (by hand).

19. Transfer cells to reagent reservoir (in cabinet under computer, next to hood) and use 12-channel pipettor with three channels empty to add 200 μL cell mix to each well in columns 3-11 of the 96-well plate. Column 2 gets 200 μL M3:10 but no cells (blank). Columns 1 and 12 are left empty.

20. Place plates on tray and put in 37°C incubator for 24 hours.

Sample Preparation

1. Prepare “MEM blank” solution to be used for making dilutions of sample. To make a 120 mL MEM blank solution (enough for six 96-well plates, or three duplicate samples), add 1.14 g Minimal Essential Medium (MEM) and 264 mg NaHCO_3 to 96 mL lab-grade water and adjust the pH to 7.1~7.2 using 1M and 2M HCl (add dropwise with pasteur pipette). If necessary, use 1M NaOH to increase pH. The pH

meter used to measure the pH is calibrated with a pH 7 standard. To the pH adjusted solution, add 12 mL sterile Fetal Bovine Serum (FBS) and 12 mL sterile SMX growth factor concentrate in the hood. Filter the solution using the Nalgene 0.22 μm pore size vacuum filtration unit.

2. Prepare “MEM concentrate” solution to be combined with the sample. To prepare 14 mL MEM concentrate (enough for three samples), add 665 mg MEM and 154 mg NaHCO_3 to 7 mL sterile FBS and 7 mL sterile SMX (these two solutions are added to a 50 mL centrifuge tube in the hood). As for the MEM blank solution, adjust the pH to 7.1~7.2. Filter the solution using the Millipore Steriflip 0.22 μm pore size vacuum filtration unit.
3. For a 15 mL final sample volume, combine 12 mL of the sample (e.g. chlorinated Nordic Lake NOM) with 3 mL of the MEM concentrate.
4. Prepare dilutions of the sample with the MEM blank solution.

Treatment of Cells with Sample

1. Place sterile surgical gauze on surface in the hood using forceps. Open up plates and empty media onto the gauze. Discard gauze and wipe up any media left in hood with ethanol and large kimwipes.
2. Take out a sterile reagent reservoir and pour MEM blank into it. Use an 8-channel pipettor to add 200 μL of MEM blank into the wells in columns 2 and 3 on duplicate plates. Empty the reservoir into a waste cup, and add the lowest concentration of sample into it. Place 200 μL of this concentration of sample into column 4 on duplicate plates. Empty the reservoir into a waste cup, add the next highest concentration of sample into it, and place 200 μL of this concentration of sample into column 5 of duplicate plates. Continue in this manner until columns 4-11 are filled with the increasing concentrations of sample.
3. Cover the wells with Alumnaseal and press down with a finger to ensure that all of the wells are sealed.
4. Place plates in 37°C incubator for 72 hours.

Preparation of Positive Control Plate

1. Add 180 μL fungizone to 90 mL of M3:10 medium in a sterile container in the hood. Cover container with lid and swirl.
2. Prepare $2 \times 10^{-5}\text{M}$ diiodoacetamide by adding 87 μL of a 1790 $\mu\text{g}/\text{mL}$ diiodoacetamide stock solution into 25 mL of M3:10 medium.
3. Prepare $7 \times 10^{-6}\text{M}$ diiodoacetamide by adding 30 μL of a 1790 $\mu\text{g}/\text{mL}$ diiodoacetamide stock solution into 25 mL of M3:10 medium.

4. Prepare dilutions of these diiodoacetamide solutions with M3:10 medium.
5. Follow the steps under “Treatment of Cells with Sample” to place the diiodoacetamide dilutions on the cells, but use M3:10 instead of MEM blank for columns 2 and 3, and only make one plate (not duplicate).

Plate Reading (this part is carried out on lab bench, rather than in sterile hood)

1. Take out several gauze mats. Place one gauze mat on lab bench and fold in thirds. Remove two or three plates from incubator at a time. Peel off Alumnaseal from plate and tap plate face down on the mat a couple times to remove the media.
2. Pour non-sterile PBS (from fridge) into reagent reservoir (label it “PBS”). Use 12-channel pipettor to add 200 μL PBS to each well.
3. Pour 100% methanol into another reagent reservoir (label it “MeOH”). Remove PBS on the mat and add 100 μL methanol to each well. Place cover on plate. Let sit for 20 minutes. Repeat steps 1-3 for all plates.
4. Pour out remaining methanol from methanol boat and add 1% crystal violet in 100% methanol to it. Add 100 μL crystal violet to each well, changing tips for each plate. Cover the plate and let sit for 20 minutes.
5. Rinse plates one at a time in cold, running tap water, being careful not to expose plates to the direct flow of the tap. Plates are ready when no dye is observed when tapping the plates on a clean surface. Prop finished plates up against a Styrofoam tube holder to dry.
6. After allowing plates to dry (~20 min or more), add 50 μL DMSO to each well. Cover the plates with foil (can stack plates 2-3 high) and place on a rotating shaker. Secure the plates to the platform with tape and turn the shaker on (switch by Hold, set at 110 rpm). Let run for 30 minutes.
7. Turn plate reader on and let warm up (takes ~30 minutes, on/off switch in back).
8. While plates are on shaker table, prepare crystal violet standard plate to run with samples. To prepare this plate: Leave bottom row (H) empty and put 50 μL water in the rest of the wells. Place 50 μL of 0.01% CV in row H. Place 50 μL of 0.01% CV in row G, then take out 50 μL from row G and add it row F, and so on up until row B. Once the 50 μL from row C has been added to row B, remove 50 μL from row B and discard. Row A will contain only water.
9. Turn the computer on. When the screen pops up, hit Okay, then Cancel. Put flash drive in USB port. Double click Wallace 1420 Workstation. Take cover off of plate and place in machine. Go to Instrument Ctrl, and click Start. Will measure absorbance at 600 nm (Alamar Blue).
10. Go to Live Display (set scale at 0.000 A – 2.000 A absorbance scale for photometry).

11. When done reading, click 3rd . Click 4th , which is plate view. Click File, then Print. Then go to File, Export, then removable disk. Include date and sample name in file name (e.g. exp091610_I2AM).
12. Make sure that the data has printed okay and saved before closing out and starting the next plate reading. Label printout with date of experiment and sample name. Sign it and make one copy for self (the other is for EPA). Do not forget the flash drive!

Sources Cited for Chapter 6

- Bohdziewicz, J. et al., 1999. The application of reverse osmosis and nanofiltration to the removal of nitrates from groundwater. *Desalination*, 121(2), pp.139-147.
- Clifford, D. & Liu, X., 1993. Ion exchange for nitrate removal. *Journal American Water Works Association*, 85(4), pp.135-143.
- Collins, M.R. et al., 1986. Molecular weight distribution, carboxylic acidity, and humic substances content of aquatic organic matter: implications for removal during water treatment. *Environmental Science & Technology*, 20(10), pp.1028-1032.
- Dotson, A.D. et al., 2010. UV/H₂O₂ treatment of drinking water increases post-chlorination DBP formation. *Water Research*, 44(12), pp.3703-3713.
- Hell, F. et al., 1998. Experience with full-scale electro dialysis for nitrate and hardness removal. *Desalination*, 117(1-3), pp.173-180.
- Linden, K.G. et al., 2012. *Impact of UV Location and Sequence on Byproduct Formation*. American Water Works Association and Water Research Foundation: Denver, Colorado.
- Plewa, M.J. et al., 2004. Halonitromethane drinking water disinfection byproducts: chemical characterization and mammalian cell cytotoxicity and genotoxicity. *Environmental Science & Technology*, 38(1), pp.62-68.
- WHO (World Health Organization), 1993. *Guidelines for Drinking-Water Quality*. 2nd Edition, World Health Organization: Geneva.